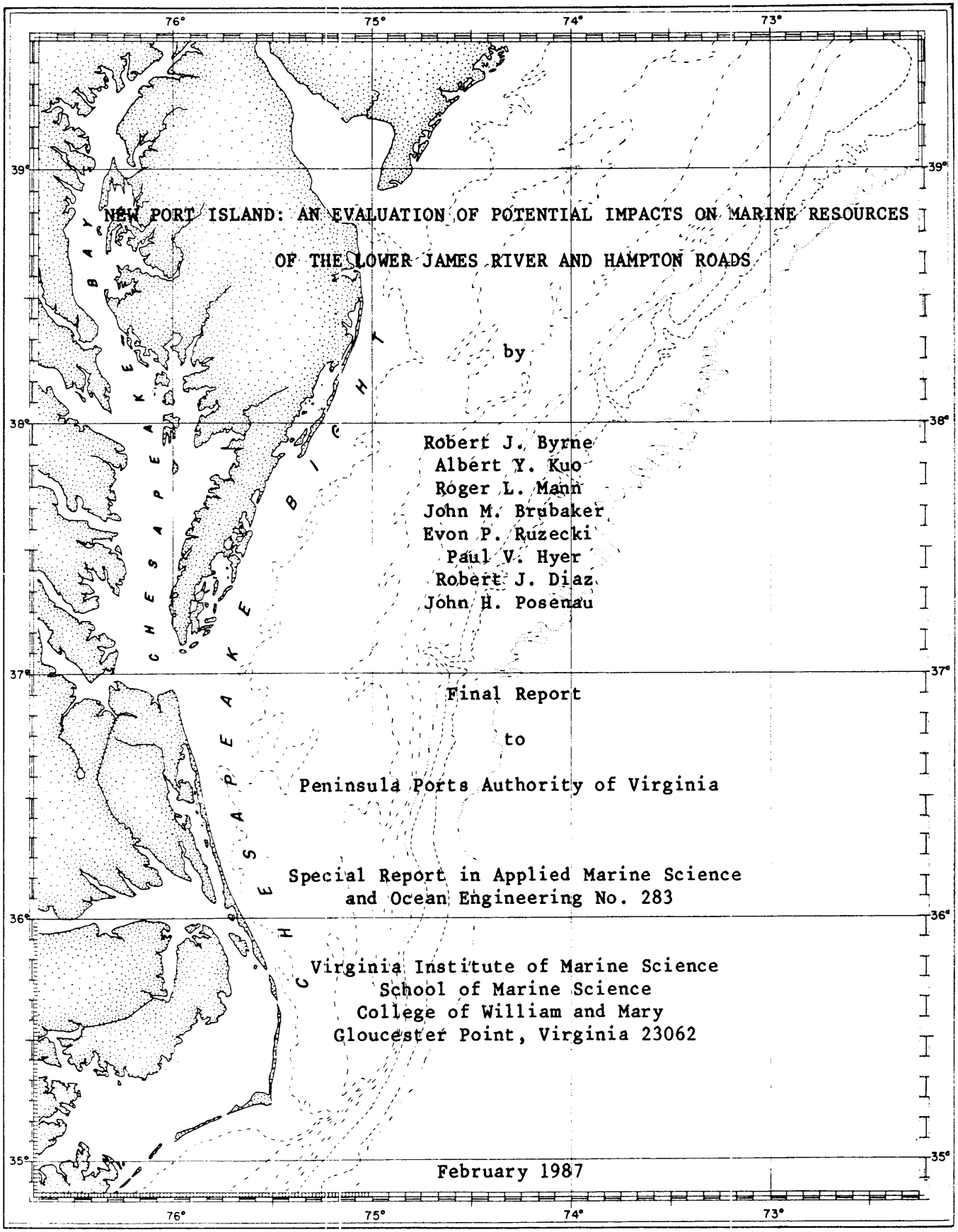

NEW PORT ISLAND: AN EVALUATION OF POTENTIAL IMPACTS ON MARINE RESOURCES OF THE LOWER JAMES RIVER AND HAMPTON ROADS

by

Robert J. Byrne
Albert Y. Kuo
Roger L. Mann
John M. Brubaker
Evon P. Ruzecki
Paul V. Hyer
Robert J. Diaz
John H. Posenau

Final Report

to

Peninsula Ports Authority of Virginia

Special Report in Applied Marine Science
and Ocean Engineering No. 283

Virginia Institute of Marine Science
School of Marine Science
College of William and Mary
Gloucester Point, Virginia 23062

February 1987

NEW PORT ISLAND: AN EVALUATION OF POTENTIAL IMPACTS ON MARINE RESOURCES OF THE LOWER JAMES RIVER AND HAMPTON ROADS

by

Robert J. Byrne
Albert Y. Kuo
Roger L. Mann
John M. Brubaker
Evon P. Ruzecki
Paul V. Hyer
Robert J. Diaz
John H. Posenau

Final Report

to

Peninsula Ports Authority of Virginia

Special Report in Applied Marine Science
and Ocean Engineering No. 283

Virginia Institute of Marine Science
School of Marine Science
College of William and Mary
Gloucester Point, Virginia 23062

February 1987

PREFACE

This study is reported in two volumes. The main body of the results, discussion, and the conclusions are presented in this volume. Explanation of methods and data summaries are presented in Volume 2, Appendices.

Acknowledgments. This work could not have been completed without the devoted effort of many of the Institute staff. The authors wish to express their deepest appreciation to William Matthews, Steve Snyder, Mark Worrall, Karl Dydak, Tracy Eanes, Samuel Wilson, and Ralph Edlow for long exhausting days of field sampling. For assistance in analysis we thank Tracy Eanes, Linda Huzzey, Mary Sue Jablonsky, and Hugh Evans. We thank Dr. John D. Boon, III, for assistance in tidal height analysis; Malcolm O. Green for analysis of wave-current interaction; and Linda Schaffner and George Thomas for assistance in the biological sampling. Dr. Jay D. Andrews provided a thoughtful and constructive review of the draft manuscript.

We thank the Vessel Operations staff for their assistance throughout the project, particularly Sharon Miller, Durand Ward, Charles Machen, and Danny Gouge.

Finally, the report itself would not have been completed without the dedicated efforts of Agnes Lewis, Barbara Cauthorn, Ruth Hershner, Janet Walker, Maxine Butler, Mary Jo Shackelford, and Sylvia Motley.

CONTENTS

LIST OF TABLES

LIST OF FIGURES

I. EXECUTIVE SUMMARY

A. Legislative Background

The Virginia General Assembly, in House Bill No. 1396, 1985 (Figure IA-1) established certain conditions for possible conveyance of submerged lands to the Peninsula Ports Authority of Virginia (PPAV) for the purpose of constructing thereon an island in order to increase port and recreational facilities. One condition of H.B. No. 1396 requires that the Virginia Institute of Marine Science shall study "the effect and potential effect of the contemplated project on the James River seed oyster beds, including but not limited to tidal flow and water circulation. In addition, the study shall include examination of the effect or potential effect of the contemplated project on other marine resources and the fisheries of the Commonwealth."

Pursuant to the conditions of H.B. 1396 the PPAV funded the Virginia Institute of Marine Science (VIMS) under a contract of July, 1985, to conduct certain studies for evaluation of the potential impact of the proposed island on the marine resources of the James River/Hampton Roads system.

B. Rationale of the Study

Proposed is a 400 acre island on the western end of Hampton Flats, a shallow embayment in Hampton Roads (Figure IB-1). Two island location options have been proposed with connection, via open piling causeway, to the mainland at Newport News Point (Figure IB-2a,b). Also shown in Figure IB-2a

LD7008101

Signed by the Governor
April 19, 1985.

HOUSE BILL NO. 1396

AMENDMENT IN THE NATURE OF A SUBSTITUTE

(Proposed by the Senate Committee for Courts of Justice on February 13, 1985)

(Patron Prior to Substitute--Delegate Diamonstein)

A BILL to authorize the Governor to convey certain submerged lands to the Peninsula Ports Authority of Virginia.

Whereas, it is proposed that the shipping channels in Hampton Roads be dredged to a depth of fifty-five feet; and

Whereas, submerged lands owned by the Commonwealth of Virginia near the City of Newport News in Hampton Roads Harbor, midway between Newport News Point and the Newport News shipping channel, sometimes referred to as the Newport News Sandbar, are a potential disposal site for the spoils from such dredging; and

Whereas, it is estimated, if such spoils are so deposited, an island of more than 400 acres may be created; and

Whereas, the Peninsula Ports Authority of Virginia needs additional land for port facilities, industrial expansion and recreation purposes; and

Whereas, the marine resources and the natural environment of the Commonwealth are irreplaceable natural resources which have been afforded special protection under Article XI of the Constitution of Virginia; and

Whereas, the deposit of such dredged spoils raises questions concerning potential effects on marine resources and the environment; now, therefore,

Be it enacted by the General Assembly of Virginia:

1. *§ 1. That the Governor of Virginia is hereby authorized and empowered, subject to the conditions set forth in §§ 2 through 7, to execute in the name of the Commonwealth a conveyance to the Peninsula Ports Authority of Virginia of the submerged lands in Hampton Roads Harbor, sometimes referred to as the Newport News Sandbar, containing 400 to 500 acres for the purpose of creating an island of dredge spoils. Exact acreage and description are to be determined by survey done at the city's expense.*

§ 2. Prior to the commencement of any further proceedings hereunder, the Authority shall obtain from the Attorney General an opinion that the conveyance and the proposed use are in conformance with the Constitution and laws of Virginia.

§ 3. The Virginia Institute of Marine Science shall study, at the expense of the Peninsula Ports Authority of Virginia, the effect and potential effect of the contemplated project on the James River seed oyster beds, including but not limited to tidal flow and water circulation. In addition, the study shall include examination of the effect or potential effect of the contemplated project on other marine resources and the fisheries of the Commonwealth.

§ 4. The Marine Resources Commission, prior to the issuance of any permit, shall conduct an evidentiary proceeding under the Administrative Process Act to determine whether it should recommend to the Governor that the conveyance be made. The Virginia Institute of Marine Science study described in § 3 shall be a part of the record of such proceeding. The Marine Resources Commission shall not recommend that the conveyance be made unless it first finds that there is no material probability that the project will

FIGURE IA-1. House Bill No. 1396.

affect the James River seed oyster beds in an adverse manner.

§ 5. All other requirements of state law, including but not limited to obtaining applicable permits, shall be complied with prior to conveyance by the Governor.

§ 6. The form of conveyance and all terms and conditions thereof shall be as determined by the Governor to be in the best interests of the Commonwealth. The instrument of conveyance shall include a provision that title to the property conveyed shall revert to the Commonwealth if the island of dredge spoils shall not have been substantially created, as determined by the Governor, by June 30, 1992.

§ 7. The form of conveyance shall be approved by the Attorney General.

Official Use By Clerks	
Passed By The House of Delegates	Passed By The Senate
without amendment ☐	without amendment ☐
with amendment ☐	with amendment ☐
substitute ☐	substitute ☐
substitute w/amdt ☐	substitute w/amdt ☐
Date: _____	Date: _____
_____	_____
Clerk of the House of Delegates	Clerk of the Senate

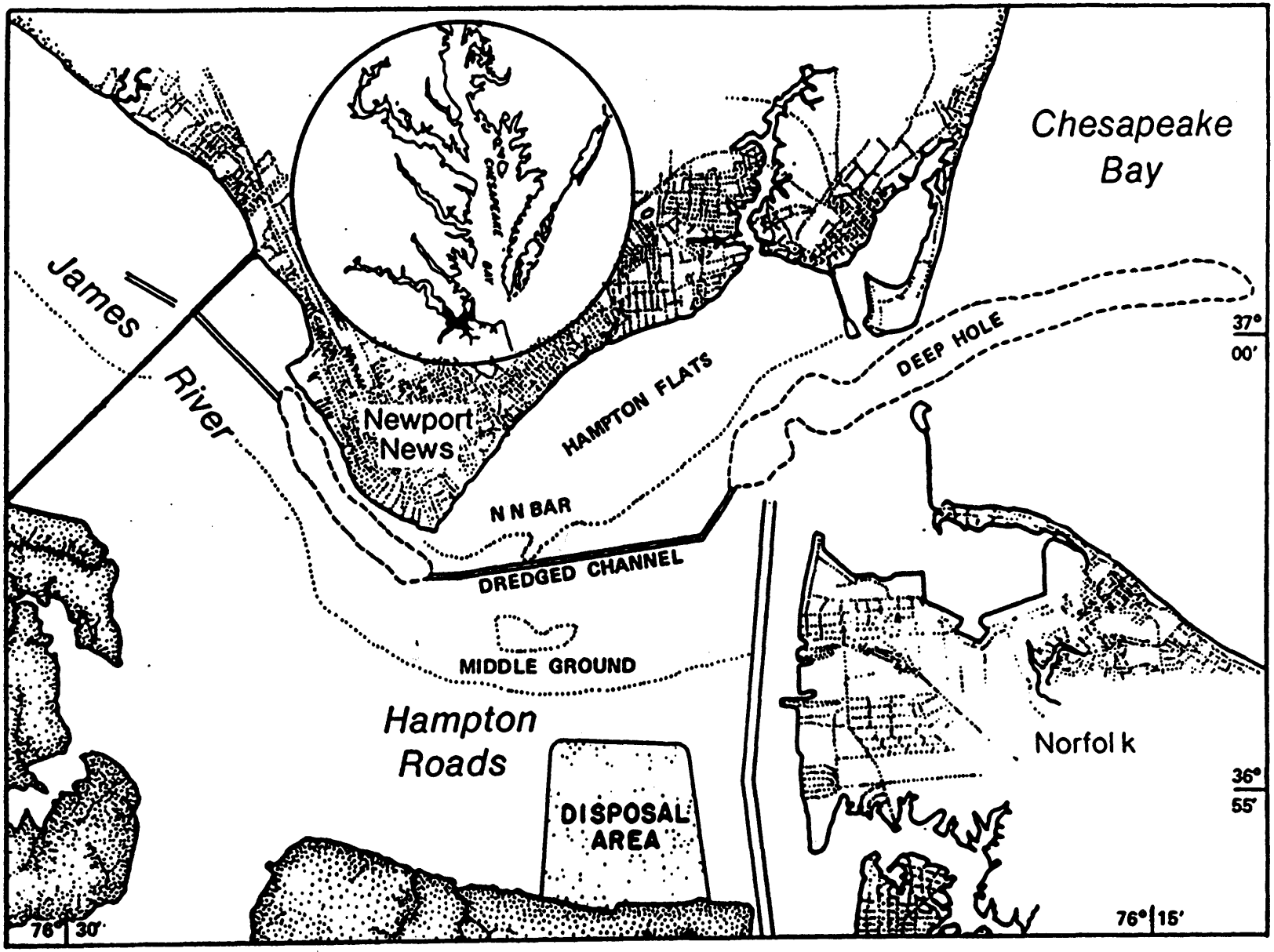

Figure IB-1. Hampton Roads and the lower James River.

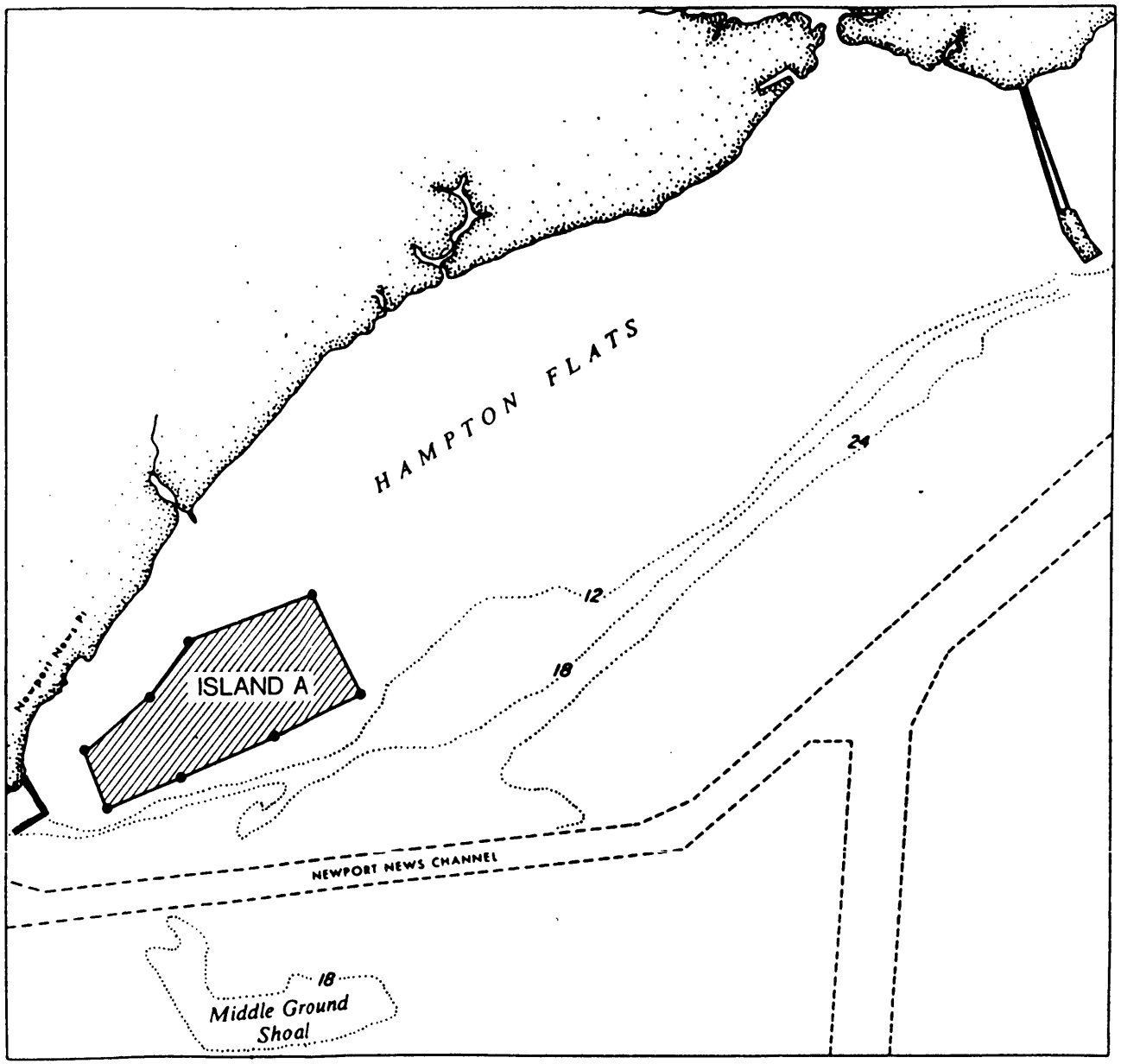

Figure IB-2a. Location of proposed New Port Island, Option A.

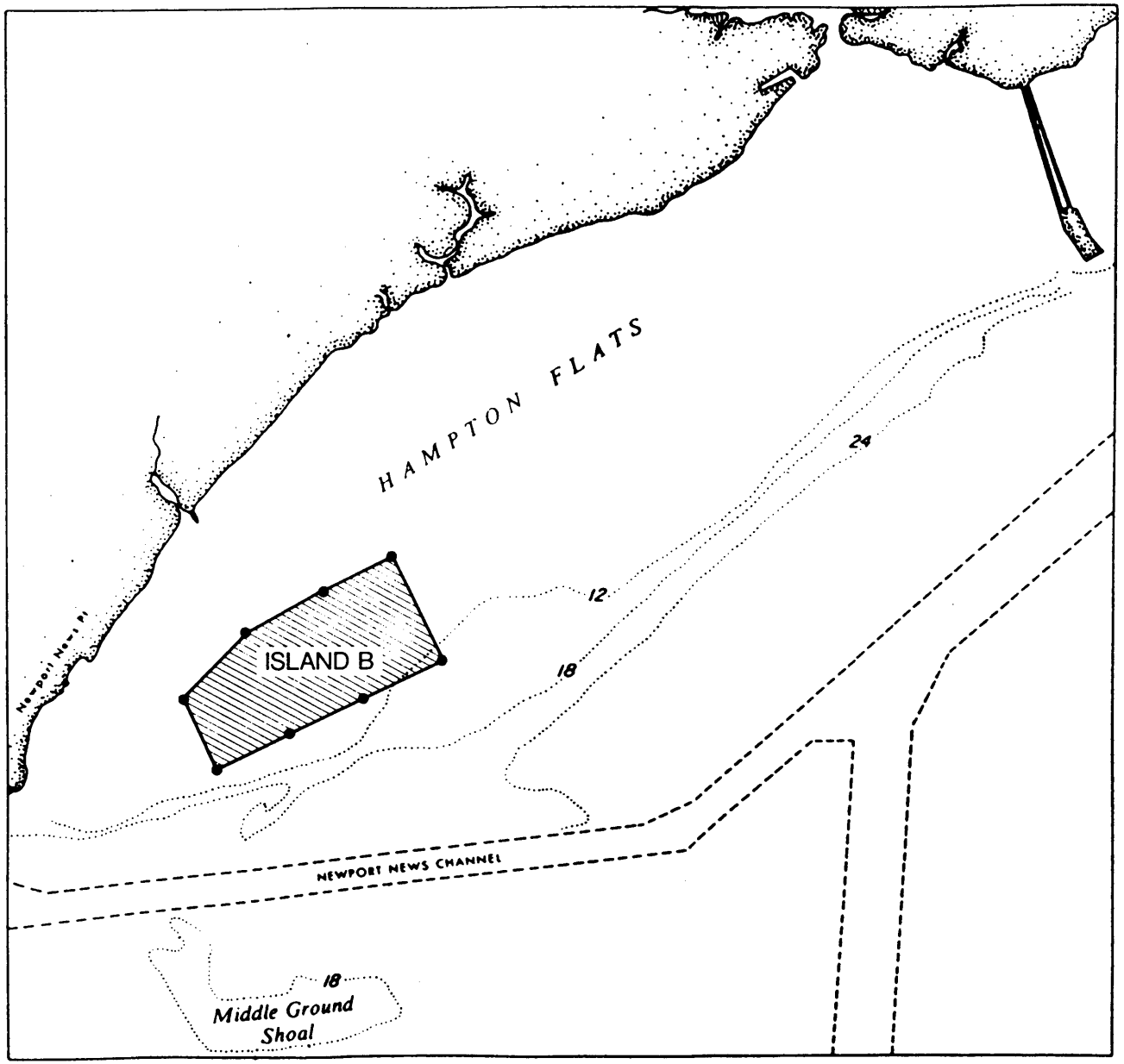

Figure IB-2b. Location of proposed New Port Island, Option B.

is the north island jetty of the I664 Hampton Roads crossing, currently under construction.

The studies herein reported have focused on the seed oyster beds of the James River, and on the hard clam resources on Hampton Flats. In addition the general benthic resources of Hampton Flats are reviewed.

There are no extant seed oyster beds in Hampton Roads (Figure IB-3). However, limited observations by VIMS in 1974 suggested that some characteristics of the water circulation in Hampton Roads may play a significant role in the transport system for oyster larvae. The James River provides conditions conducive for the maintenance of oyster populations via an annual strike of oyster larvae. While salinity regimes undoubtedly play significant roles, it appears that favorable larval retention within the system is the major factor in maintenance of the seed oyster beds.

Oyster larvae remain in the water column for a period of two to three weeks and are carried by the water movements. However, larvae do swim vertically in a tight helical motion whereby feeding, respiration, and depth regulation are achieved. In the final stage of development larvae seek an appropriate hard substrate for attachment and metamorphosis. The horizontal dispersal of planktonic larvae is determined principally by circulation patterns within the estuary. Evidence to date indicates that the larvae are carried in a net counterclockwise circulation wherein surface water (upper 4 meters) moves downriver on the southern side of the river and then turns within Hampton Roads toward the north. The surface waters of the northern flank of the James also have net downriver movement, albeit a weaker movement than on the southern side. How then are oyster larvae advected into Hampton Roads returned upriver to the seed oyster beds? In 1974 limited observations indicated a flow convergence off Newport News Point wherein

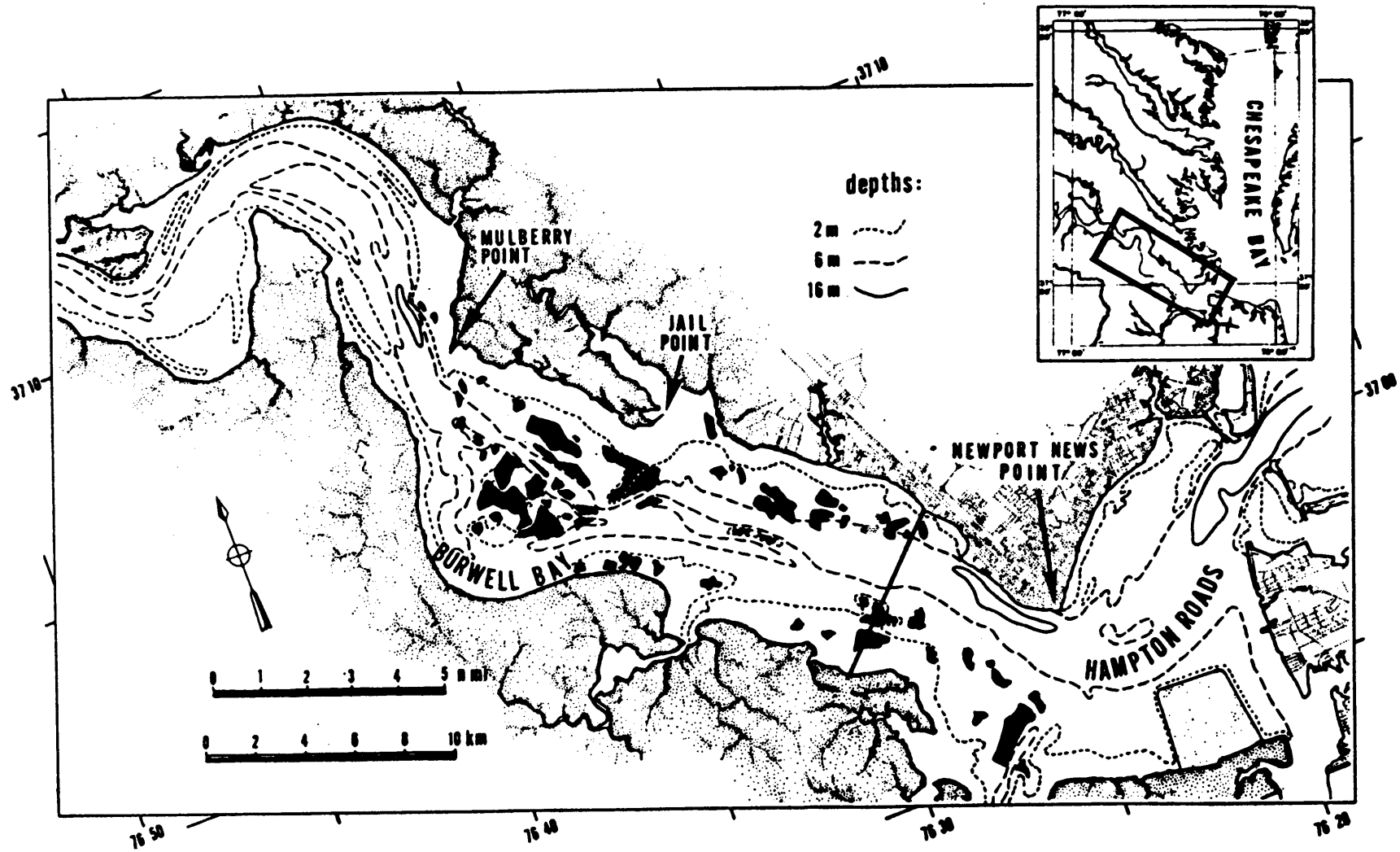

Figure IB-3. The James River Estuary from Old Point Comfort, at the mouth, to Jamestown Island (upper left corner). Seed oyster beds are shown as irregularly shaped darkened areas.

surface waters flowing upriver over Hampton Flats, during flood phase, descend beneath the waters of the lower James. The potential importance of the convergence phenomenon (called hereafter a frontal system) is centered on the hypothesis that it provides a mechanism to inject larvae-laden waters into deeper depths for recycling by net upriver transport induced by longitudinal salinity gradients. The task was to test this hypothesis and, if the frontal system was demonstrated to be a significant link in the larval transport system, to address the central question:

> Will the New Port Island project have a material adverse impact on the larval transport system via disruption or reduction of the transport efficiency of the frontal system at Newport News Point?

The issue of potential far-field impacts on the seed oyster beds is very complex because construction of projects other than the proposed island are involved also. There will be modifications of the shore boundary at Newport News Point due to the jetty and north island of I664, and the south island of I664 may be expected to modify the flow field. The second element of construction is the proposed deepening of the Newport News Channel from its current project depth of 45 feet to 55 feet. Thus, the effects of these construction programs must be differentiated from those associated with the construction of the proposed island.

The bottoms of Hampton Flats and adjacent slopes contain a significant fishery of local hard clam (Mercenaria mercenaria). The principal concern was whether the proposed island would alter circulation patterns on Hampton Flats to induce deposition of fine-grained sediments. Laboratory studies (Keck et al. 1974) indicate that a sandy substrate is preferred to mud for setting of hard clams.

C. Design of the Study

1. Frontal System and Larval Transport

At the onset of the study little was known about the characteristics of the frontal system. Investigations were undertaken to determine:

a. Whether the frontal system is a persistent feature. That is, does the feature form under all flood current conditions throughout the range of tides within the lunar month, and under the normal range of fresh water inflow.

b. The depth of injection, or mixing, of surface waters intercepted by the frontal system.

c. How much of the flow across the lower James/Hampton Roads transverse cross-section is involved in the frontal system activity.

These components of the study were achieved by a program of extensive field observations including examination of the water column density structure, and dye injection experiments to trace flow paths to the fronts and subsequent depth of diving below the front. Current meters were deployed to examine the phase and strength of tidal flow in the vicinity of the front.

The ensemble of field observations was intended to establish the conditions pertaining to formation and behavior of the frontal system, and to provide a basis to argue why the frontal system forms. As well, these observations provide a data set to test the applicability of the theory of estuarine fronts.

The distribution of oyster larvae in the water column was also deemed highly important. If larvae were confined to the lower portion of the water column then downward mixing of surface waters induced by the frontal system would be relatively less important in the larval transport process.

Accordingly, a program for field observation of larval distribution in the water column was undertaken in the late summer of 1985. Sampling was guided by earlier surveys of the frontal system density structure, and by dye injection experiments.

Larval swimming behavior was examined in laboratory experiments to test whether sharp salinity gradients constituted a barrier, and to measure swimming rates at various stages of development.

2. Sedimentation on Hampton Flats

Hampton Flats offers a favorable habitat for hard clams. A first step toward evaluation of impacts of construction was characterization of surface sediments, and of the flow field. Surface sediments were collected and analyzed for sand, silt, and clay ratios and the grain size distribution of the sand fraction. A two-dimensional hydrodynamic model was utilized to characterize the flow field due to tidal currents.

Qualitative assessment of the sediment transport/deposition potential was formulated by comparing the bottom shear stress induced by tidal currents to the threshold shear stress for resuspension.

3. Evaluation of Potential Impacts

As previously mentioned, there were several elements of construction to be evaluated with respect to the frontal transport system and to sedimentation on Hampton Flats. These were:

BASE	Conditions pertaining prior to I664 construction, channel deepening, and island construction.
I664-45	The condition of I664 in place with the present project depth of 45 feet for Newport News Channel.
I664-55	The condition of I664 in place but with Newport News Channel deepened to 55 feet.
Island A	The condition of I664 in place and Newport News Channel at 55 feet depth, with the proposed Island Option A (Figure IB-2a).

Island B The condition of I664 in place, 55 foot channel depth, and the proposed Island Option B (Figure IB-2b).

The results of the investigation suggested that an island position shifted to the east of the two options proposed may have reduced impact on the frontal transport system. Accordingly, the analysis was extended (Figure IC-1a,b) to illustrate the sensitivity of island location on Hampton Flats:

Island C The condition of I664 in place, deepened channel and Island C.

Island D The condition as above but with the island located in a position intermediate to the proposed Option B and that of Island C.

Whereas the island size tested for Island Options A and B was approximately 415 acres, the area of Island C was 370 acres and Island D was 323 acres. The configurations for C and D were dictated by the grid size used in the numerical hydrodynamic model.

Evaluation of potential impacts due to construction was achieved by integrating the results of advances in the theory of fronts with the results of the two-dimensional hydrodynamic model for changes in the flow field, and past hydraulic model studies for changes in the density (salinity) fields.

D. Principal Findings

1. Characteristics of the Frontal System and Implications on Oyster Larvae Transport

a. Observations made in the course of the study indicate that the estuarine front system in the vicinity of Newport News Point:

1) Is a persistent phenomenon which may be expected to occur during times of flood current under normal combinations of tidal

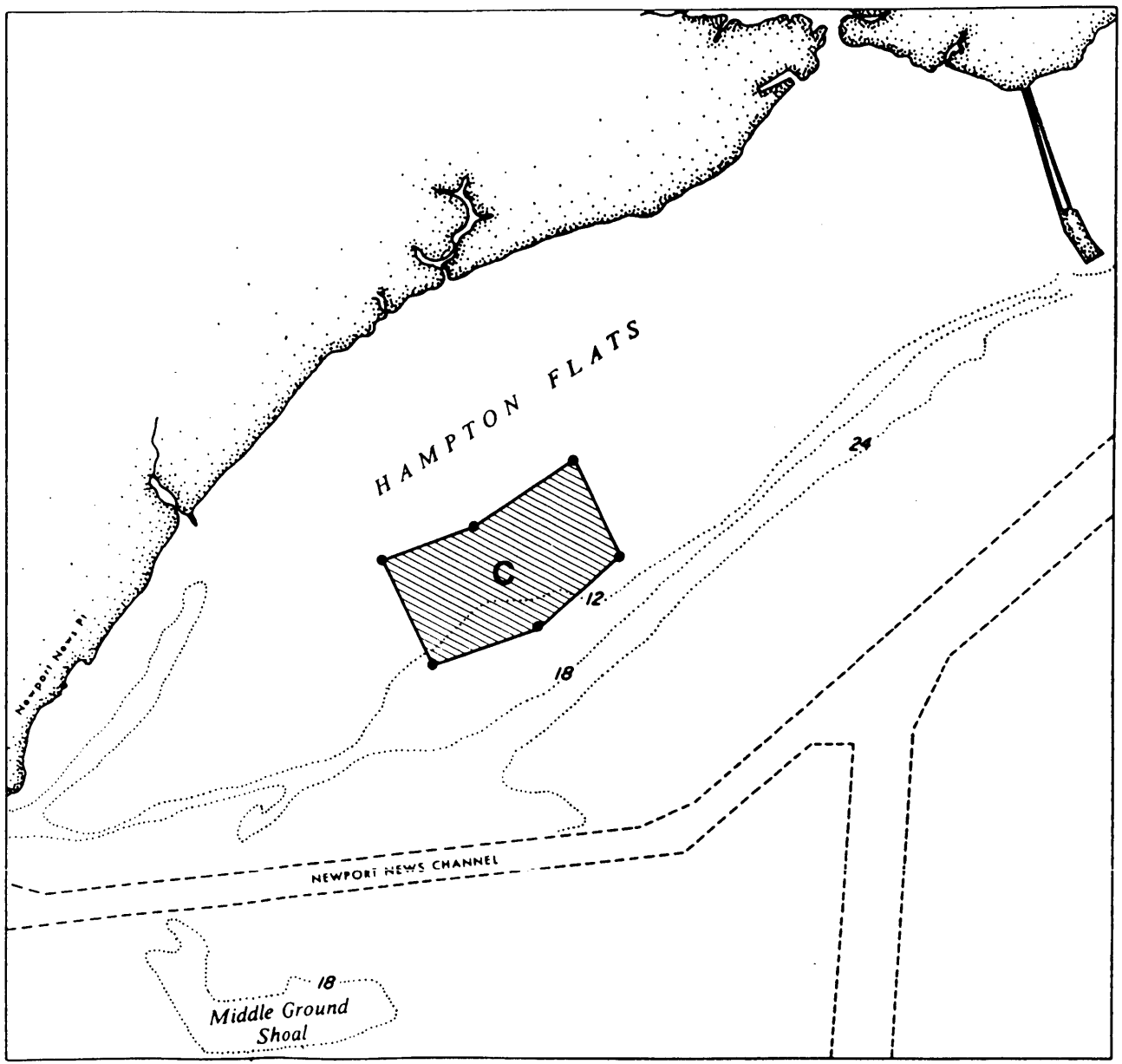

Figure IC-1a. Location of test Island C.

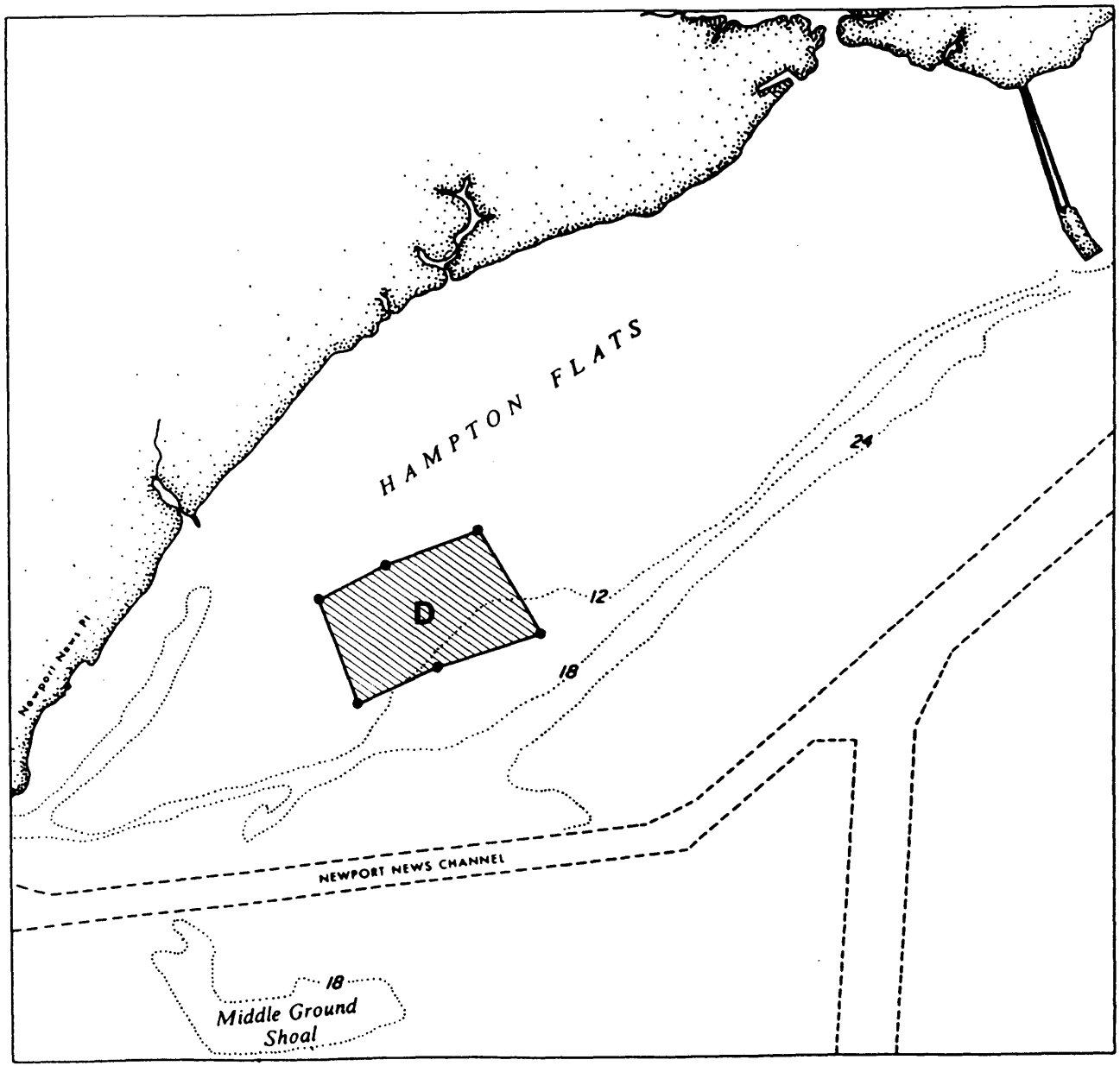

Figure IC-1b. Location of test Island D.

range, fresh water inflow, and meteorological conditions. The location and duration of the feature may be affected during unusual combinations of the forcing functions.

2) Involves not only the flow coursing over Hampton Flats but also much of the channel flood current flow between Hampton Flats and Newport News Middleground Shoal. The feature is compound in that the earliest contribution arises from flow across Hampton Flats and is progressively followed by contributions from the channel section.

3) Arises as a result of the geometry of Hampton Roads (including Hampton Flats) relative to the orientation of the James River, and the salinity distribution prevailing at slack water before flood currents begin.

4) Tends to be 'arrested' (or stabilized) and enhanced by the depth transition at Newport News Point. Numerous dye studies have demonstrated that surface waters are injected to depths of four meters or more in the vicinity of the depth transition.

b. Limited observations of the distribution of oyster larvae indicated presence of larvae of various sizes throughout the water column. Sampling of oyster larvae on the downriver and upriver sides of the front support the hypothesis that they are passively injected via the frontal activity to depths with net upriver transport.

c. Laboratory studies of larva swimming behavior indicate that they can swim through vertical salinity gradients typically found in the frontal system. However, the vertical swimming rates are ten times smaller than calculated downward injection rates induced by the frontal system. The larval swimming rate cannot counteract the vertical transport rate of the frontal system.

d. The sum of evidence obtained concerning the circulation associated with the frontal system supports the hypothesis that the frontal system plays a significant role in the larval transport and retention within the James River seed beds. Studies of horizontal circulation indicate an elongate counterclockwise net movement of water within the lower James River/Hampton Roads wherein the flow is downstream on the southern side of the James, veers within Hampton Roads (with leakage to the Bay), and transits up the northern side of the James. The importance of the convergence of the front off Newport News Point rests in the fact that the vertical circulation associated with the frontal system provides a mechanism to inject larvae laden waters into deeper waters for cycling upriver by the net upriver transport induced by gravitational circulation.

e. Prior to the onset of the oyster disease, MSX, Hampton Flats was planted with seed oysters from upriver beds. These oysters were allowed to grow for harvest. Evaluation of dye studies in a hydraulic model, coupled with information on oyster size and quality, indicates that Hampton Flats was probably the largest contributor of oyster larvae to the entire seed bed system. Thus, if MSX resistant stocks could be reestablished on Hampton Flats that area would again contribute to the larval pool.

f. The body of theory on frontal processes has been advanced in this study so that the behavior of a front passing over the depth transition can be estimated. Although the theory is developed for the two-dimensional case with two fluids of discrete density contrast, the observed phenomena show close correspondence with the theory.

g. Application of the theory, utilizing the results of the two-dimensional hydrodynamic model and previous studies on salinity distributions, provide the following findings:

1) The frontal activity will persist regardless of the various construction elements (I664, channel deepening, or the proposed New Port Island). However,

2) The transport effectiveness of the frontal system would be markedly reduced with New Port Island in either of the two locations proposed (either Option A or B). The principal reduction is due to blockage of flow from Hampton Flats. Island locations A or B result in a reduction of flood tidal flow onto Hampton Flats of about 14% relative to the I664 condition. Both configurations result in dramatically reduced outflow through the passage between the island and the mainland. At the eastern end of the island large water volumes are deflected toward the channel at a position remote from the front.

Both surface and deeper water contribute to the frontal system. Surface waters (4 meters or less) receive relatively large vertical displacement and are injected into the zone of net upriver transport. Thus, the contribution of surface water is considered to be particularly significant. Deeper water, although receiving additional displacement due to the front, would participate in the net upriver transport with or without the front.

The results are summarized in terms of the flood current water transport budget (Table ID-1). A full discussion is presented in Part IV. The budget considers flow into two branches of the frontal system (Figure IC-2). Branch I considers flow passing over Hampton Flats (Segment 1) and that passing along the shallow flanks (Segment 2). Branch II considers the

Table ID-1. Flood Current Water Transport Budget.

	BRANCH I		BRANCH II				% change Relative to I664-45	
	Segment 1	Segment 2	Segment 3 <4m	Segment 3 >4m	SUBTOTAL <4m	TOTAL FLUX	<4m	Total
BASE								
Volume	20.4*	15.2	41.2	41.2				
Contributing	20.4	10.0	22.2	22.2	52.6	74.8	N/A	N/A
Noncontributing	-0-	5.2	19.0	19.0	24.2	43.2		
I664-45								
Volume	16.0	14.7	38.3	36.8				
Contributing	16.0	9.7	22.7	21.8	48.4	70.2	N/A	N/A
Noncontributing	-0-	5.0	15.6	15.0	20.6	35.6		
I664-55								
Volume	14.9	14.2	41.9	43.7				
Contributing	14.9	9.2	22.4	23.4	46.5	69.9	-3.9	-0.4
Noncontributing	-0-	5.0	19.5	20.3	24.5	44.8		
ISLAND A								
Volume	6.7	11.5	42.5	44.2				
Contributing	6.7	7.5	22.4	23.4	36.6	60.0	-24.4	-14.5
Noncontributing	-0-	4.0	20.1	20.8	24.1	44.9		
ISLAND B								
Volume	9.4	10.3	40.8	44.3				
Contributing	9.4	6.6	22.4	23.4	38.4	61.8	-20.7	-12.0
Noncontributing	-0-	3.7	18.4	20.9	22.1	43.0		
ISLAND C-45								
Volume	15.6	14.1	39.3	37.3				
Contributing	15.6	9.0	22.7	21.8	47.3	69.1	-2.2	-1.6
Noncontributing	-0-	5.1	16.6	15.5	21.7	37.2		
ISLAND C-55								
Volume	14.9	13.8	38.8	40.3				
Contributing	14.9	8.7	22.4	23.4	46.0	69.4	-5.0	-1.1
Noncontributing	-0-	5.1	16.4	16.9	21.5	38.4		
ISLAND D-55								
Volume	14.6	13.2	38.4	40.0				
Contributing	14.6	8.3	22.4	23.4	45.3	68.7	-6.4	-2.1
Noncontributing	-0-	4.9	16.0	16.6	20.9	37.5		

* All values x $10^6 m^3$

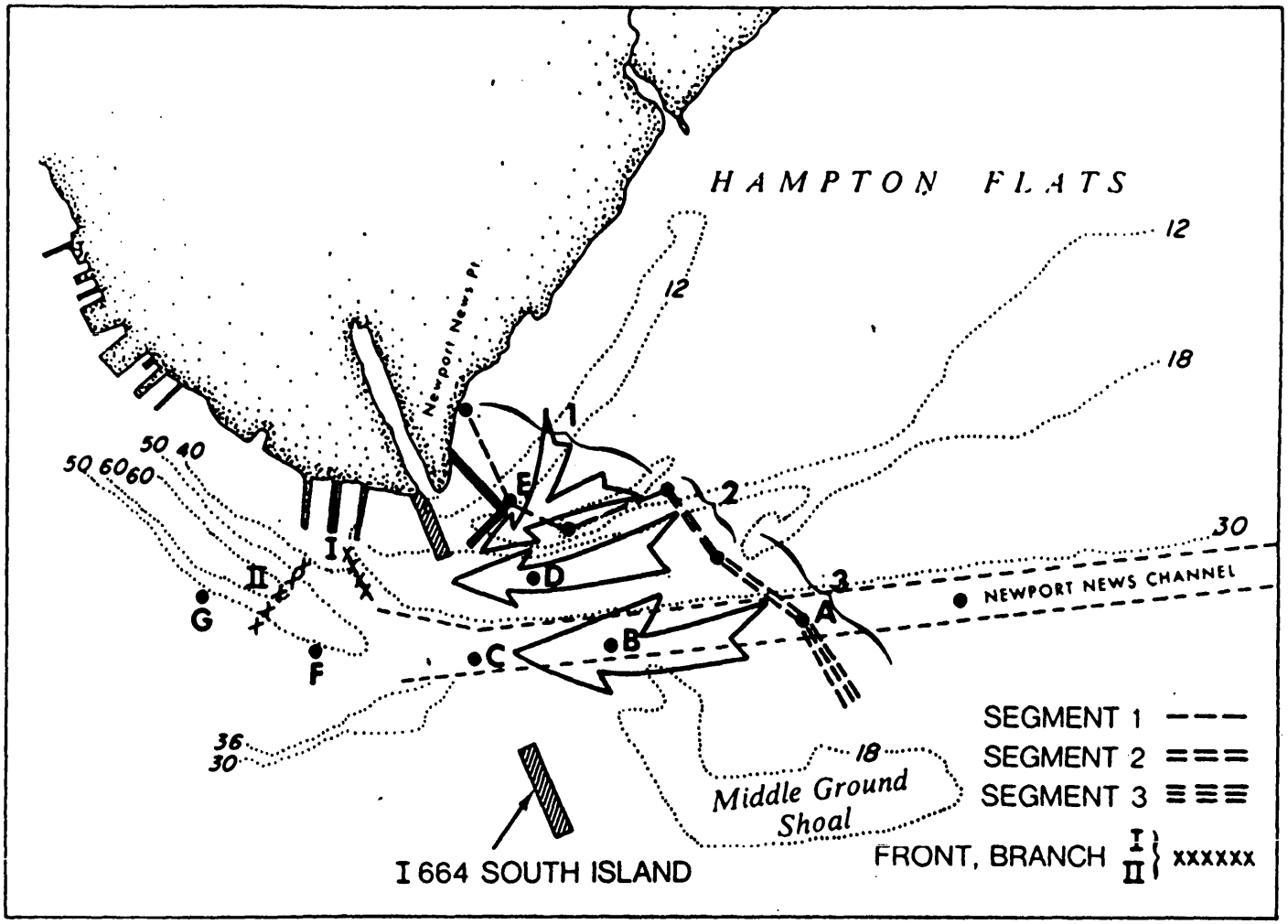

Figure IC-2. **Segments used in calculation of flux to the frontal system, 1664 and Island conditions.**

flow through the section containing Newport News Channel. The percent of flow reduction is summarized with respect to transport associated with I664 in place and the Newport News Channel depth at forty-five feet. The proposed island locations, Island A and Island B, result in reductions of 24.4 and 20.7 percent, respectively, of the total surface water flow (<4 m) participating in the frontal systems. The total flow transport is reduced by 14.5 and 12.0 percent respectively. Particularly noteworthy is the reduction of flow in Segment 1. That reduction represents the retardation of flow induced by the islands.

Due to the assumptions embodied in the application of the theory and the relative accuracy of a coarse grid numerical model, the stated reductions must be considered as rather gross estimates. However, the application of the procedures is internally consistent between the cases posed. Thus, there is a firm basis to argue that the effects on the transport system of the proposed locations for New Port Island would be pronounced.

3) The analyses conducted for the proposed location suggested that an island location further to the east may have less impact on the frontal transport system. Additional analyses were performed as a diagnostic test for two conditions. Island C and Island D (Figure IC-1a,b) represent areas of 370 acres and 323 acres respectively. The configurations were dictated by the grid layout of the numerical hydrodynamic model.

The results of Island C and D indicate a remarkable difference compared to the proposed locations (Islands A or B). The transport via Segment I is restored and the percent reduction of surface water transport is 5 and 6.4 percent, respectively, for Island C-55 and Island D-55. Moreover, the

values for reductions in total transport are very small, 1.1 and 2.1 respectively. The values associated with Islands C and D are considered to be within the resolution of the present analysis. Thus, these preliminary tests suggest that the effectiveness of the frontal transport system could be virtually maintained with an island location shifted to a more easterly position.

2. Sedimentation on Hampton Flats and Inferences Relating to Hard Clam Resources

a. Hampton Flats, an embayment of approximately 4,500 acres, is relatively shallow with depths generally less than twelve feet. Investigations conducted during the course of this study indicate that:

1) The surface sediments are fine to medium sand with silt/clay content ranging between 3 and 25 percent. Sources of sediment are limited to shore erosion and suspended solids advected over the flats by tidal currents. Limited measurements in past studies indicate that the normal suspended solids concentrations range between 5 to 10 milligrams per liter.

2) The surface sediments are exposed to hydrodynamic forces sufficient for entrainment. Limited field measurements and the results of the hydrodynamic model suggest that tidal currents associated with the mean tide range are sufficient to entrain the sediment sizes found. Benthic biological activity may tend to stabilize the surface.

b. Hampton Flats contains commercially important quantities of hard clams. Recruitment on Hampton Flats occurs in a dynamic environment. Sediment reworking and resuspension are sufficient to maintain a sandy substrate. Mechanisms for resuspension include scour due to tidal current

and waves, and probably resuspension of bottom materials due to clam harvesting. In order to estimate the changes in resuspension potential due to the various construction elements the hydrodynamic model results were used. The ratio of current induced bottom shear to the entrainment shear stress is taken as the representative index. These results indicate that:

1) The construction of I664 (channel depth at 45 or 55 feet) should result in an increase in deposition in the shallower waters of the northwest sector of Hampton Flats. This finding is consistent with those of studies conducted in the hydraulic model (VIMS, 1972 and 1979) and mathematical model simulations (Corps of Engineers, 1984).

2) Construction of New Port Island, Option A, would increase the area of expected deposition to at least the entire northwest sector of Hampton Flats. In large measure this is due to the dramatically reduced flow speeds expected in the passage between Island A and the mainland to the northwest. Most important, this configuration is likely to result in blanket mud deposits between the island and the mainland. This condition unsuitable for settlement and survival of clam larvae.

3) Construction of New Port Island, Option B, would also increase the area of expected deposition. However, there are important differences relative to the Option A configuration. Although Option B also results in a reduction of the tidal flux onto Hampton Flats (about 14 percent), the more eastward position results in appreciably larger flow speeds in the northwest passage between Island B and the mainland. Thus in the case of Island B the zone of enhanced sedimentation is shifted to a more central position on Hampton Flats. This zone is more susceptible to resuspension by wave-current interactions than is the western sector. Thus, the net sedimentation enhancement is expected to be less for Island B than

Island A configuration. However, the central zone of Hampton Flats is also the most productive in hard clam yield.

4) Tests with island location at positions C and D indicate significant differences relative to the proposed island locations (A and B). Of the four positions tested, location C results in the minimum perturbation to sedimentation potential on Hampton Flats. A nondepositional mode is predicted for the passage between this island location and the mainland. Moreover, the areal extent of deposition tendency due to I664 is reduced. Those limited areas predicted to have reduced tidal scour are susceptible to wave induced sediment resuspension.

Island location D, intermediate to C and B in position, is predicted to have sedimentation enhancement over a total area similar to Island B. However, the subareas with higher sedimentation potential are more exposed to wave driven resuspension.

5) The extent to which the altered sedimentation patterns would affect clam recruitment and/or clam production cannot be quantitatively predicted. However, the various construction elements may be ranked in terms of perturbations to the existing conditions. In order of increasing depositional tendency these are:

I664-45

I664-55

ISLAND-C

ISLAND-D

ISLAND-B

ISLAND-A

3. Benthic Resource Evaluation

The relative benthic resource value of the Hampton Flats system was determined from field investigation and the results from previous studies. Within the framework of necessary assumptions these data indicate that the bottom with high resource value occurs in water depths between 2 and 5 meters, moderate resource value at depths greater than 5 meters, and lower resource value in depths less than 2 meters. The area which would be covered by island construction represents a loss of about 9 percent of the bottom with high relative benthic resource value.

E. CONCLUSIONS

1. Impacts on the Larval Transport System

a. Due to Proposed Island Locations A and B. Application of front theory and the results of the two-dimensional hydrodynamic model, when combined with inferences from oyster larvae studies, indicate that the transport effectiveness of the frontal system would be markedly reduced by island construction in either of the locations (A or B) proposed.

No quantitative assessment can be made as to the extent to which the estimated reductions in frontal transport would impact the recruitment to the seed oyster beds. However, logical extension of the present findings leads to the conclusion that there would be a material probability of adverse impact on the seed oyster beds if New Port Island were constructed at either of the locations (A or B) proposed.

b. Due to Alternate Island Locations C and D. Preliminary testing for an island location shifted to a more easterly position suggests that the effectiveness of the frontal transport system could be virtually

maintained. Calculations indicate a transport reduction of a few percent, but these values are considered to be within the limitations of the present analysis. The tests conducted were for island areas of 370 acres (C) and 323 acres (D). Expansion of the area to 400 acres may modify the results.

2. Impacts on the Hampton Flats Hard Clam Habitat

The results do not permit a strictly quantitative assessment of the impact on the hard clam habitat due to modifications of the sedimentation patterns. Relative comparisons between cases can, however, be made.

Of the four island locations tested, the proposed locations, A and B, are projected to induce the more severe impacts. Configuration A is projected to cause the formation of blanket mud deposits in the area between the island and the mainland.

The preliminary tests performed for positions C and D indicate that C would have the least likelihood to cause deposition of fine grained sediments over a large area. Configuration D would induce an areal pattern of potential deposition comparable to configuration B. However, the degree of fine grained sediment deposition would be less than configuration B.

3. Combined Impact

Island construction at either of the locations proposed (A or B) would present a material probability of adverse impact on the seed oyster beds. Moreover, construction at locations A or B is projected to cause the largest adverse impact on the hard clam habitat on Hampton Flats.

Of the four island locations considered in this study the 370 acre island at location C is projected to have minimum combined impact.

F. Recommendations

This study has provided a basis for estimating the impacts of the proposed New Port Island construction on the lower James River seed oyster beds and on potential sedimentation at hampton Flats. However, there are a number of refinements which would provide better estimates:

1. Application of a Three-Dimensional Hydrodynamic Model to the Frontal Transport System

Evaluation of potential impacts on the effectiveness of the frontal transport system was accomplished by integrating the results of two-dimensional theory of fronts with those of a vertically integrated numerical hydrodynamic model for predictions of changes in the horizontal flow field due to construction. The numerical model did not include salt transport.

Application of an appropriate three-dimensional hydrodynamic model with salt transport would yield very useful results if frontal phenomena are successfully simulated. Superior estimates of the transport capability of the front system and changes due to construction would be provided.

The Virginia Institute of Marine Science (VIMS)has recently contracted to acquire a state-of-the-art three-dimensional model for initial applications to the lower James River-Hampton Roads system. Investigation of the frontal phenomena near Newport News Point is planned during the 1988-1989 time period.

2. Application of a Hydrodynamic and Sediment Transport Model to Further Investigate Sedimentation Trends on Hampton Flats

In the present study the potential impacts on Hampton Flats due to sedimentation were gauged by evaluating the extent to which the entrainment (or resuspension) potential would be reduced. This procedure permitted a

qualitative assessment of impacts wherein the relative difference between cases could be portrayed. The procedure does not formally simulate transport of sediments and calculation of the depth of deposition or scour. Application of a formal sediment transport model coupled with a time varying hydrodynamic model would enable determination of at least semi-quantitative estimates of deposition rates. This could be achieved using either a vertically integrated hydrodynamic sediment transport model or a fully three-dimensional model. The three-dimensional model being acquired by VIMS will have the required capability and such application is planned in 1989-1990.

3. Further Evaluation of Alternate Island Locations

Preliminary results for two alternate island locations have been discussed. These findings suggest that the transport effectiveness of the frontal system is virtually maintained for island locations placed further to the east on Hampton Flats (locations D and C). The tests conducted were for island areas of 370 acres (C) and 323 acres (D), sizes dictated by the model grid. Further study with a more refined grid would be required to test for an optimum 400 acre site. The results to date suggest that the optimum location would likely be in the vicinity of site C.

4. Evaluation of the Influence Island Shape

The tests conducted of four island locations clearly demonstrate that proximity of island location to Newport News Point is a dominant influence in controlling flood current transport to one segment of the frontal system. As noted in Figures IB-2a,b and IC-1a,b the island shapes are roughly rectangular. The boundary conditions of the numerical hydrodynamic model require assignment of a small depth (1 meter) at the island boundaries. Some flow in the model does cross the corners. In effect, this rounds off the corners of the flat, blunt face.

Investigation of island shapes significantly departing from the geometry tested (i.e. an ellipse, or a wedge) would require a much finer grid. Use of a fine grid would also reduce the flow crossing the boundary of the island.

II. BACKGROUND

A. Hydrography of the Lower James-Hampton Roads and Interaction with Seed Oyster Beds

1. Hydrography

a. Description. The James River is the southernmost of the major tributaries to Chesapeake Bay. Along its 530 km (330 mile) course from where it is formed by the confluence of the Jackson and Cowpasture rivers in Botetourt County to Old Point Comfort at its mouth, the James drains about 25% of the surface area of the Commonwealth (26,000 km^2 or 10,000 mi^2). Approximately 30% of its length (the 160 km segment seaward of Richmond) is tidal and over 35% of this (60 km) is estuarine (Figure IIA-1). The central half of the estuarine portion of the James contains some of the most productive seed oyster beds in the world. These beds (Figure IIA-2) cover an area of 25,000 acres, of which 16,150 acres have been determined to be highly or moderately productive (Haven and Whitcomb, 1983).

1) Basin geometry. The isobaths (depth contours) in Figure IIA-2 give an indication of the configuration of the estuary's basin. In general, the basin is on the order of 7 km wide from its mouth at Old Point Comfort to a constricted region at Mulberry Point, just upstream of the broader (10 km wide) region of Burwell Bay. The remaining portion of the estuary, from Mulberry Point to Jamestown Island (at the upper left of Figure IIA-2) is from 4 to 6 km wide. Average depths are on the order of 3-4 m with deeper natural channels (up to 25 to 30 m) off Old Point Comfort, Newport News Point and just upstream of Mulberry Point. These natural channels have been interconnected with dredged navigation channels.

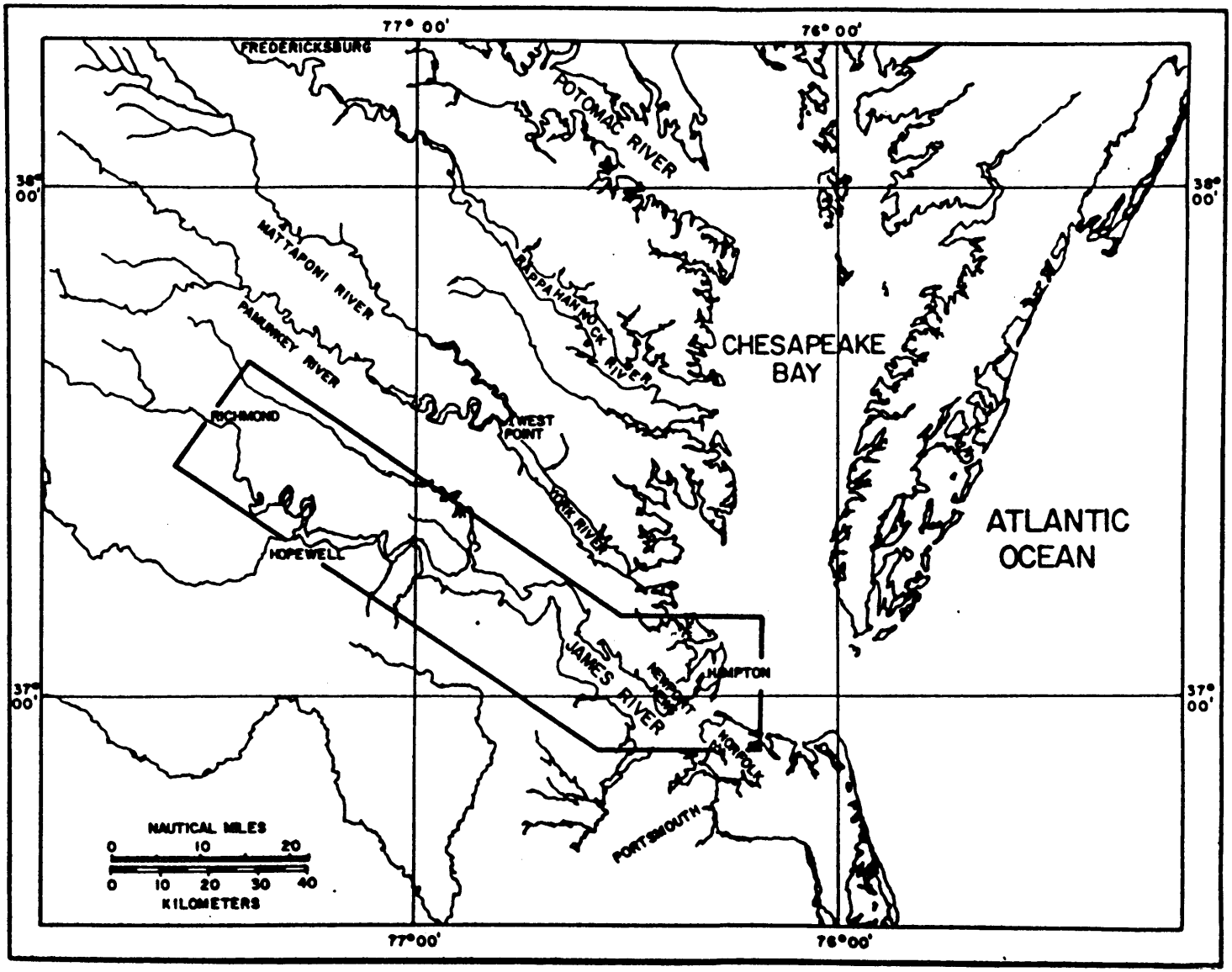

Figure IIA-1. The James River and its major tributaries.

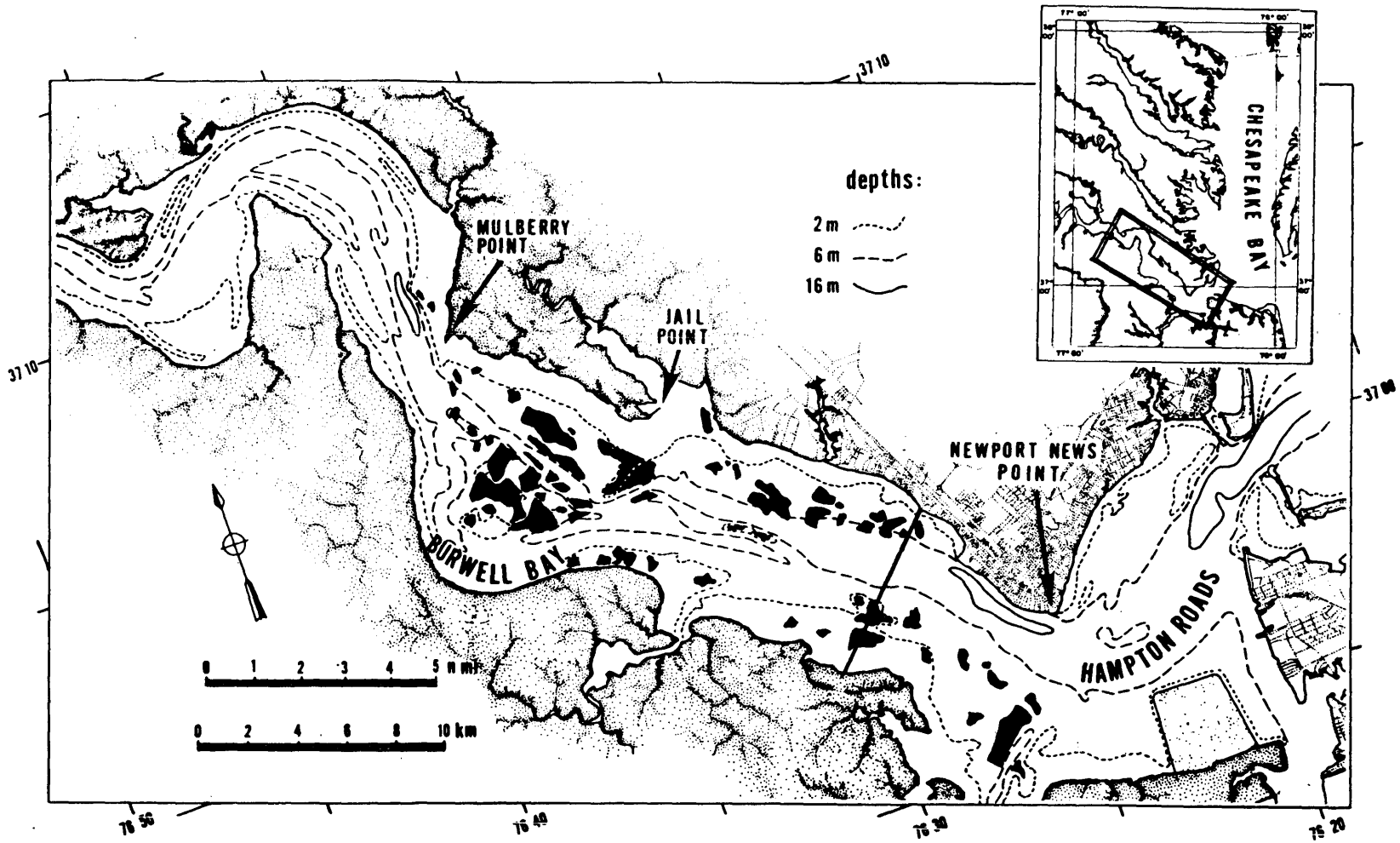

Figure IIA-2. The James River Estuary from Old Point Comfort, at the mouth, to Jamestown Island (upper left corner). Seed oyster beds are shown as irregularly shaped darkened areas.

2) Estuarine circulation and salinity distribution. Pritchard (1967) defined an estuary as "a semi-enclosed coastal body of water which has a free connection with the open sea and within which sea water is measurably diluted with fresh water derived from land drainage." The Chesapeake Bay estuarine system was formed by the drowning of a cascading series of river valleys, the most seaward of which was the James. Estuaries thus formed are called coastal plain estuaries and the distribution of salt and currents within them covers a spectrum of conditions or estuarine types depending on the balance achieved between the various forces that drive or retard mixing and water motion. The primary forcing functions are: gravitational circulation which is dependent on freshwater discharge; tidal mixing which depends on the tide range and basin configuration; and Coriolis force which is an artifact of the earth's rotation coupled with fluid motion.

Gravitational circulation and tidal mixing can be illustrated by an example. Consider a long trough, closed at one end, which is slightly tilted upwards, a partitioning wall midway along its length, and a large basin at the downstream end. The large basin is filled with dense salt water that occupies the portion of the trough downstream from the barrier and the closed portion of the trough is filled with lighter, fresh water. Removal of the partitioning wall would result in an exchange of fresh and salt water within the trough such that the salt water would encroach upstream under the lighter fresh water and the fresh water would slide downstream over the salt water. If, now, a large discharge of fresh water is imposed at the closed end of the trough, the intruding salt water will be forced downstream and take a wedge shape. Friction between the fresh and salt water layers will cause upward mixing of the salt water which, in turn,

will be transported downstream in the surface layer and increase its salinity in that direction. Reduction of the freshwater discharge would permit upstream encroachment of the salt wedge while an increase in freshwater discharge would have the opposite effect. Thus, depending on the strength of the discharge and the amount of mixing between the fresh and salt water, various "balance" positions of the salt wedge can be achieved along the channel. Within the salt wedge, there will be a slow upstream transport of water to replace that which is mixed upward and removed by the fresh water. The salinity in the salt wedge will remain constant while that in the downstream flowing surface water will increase towards the mouth. This type of circulation, wherein gravity forces the fresh water downstream at the surface and the saltier water upstream at the bottom, is called **gravitational** circulation. It exists to some degree in all estuaries provided some freshwater discharge is present. An estuary where gravitational circulation is the dominant driving force is called a **salt wedge estuary**.

A slow, vertical oscillation of the surface of the salt water reservoir (tides) will result in wave-type motion progressing up the trough. This tidal oscillation will tend to increase mixing between the salt and freshwater layers and reduce the effectiveness of the gravitational circulation. Increased mixing due to tides will result in the transport of larger volumes of salt water into the upper layers, thus increasing the overall volume of discharge in this layer and also increasing the volume of replacement salt water entering the trough from the basin in any given period of time. Additionally, there will be some downward mixing of fresh water into the salt water layer. Once again, a balance will be reached between the gravitational circulation induced by freshwater discharge and the mixing

resulting from the tides. If freshwater discharge is held constant, this new balance will involve upstream transport of a larger volume of salt water in the lower layers, and downstream transport of a larger volume of the salt-fresh mixture in the upper layers. These larger volume transports will be affected by the earth's rotation and tend to be pushed to the right of their (tidally averaged) directions of motion. The sides of the trough constrain this lateral motion with the result that there will be a lateral tilt to the now less distinct freshwater-saltwater interface. The tilt of the interface will be upwards on the right side of the trough looking upstream. Tides will induce an oscillating upstream-downstream motion along the axis of the trough but the vertical and cross stream effects of gravitational circulation and tidal mixing will result in stronger and longer downstream motion in the fresher portion of any given cross section. When averaged over a series of tidal cycles, there will be a net downstream flow of fresher surface water and a net upstream flow of saltier bottom water, with a tilted intermediate region of no net motion. This intermediate region will be in the vicinity of the maximium change of salinity with depth (the halocline). Along the axis of the trough, salinities will increase with depth as well as in the downstream direction at any given depth. A coastal plain estuary exhibiting these salinity and circulation characteristics is called a **partially mixed estuary**. Pritchard (1985) has identified two subclasses of partially mixed estuaries: **strong** and **weak**. In a strong partially mixed estuary, the laterally tilted level of no net motion and halocline are always found below the water surface, hence the net motion of surface water is downstream everywhere. In a weak partially mixed estuary, these tilted interfaces intersect the water surface and, at some locations (usually on the right side looking upstream) net motion of surface water is

upstream and these surface waters have salinities more closely related to those of the bottom water.

An additional reduction in freshwater discharge and/or increase in tidal mixing will shift the balance between gravitational circulation and tidal mixing to where tidal mixing overwhelms the gravitational circulation. In this case, the balance achieved results in predominance of tidally averaged upstream movement of saltier water on the right hand side of the trough (looking upstream) and downstream movement of fresher water on the left hand side. At any location, there is little or no change in salinity from the water surface to the bottom and salinity increases in the downstream direction as well as from left to right at any cross section (when looking upstream). The region of no net motion and the region of maximum salinity gradient are both vertical while net upstream transport on the right and downstream transport on the left greatly exceed freshwater discharge over any series of tidal cycles. An estuary exhibiting these characteristics is called a **vertically homogenous estuary.**

In order to have the model estuary trough conform to the James River, the basin configuration must first be changed. There is a general linear decrease in cross sectional area of the estuarine portion of the James (Old Point Comfort to Jamestown Island - the seaward 60 km of the river) from approximately $4x10^4 m^2$ at the mouth to $10^4 m^2$ near Jamestown (see Figure IIA-3,a). Similar generally linear reductions are evident in average width and surface area (Figures IIA-3,b; IIA-3,c) which vary from approximately 8 to 3 km and approximately 15x106 to $6x10^6 m^2$ respectively in this 60 km reach. Notable exceptions to these general trends are the broad regions of Hampton Roads, Burwell Bay and Cobham Bay downstream from Jamestown Island (compare Figures IIA-3,a,b,c with Figure IIA-2). In these regions, average water

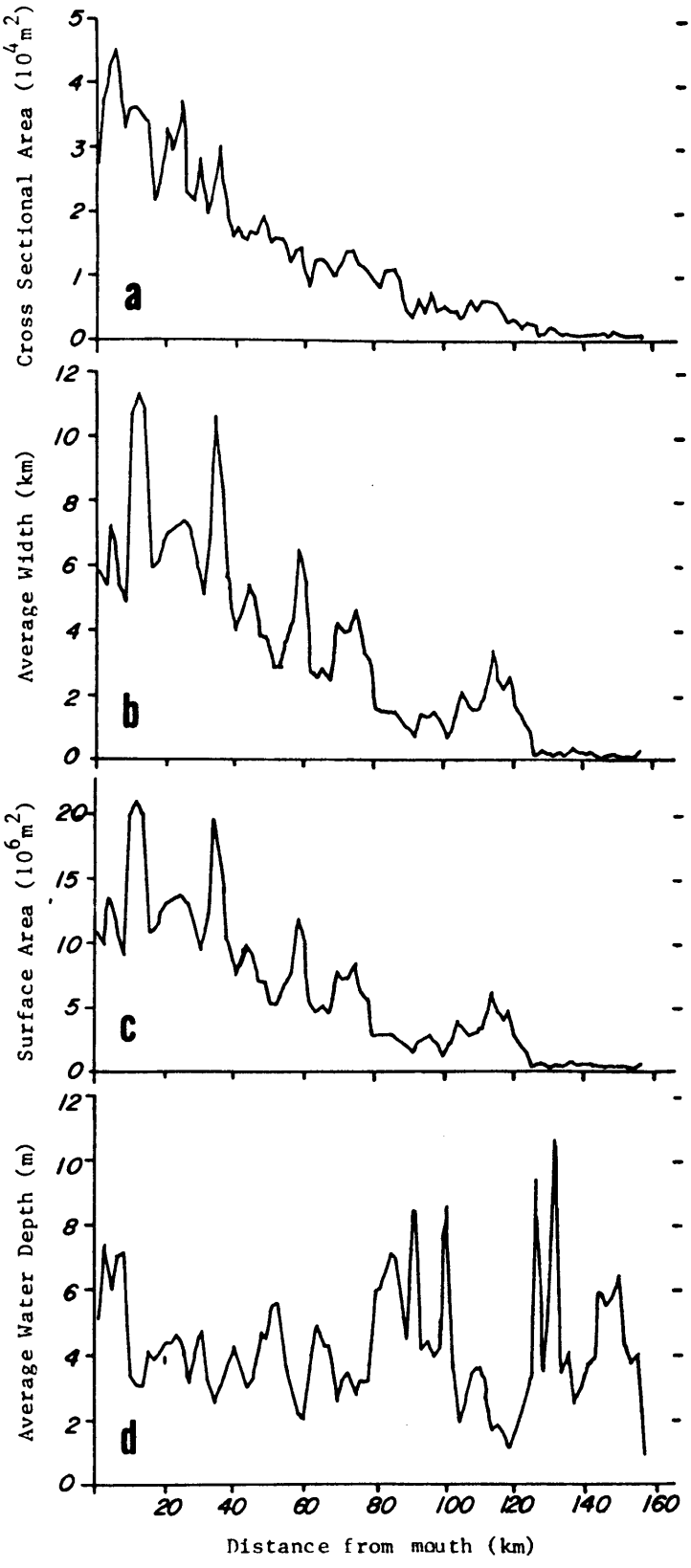

Figure IIA-3. Variations in geometry of the James River Estuary as a function of distance upstream: a)Cross sectional area; b)Average width; c)Surface area; and d)Average cross sectional depth.

depths tend to be less than the 4 m of longitudinally adjacent portions of the estuary (Figure IIA-3,d). In general, the trough would have to be broad with extensive shoals flanking a more or less central, deeper channel. Finally, the trough must be bent and twisted to conform to the changes in basin direction shown in Figure IIA-2.

The tide in the James River has mean and spring ranges of .76 and .90 m at Old Point Comfort, .79 and .94 m at Newport News Point, .73 and .88 m in Burwell Bay and .61 and .73 m at Jamestown Island. Assuming similar differences between mean and neap tides, tidal variations along the estuary are shown in Table IIA-1.

TABLE IIA-1

Tidal Variations Along the Estuarine Portion of the James River

	Tide Range (m)		
Location	Spring	Mean	Neap
Old Point Comfort	0.90	0.76	0.62
Newport News Point	0.94	0.79	0.64
Burwell Bay	0.88	0.73	0.58
Jamestown Island	0.73	0.61	0.49

With shoal depths on the order of 3 to 4 m, spring tide ranges would result in an 18 to 30% change in water level while, during neap tides, these changes would be from 12 to 21% of shoal water depths. Differences in tidal range result in variations in tidal mixing and a shift in the balance between gravitational circulation and tidal mixing during the fortnightly neap-spring cycling of tides. The balance would also change on a seasonal

basis in response to variations in freshwater discharge into the James (Figure IIA-4).

Basin configuration, coupled with variations in tide range and freshwater discharge yield circulation patterns and salinity distributions in the James that vary from those of a strong partially mixed to a vertically homogeneous estuary. These patterns tend to follow the seasonal variation in freshwater discharge with strong partially mixed conditions found in the "wet" months of February, March and April while the tendency towards weak partially mixed or even vertically homogeneous conditions are found in the "dry" months of August, September and October. Fortnightly variations in tidal mixing modify these seasonal patterns to produce variations in stratification which increases shortly after neap tides and decreases after spring tides. Additionally, the variations in freshwater discharge will result in longitudinal shifts in salinity patterns. This is particularly noticeable during periods of extreme drought (as in the summer of 1980) and after severe flooding (as from Tropical Storm Agnes in 1972). This is evident in Table IIA-2 which gives average and extreme surface and bottom salinities at 10 km incremental distances between the mouth of the James and the Burwell Bay region for the period 1971-1980 (Brooks and Fang, 1983).

TABLE IIA-2

Surface and Bottom Mean and Extreme Salinities (^{o}/oo) in the James River Estuary at Various Distances From the Mouth

		Distance from mouth (km)			
		0	10	20	30
Surface	Min	8.0	4.3	1.8	0.0
	Mean	17.6	15.8	12.7	8.3
	Max	25.0	24.2	23.8	22.0
Bottom	Min	17.5	13.0	8.4	2.0
	Mean	24.0	19.3	17.6	12.6
	Max	32.2	27.0	24.4	24.2

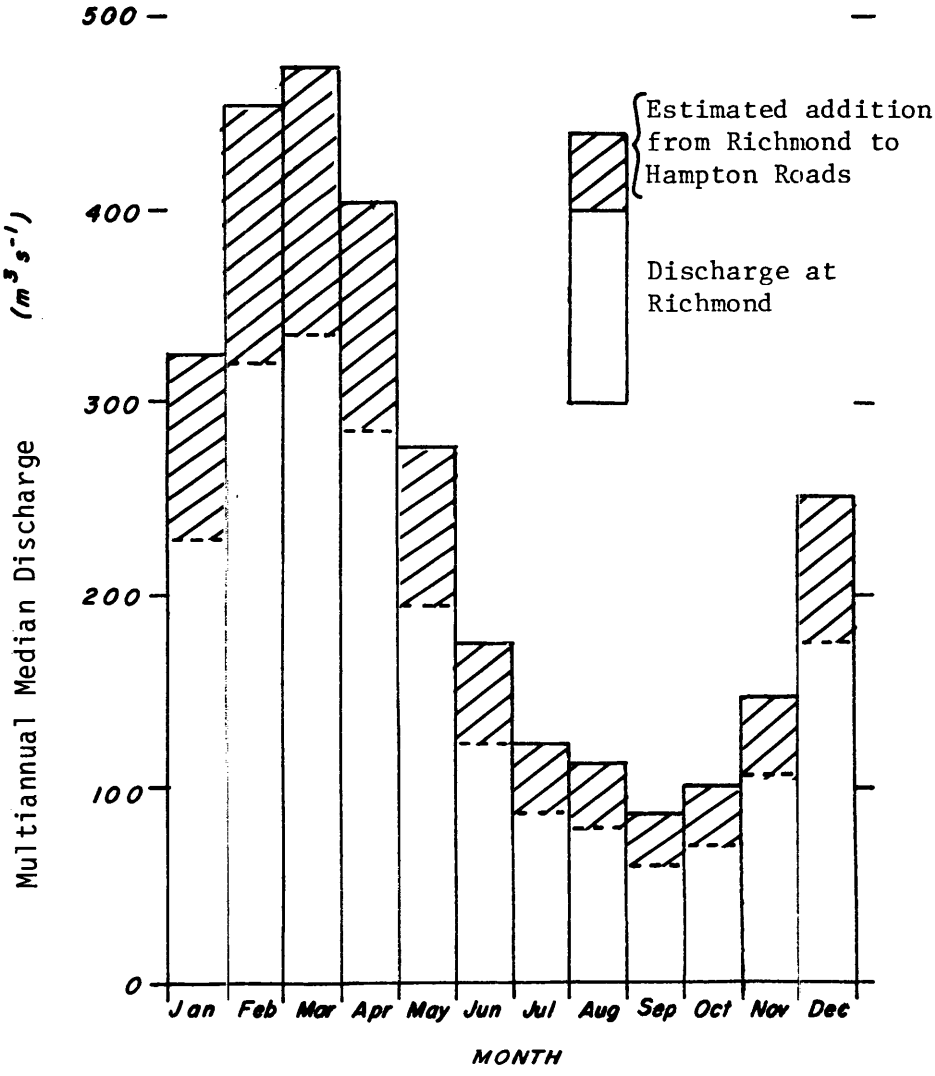

Figure IIA-4. Estimated monthly median discharge of fresh water into the James River based on records from 1925 to 1975 taken at Cartersville, Va. and corrected to include total drainage basin (to Hampton Roads).

b. James River Estuary Horizontal Circulation. Circulation patterns in the James River Estuary were examined by analysis of a series of hydraulic model dye experiments conducted at the Corps of Engineers Waterways Experiment Station in Vicksburg, Mississippi in 1968. The experiments are described in Appendix IA and were initially reported by Ruzecki and Moncure (1969) with a subsequent re-examination of results by Ruzecki and Hargis (1985). The primary purpose of the experiments was to determine the optimum location for placement of disease resistant oysters to produce maximum spatfall over seed oyster beds.

In the experiments, dye was released at six locations in the model and periodically sampled at 108 multilevel stations for the period covering 20-40 tidal cycles (10 -20 days) after release. Dye injection and sampling locations are shown in Figure IIA-5. To match late summer "dry" conditions that exist during the oyster spawning period, freshwater discharge into the model was held constant at the equivalent of 118 m^3s^{-1}, ocean salinities were maintained at 26 $^o/oo$ and a mean tide was generated in the ocean portion of the model for the duration of the experiments.

As a portion of the results of their analysis, Ruzecki and Hargis (1985) showed temporal variations in total dye per square meter of model bottom found in the upper 6 cm (6 m prototype) at slack water before flood (SBF) and slack water before ebb (SBE) over six seed oyster bed regions resulting from the six dye injections. These values were taken to represent a relative measure of possible spatfall in each sampling area. Their results are reproduced here as Figure IIA-6 which shows the sampling regions of interest (Point of Shoals, Wreck Shoal region, Brown Shoal Reach, White Shoal, Naseway Shoal and Nansemond Ridge region). Vertical panels show variations of dye at SBF (dashed lines) and SBE (solid lines) from each

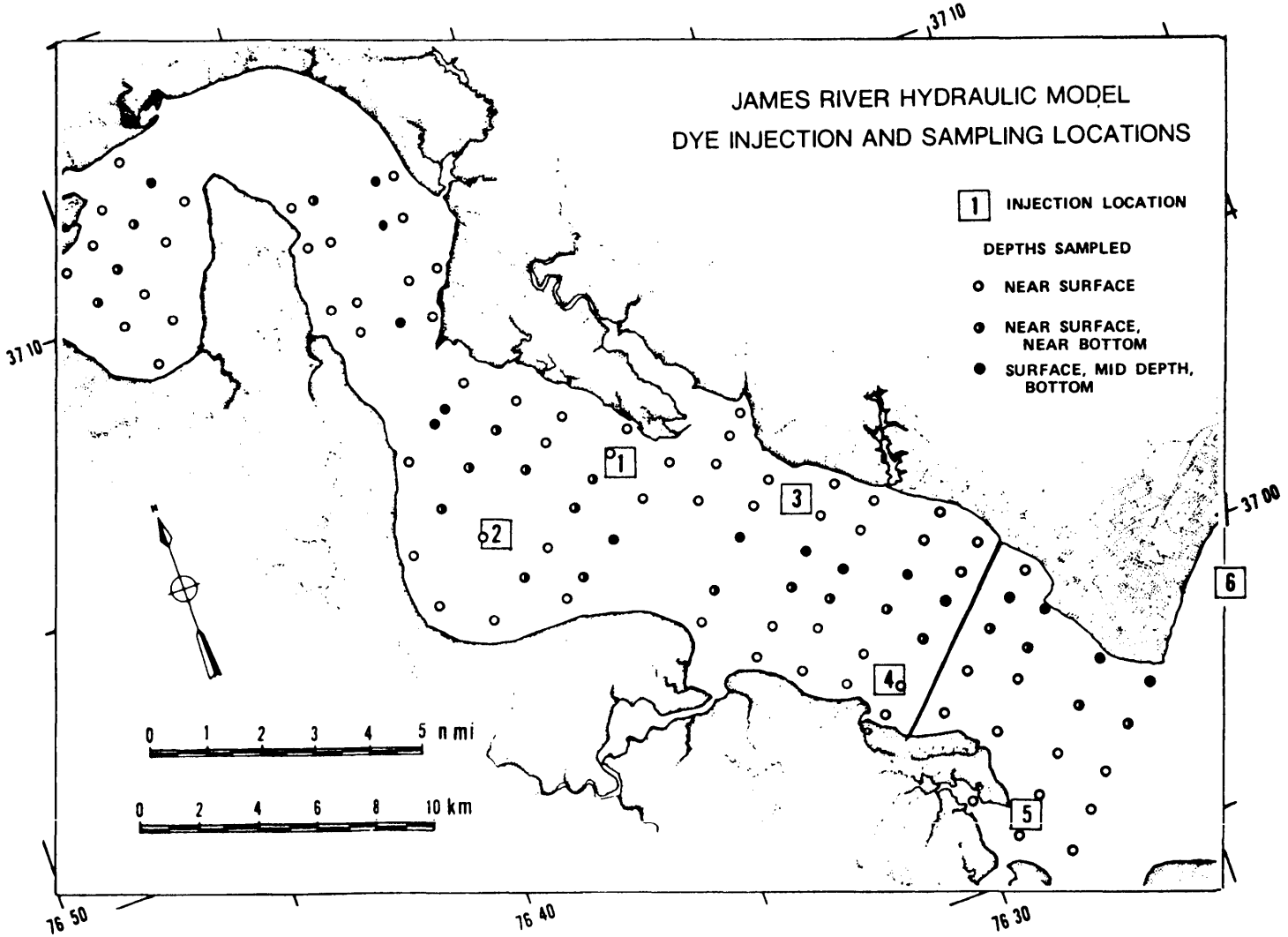

Figure IIA-5. Dye injection and sampling locations in a portion of the James River Hydraulic model. (After Ruzecki and Hargis, 1985).

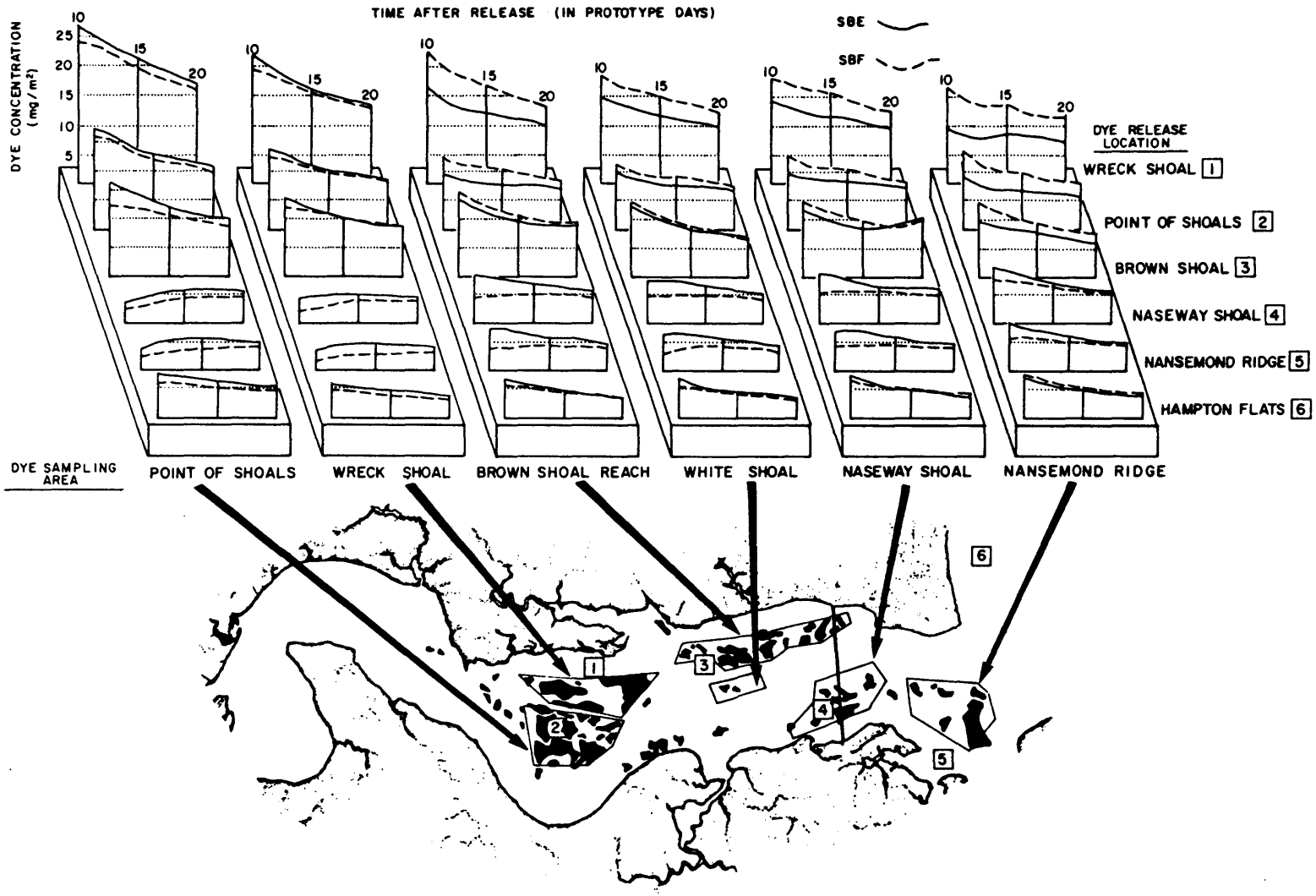

Figure IIA-6. Lower portion: Dye injection locations and oyster rock regions of interest. Upper portion: Temporal variation of dye concentrations at SBF and SBE in six sampling regions resulting from six dye injections. (After Ruzecki and Hargis, 1985).

release location (identified to the right) as measured in each sampling region (indicated by horizontal blocks). When comparing SBF and SBE values on each panel, higher concentrations at SBF indicate that greater quantities of dye in the surface layer were upstream from the sampling region during a particular tidal cycle. Conversely, higher SBE values indicate greater quantities of dye downstream, and, when SBF and SBE values were equal, the maximum surface layer quantities were in the vicinity of the sampling region.

Surface dye concentrations (which, because of sampling depths, give a measure of integrated dye concentrations in the upper 3 m (prototype) of the water column) were plotted for each SBF and SBE sampling period after the dye injection at Wreck Shoal (location 1 in Figure IIA-5). Plots of the dye centroid, shown in Figure IIA-7, show movement of dye across Burwell Bay and downstream along the southern shore of the model. By SBF cycle 32 (16 days after release) the dye centroid had extended to near the mouth of the Nansemond River and remained there three slack waters later (SBE-34). This gives an estimate of the time the bulk of material released at Wreck Shoal would take to move, by diffusive and advective processes, through the upstream cyclonic segment of circulation.

The upriver progression of dye from injection locations on Hampton Flats (Location 6) and near the mouth of the Nansemond River (Location 5) is illustrated in Figures IIA-8a,b and IIA-9a,b which show isopleths of dye concentration along the main channel. Subfigures a of these figures show dye distribution (in parts per billion) at local SBF and subfigures b show distributions at SBE. The latter show vertically homogeneous conditions off Newport News Point (right edge of each panel) with an indication of greater bottom upstream movement along the section 5-10 km (prototype) upstream from

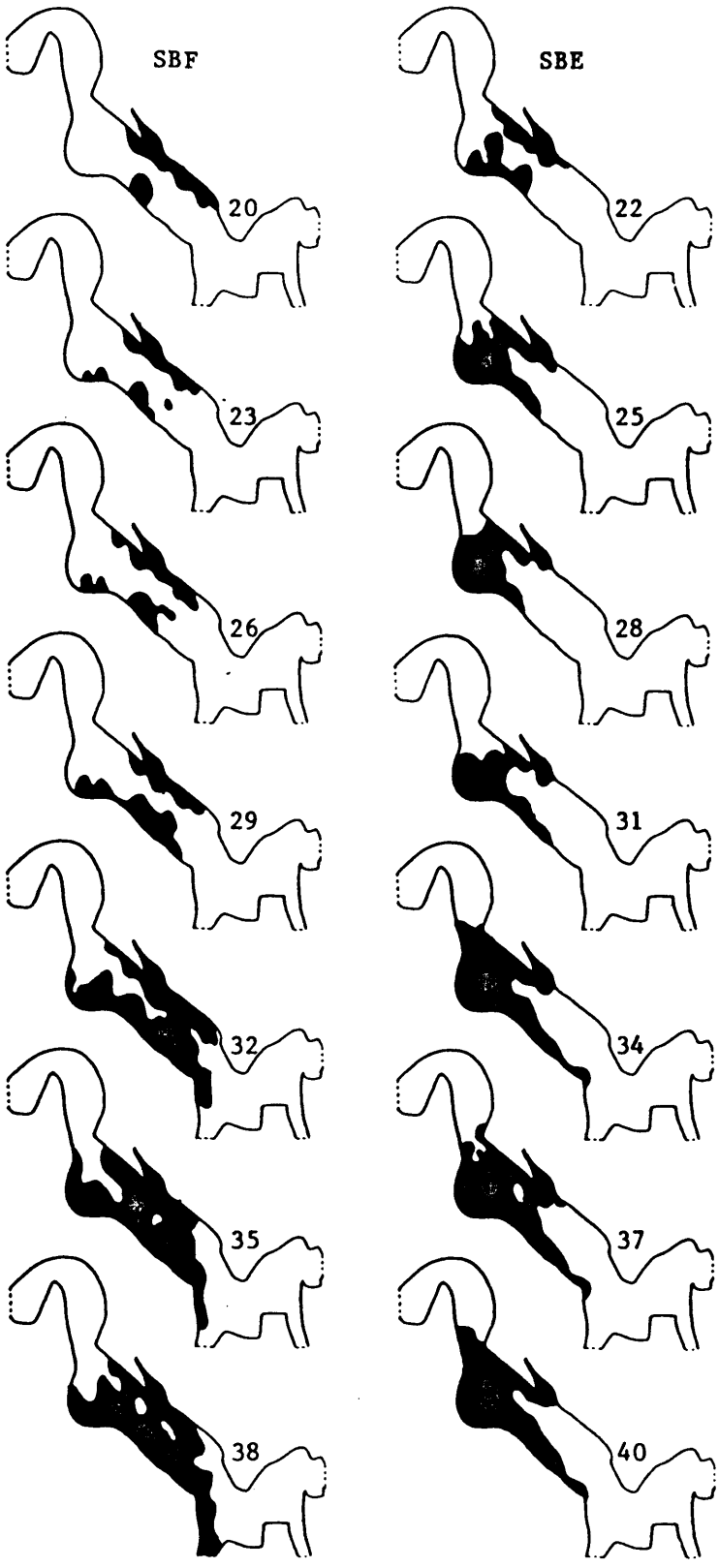

Figure IIA-7. Centroid of dye resulting from injection at Wreck Shoal (1 in Figure IIA-5) at each slack water sampling. Number in Newport News Point region of each subfigure indicates tidal cycles after dye injection.

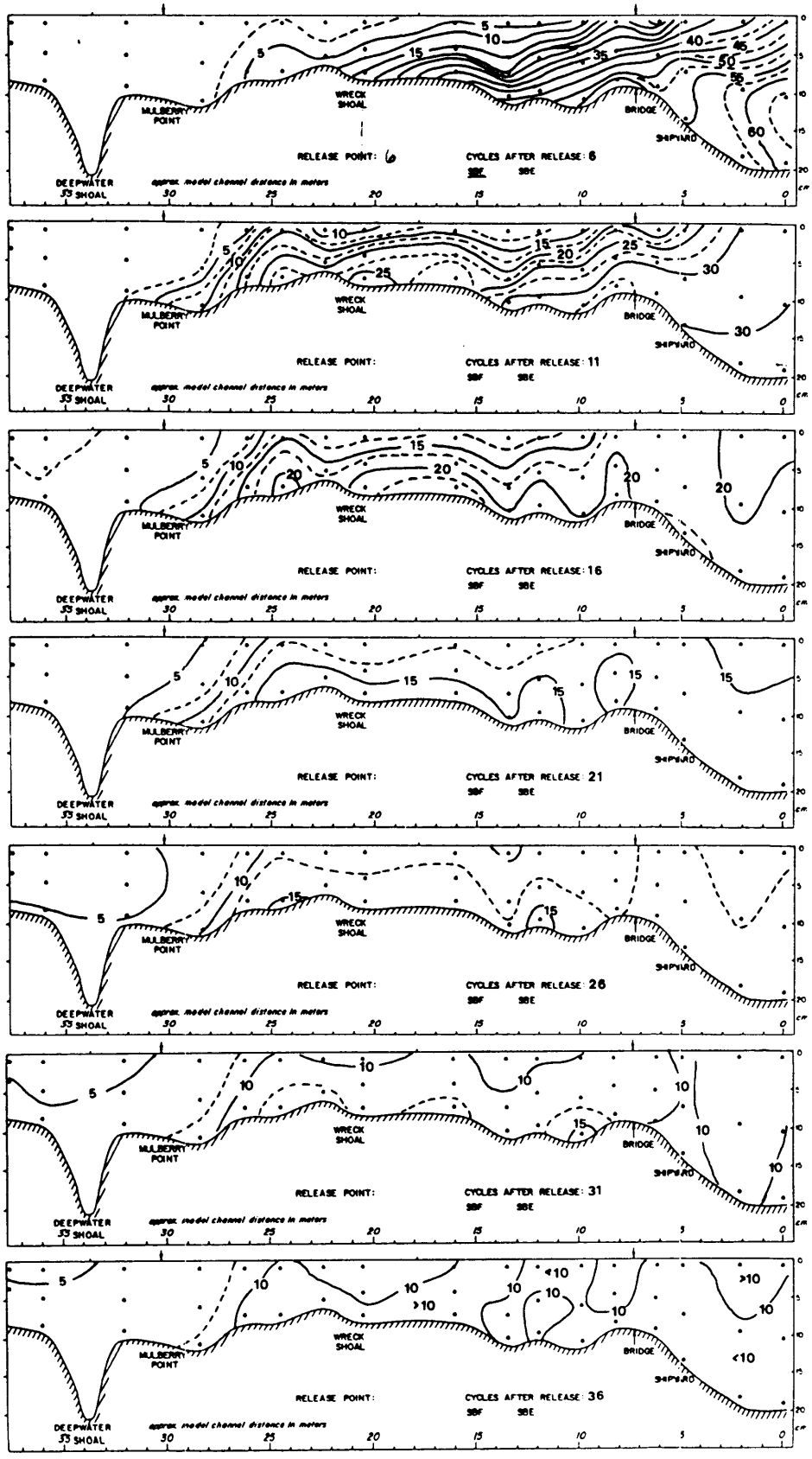

Figure IIA-8a. SBF dye concentrations (ppb) along the axis of the James resulting from injection at Hampton Flats (6 in Figure IIA-5).

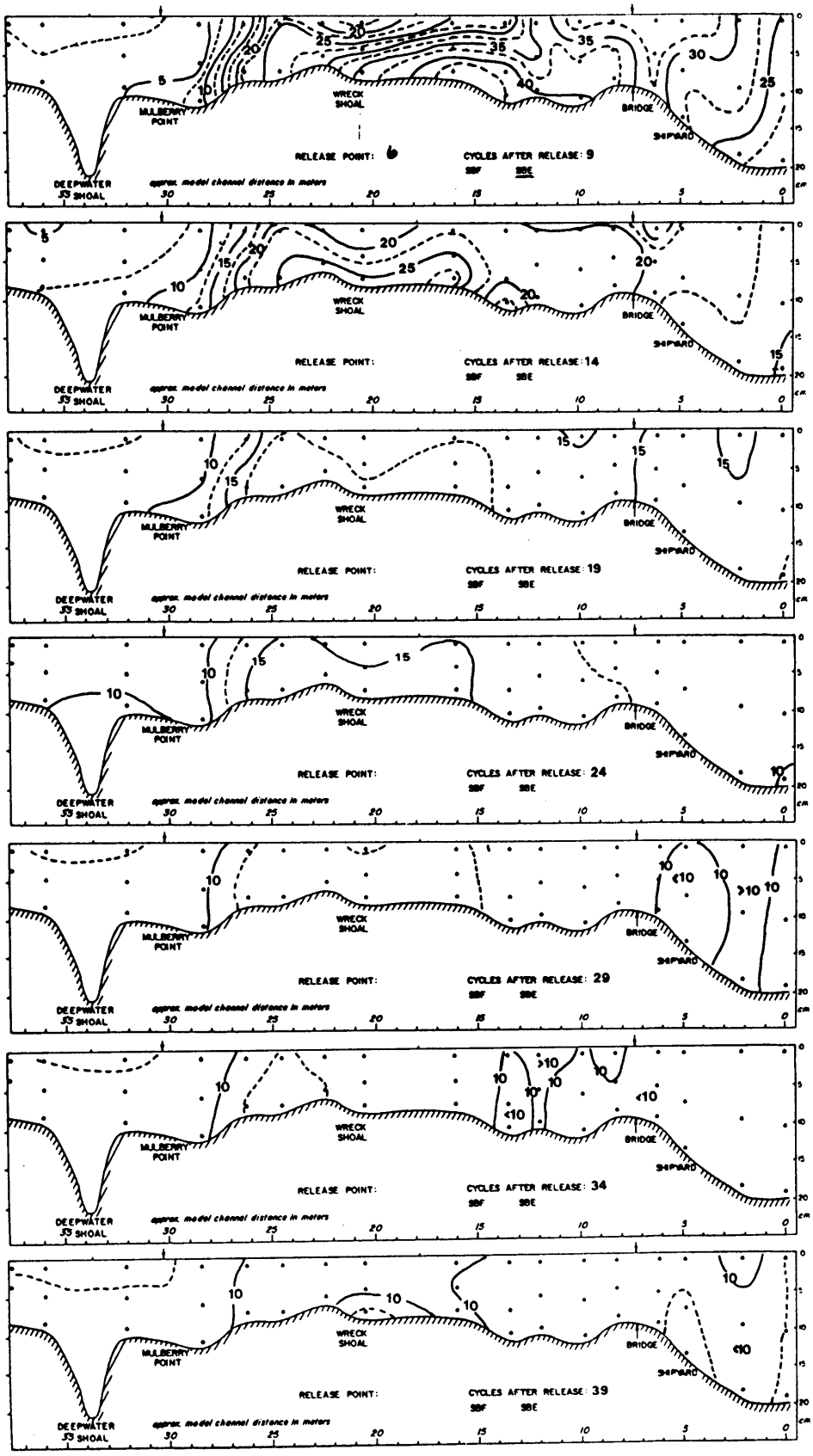

Figure IIA-8b SBE dye concentrations (ppb) along the axis of the James resulting from injection at Hampton Flats (6 in Figure IIA-5).

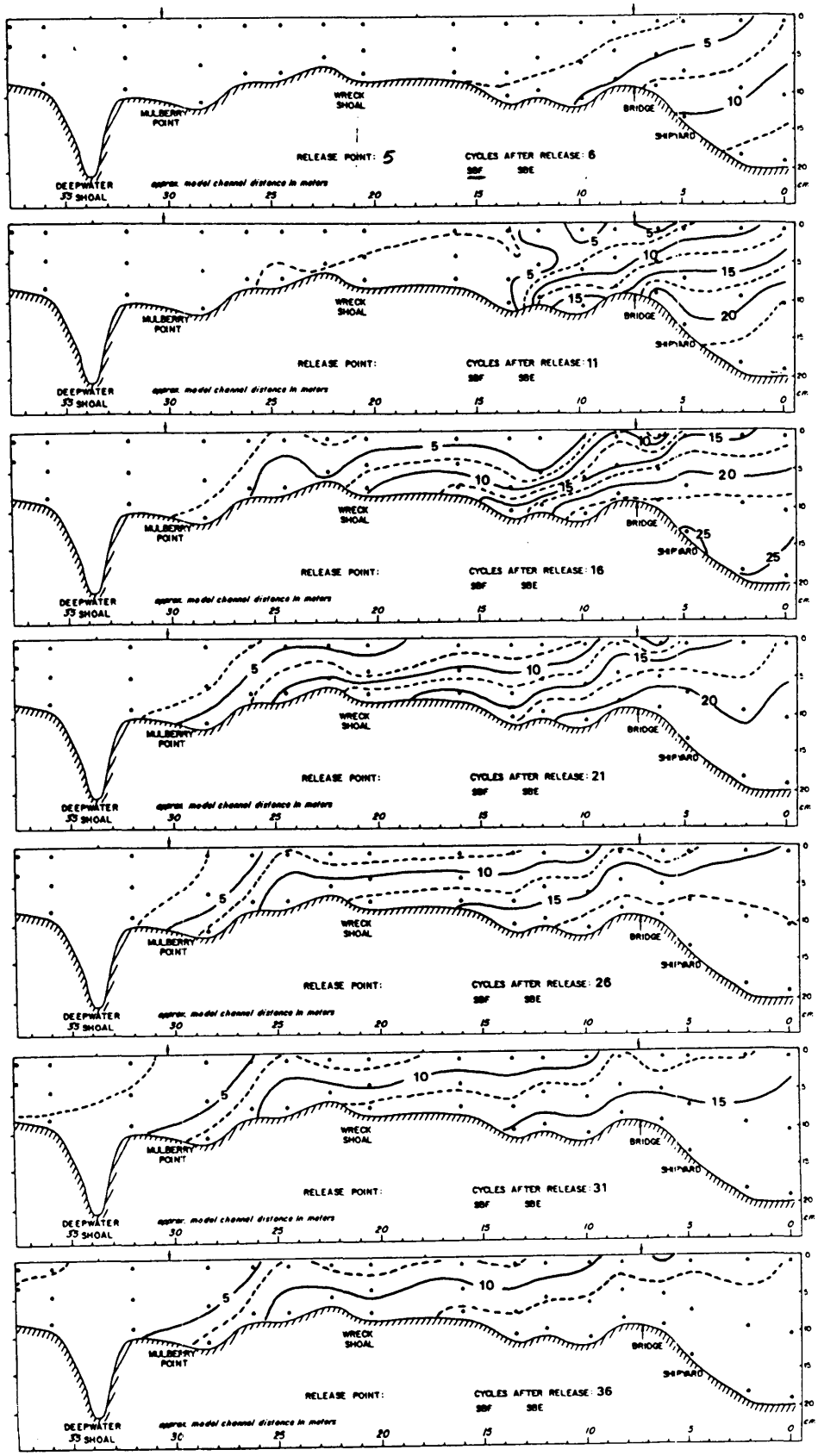

Figure IIA-9a SBF dye concentrations (ppb) along the axis of the James resulting from injection near the mouth of the Nansemond River (5 in Figure IIA-5).

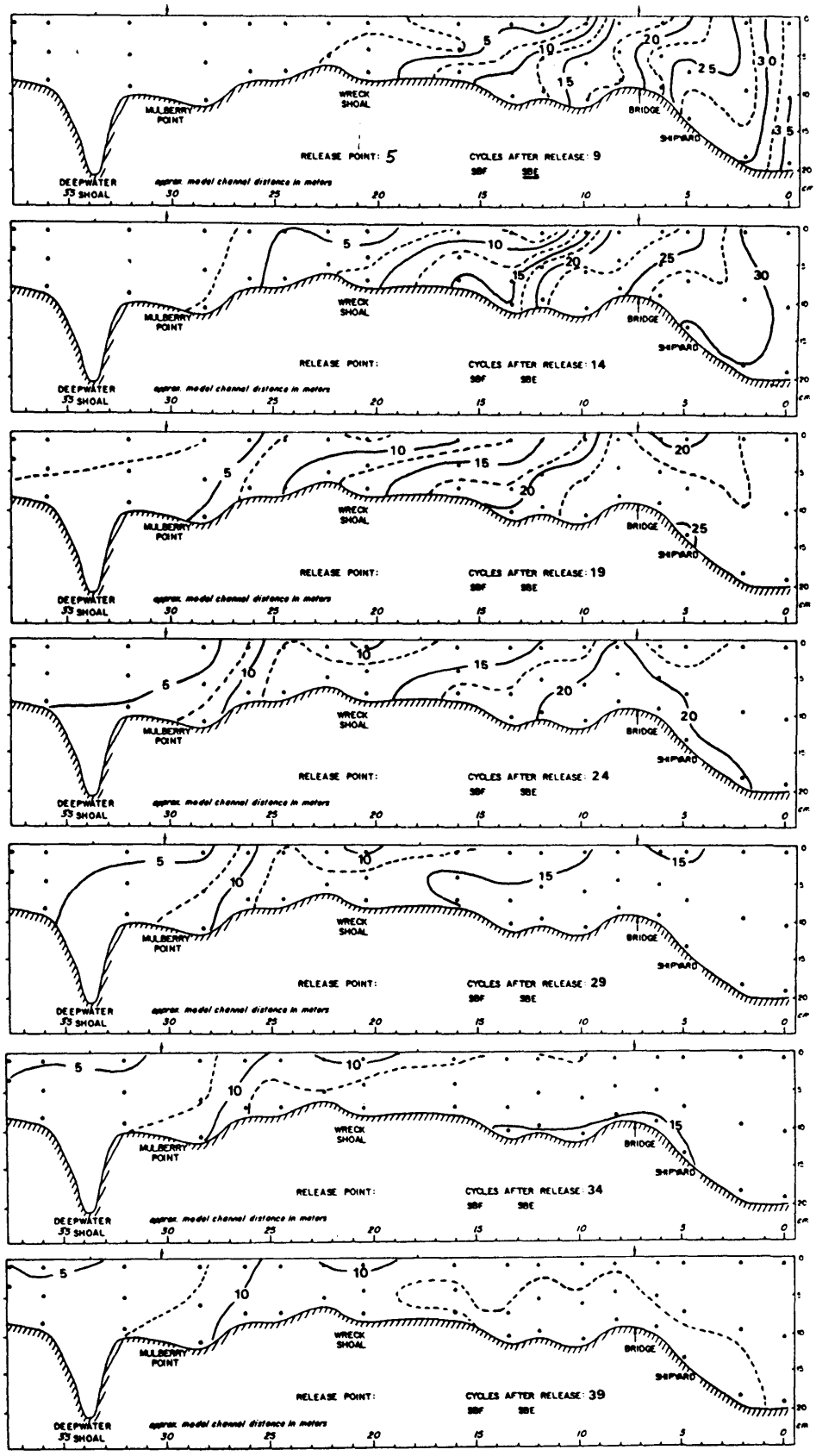

Figure IIA-9b SBE dye concentrations (ppb) along the axis of the James resulting from injection near the mouth of the Nansemond River (5 in Figure IIA-5).

this location. In general, vertical distributions at the end of flood tide are more uniform than those at the end of ebb tide (SBF - Subfigures, a) indicating the stronger downstream motion of surface waters. When averaged over individual tidal cycles, these distributions indicate a net upstream intrusion of dye at all levels but primarily along the bottom of the estuary. The constriction at Mulberry Point (Figure IIA-2) imposes a geometric barrier to dye transport upstream of this location. Dye released at locations near the mouth of the Nansemond moved upstream along the channel on the opposite side of the river suggesting south to north cross stream transport in the (unsampled) Hampton Roads region. Comparison of Figures IIA-8a and IIA-9a suggests a 10 tidal cycle (5 day) difference between similar along-channel distributions of dye released on Hampton Flats and off the mouth of the Nansemond. Temporal variations of dye distributions resulting from all releases were used to formulate the general horizontal circulation pattern of surface and bottom waters in the James River estuary shown in Figure IIA-10. This circulation pattern shows the lower James River as a "leaky closed system" wherein surface circulation is expressed as an elongated cyclonic (counter clockwise) gyre with slight losses of material upstream past Mulberry Point and substantial losses downstream past Sewells Point. Bottom circulation has a net upstream progression with some indication of cyclonic tendency in the upper reaches of Burwell Bay. In general, this description of circulation conforms with that described by Pritchard (1985) for a **weak partially mixed estuary**.

c. Field Confirmation of Net (nontidal) Circulation. This circulation pattern was, in part, substantiated by results of a current measurement experiment conducted near the James River Bridge in the summer of 1985. In this experiment, 13 recording current meters were placed on a

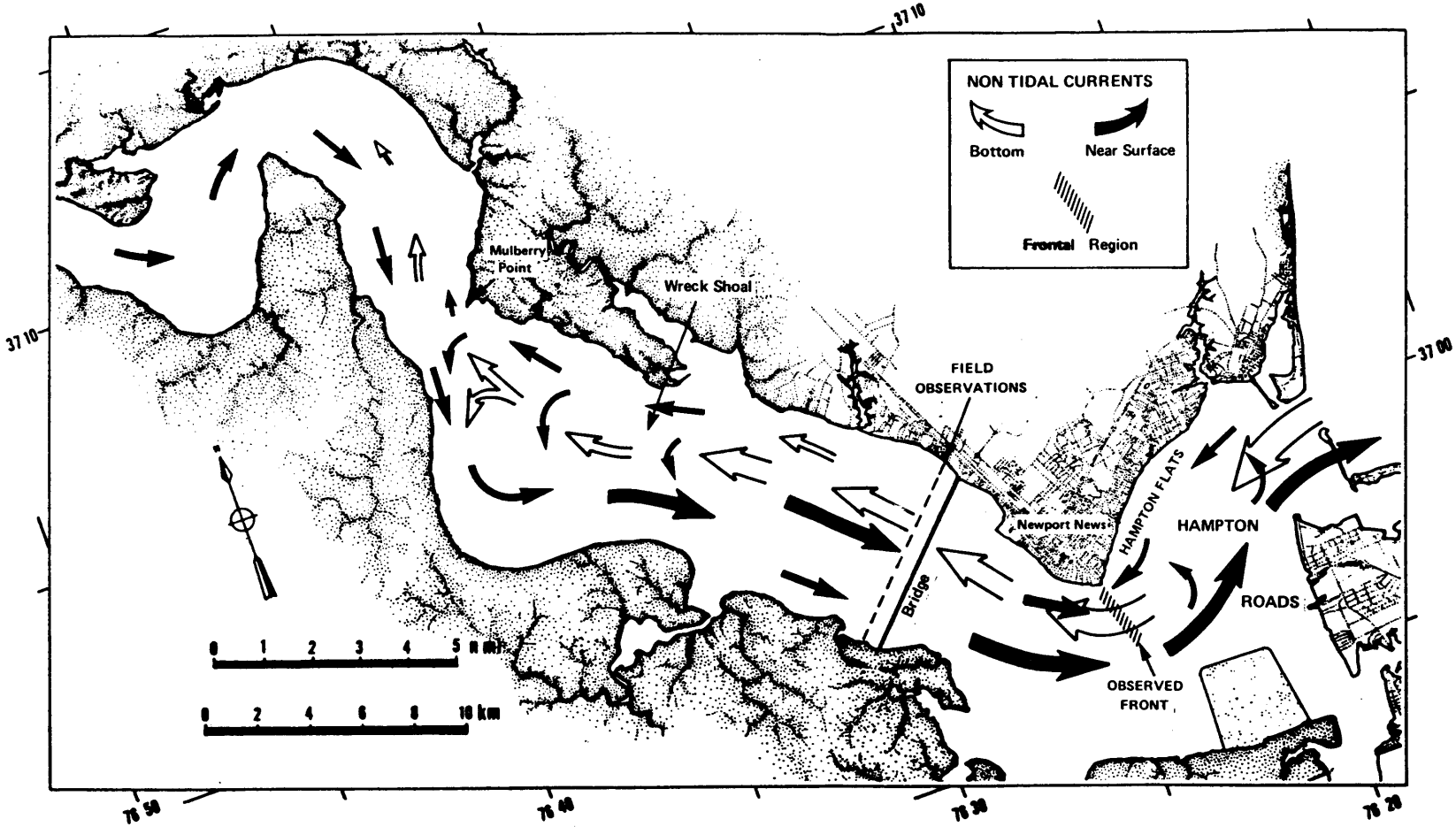

Figure IIA-10. Hypothesized surface and bottom non-tidal circulation in the James River Estuary based on variations in dye concentrations (after Ruzecki and Hargis, 1985).

transect just upstream from the bridge and kept in place for 29 days. The longitudinal component of averaged currents (Figure IIA-11) shows a circulation pattern at this location that matches that of a **strong partially mixed estuary** as described by Pritchard (1985). Note the level of no net motion (0 cm s^{-1}) in Figure IIA-11 is higher on the left when looking **downstream.**

The match between hydraulic model (Figure IIA-10) and field (Figure IIA-11) results is excellent when model and field conditions are compared. In particular, field measurements were made under variable winds and neap-spring tides, neither of which were duplicated in the hydraulic model. The greatest apparent disparity between model and field results is that averaged near-surface currents over the northeast (Newport News) shoals were slightly greater than 1 cm/sec downstream in the field experiment whereas the model showed net upstream surface motion near this location. However, "surface" dye concentrations in the model experiments were from samples taken at 3 cm (3 m prototype). When this correction for "surface" values is made, the field and model results are comparable.

d. Circulation in Hampton Roads Based on Hydraulic Model Experiments. To further investigate the cyclonic nature of circulation in Hampton Roads, available measurements of surface circulation made with the use of time exposure photography of material floating in the hydraulic model were examined. Such photographs taken during various model tests show streaks which represent movement of floating objects over a prototype time period of five minutes. Photographs were taken once every (prototype) hour for one tidal cycle when a constant mean tide was generated in the model and river discharge was regulated to equal the multiannual mean flows in the James (212.4 m^3/s as measured at Richmond). Timing of the photographs was keyed to the moon's passage over the 76th meridian (the mouth of Chesapeake

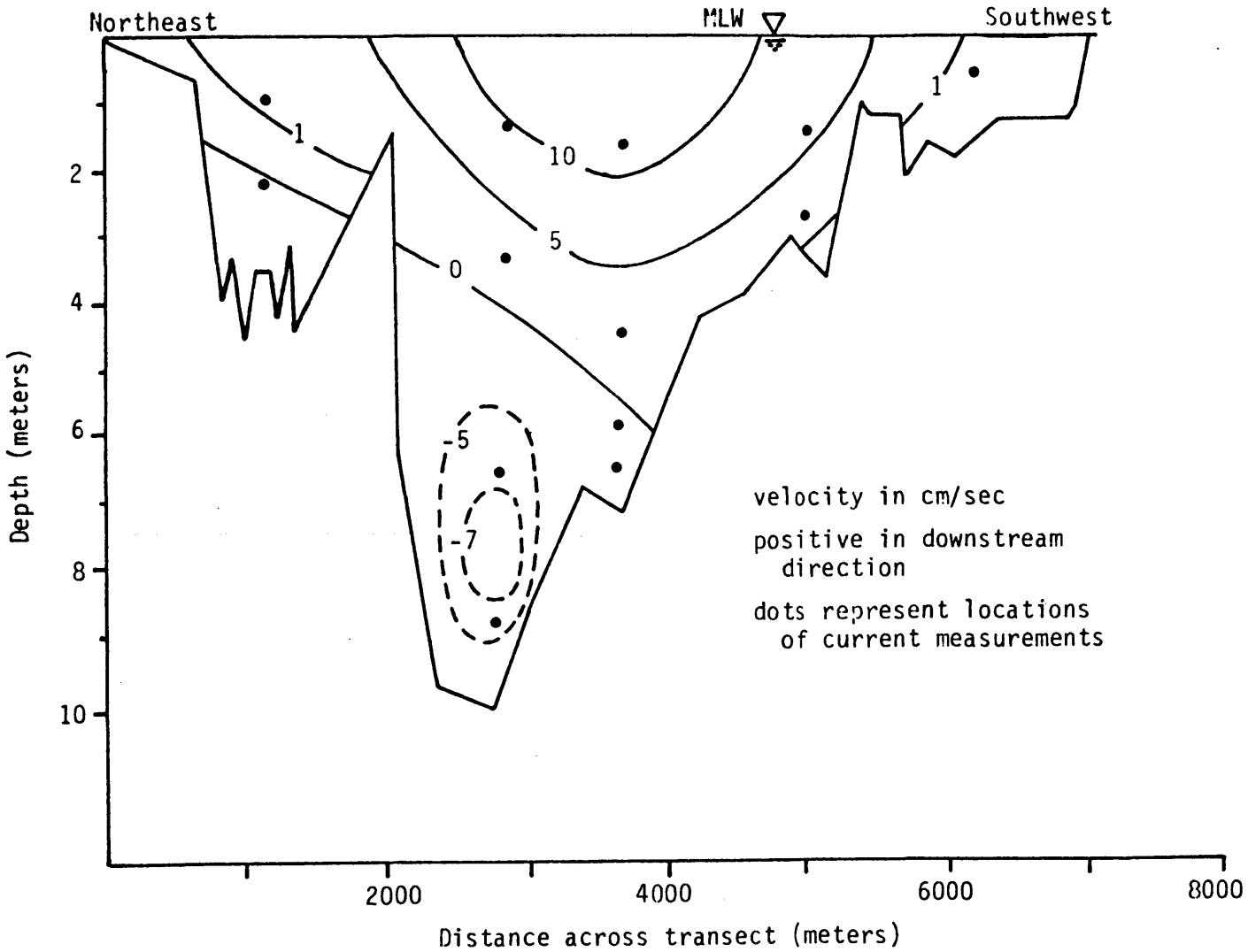

Figure IIA-11. Average velocity (29 day average) in a transect near James River Bridge.

Bay) with the photograph at hour 5 representing the end of ebb and beginning of flood tide in Hampton Roads. An example of one of these "confetti" photographs is shown in Figure IIA-12.

Information from confetti photographs was translated to a regular .25 x .25 km grid for examination of surface water movement forced by a steady mean tide and constant multiannual mean discharge using the 1975 channel conditions without I664 tunnels, causways or jetties. Gridded trajectory information was then augmented with arrows to show the estimated trajectory of a floating object over the full hour represented by each photograph.

Results of this analysis are shown in Figure IIA-13,a,b,c representing hours 4, 5 and 6. Note that at hour 4 (Figure IIA-13a) general surface ebbing persists in Hampton Roads all along the primary natural channel (see subfigure IIA-13,d for detailed bathymetry) but regions of localized flooding (upstream motion) are evident: (a) over Hampton Flats along the Hampton-Newport News shoreline; (b) at the confluence of the James and Nansemond rivers; (c) in the Elizabeth River upstream from Craney Island; and (d) along the Norfolk shoreline seaward of Sewells Point (at the entrance to Willoughby Bay).

The early local flooding over Hampton Flats and at the entrance to Willoughby Bay is associated with what appears to be gyre-type circulation that is usually encountered with flow past a headland. This type circulation transports downstream flowing water from the main channel over the flanking shoals and, on a very local basis, back upstream to the vicinity of the protruding headland (in this case, Newport News Point and Sewells Point). To a much lesser extent, a similar gyre results from ebbing flow past the upstream corner of the Craney Island disposal area. The upstream transported water then becomes entrained in the general ebbing flow of the

Figure IIA-12. Example of a "confetti" photograph mosaic of the Hampton Roads portion of the James River Hydraulic model.

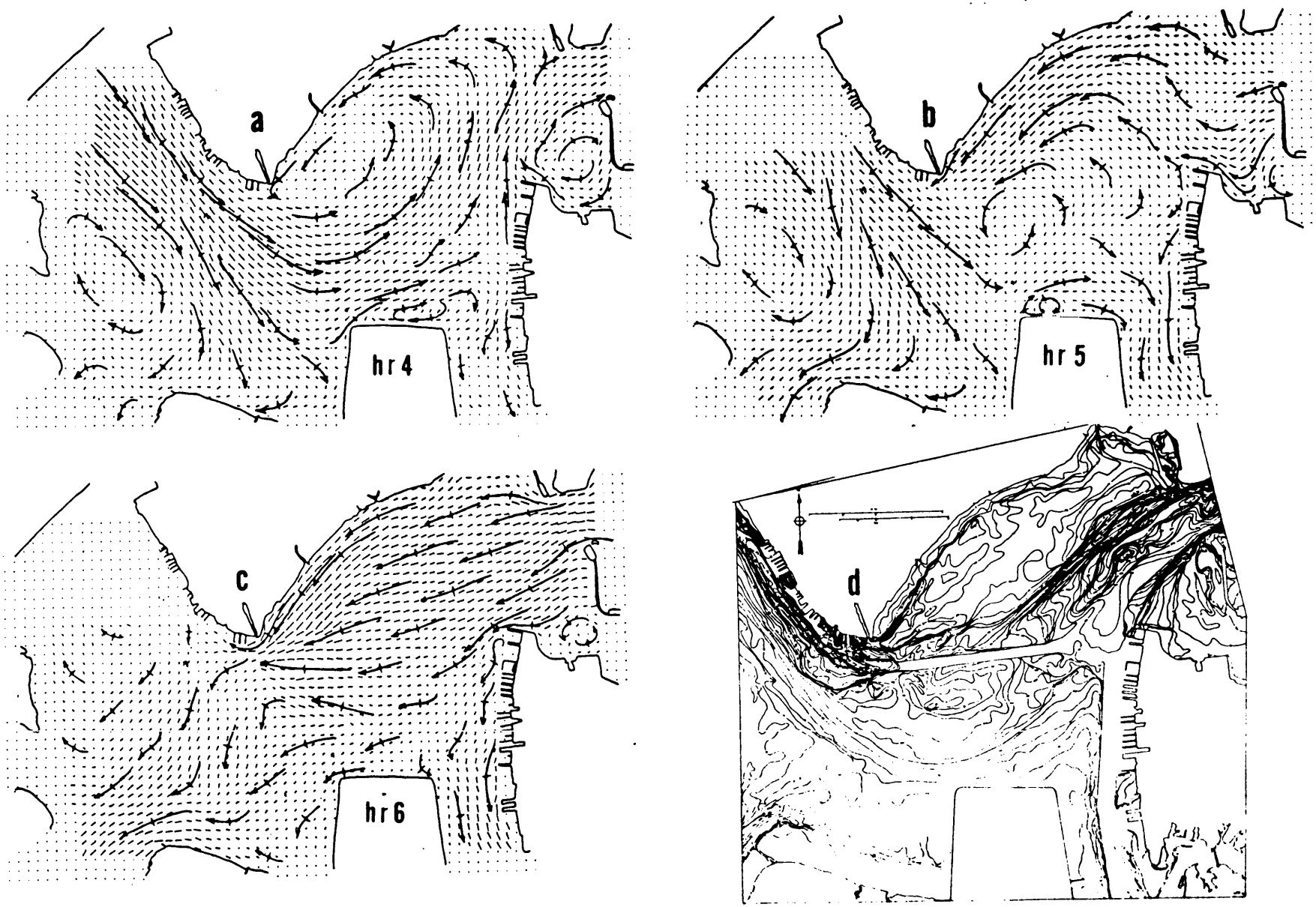

Figure IIA-13. Surface circulation in the James River Hydraulic model (Hampton Roads portion) at lunar hour 4 (a), 5(b) and 6(c) and bathymetry of Hampton Roads (d) at 2 ft intervals.

main channel providing a mechanism for retention of a portion of the surface water that would otherwise have left the system at the end of the ebbing tide. One consequence of the gyre type circulation would be the upstream injection of higher salinity surface waters from downstream locations. The cyclonic gyre over Hampton Flats appears to be centered over Newport News Bar at hour 4. Further upstream in the James, an anticyclonic (clockwise) gyre is starting to inject ebbing water from the James into the Nansemond to produce an early localized flooding condition at the mouth of this tributary.

One hour later (Figure IIA-13,b) a flooding tide is encountered across the mouth of the James (Old Point Comfort to Sewells Point) while general ebbing still persists upstream of Newport News Point. The center of the cyclonic gyre over Hampton Flats has shifted southward and is located over Newport News Middle Ground resulting in strong flooding conditions over all of Hampton Flats and cross stream cyclonic surface flow between Sewells Point and Newport News Middle Ground. Entrainment off Newport News Point is now replaced by a region of surface convergence indicated by little or no surface motion in the region between strong flooding over Hampton Flats and strong ebbing past Newport News Point. Continuity can be maintained by the denser more saline flooding water from Hampton Flats moving vertically downwards under the fresher lighter ebbing water off Newport News Point. Ebbing surface waters from the James continue their anticyclonic motion at the mouth of the Nansemond and participate in the intensified flooding of this tributary. Ebbing surface water from the James also participates in the increasing flooding at the mouth of the Elizabeth River generally to the south of a line connecting Newport News Middle Ground with Sewells Point.

North of this line of divergence, ebbing waters in the James are directed towards Hampton Flats.

The final illustration in this sequence (hour 6 - Figure IIA-13,c) shows well organized flooding throughout the portion of Hampton Roads downstream from a line between Newport News Point and the western corner of the Craney Island Disposal Area. Upstream from this line, surface motion is directed cross stream towards the Nansemond with a convergent region 1 to 2 km upstream from where it was the previous hour. The line of ebbing divergence between Newport News Middle Ground and Sewells Point is replaced by a line of flooding divergence which runs from Sewells Point to the center of the northern shoreline of Craney Island. A poorly organized line of surface convergence is suggested in the region between Newport News Middle Ground and Pig Point (the eastern portion of the mouth of the Nansemond).

e. Transport Through Cross-sections at Newport News Point and Newport News Bar. Field data collections associated with verification of the James River Hydraulic Model (Shidler and MacIntyre, 1967) included the measurement of currents in the vicinity of Newport News Point and Newport News Bar. Station locations and measurement depths at each station are shown in Figure IIA-14. Measurements at stations 5 through 9 were made on 10 September 1964 while those at stations 47, 48 and 49 were made from 6-10 July 1964. Longitudinal components (flood and ebb normal to each section) were determined from current speed and direction measurements and plotted as isotachs for each section at half hour intervals. All data was referred to the time of predicted slack water before flood (SBF) at Chesapeake Bay Entrance (CBE) based on tidal current tables (USC&GS, 1963). Results for the Newport News Point section are shown in Figure IIA-15 and those for the Newport News Bar section in Figure IIA-16.

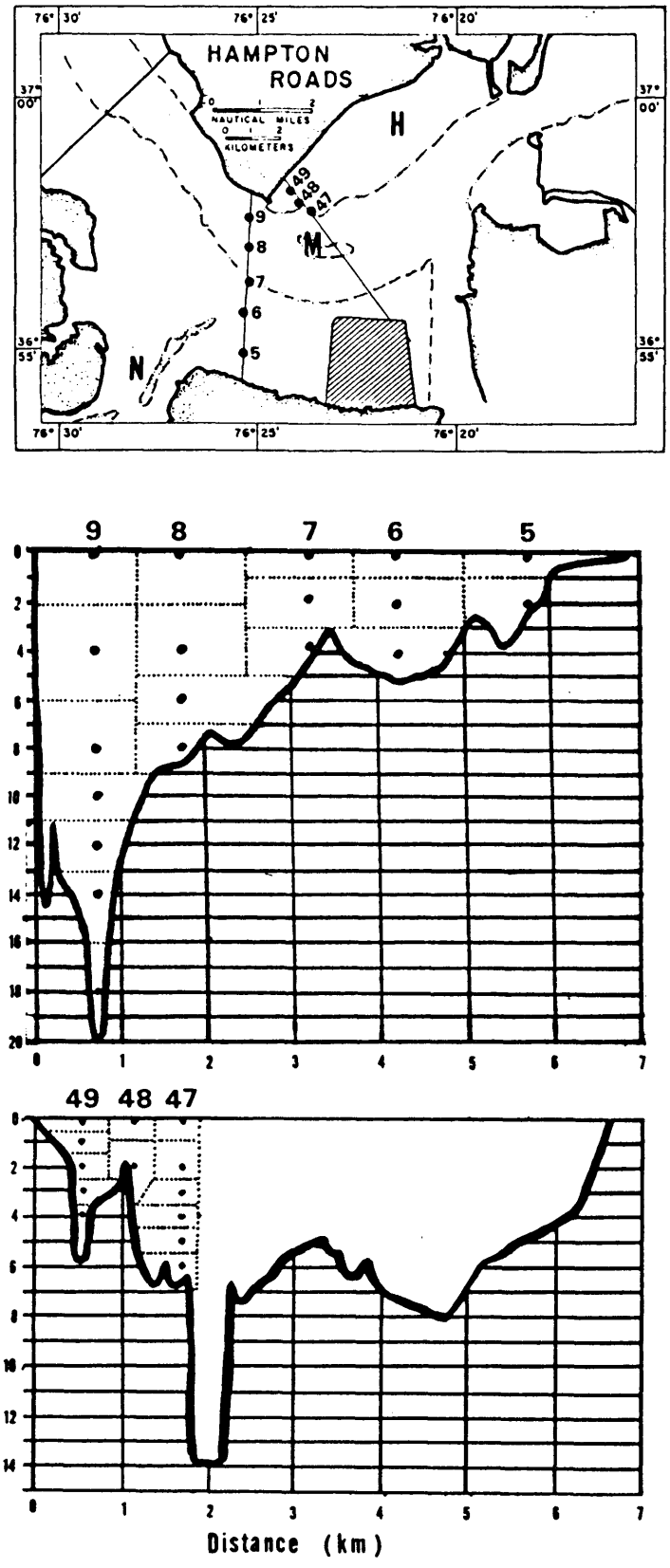

Figure IIA-14. Current measurement stations near Newport News Point occupied during "Operation James River-1964". A: Station locations, Mouth of Nansemond River (N) Hampton Flats (H) and Newport News Middle Ground Shoal (M) are identified; B: Measurement depths south of Newport News Point; C: Measurement depths across Newport News Bar. Dotted polygons in B and C delineate portions of cross-sectional area applied to currents to obtain instantaneous transport.

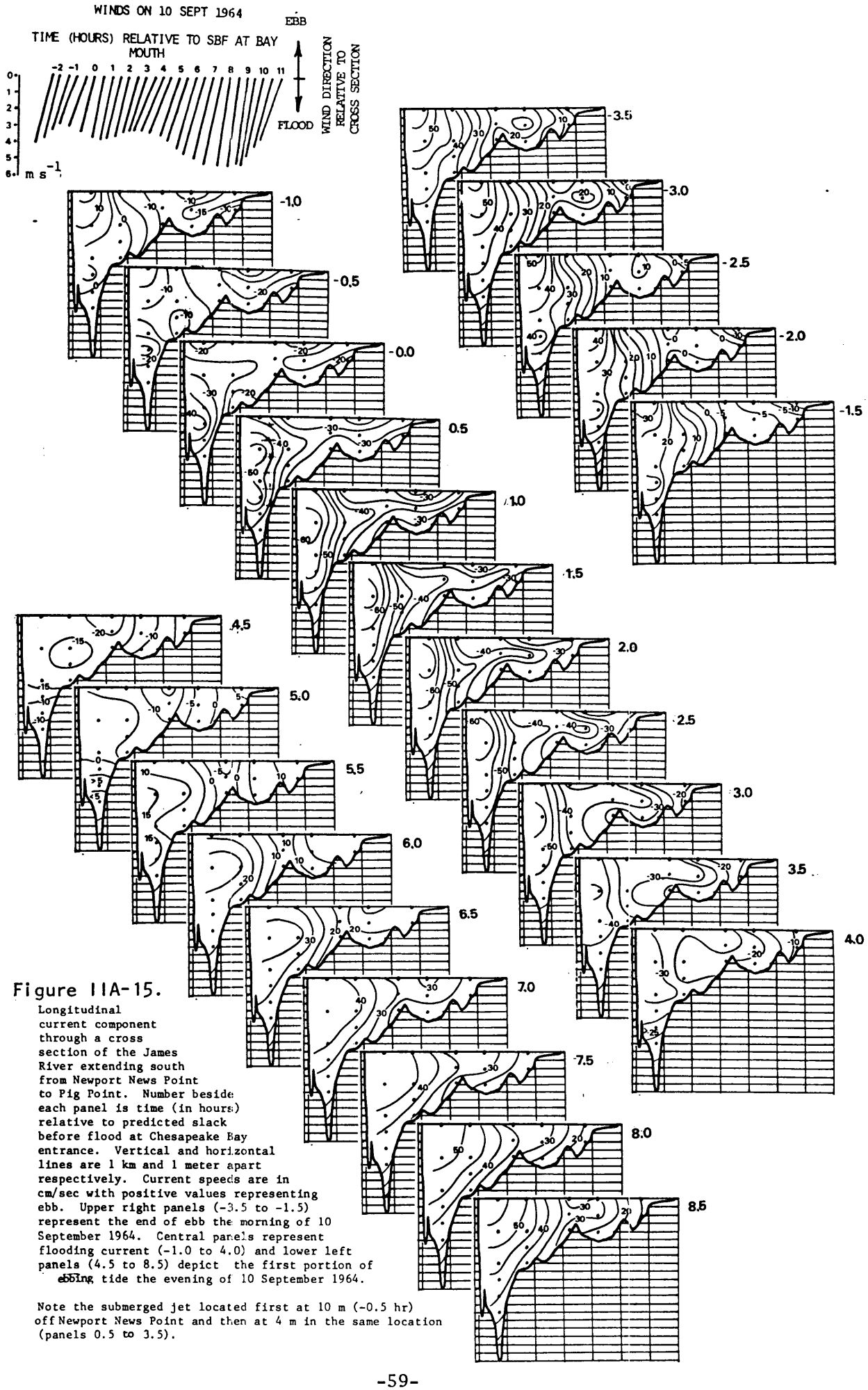

Figure 11A-15.

Longitudinal current component through a cross section of the James River extending south from Newport News Point to Pig Point. Number beside each panel is time (in hours) relative to predicted slack before flood at Chesapeake Bay entrance. Vertical and horizontal lines are 1 km and 1 meter apart respectively. Current speeds are in cm/sec with positive values representing ebb. Upper right panels (-3.5 to -1.5) represent the end of ebb the morning of 10 September 1964. Central panels represent flooding current (-1.0 to 4.0) and lower left panels (4.5 to 8.5) depict the first portion of ebbing tide the evening of 10 September 1964.

Note the submerged jet located first at 10 m (-0.5 hr) off Newport News Point and then at 4 m in the same location (panels 0.5 to 3.5).

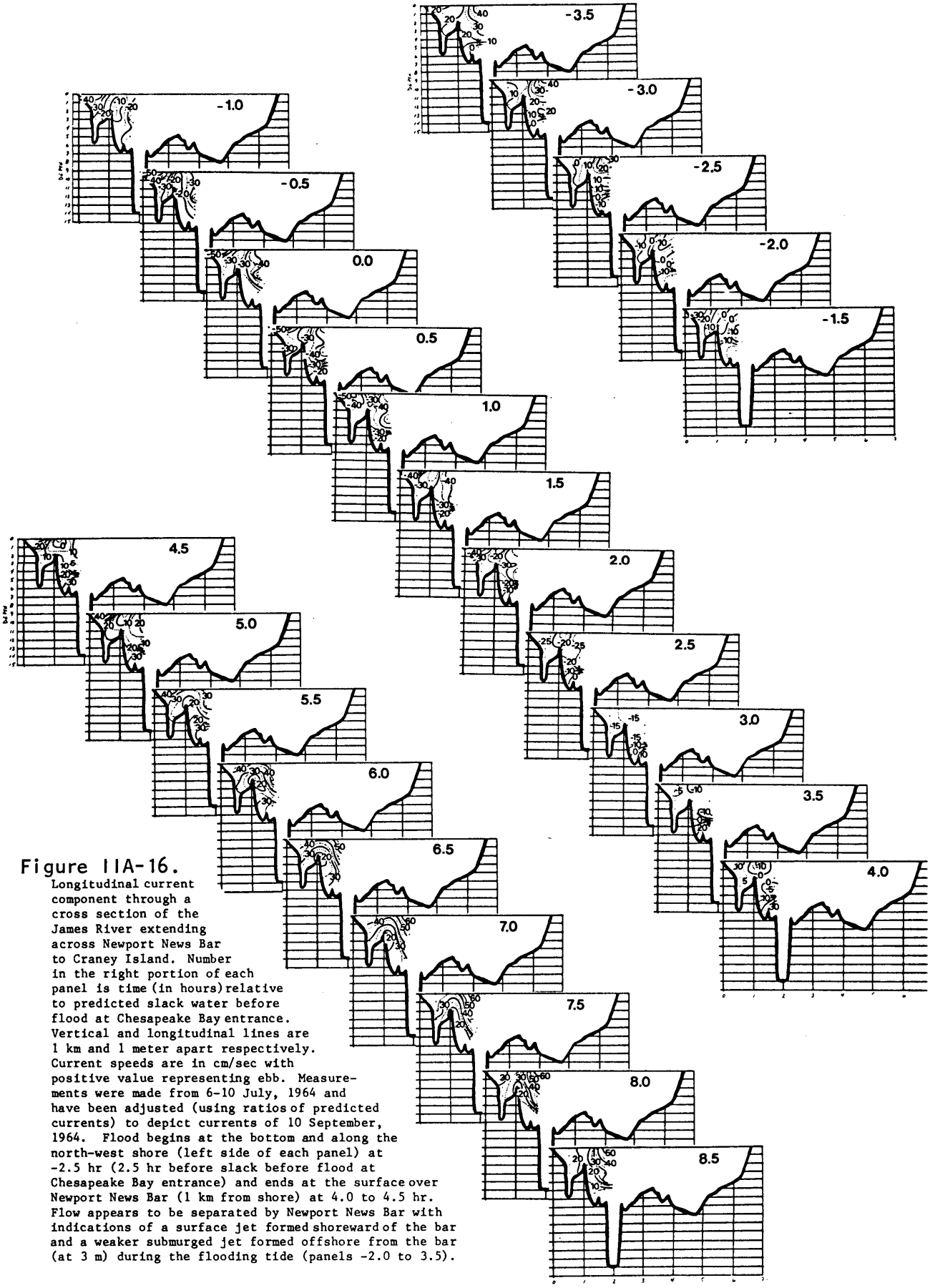

Figure IIA-16.
Longitudinal current component through a cross section of the James River extending across Newport News Bar to Craney Island. Number in the right portion of each panel is time (in hours) relative to predicted slack water before flood at Chesapeake Bay entrance. Vertical and longitudinal lines are 1 km and 1 meter apart respectively. Current speeds are in cm/sec with positive value representing ebb. Measurements were made from 6-10 July, 1964 and have been adjusted (using ratios of predicted currents) to depict currents of 10 September, 1964. Flood begins at the bottom and along the north-west shore (left side of each panel) at -2.5 hr (2.5 hr before slack before flood at Chesapeake Bay entrance) and ends at the surface over Newport News Bar (1 km from shore) at 4.0 to 4.5 hr. Flow appears to be separated by Newport News Bar with indications of a surface jet formed shoreward of the bar and a weaker submurged jet formed offshore from the bar (at 3 m) during the flooding tide (panels -2.0 to 3.5).

1) Temporal variations in currents. Figure IIA-15 shows that flow through the southern portion of the section off Newport News Point is strongly influenced by the Nansemond River (Stations 5 and 6) while the main channel of the James dominates water movement on the opposite side (Stations 8 and 9). Station 7 on this section is, for most of the time, at the boundary between these two flow regimes. On the flooding tide (negative isotachs in Figures IIA-15 and IIA-16), the influence of Newport News Middle Ground Shoal (M in Figure IIA-14,a) is evident primarily at Station 9.

Indications of the formation of a submerged jet during the flooding tide are seen at station 9 from -0.5 to 3.5 hr. Upstream flow greater than 25 cm s^{-1} was measured at 10 m at station 9 at -0.5 hr. One hour later speeds greater than 50 cm s^{-1} were measured at 4 and 10 m. Greatest flooding speeds (66 cm s^{-1}) were measured one hour later at 4 m. The current maximum persisted at this depth until 3.5 hr after SBF at CBE.

A phase difference in flooding of the Nansemond and the main portion of the James is evident in Figure IIA-15 with the former leading the latter by approximately 2 hours. Note station 5 surface speeds at -3.0 hr and 10 m speeds at station 9 at -1.0 hr. Isotachs from these two locations "grow" towards each other to produce a tilted layer of maximum flooding motion that persists for two hours (0.0 to 2.0). Slower surface currents in this region were not the result of opposing winds as evident from the stick plot of wind vectors (in the upper left corner of Figure IIA-15) which show winds blowing in the flood direction from 3 to 5 m s^{-1}.

Examination of half-hour isotach plots for the northern portion of the Newport News Bar section (Figure IIA-16) shows similarities with Figure IIA-15. As would be expected, Newport News Bar (at Station 48 in Figure IIA-14,a) appears to separate the flow along Hampton Flats. The formation of

three current maxima are evident during flood: at the surface shoreward of the bar (station 49) and offshore from the bar (station 47) at the surface and at 3 m. The inshore surface current maximum starts at between -2.0 and -2.5 hr., reaches greatest strength (58 cm s^{-1})at 0.5 hr and persists as a local maximum until 3.5 hr. At station 47 the submerged flooding current maximum begins at -3.0 hr at 5 m, moves upwards in the water column to 3 m by -1.5 hr, reaches a local maximum strength (49 cm s^{-1}) at 0.5 hr and persists until 2.5 hr. The surface maximum at this station is shorter lived starting at -0.5 hr, reaching a local maximum (also 49 cm s^{-1}) at 1.0 hr and persists until 2.5 hr. In general, there appears to be a 1.5 hr phase lag in currents from the northern portion of the Newport News Bar section to stations 8 and 9 off Newport News Point.

A conceptual model of water movement over Hampton Flats, around Newport News Bar and past Newport News Point can be formulated from the examination of the 1964 current measurements and more recent field experiments:

> On the flooding tide, water courses over Hampton Flats and is diverted around either side of Newport News Bar forming both inshore and offshore jet-like features. The inshore jet is formed first and reaches speeds in excess of 50 cm s^{-1} at the surface (- 0.5 to 1.0 hr, Figure IIA-16) while the jet offshore from Newport News Bar only shows currents in excess of 50 cm s^{-1} at 1.0 hr (Figure IIA-16) and is centered at 3 m. Flooding water around the bar converges downstream from Newport News Point where it encounters fresher ebbing water. A frontal region is formed where the denser, more saline flooding water descends and is

incorporated in the flooding submerged jet off Newport News Point (see Figure IIA-15, 0.5 to 3.5 hrs).

2) Longitudinal transport. The longitudinal component of flood and ebb transport of water through the Newport News Point section and the northern portion of the Newport News Bar section was estimated for each half hourly interval by taking the product of measured longitudinal current components and the appropriate portion of cross sectional area (as delineated by dotted lines in Figures IIA-14,b,c). Total flood and ebb volume transport for each station was determined by trapezoidal integration. To check the accuracy of these calculations, total flooding volume through the Newport News Point section was compared to the James River intertidal volume upstream from a section 5 nautical miles from the mouth of the James (2 km downstream from the Newport News Point section) as computed by Cronin (1971). Our calculations show 2.85×10^8 m^3 of water was transported upstream from slack before flood to slack before ebb. Cronin (1971) gives an intertidal volume of 2.24×10^8 m^3 or 79% of our calculated transport. The difference may be due to several factors: our measurements (10 Sept '64) were made between spring and mean tides while Cronin's calculations are referenced to mean tide; we have not imposed a no-slip boundary condition in our calculations; tidally averaged estuarine circulation patterns can vary from the classical two layered type (Schubel and Carter, 1984); there is a 19% variation in tidal range from mean to spring tides and, the previously mentioned upstream directed wind could have forced additional water in that direction.

Temporal variation of cumulative volume transport past Newport News Point from 0-6 m, 2-6 m, 0-9 m and surface to bottom (for station 9 of

Figure IIA-14) and around either side of Newport News Bar (station 47 and half of 48 for offshore and station 49 and half of 48 for inshore - Figure IIA-14) was determined and is shown in Table IIA-3. For ease of comparison, inshore, offshore and total flooding transports through the Newport News Bar section were lagged by 2, 1 and 1.5 hours respectively to put them in phase with transport past station 9. Data from Table IIA-3 are plotted in Figure IIA-17. At station 9 flooding starts at 0.75 to 0.50 hrs before SBF at CBE and continues to 5.0 hrs after SBF at CBE with nearly 136 million m^3 of water moving upstream. The submerged jet at station 9 (2 - 6 m) is responsible for 31% of the flood transport past station 9. Over one tidal cycle (-0.5 to 12.0 hr) the net transport of water through station 9 is downstream with most of this flow in the upper 2 m.

Flood transport around Newport News Bar is greater inshore than offshore with a net flooding of water over a tidal cycle inshore (-0.5 to 12 hr) and a net ebbing offshore as shown inFigure IIA-17.

Comparisons of total time dependent flood transport past Newport News Bar and around Newport News Point (station 9) are made on a percent basis. Table IIA-4 and Figure IIA-18 show the percent of flooding water from 0-6 m, 2-6 m, 0-9 m and surface to bottom that could have come from the vicinity of Newport News Bar (inshore, offshore and total). These calculations give quantitative support to the conceptual model and show that during the flooding tide, (-0.5 to 5.0 hr) at Newport News Point, water passing inshore of Newport News Bar could supply half the transport between 2 and 6 m, one third the water from the surface to 6 m, nearly a quarter of the water from the surface to 9 m and over 15% of the total flooding water at station 9. Transport offshore from the bar would supply 37%, one quarter, 16% and 11%

TABLE IIA-3

CUMULATIVE FLOOD DIRECTED TRANSPORT OFF NEWPORT NEWS POINT AND OVER NEWPORT NEWS BAR IN MILLIONS OF m^3

	--STATION 9 OFF NN PT.--				INSHORE OF BAR	OFFSHORE OF BAR	TOTAL
TIME	0-6m	0-9m	SFC TO BOTTOM	2-6m	2 Hr lag	1 Hr lag	1.5 Hr Lag
-0.5	0.166	0.800	1.446	0.037	0.015	0.240	0.105
0.0	2.300	4.677	8.068	1.661	0.335	1.004	1.192
0.5	7.134	12.291	19.551	5.117	1.223	2.451	3.430
1.0	14.273	22.954	34.803	10.040	2.661	4.364	6.818
1.5	22.699	35.263	52.117	15.645	4.638	6.587	11.150
2.0	31.550	48.093	70.158	21.423	7.057	8.908	16.038
2.5	40.182	60.622	87.869	27.092	9.720	11.131	21.110
3.0	48.074	72.159	104.257	32.370	12.472	13.066	26.040
3.5	54.730	82.007	118.280	36.839	15.179	14.562	30.477
4.0	59.767	89.545	128.922	40.191	17.680	15.546	34.099
4.5	62.993	94.407	135.477	42.251	19.808	16.006*	36.728
5.0	64.307*	96.413*	137.759*	42.949*	21.446	15.963	38.247
5.5	63.683	95.576	136.047	42.268	22.495	15.457	38.511*
6.0	61.175	91.991	130.681	40.348	22.815*	14.491	37.444
6.5	57.026	85.980	122.181	37.432	22.254	13.043	35.149
7.0	51.650	78.169	111.340	33.819	20.925	11.121	31.852
7.5	45.388	69.127	98.878	29.733	19.056	8.869	27.809
8.0	38.468	59.228	85.306	25.299	16.914	6.439	23.378
8.5	31.147	49.847	71.092	20.655	14.736	3.950	18.889
9.0	23.659	38.313	56.676	15.941	12.676	1.594	14.545
9.5	16.259	27.960	42.458	11.325	10.822	-0.406**	10.596
10.0	9.100	18.021	28.742	6.863	9.228	-1.899	7.300
10.5	2.437	8.791	15.945	2.743	7.932	-3.322	4.855
11.0	-3.329**	0.750	4.704	-0.732**	6.980	-4.705	2.452
11.5	-7.805	-5.414**	-3.955**	-3.298	6.001	-5.578	0.156
12.0	-10.412	-8.726	-8.304	-5.091	5.087	-5.966	-1.190

* INDICATES END OF FLOODING CURRENTS

** NEGATIVE VALUES INDICATE NET EBBING TRANSPORT OVER THE TIDAL CYCLE MEASURED.

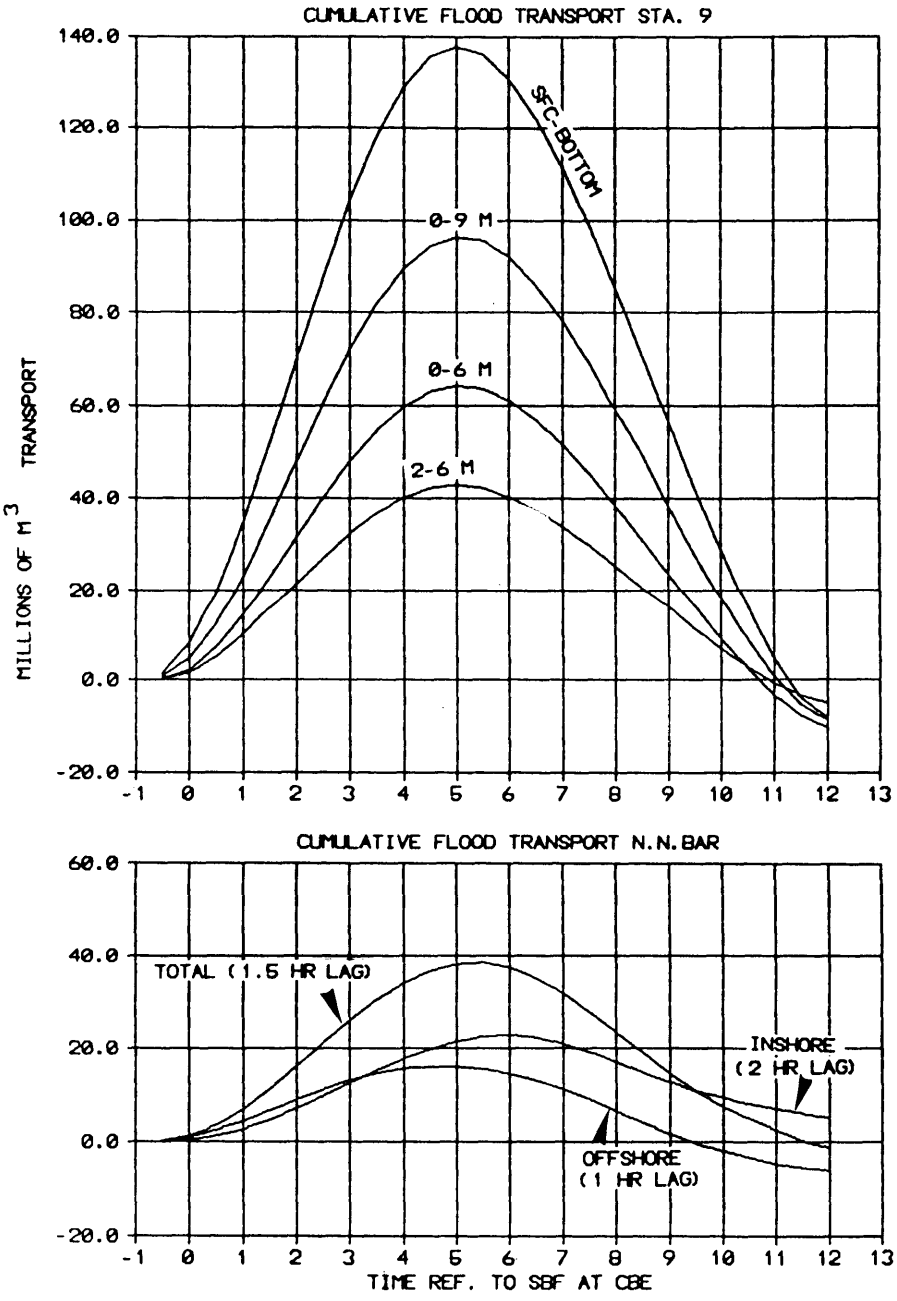

Figure IIA-17. Transport past Newport News Point (upper) and Newport News Bar (lower) during a tidal cycle.

Flood transport around Newport News Bar is greater inshore than offshore with a net flooding of water over a tidal cycle inshore (-0.5 to 12 hr) and a net ebbing offshore as shown in Figure IIA-17.

Comparisons of total time dependent flood transport past Newport News Bar and around Newport News Point (station 9) are made on a percent basis. Table IIA-4 and Figure IIA-18 show the percent of flooding water from 0-6 m, 2-6 m, 0-9 m and surface to bottom that could have come from the vicinity of Newport News Bar (inshore, offshore and total). These calculations give quantitative support to the conceptual model and show that during the flooding tide, (-0.5 to 5.0 hr) at Newport News Point, water passing inshore of Newport News Bar could supply half the transport between 2 and 6 m, one third the water from the surface to 6 m, nearly a quarter of the water from the surface to 9 m and over 15% of the total flooding water at station 9. Transport offshore from the bar would supply 37%, one quarter, 16% and 11% of the water for these depths and total transport around the bar would yield 89%, 59%, 40% and 28% of this water respectively.

TABLE IIA-4

PERCENT OF WATER PASSING THROUGH VARIOUS DEPTH INCREMENTS OF STATION 9 OFF NEWPORT NEWS POINT THAT COULD HAVE COME FROM HAMPTON FLATS NEAR NEWPORT NEWS BAR INSHORE (A) OFFSHORE (B) OF N.N. BAR AND TOTAL (C)

	A (2 HR LAG) DEPTH INCREMENTS STA 9				B (1 HR LAG) DEPTH INCREMENTS STA 9				C (1.5 HR LAG) DEPTH INCREMENTS STA 9			
TIME	0-6m	0-9m	0-BTM	2-6m	0-6m	0-9m	0-BTM	2-6m	0-6m	0-9m	0-BTM	2-6m
-0.5	9.0	1.9	1.0	40.5	144.6*	30.0	16.6	648.6*	63.3	13.1	7.3	283.8*
0.0	14.6	7.2	4.2	20.2	45.2	22.2	12.9	60.4	51.8	25.5	14.8	71.8
0.5	17.1	10.0	6.3	23.9	34.4	19.9	12.5	47.9	48.1	27.9	17.5	67.0
1.0	18.6	11.6	7.6	26.5	30.6	19.0	12.5	43.5	47.8	29.7	19.6	67.9
1.5	20.4	13.2	8.9	29.6	29.0	18.7	12.6	42.1	49.1	31.6	21.4	71.3
2.0	22.4	14.7	10.1	32.9	28.2	18.5	12.7	41.6	50.8	33.3	22.9	74.9
2.5	24.2	16.0	11.1	35.9	27.7	18.4	12.7	41.1	52.5	34.8	24.0	77.9
3.0	25.9	17.3	12.0	38.5	27.2	18.1	12.5	40.4	54.2	36.1	25.0	80.4
3.5	27.7	18.5	12.8	41.2	26.6	17.8	12.3	39.5	55.7	37.2	25.8	82.7
4.0	29.6	19.7	13.7	44.0	26.0	17.4	12.1	38.7	57.1	38.1	26.4	84.8
4.5	31.4	21.0	14.6	46.9	25.5	17.0	11.8	37.9	58.3	38.9	27.1	86.9
5.0	33.9	22.2	15.6	49.9	24.8	16.6	11.6	37.2	59.5	39.7	27.8	89.1
5.5	35.3	23.5	16.5	53.2	24.3	16.2	11.4	36.6	60.5	40.3	28.3	91.1
6.0	37.3	24.8	17.5	56.5	23.7	15.8	11.1	35.9	61.2	40.7	28.7	92.8
6.5	39.0	25.9	18.2	59.5	22.9	15.2	10.7	34.8	61.6	40.9	28.8	93.9
7.0	40.5	26.8	18.6	61.9	21.5	14.2	10.0	32.9	61.7	40.7	28.6	94.2
7.5	42.0	27.6	19.3	64.1	19.5	12.8	9.0	29.8	61.3	40.2	28.1	93.5
8.0	44.0	28.6	19.8	66.9	16.7	10.9	7.5	25.5	60.8	39.5	27.4	92.4
8.5	47.3	29.6	20.7	71.3	12.7	7.9	5.6	19.1	60.6	37.9	26.6	91.5
9.0	53.6	33.1	22.4	79.5	6.7	4.2	2.8	10.0	61.5	38.0	25.7	91.2

* Transport around Newport News Bar during a given time which exceeds near surface transport past Newport News Point, (even when the former is lagged to allow for movement to the Point) indicates the imported water could not have remained at the surface (assuming continued upstream flow) but must have descended to greater depth on its way upstream.

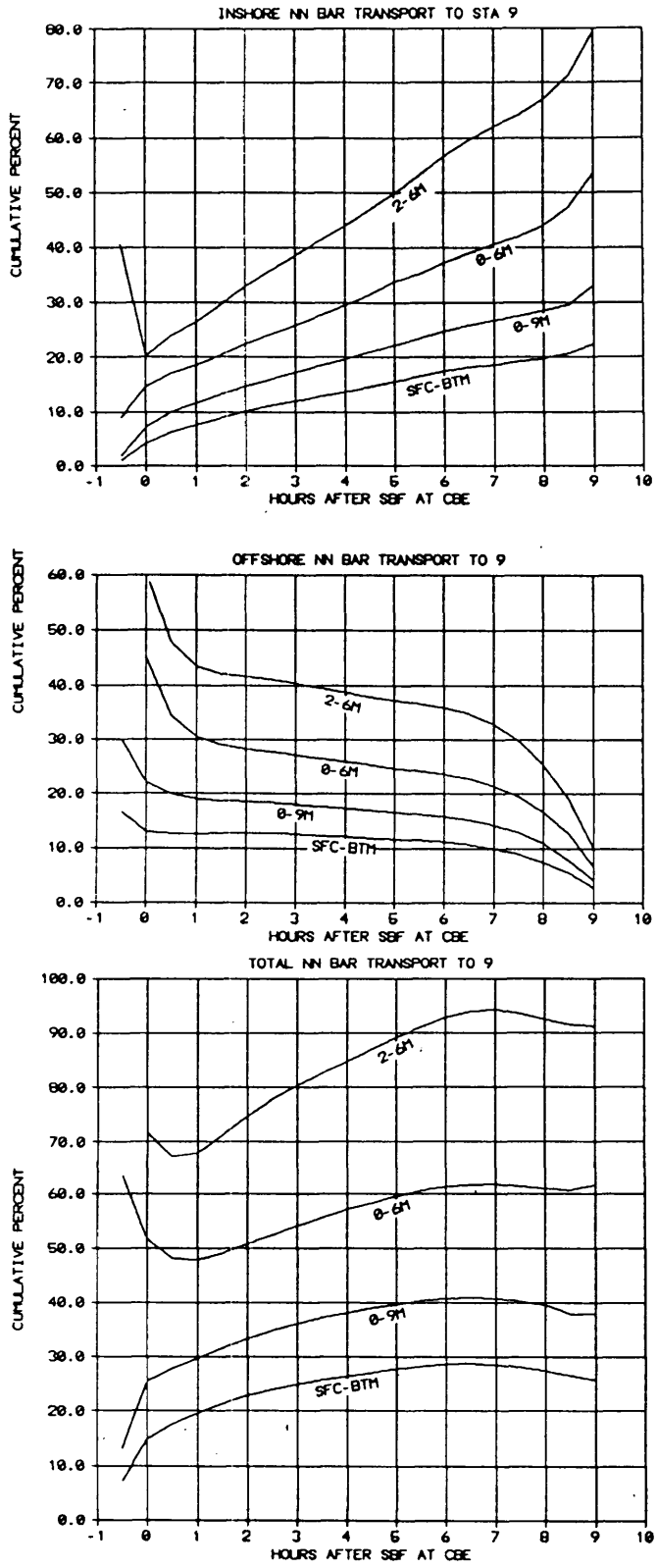

Figure IIA-18. Cumulative percent of transport past Newport News Bar that could participate in transport past Newport News Point during a tidal cycle.

of the water for these depths and total transport around the bar would yield 89%, 59%, 40% and 28% of this water respectively.

2. Interaction Between Circulation and Seed Oyster Beds

a. Dye Experiment Results.

1) Individual oyster rocks. Data representing the relative measure of spatfall over individual oyster rocks were examined to determine the average quantity of dye over each oyster rock region fifteen (prototype) days after release as well as mean quantities and standard deviations of dye over the rocks for the period 20 to 40 tidal cycles, after release. Results of this analysis are shown in Table IIA-5 for the various sampling sites and individual release points. Examination of these results show only slight differences between the average concentrations estimated for the fifteenth (prototype) day and means for the 20-40 tidal cycle period (maximum differences were less than 5% while the average difference was 1.6%) indicating concentrations on the 15th day after release provide a reasonable estimate of mean concentrations during the setting period. Information shown in Table IIA-5 was used to rank the effectiveness of each release point in providing dye to the seed bed regions and to rank the seed bed regions with regard to receiving dye from the various release points. Rankings are shown in Table IIA-6 which indicates the best release points were those in the upstream portion of the model and on the northeastern shoals while all but the Wreck Shoal and White Shoal seed oyster bed regions are excellent to moderately good locations for receiving dye from all release points.

2) Dye retention. Vertically integrated dye concentrations at each sampling station were analyzed to determine temporal variations of dye in model segments delineated by dams emplaced after the

Table IIA-5

Dye Concentrations (as 100 x mg/m^2) Over Selected Seed Oyster Rock Regions
20 to 40 Tidal Cycles (10-20 Days) After Release
From Six Candidate Brood Stock Areas

Test I

	Release Point 1 (Wreck Shoals)			Release Point 2 (Point of Shoals)		
	Avg for	Cycles 20-40		Avg for	Cycles 20-40	
Sampling Region	Day 15	Mean	Std.Dev.	Day 15	Mean	Std.Dev.
Point of Shoals	2073.4	2064.1	291.3	1259.0	1289.4	201.4
Wreck Shoals	1593.3	1600.7	233.3	1022.3	1038.8	135.3
White Shoal	1312.8	1308.4	248.5	817.7	829.9	116.3
Brown Shoal Reach	1437.7	1438.2	354.0	905.5	898.2	164.2
Naseway Shoal	1341.0	1316.0	257.4	922.0	902.7	151.3
Nansemond Ridge	1080.2	1040.5	295.2	821.5	812.0	206.5

Test II

	Release Point 3 (Naseway Shoals)			Release Point 4 (Brown Shoal)		
		Cycles 21-39			Cycles 21-39	
Point of Shoals	494.0	472.4	75.8	1124.7	1132.8	199.8
Wreck Shoals	424.4	408.5	66.1	971.5	981.5	142.0
White Shoal	555.9	552.0	105.6	858.1	867.9	141.7
Brown Shoal	583.7	585.4	125.3	1002.2	1028.0	128.0
Naseway Shoal	587.0	593.5	104.3	908.5	952.2	95.1
Nansemond Ridge	656.9	667.1	130.4	843.8	830.8	123.5

Test III

	Release Point 5 (Nansemond Ridge)			Release Point 6 (Hampton Flats)		
		Cycles 21-39			Cycles 21-39	
Point of Shoals	429.3	417.3	91.9	559.7	557.3	74.3
Wreck Shoals	361.4	345.5	92.0	432.8	427.7	54.9
White Shoal	485.0	466.4	96.0	442.3	442.7	65.7
Brown Shoal	497.7	491.9	107.5	461.3	453.7	58.7
Naseway Shoal	502.8	501.1	80.1	495.2	494.1	74.1
Nansemond Ridge	561.6	551.9	91.7	503.0	504.8	95.9

Table IIA-6

A. Ranking of Release Points with Regard to Delivery of Dye to Seed Bed Regions

Ranking	Score*	Release Point
1	30	Wreck Shoal
2	22	Brown Shoal
3	20	Point of Shoals
4	10	Naseway Shoal
5	4	Nansemond Ridge
5	4	Hampton Flats

B. Ranking of Seed Oyster Bed Regions With Regard to Receipt of Dye from all Release Points

Ranking	Score*	Seed Oyster Bed Region
1	22	Point of Shoals
2	18	Naseway Shoal
3	17	Brown Shoal Reach
4	15	Nansemond Ridge
5	11	Wreck Shoal
6	7	White Shoal

*Scoring assigned 5 points to highest concentration and and 0 points to lowest for each of six dye releases. Consistency in ranking of release points or seed oyster bed regions would have yielded scores of 30,24,18,12,6 and 0.

40th tidal cycle (Figure IIA-19). Of primary interest were the seed oyster bed regions between Newport News Point and Mulberry Point (Figure IIA-2). Dye retention in this region of the model was examined as a function of time and and inventory of dye for the end of each test was established. Temporal variations of dye within the seed oyster bed region are shown in Figure IIA-20 as percent of released dye retained in model segments A and B and the Newport News Point - Mulberry Point reach. Percentages shown are from each release from the 20th to the 40th tidal cycle with optimal setting time (30th and 31st tidal cycles) indicated. The data set was also used to determine the average percent of dye in each of these subregions on the 15th (prototype) day after release as well as the means and standard deviations of percentages from 20 to 40 tidal cycles after release. These values are shown in Table IIA-7 which can be used to rank release points with regard to larval retention within the system. The ranking, shown in Table IIA-8, is similar to that shown in Table IIA-6, with the following exceptions:

- Reversal of the ranks of the Brown Shoal and Point of Shoals release points for the Burwell Bay (region B) and Newport News/Mulberry Point reach portions of the model; and
- Higher ranking of the Hampton Flats release point with regard to dye retention in the Burwell Bay (region B) portion of the model.

The latter exception supports the two-layered circulation theory for partially-mixed estuaries (Pritchard, 1952) and shows that, although farthest down stream, the dye released on Hampton Flats is transported to the Burwell Bay region slightly more efficiently than that released farther upstream (at Nansemond ridge and Naseway Shoal). Nonetheless, the three upstream release points are the best injection locations with respect to retention of dye within the seed oyster bed portion of the model.

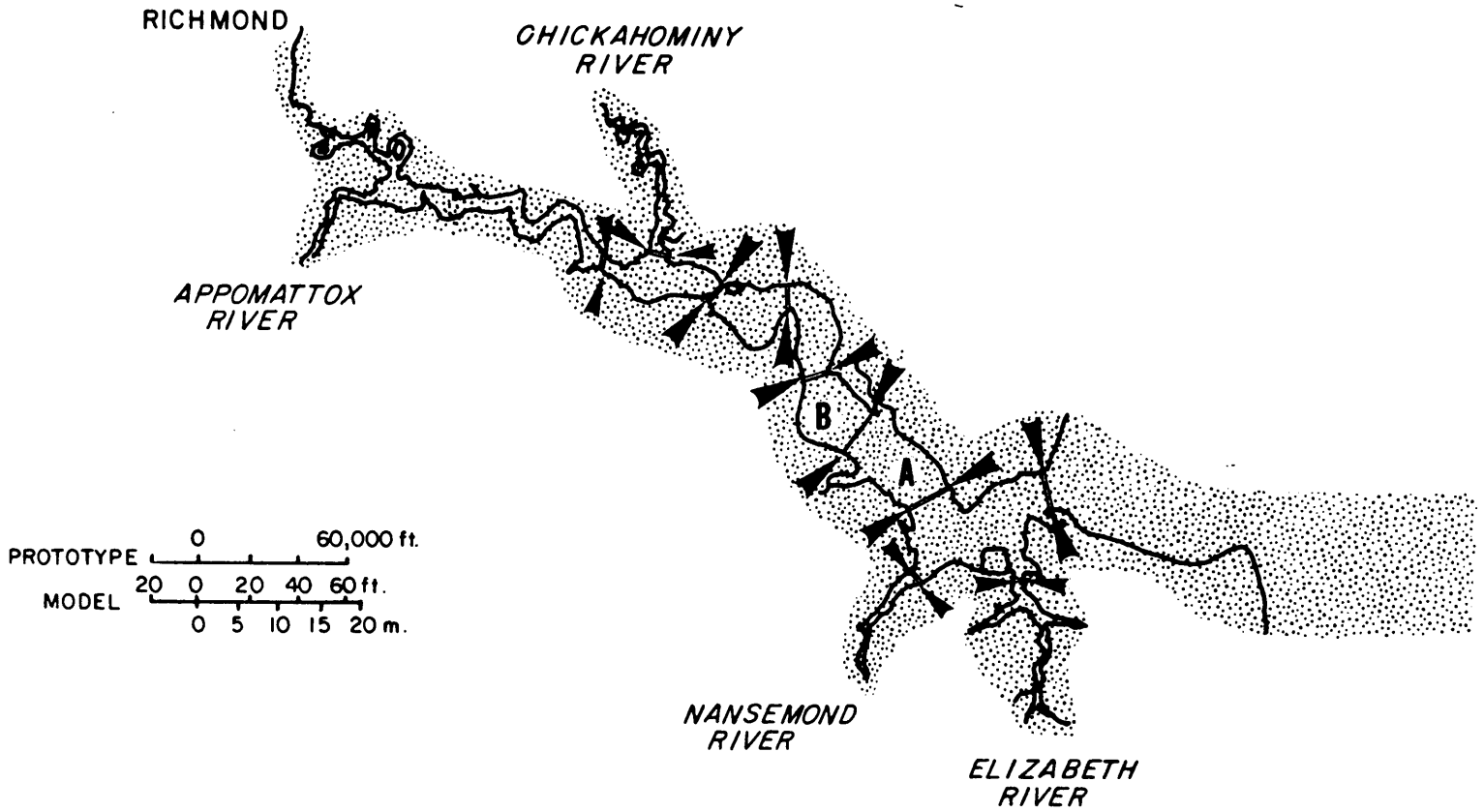

Figure IIA-19 James River Hydraulic Model segmentation with dams after dye experiments. A and B segments are primary seed oyster grounds.

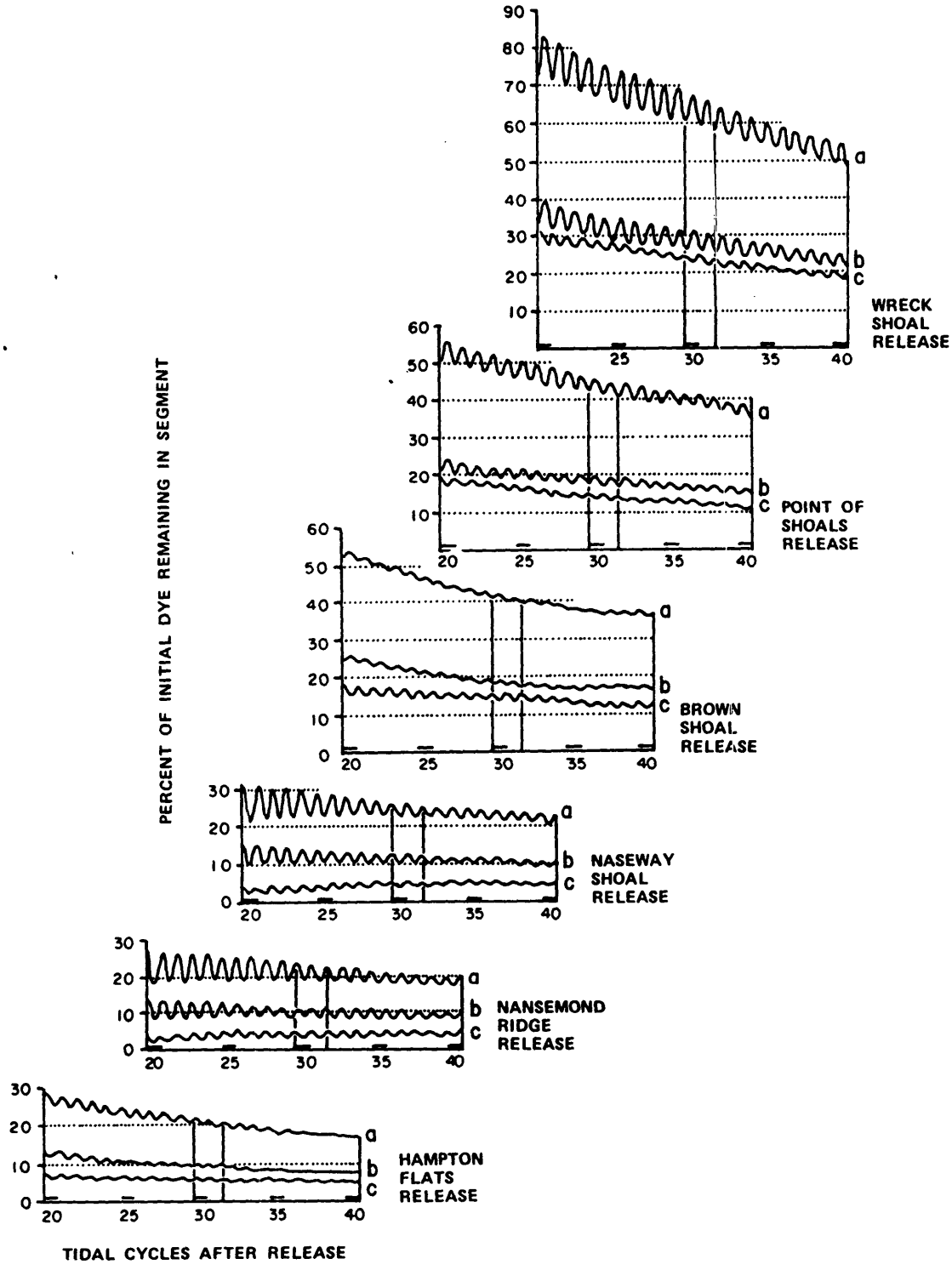

Figure 11A-20 Variation of dye retained in primary seed oyster grounds (A and B of Figure 11A-19) and C (between Newport News Point and segment A.

Table IIA-7

Percent of Dye Retained in Regions of Interest From Each Release Point

Release Point	Region	Average Day 15	20 to 40 Tidal Cycles Mean	Std. Dev.
Wreck Shoal	II	29.29	29.12	5.45
	III*	24.61	24.57	3.40
	N/M*	65.01	64.34	9.81
Point of Shoals	II	18.98	18.84	2.80
	III	14.77	15.03	2.30
	N/M	44.62	44.62	5.88
Naseway Shoal	II	11.69	11.68	2.05
	III	4.98	4.78	0.74
	N/M	24.66	24.53	3.58
Brown Shoal	II	19.06	19.42	2.58
	III	14.66	14.50	1.83
	N/M	42.44	42.63	4.94
Nansemond Ridge	II	9.97	9.75	1.74
	III	4.47	4.33	1.09
	N/M	21.36	20.91	3.11
Hampton Flats	II	9.75	9.69	1.34
	III	6.14	6.05	0.78
	N/M	21.28	21.14	2.79

*N/M = Newport News Point to Mulberry Point Reach of Model.

Table IIA-8

Dye Release Point Ranking According to Dye Retention in Model Segments

a) 15 (Prototype) Days After Release and
b) For the Period 20-40 Tidal Cycles After Release

	Rank	Region II	Region III	Newport News-Mulberry Point Reach
a)	1	Wreck Shoal	Wreck Shoal	Wreck Shoal
	2	Brown Shoal	Point of Shoals	Point of Shoals
	3	Point of Shoals	Brown Shoal	Brown Shoal
	4	Naseway Shoal	Hampton Flats	Naseway Shoal
	5	Nansemond Ridge	Naseway Shoal	Nansemond Ridge
	6	Hampton Flats	Nansemond Ridge	Hampton Flats
b)	1	Wreck Shoal	Wreck Shoal	Wreck Shoal
	2	Brown Shoal	Point of Shoals	Point of Shoals
	3	Point of Shoals	Brown Shoal	Brown Shoal
	4	Naseway Shoal	Hampton Flats	Naseway Shoal
	5	Nansemond Ridge	Naseway Shoal	Hampton Flats
	6	Hampton Flats	Nansemond Ridge	Nansemond Ridge

Results of our final inventory of dye have been arranged according to retention in desirable regions of the model in the following cascading order:

- Primary seed oyster beds (regions A and B);
- The historically important oystering regions of Hampton Roads (river mouth to region A);
- Large downstream tributaries (the Elizabeth and Nansemond Rivers) where oyster beds exist or could be established if presently polluted areas could be restored;
- Losses to the low salinity portions of the system (upstream of Region B); and
- Losses at the mouth of the James River.

These results are presented in Figure IIA-21 and show the Wreck Shoal release point provides best retention of dye within the desirable portion of the system while loss of dye from the James estuary is greatest (over 60%) from the Hampton Flats release point. The Point of Shoals release location contributes most of the upstream loss of dye (>30%).

b. Ranking of Seed Oyster Areas Adjusted for Brood Stock Density and Condition. As thus far presented, results of the 1968 James River Hydraulic Model tests indicate a possible ranking for candidate brood stock regions in the James Estuary (Tables IIA-6 and IIA-8). In general, this ranking favors upstream regions over those downstream and regions along the northern shoal over those on the opposite side of the river. The ranking is based on release of equal quantities of dye at all injection locations, and presumes that an equal number of brood stock oysters planted at any of the six proposed brood stock regions will produce the same quantity of larvae regardless of their location. Historical field data

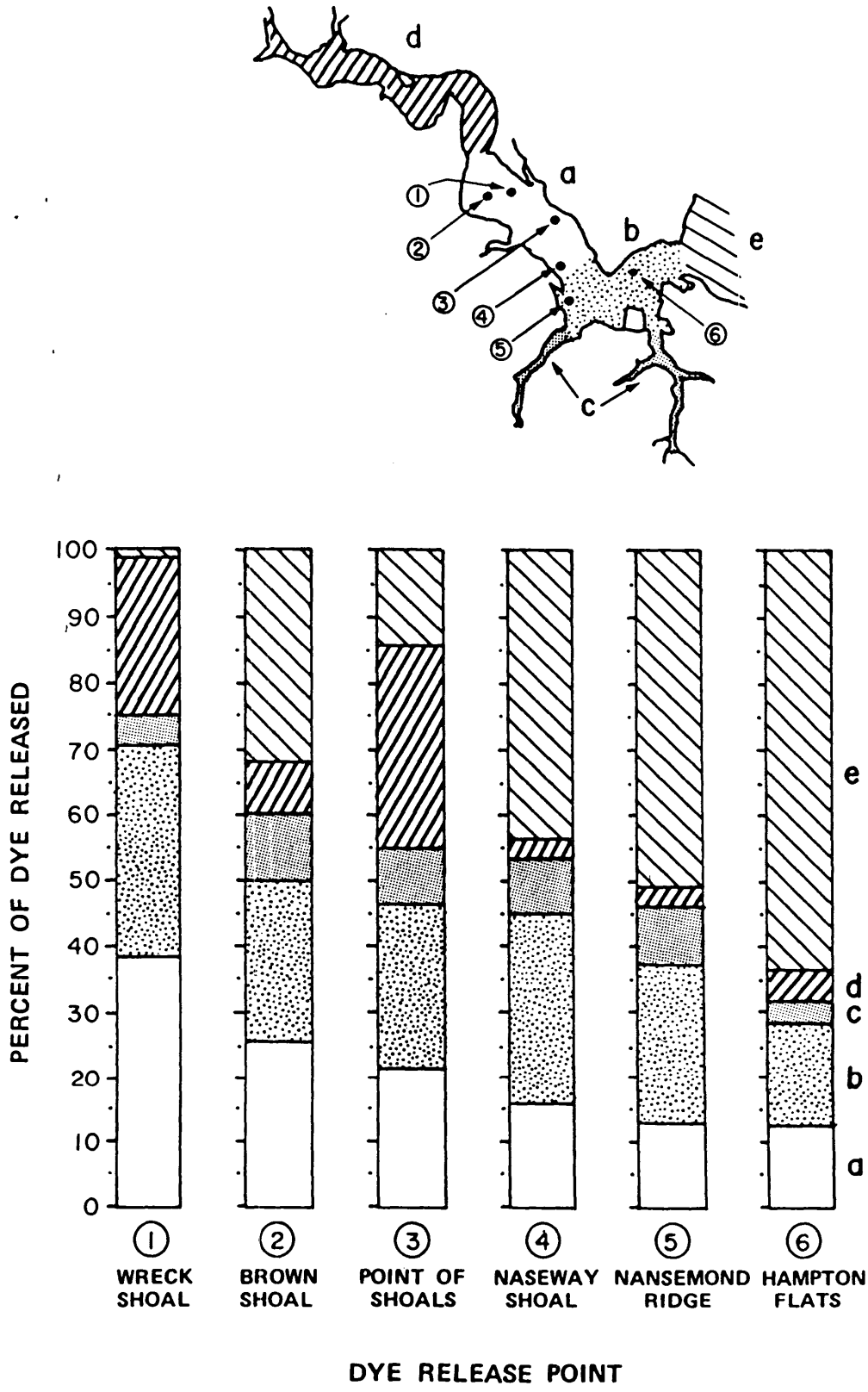

Figure IIA-21 Inventory of dye in various model segments 40 tidal cycles after release.

collected over the last 30 years indicates this presumption is incorrect (Haven, pers. comm.). Results of oyster condition index surveys during early summer, and fall inventory surveys, conducted after late summer spawning, show a general trend that greater numbers of large oysters in better condition are found in the more saline portions of the James. The condition index measures the "fullness" of oyster shell cavities and is essentially a measure of the density,

$$(C.I. = \frac{100 \times \text{meat dry weight in gm}}{\text{shell cavity volume in cm}^3}).$$

Fall inventory surveys provide a measure of oyster size distributions over various oyster rocks as counts of spat, yearlings, small (less than market size but older than 1 year) and market size (>3") oysters per bushel of cultch. The condition index prior to spawning can be used to indicate potential gamete production (Mann, pers. comm.). Additionally, regions with greater numbers of small and market size oysters will most likely have more potential for gamete production. Condition index is combined with fall survey results to provide comparative estimates of gamete production per unit bottom area for portions of the James Estuary that coincide with model dye release points. The range of condition index values is generally between 3.0 and 9.0. Oysters with a C.I. of 3 are in "poor" condition while those with a C.I. of 7.5 or over give an above average yield of meats per bushel and can be considered excellent gamete producers.

A substantial amount of condition index and fall survey data is available for various rocks in the James. These data have been used to provide an estimate of larvae production for various rocks which can, by utilizing the hydraulic model dye test data be used to estimate larval contributions from the various seed beds.

Assuming a condition index of 3 is marginal, a "larval production number" of unity is assigned to those oysters with this condition. It is further assumed that oysters with a C.I. of 9 are capable of producing 100 times the larvae produced by those of C.I.3. Using these assumptions, a fecundity factor (FF) is proposed such that $FF = \frac{CI-3}{3}$, which is the relative quantity of gametes produced by an oyster with a given CI.

Yearling, small and market oysters (as counted in fall surveys) are all able to produce gametes according to their size. Using "average" shell cavity volumes of 5, 10 and 20 cm^3 respectively (Haven, pers. comm.), the average summer condition index and fall survey data are combined to estimate gamete production per unit area of oyster rock. These estimates, when multiplied by areas of various oyster rock regions provide a means to formulate dye concentration correction factors for possible reinterpretation of the dye test results.

Results of Fall Surveys for the decades of the '50's, '60's and '70's as well as gamete production factors (based on condition index) and estimates of relative oyster area size are presented in Table IIA-9). From these estimates, relative quantities of oyster larvae released from possible brood stock areas in the James River have been calculated and are given in Table IIA-10 for the three decades when data are available.

Information from Table IIA-10 can be used to "adjust" results of the 1968 dye study to provide an estimate of possible oyster larvae contributions from the six release locations. The adjustment is shown in Table IIA-11 which is Table IIA-6 multiplied by the "Average" column of Table IIA-10 and then normalized to Wreck Shoal release point values. It is evident that, when some adjustments are made for possible variations in fecundity and numbers of adult oysters in a region, a brood stock at Hampton Flats,

Table IIA-9

Location	Fall Survey as Normalized, Size Weighted Oysters/Bushel of Culch 1950-59	1960-69	1970-79	Gamete Production Factor May, June, July	Decade	Area Size (Acres)
Hampton Flats+	0.66	1.02	1.39	184.8	'50's	1822**
Nansemond Ridge	0.45	0.41	0.64	30*		100
Naseway Shoal	-	-	0.94	24*		300
Brown Shoal	0.97	0.61	0.50	20.4	'70's	500
Point of Shoals	0.91	1.35	0.95	17.1	'70's	500
Wreck Shoal	1.59	1.67	1.42	10.8	'70's	510

* interpolated based on adjacent values and distance between locations
** 3644 acres leased in Hampton Roads. We assume half this area is planted and half is used as a buffer (Haven, pers. comm.).
+ estimate

No fall survey data was available for the Hampton Flats region. Values shown are estimates based on the following assumptions, facts and conditions.

1) Hampton Flats is a leased area and, prior to the mid 1960's was planted with seed oysters from the James beds upriver. These oysters were allowed to grow and were harvested.

2) Hampton Flats is presently used for clam, not oyster harvest and seed oysters are no longer planted at this location.

3) We assume planters operate on a three year cycle: Seed is planted and oysters are harvested three years later. Thus, continuous production would have one third of leased oyster grounds devoted to seed one third to yearlings and one third to small oysters. Market sized oysters are presumed to have been removed and replaced by seed oysters. Under this hypothetical arrangement, during the spawning season the distribution of oysters in an average bushel of culch would be 1/2 yearlings, 1/3 small and 1/6 market. We also, conservatively assume 90 market oysters per bushel of culch resulting in fall survey estimates of 270, 180 and 90 or weighted value of 141.4. Values shown here for Hampton Flats have been normalized against means for all other locations considered.

Table IIA-10

Relative numbers of oyster larvae released from possible brood stock regions in the James Estuary.

Location	1950-57	1960-69	1970-79	Avg.
Hampton Flats	165	280	0*	222**
Nansemond Ridge	1	1	0	1
Naseway Shoal	-	-	4	4
Brown Shoal Reach	7	5	3	5
Point of Shoals	6	9	4	6
Wreck Shoal	6	7	4	6

*All adult oysters lost to disease or removed for sale.

**Based on 1950-69 assumptions.

Table IIA-11

Dye Density (Relative to Wreck Shoal Release) Adjusted for Assumed Fecundity and Numbers of Adult Oysters in Blood Stock Area.

Sampling Region	Release Point: Wreck Shoal	Point of Shoals	Brown Shoal	Naseway Shoal	Nansemond Ridge	Hampton Flats
Point of Shoals	1.00	0.61	0.45	0.16	0.03	10.00
Wreck Shoal	1.00	0.64	0.51	0.18	0.05	10.06
White Shoal	1.00	0.62	0.55	0.28	0.06	12.47
Brown Shoal Reach	1.00	0.63	0.58	0.27	0.06	11.88
Naseway Shoal	1.00	0.69	0.57	0.29	0.06	13.65
Nansemond Ridge	1.00	0.76	0.65	0.41	0.09	17.24

Note that differences are less than an order of magnitude and the greatest difference is between releases from Wreck Shoal and Nansemond Ridge samples at Point of Shoals (a five fold difference in average dye concentrations).

even though subjected to harvesting, yields at least an order of magnitude greater number of larvae over all seed bed areas examined in the model.

Additional information relevant to the James River oyster fishery is available in an annotated bibliography included in the appendix to this report.

B. Hard Clam Resources in Hampton Roads

For the present studies no surveys of hard clam (Mercenaria mercenaria) resource on Hampton Flat and the surrounding area were made. The Hampton Flats region has, however, been the site of several studies and surveys relating to hard clams in the past fifteen years. It is worth noting at this juncture that as these data sets "grow older" they become less valuable as true facsimiles of the present populations due to possible changes (both natural and fishing related) that have occurred in the intervening period. Notable studies prior to 1980 were made by Haven and Loesch (1972a,b), Haven, Loesch and Whitcomb (1973) and Haven and Kendall (1974, 1975). These data are summarized in Figure 4 and Table 10 of Haven and Morales-Alamo (1980). The following are extracted from Haven and Morales-Alamo (1980) and described by area as noted in Figure IIB-1:

1. Newport News Bar: An area of ~680 acres at a density of 65 bushels per acre. An estimated total of 44,200 bushels of clams containing 282,000 kg of meat.

2. Hampton Flat: 2266 acres at a mean density of 109.8 bu/acre. 248,807 bushels of total clams containing 1,587,000 kg of meat.

3. Inshore of Hampton Flat: 488 acres at 109.8 bu/acre. 53,582 bushels containing 342,000 kg of meat.

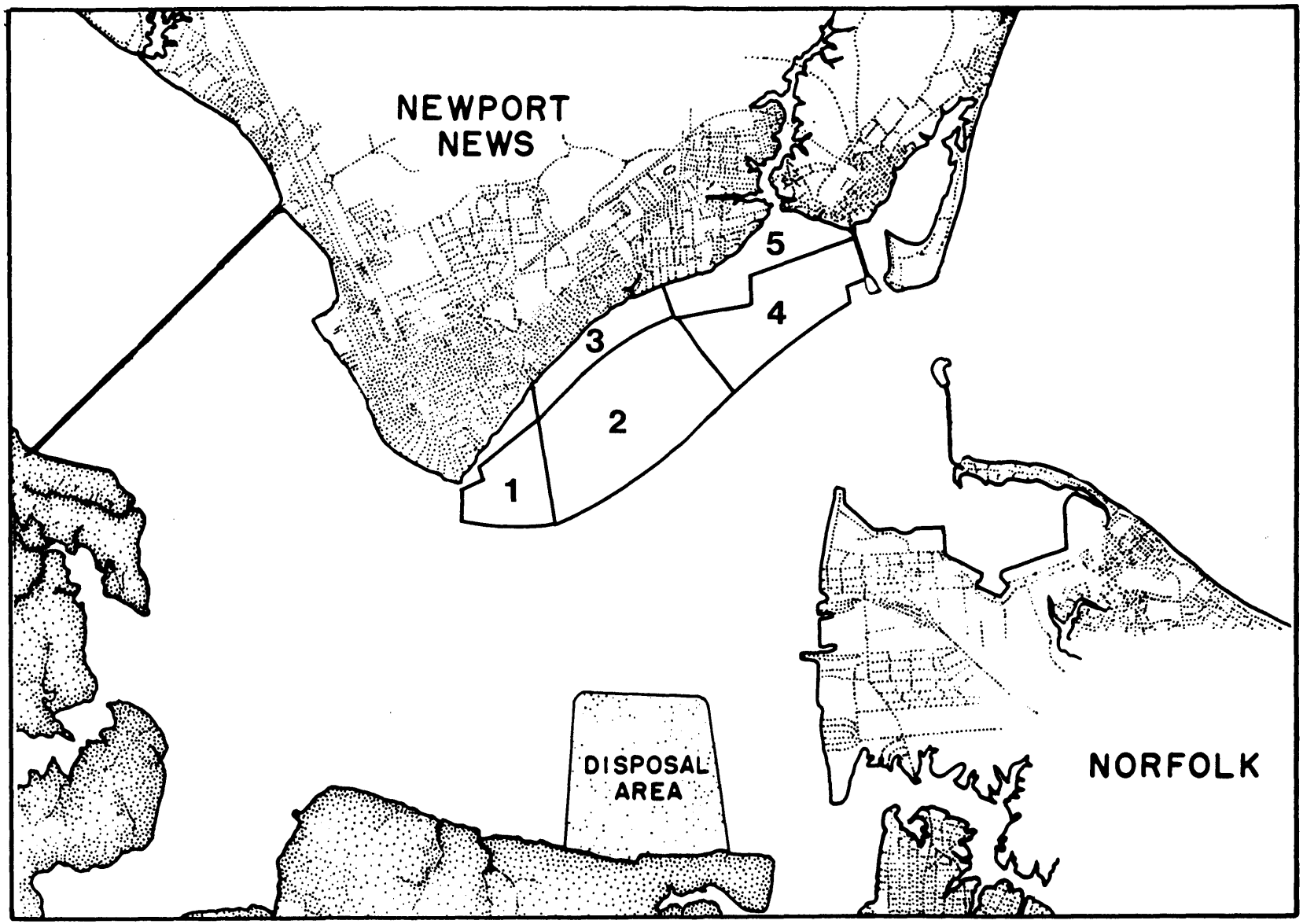

Figure IIB-1. Hard clam resources in Hampton Roads: areas of Hampton Roads corresponding to data summarized in Haven and Morales-Alamo (1980); 1) Newport News Bar, 2) Hampton Flat, 3) Inshore of Hampton Flat, 4) Hampton Bar, and 5) Mouth of Hampton River. See text for further details.

4. Hampton Bar; Offshore: 1473 acres at 24.12 bu/acre. 35,529 bushels containing 227,000 kg of meat.

5. Mouth of Hampton River; Inshore: 691 acres at an estimated 25 bu/acre. 17,275 bushels containing 110,000 kg of meat.

When 1 through 5 added together a grand total of 5598 acres, bounded by the shoreline from Newport News to the present north terminus of the Hampton Roads bridge tunnel (I64), and by the ship channel to the south, is included. This region was estimated to contain 399,390 bushels of hard clams containing 2,206,000 kg of meat.

During July of 1985 a small survey was completed by VIMS personnel of hard clam resources in an area close to Newport News Small Boat Harbor entrance and adjacent to the site of present activity related to I664 construction and jetty construction. Hard clams were only in moderate abundance in this area, which corresponds approximately to a section within the Newport News Bar area (above) as extracted from Haven and Morales Alamo (1980), and had an average density of 12,981 clams/acre valued at $659/acre.

All of the above data on the clam resource do not, however, accurately reflect present day fishing activity for hard clams in the Hampton Flat and Hampton Roads region. Harvesting of hard clams in the Hampton Roads and Willoughby Area is restricted in that stock must be relayed for depuration before marketing. A record is maintained of numbers of clams harvested and relayed by the Virginia Marine Resources Commission. VMRC records are maintained as monthly or bimonthly running totals from April through September for the combined Hampton Roads and Willoughby Bay areas, a total area larger than that pertinent to the present discussion (Figure IIB-2). Nonetheless, the data provide a good basis for discussion of the magnitude of the hard clam fishery and its true economic value at present. During

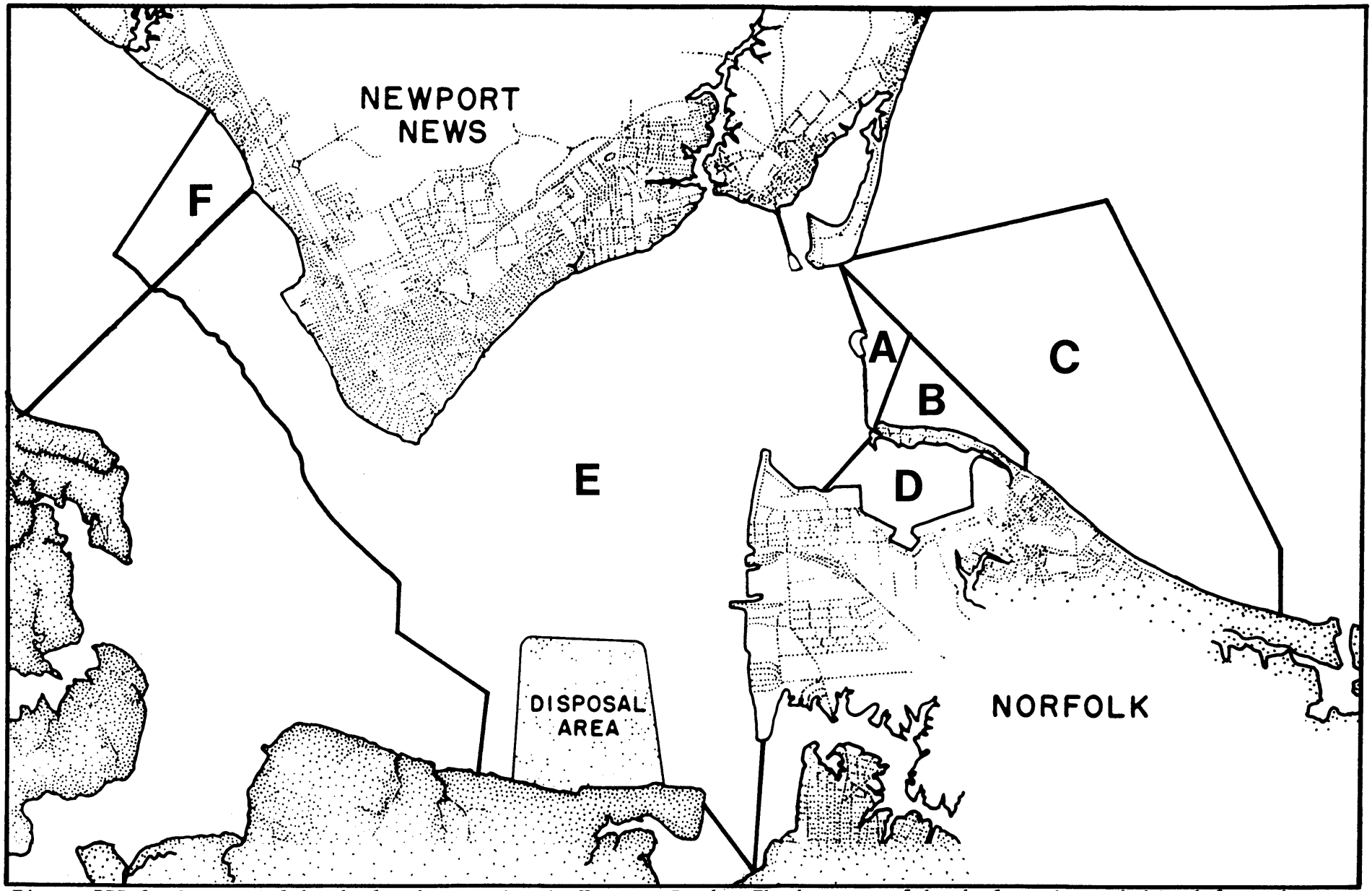

Figure IIB-2. Commercial hard clam harvesting in Hampton Roads. The harvest of hard clams is prohibited from the Elizabeth and Lafayette rivers. Areas A, B and C are conditionally approved for harvesting (Virginia State Department of Health, 15 June 1983); however, areas D, E and F are condemned. Shellfish from condemned ground must be relayed for depuration (see text). Note that the combined area of D, E and F exceeds that of areas 1-5 inclusive of Figure IIB-1 (see also comment in text).

1984 a total of 12,762,946 clams were harvested from this combined area. In 1985 this total increased to 16,567, 125 clams. Assuming that these were predominantly "chowder" size clams (size class data are not available) that have a value of ~4 ¢ each after depuration, these totals correspond to $510,517.84¢ and $662,685 respectively for 1984 and 1985. Note, however, that these dollar values are probably overestimates of true value in that (a) a clam that requires relaying will not command a 4¢ price and (b) a small but significant percentage of the relayed clams will be lost to mortality or incomplete recovery before they reach a final market.

C. Estuarine Fronts

1. Introduction

In recent years, the widespread occurrence of fronts in estuarine and coastal waters has been well established, as has appreciation for their potentially key role in determining characteristics of circulation and mixing in a variety of physical settings. Implications for a range of ecological and environmental questions have provided ample motivation for research, which has dealt with various aspects of fronts, including: the generation or development of frontal structure (frontogenesis), the dynamics of existing fronts, the dissipation or collapse of frontal structure (frontolysis), interaction of fronts and wave phenomena, details of small-scale (i.e. smaller than front scale) processes of turbulence and mixing, and the relationship of frontal structures to larger scale circulation and mixing.

Although the last topic might seem to be the primary focus of the present investigation into the potential impact of the proposed construction

of New Port Island, it is not possible at the present level of understanding of fronts to address the question of net, large-scale effect of a front (with any predictive capability) without paying considerable attention to variability at the frontal scale. Herein, some observations of frontal scale variability are presented.

2. Classes of Fronts

Fronts occur over a wide range of scales. For large-scale oceanic fronts, the influence of the Earth's rotation is a dominant factor in the dynamics. Although rotational effects on stratified flows can enter at scales smaller than the basin dimensions around Newport News Point, we will assume their influence on the frontal processes there is minor, and restrict attention here to fronts where rotation has been neglected.

a. Plume Fronts. Where major rivers or estuaries empty into the coastal ocean, the less dense discharge flows out as a buoyant layer over the heavier coastal water. In general, there will be some mixing between the two water masses, the extent of which will depend on the strength of sources of turbulent kinetic energy such as wind stress and bottom stress associated with tidal currents. The behavior of the outflow will also be influenced by (and will influence) the nature of the coastal circulation in the vicinity. Often, despite some mixing, the brackish outflow will retain its identity over a considerable distance as a distinct plume. The plume boundary may be extremely sharp, marked by typical frontal characteristics: strong local horizontal gradients in density as well as in color and in surface roughness, and evidence of convergent flow at the surface such as accumulations of foam, debris, etc.

A well-documented example of a plume front has been reported by Garvine and Monk (1974), who investigated the hydrography and currents in the area

of the Connecticut River outflow into Long Island Sound. The presence of a distinct plume, and associated frontal boundary were apparent only during the ebb phase of the tide.

b. Tidal Intrusion Fronts. In coastal areas where tidal currents are strong enough, outflow plumes may be swept back into the estuary by the flood current, forming what have been termed tidal intrusion fronts by Simpson and Nunes (1981). An interesting feature of the frontal boundary observed by them in the Seiont estuary in North Wales was that it tended to form into a pronounced V-shaped configuration with strong point convergence at the apex of the V. With the large tide range of this estuary, it was virtually evacuated of salt water at the end of each ebb flow. Simpson and Nunes suggest that this extreme is not necessarily a requirement for the existence of a tidal intrusion front, but, rather, that they will be prominent in estuaries which have a suitable range of tidal inflow in relation to the freshwater flow, that is, where the flood current is strong enough to force the plume back into the estuary, but where tidally-induced vertical mixing is not so strong as to obliterate the stratification.

c. Axial Convergence Front. In estuaries where tidal mixing is sufficient to inhibit development of persistent stratification, vertical and lateral shear in the flood current may interact with the longitudinal density gradient to produce relatively heavy water in the central part of the channel. The associated pressure field could drive a transverse, two-cell circulation, with surface flow toward the estuary axis resulting in strong convergence and sinking there. Heavy foam lines extending for kilometers along the axis of the Conway estuary, observed only in reaches with substantial longitudinal salinity gradient and only during flood tide, are consistent with the proposed concepts, and Simpson and Turrell (1985)

have reported preliminary results of current measurements that confirm the existence of full-depth transverse circulation cells.

d. General Differential Advection. The axial convergence just described is a specific example of the general phenomenon of a non-uniform flow interacting with a non-uniform (but perhaps weakly and smoothly varying) density field to produce locally intensified horizontal density gradients, i.e., fronts. For example, frontal structures could be produced during ebb flow, when relatively fast channel currents bring relatively fresh upstream water alongside slower, heavier water over the shallow flanks of an estuary. In contrast to the axial convergence flood front, the conditions during ebb flow would supply buoyant water to the channel region of the cross section, causing shoreward surface flow, divergence over the channel axis, and a tendency for front formation along either side of the channel. Transverse circulation cells would not necessarily occupy the full depth, but could develop over the pycnocline of a partially mixed estuary.

It would seem that variations on this theme, for example those related to channel curvature, shoreline irregularities, lateral gradients of tidal phase due to nearshore frictional boundary layers, etc., could in some circumstances produce frontal structures.

e. Bathymetrically Arrested Front. In the classes of front discussed so far, the role of topographic variability is either minor or indirect. However, Huzzey (1982) has investigated a front occurring regularly in the Port Hacking Estuary that is specifically controlled by bottom slope. Flood tide current at the study site flows as a shallow, well-mixed layer across a delta and then over a steep slope into a considerably deeper basin of fresher, virtually stagnant water. At a critical depth on the slope, the incoming flow plunges under the brackish water. The

front at the plunge line represents the surface boundary between the two water masses, and exhibits strongly convergent flow.

f. Stratification Boundary. Another mechanism which links fronts directly to topographic variations has been proposed by Bowman and Iverson (1977). Essentially, they suggest that a concept, developed by Simpson and Hunter (1974), which has proved very successful in delineating fronts in shallow seas may be applicable to estuaries as well. The idea is that of a competition between buoyancy inputs tending to stratify the water column, and tidally-induced stirring tending to mix it. If the water is deep enough, for a given buoyancy input and tidal current, the water column will remain stratified. In shallow enough water, the stirring can overcome the buoyancy input, and the water column will be well mixed. Fronts have been observed to form in shallow seas at the boundary between stratified and well-mixed water. There, the buoyancy input is due to solar insolation whereas in estuaries it would be related primarily to salinity variations.

g. Hybrids. The classification of fronts set out above focuses on an idealized isolation of relevant factors. In many estuarine settings, a combination of several of these factors is likely, which may enhance or inhibit frontal formation, or perhaps lead to the simultaneous production of a complex system of fronts.

D. Past Studies Related to I664 and Channel Deepening

There are four previous studies particularly relevant to this investigation:

1. Physical and Geological Studies of the Proposed I664 Bridge-Tunnel Crossing of Hampton Roads Near Craney Island (C.S. Fang et al. 1972. SRAMSOE No. 24. Virginia Institute of Marine Science)

The James River hydraulic model at Vicksburg, Mississippi, was utilized to examine and compare three different I664 crossing routes, each with and without a westward extension to the Craney Island disposal site. Two of the crossing routes had the north tunnel island in the immediate vicinity of Newport News Point. In all tests the Hampton Roads navigational channel system was at the current project depth.

Hydraulic measurements included tides, currents, and salinities. Additionally, Gilsonite tests were conducted for qualitative comparisons of shoaling patterns.

Results. The hydraulic tests indicated that the salinity structure within Hampton Roads was not significantly altered by the addition of the proposed tunnel islands and causeways. The investigation of currents documented the phase lead on Hampton Flats. In addition, those crossings from Newport News Point were found, as expected, to induce a local increase in current speed. Tidal height variation was found to be small, generally within 4 percent.

The shoaling tests indicated that there would be increased deposition in the nearshore regions of Hampton Flats for the two routes passing from Newport News Point.

2. James River Hydraulic Model Study with Respect to the Proposed Third Bridge-Tunnel Causeway in Hampton Roads (C.S. Fang et al. 1979. SRAMSOE No. 212. Virginia Institute of Marine Science)

The James River hydraulic model was again utilized to examine the I664 crossing route selected. This routing (under construction in 1986) has the

north tunnel island departing from Newport News Point. Again, the Hampton Roads navigational channel system was at current project depth.

Hydraulic measurements included tides, currents, and salinities. Additionally, Gilsonite tests were conducted for qualitative comparisons of shoaling patterns.

Results. Although the I664 project blocks about 20 percent of the cross-section area the tidal flow is not blocked. Variations in upriver tidal height and phase differences were found to be within the accuracy of the model (about 3 percent). Again the tidal velocities between the tunnel islands were predicted to be increased. No alteration in the upriver salinity structure was detected. Downstream of the project salinity concentrations were found to vary but the variations were substantially less than top to bottom differences existing in the baseline configuration.

These tests also incorporated a jetty on the east side of the entrance to the Small Boat Harbor. This installation resulted from recommendations of the 1972 study. The intent was to shelter vessels using the harbor from potentially hazardous situations arising from flood currents and easterly winds. The jetty was found to deflect the flood currents from Hampton Flats, and to enhance the shadow zone to ebb current flow. Again the Gilsonite tests indicated there would be enhanced sedimentation on the nearshore portion of the northwest sector of Hampton Flats.

3. Norfolk Harbor and Channel Deepening Study

Report 1: Physical Model Results (D.R. Richards and M.R. Morton 1983. Technical Report HL-83-13, U.S. Army Engineers Waterways Experiment Station).

Report 2: Sedimentation Investigation (R.C. Berger et al. 1985. Technical Report HL-83-13, U.S. Army Engineers Waterways Experiment Station).

a. Report 1. The physical model tests were conducted in the Chesapeake Bay Model at Kent Island. The study investigated the changes associated with deepening the Norfolk Harbor channel network, which includes deepening the Newport News Channel to 55 feet. These tests did not include the I664 crossing. This discussion will concentrate on results pertaining to the Newport News Channel and upriver.

Results. The study concluded that changes in tidal elevations, amplitudes and phase were sufficiently small to be within the error of measurement. At the western end of the Newport News Channel the current velocity was found to decrease as a result of channel deepening. At the same station channel deepening increases the flood flow dominance at the lower depths. Salinity was observed to increase by 0.5 to 1 ppt. As well, channel deepening did cause a slight change in the neap-spring tide salinity response.

b. Report 2. In this investigation a vertically integrated hydrodynamic and sediment transport model was used to investigate changes in sedimentation characteristics due to channel deepening. The I664 crossing was not included. The tide and velocity field conditions from the physical model tests were used for calibration and verification.

Results. The study focused on sedimentation within the Elizabeth River and the Thimble Shoal reach. No specific results are presented for the Newport News Channel reach, or for general sedimentation characteristics within Hampton Roads and the lower James River.

4. I664 Bridge-Tunnel Study; Sedimentation and Circulation Study (S.B. Heltzel 1984. Draft Technical Report, U.S. Army Engineers Waterways Experiment Station)

This study focused on general sedimentation characteristics within the lower James River and Hampton Roads. The numerical hydrodynamic and sedimentation models were utilized. The physical boundary conditions included the deepened channels (Newport News Channel at 55 feet) and the I664 crossing. Salt transport was not included.

Results. The model indicated that sedimentation would not increase in the Newport News Channel as a result of the I664 Bridge-Tunnel complex. Sedimentation increases were predicted in the northwest sector of Hampton Flats, particularly in the vicinity of Newport News Point. The areas predicted to experience unchanged or slightly reduced sedimentation rates include the oyster grounds of the lower James River.

5. A fifth study is also noteworthy

In 1967 the City of Newport News commissioned the U. S. Army Engineers Waterways Experiment Station to conduct hydraulic model studies of a proposed waterfront development at Newport News Point (Effects of Proposed Waterfront Developments at Newport News Point on Tides, Currents, Salinities, and Shoaling; N. J. Brogdon, Jr., and W. H. Bobb, 1967; Draft Summary Report). Specifically proposed was a triangular fill at the tip of Hampton Flats to provide for additional wharf space and supporting infrastructure.

Results. The study concluded that the proposed structure would not cause any major changes in salinity, velocity, or tidal conditions in the immediate vicinity of Newport News Point, or the entire estuary. No

specific mention is made as to whether the flow field on Hampton Flats would be altered, or as to the sedimentation characteristics.

III. RESULTS AND DISCUSSION

A. Description of Frontal System

1. The Front

Field observations reveal that the front in the lower James/Hampton Roads is persistent in terms of its occurrence. It appears in a small area off Newport News Point of the James River and occurs every flood tide under the normal lunar variation of tidal range. However, its evolution with time is variable. Even though there appears to be a general trend of evolution, the details of the feature vary from tide to tide. During its life span the front manifests itself as a narrow zone of surface flow convergence and strong vertical transport. Depending upon the wind conditions these manifestations included well defined foam and litter lines, water color differences, and surface wave roughness. The surface signature tends to be weaker when there is a strong component of easterly wind.

Two factors are essential to the formation of the front. They are the convergence of surface currents and the density contrast between the convergent flows. As the heavier water pushes against the lighter water at the convergence, it dives beneath the lighter water as a result of gravitational force. On the flood phase of tide, the incoming water in Hampton Roads meets the ebbing water of the lower James off Newport News Point. The density difference between the two water masses is large enough to make the more saline Hampton Roads water dive beneath the fresher water of the lower James. As the heavier water, either from Hampton Flats/Newport News Bar or flowing along Newport News channel, meets the lighter water off Newport News Point, it also encounters a steep drop of bottom elevation. This steep

topographic gradient not only enhances the diving of heavier water but also tends to stabilize the location of the front.

Field observations suggest that the frontal system and its general evolution may be described in terms of three segments as shown in Figure IIIA-1a,b. The initial phase in frontal development is associated with flow exiting Hampton Flats near Newport News Point, designated as branch Ia of the frontal system. During the early phase of flood tide there is also a distinct boundary parabathytic with the southern flank of Hampton Flats. This boundary designated as branch Ib, apparently represents flow contributions from Hampton Flats and contributions from flow coursing between Hampton Flats and the navigation channel. These two segments usually join together at the western edge of Newport News Bar to form a V shape front. The front position generally rests in the vicinity of the 9 meter contour. The third segment, branch II, of the frontal system is that associated with the advancing flood current along the Newport News Channel. As the flood tide currents progress up the channel section the more saline waters entering Hampton Roads encounter the estuarine salinity gradient. Another boundary segment is formed which progresses upriver with the flood tide, and frequently joins an apex formed by the three boundaries on the slope leading to the deep water of the lower James (Figure IIIA-1b).

The vertical transport across the frontal system was studied with the aid of tracer injection experiments. Dye was pumped into the uppermost half meter of the water column at the downriver side of the front. For each experiment, the dye release location was chosen such that either branch I or branch II of the front was studied. Figure IIIA-2 presents the locations of dye releases. The dye injection was continuous at a constant rate for a period of several hours over the first part of the flood tide. The dye was

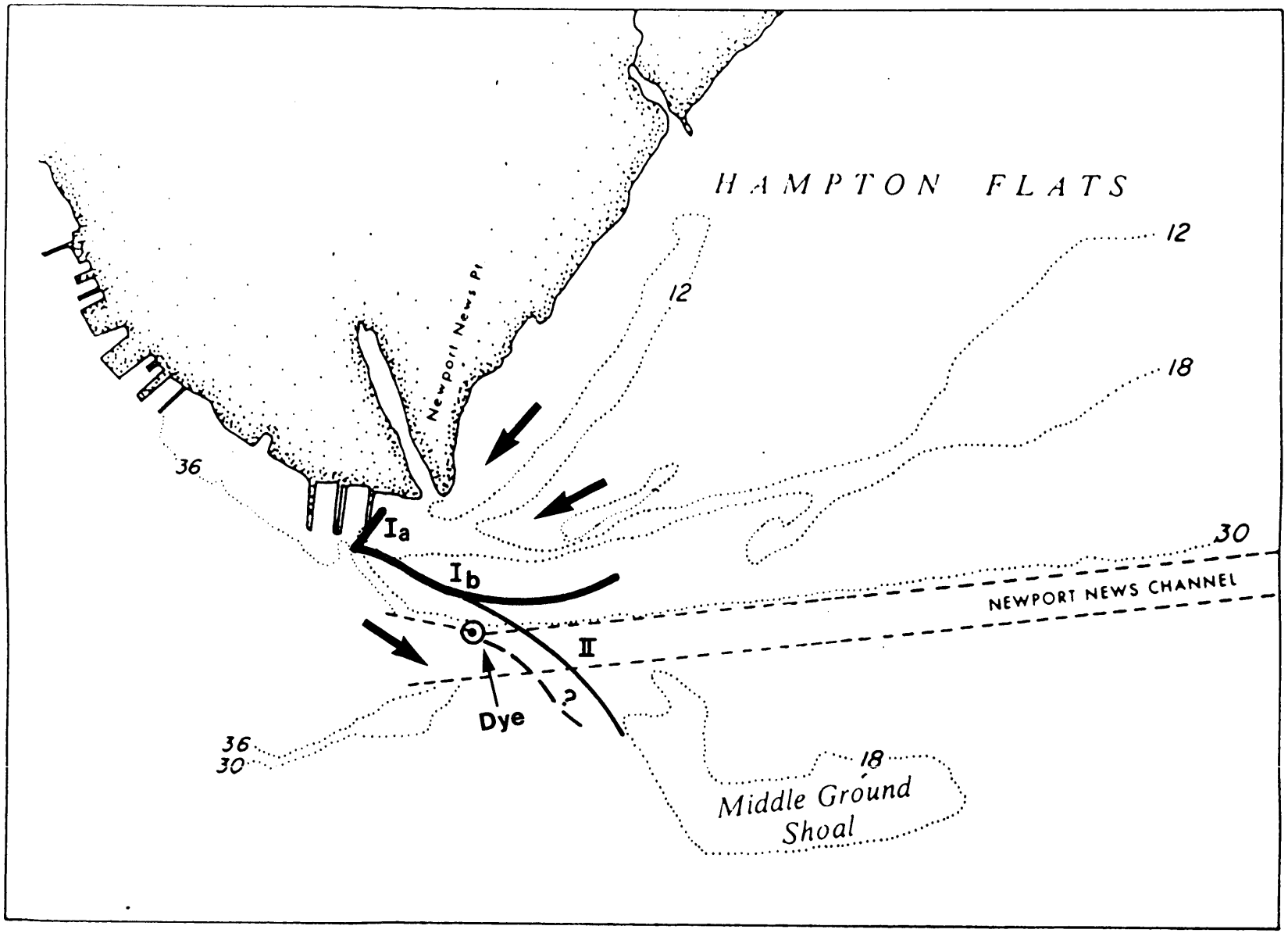

Figure IIIA-1a. Configuration of fronts at 1118 hrs. From aerial photographs of 29 August 1985. Generalized flow direction shown by arrows. (Dotted lines are depth contours, in feet).

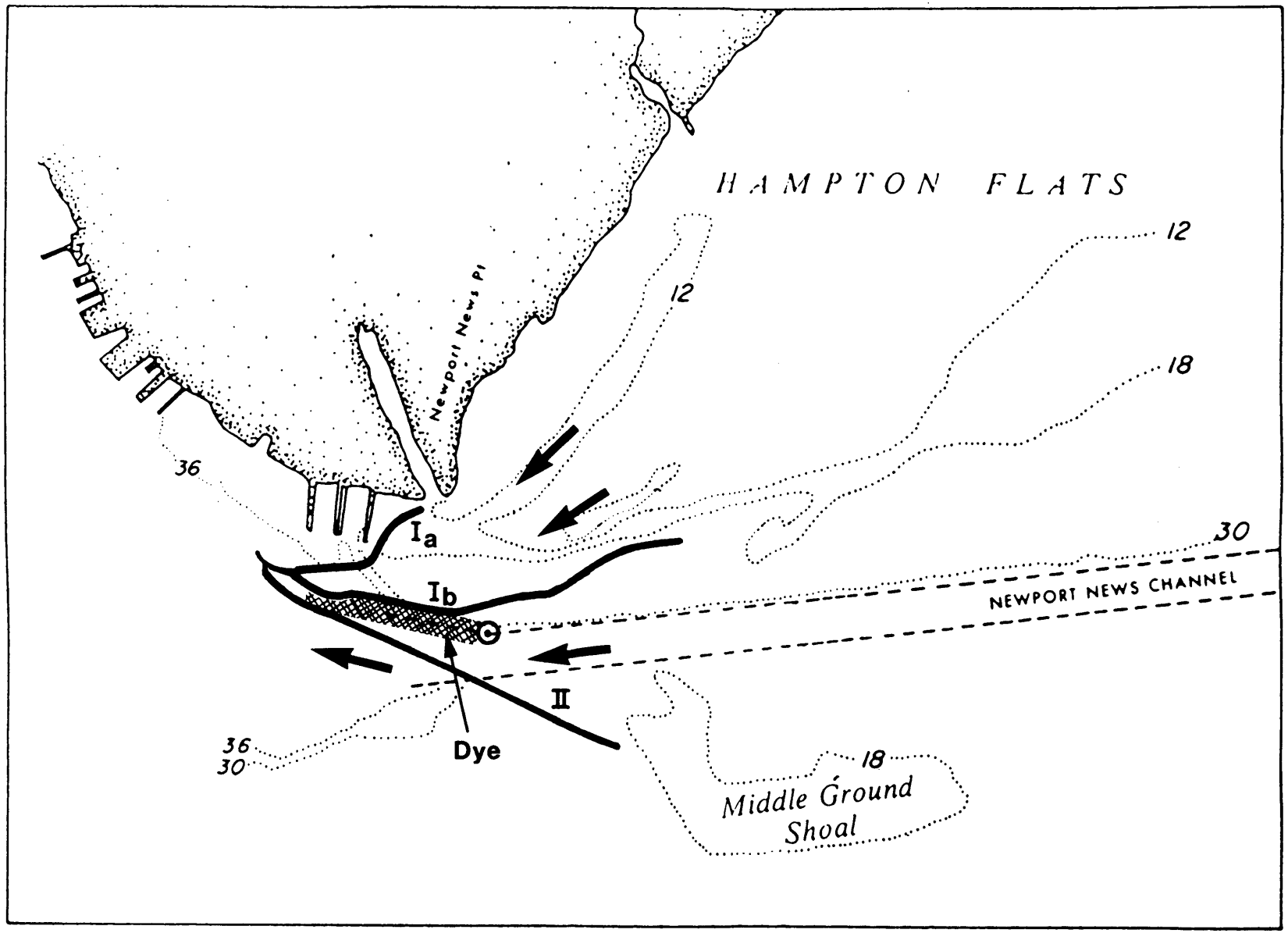

Figure IIIA-1b. Configuration of fronts at 1400 hrs. Generalized flow direction shown by arrows.

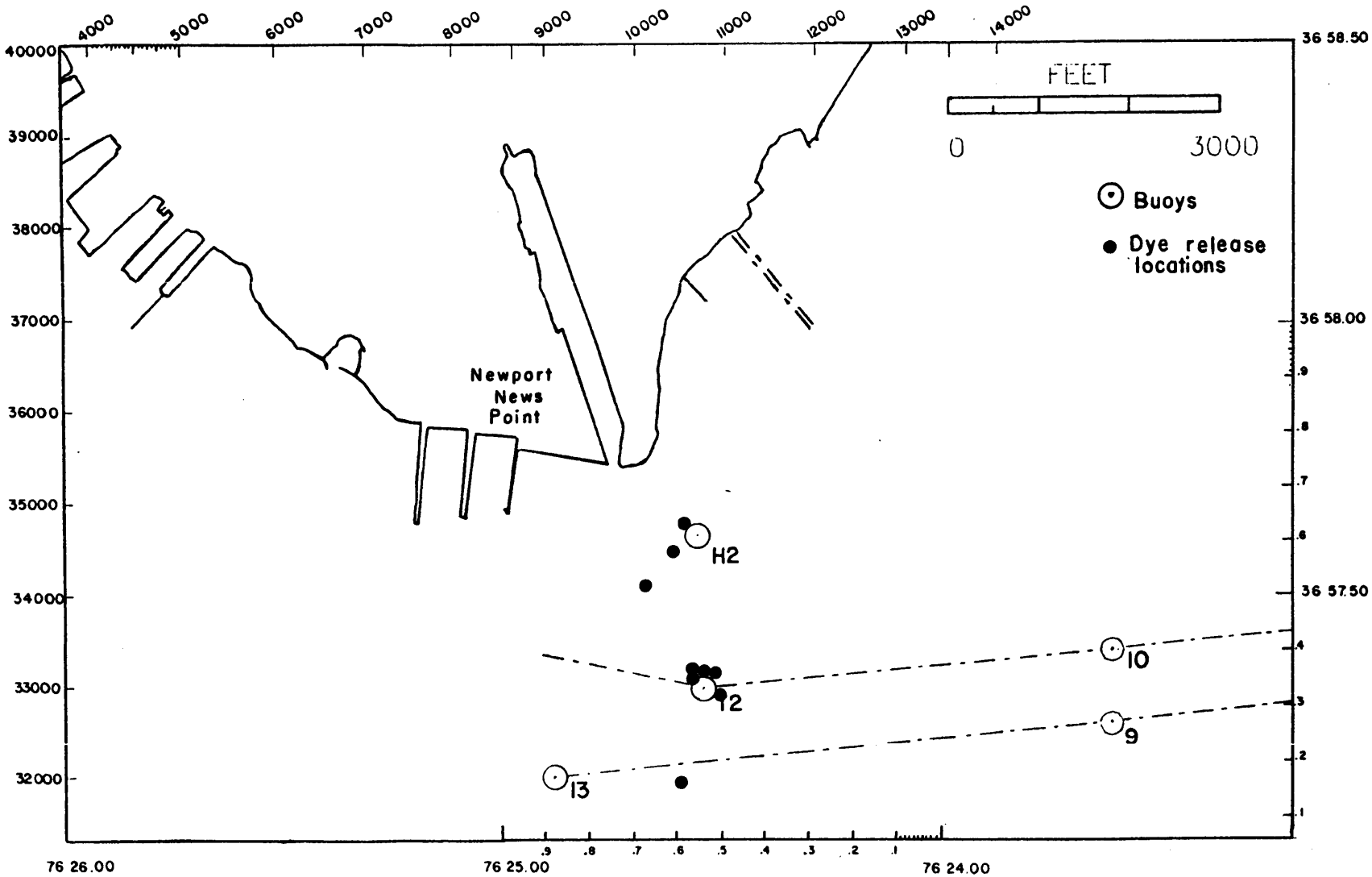

Figure IIIA-2. Locations of dye release to trace the path of surface water across the frontal system.

visible on the water surface as a streak streaming from the release location until it intersected the front. Figure IIIA-1b also shows the trace of dye streak which originated from a release point at Buoy 12. No dye was visible upriver of the front. There, the dye distribution was traced with one or two tracking boats equipped with submersible pump metering water through a fluorometer. The dye distributions were presented as concentration contours as well as tabulated data in Appendix IIA1. The contour maps indicate that peak dye concentration penetrated to depths exceeding 4 to 5 meters. Table IIIA-1 summarizes the depths of peak concentrations observed in the sampling transects. When the upriver water column was stratified the peak dye concentration tended to locate at depth where the vertical salinity gradient was the greatest. Therefore, the materials contained in the upper portion of the water column are injected, through frontal activity, into lower horizons where the net estuarine transport is upriver.

2. Flow Field in the Vicinity of the Front

The primary feature of the surrounding flow field which sets up the condition for flow convergence is a pronounced phase difference of tidal currents. Results of current measurements indicate that flood tide currents on Hampton Flats lead the current along the Newport News Channel section and, more so, the current upriver of Newport News Point. This sequence of flood current phasing is illustrated in Figure IIIA-3a,b,c which shows the pattern of surface currents in the James River hydraulic model for three hours of the tidal cycles. Figure IIIA-3a shows a recirculating eddy on the east end of Hampton Flats while the current in the channel is still ebbing. When the currents within the channel section are slack, the flood current over the shallow Hampton Flats converges at Newport News Point (Figure IIIA-3b). There it encounters ebbing waters of less density from the lower James

TABLE IIIA-1

Depths of Peak Dye Concentrations Upriver of the Front

Date	Release Location	ΔS °/oo	Depth Meter
8/21/85	buoy H2	2.5	5
		-	4
		-	5
8/23	245 m SW	-	6
	of H2	4	5
9/3	south of channel	-	6
9/6	buoy 12	2.5	4
		-	4
9/19	buoy 12	0.5	6
		0	2.5
		-	8.5
9/20	buoy 12	0	20*
11/19	buoy 12	4	6
11/21	buoy H2	3	8
6/11/86	bouy 12	3	10 to 12
6/12	305 m NE of H2	6	15*
		4.5	13.5
		3	6.5
6/13	buoy 9	2	7

*bottom

Figure IIIA-3a. Surface currents in Hampton Roads, tidal hour 4.

Figure IIIA-3b. Surface currents in Hampton Roads, tidal hour 5.

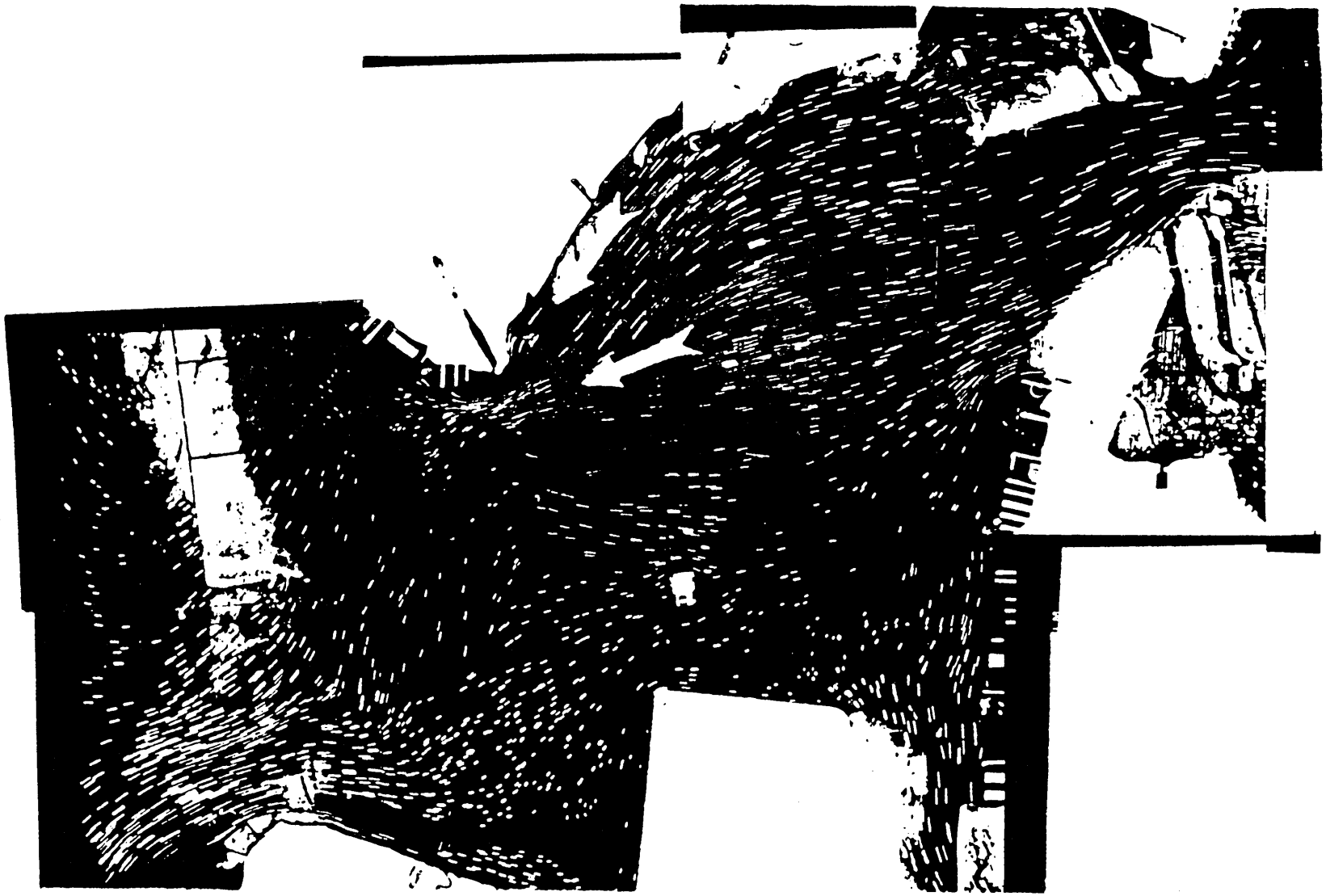

Figure IIIa-3c. Surface currents in Hampton Roads, tidal hour 6.

and dives beneath the less dense water. As the flood tide currents progress up the channel section (Figure IIIA-3c), another front is formed which progresses upriver with the flood tide. As the front moves over the topographic gradient at the western end of the dredged channel, the increase in water depth slows down the upriver movement of the front and also augments the diving action of surface water.

With the advance of flood currents, the two branches of front converge upriver of Newport News Point. At this stage of development, the currents are flooding throughout Hampton Roads.

The substantial lead of flood current on Hampton Flats over those in deep waters in the channel may be attributed to several mechanisms:

a. Topographic Eddy. The channel makes a 90^{o} bend around Newport News Point. As the ebb flow from the lower James tries to negotiate the bend, a topographic eddy begins to evolve on the shallow flanks. Toward the late stage of ebb tide, the eddy is fully developed into a counterclockwise circulation over Hampton Flats. The circulation advances the flood phase of tide and enhances the strength of flood current, at least in its early stage.

b. Modification of Tide Due to Friction. One dimensional analysis of tidal dynamics indicates that the friction tends to advance the phase of tidal current relative to that of tidal stage (e.g. Ippen, 1966, p. 509). Boundary layer theory also indicates that the oscillating current near the boundary will lead that of the interior flow (e.g. Lamb, 1962, p. 62). Therefore, it is expected that flood current on Hampton flats would lead those in the channel. The theoretical maximum of phase lead is /4, i.e., 1.55 hours for M_2 tide. This is of the same order of magnitude as observed and, thus, the friction, due both to the shallow depth and lateral

boundary, plays a role in the phase sequence of tidal current around Newport News Point.

c. Anti-node of Damped Co-oscillating Tide. Newport News Point is about one-half tidal wave length from the head of tide, i.e. the anti-node of a damped co-oscillating tide. Tide table data show a local maximum of tidal range at this location, and a local minimum at an upriver location about one-quarter wave length from head of tide. A damped co-oscillating tide would possess the same features. The analysis by Redfield (1950) indicated that tidal current phase changes substantially across the anti-node. The flood current on the downriver side starts much earlier than that on the upriver side, resulting in convergent flow at the anti-node during early stage of flood tide. The tidal data along the James River (after adjusting for geometrical variation) were fitted into a damped co-oscillating tide model. The damping factor resulting from the computation is so large as to preclude the conclusion that tidal co-oscillation accounts for the phasing in current around Newport News Point.

3. Density Field in the Vicinity of the Front

The lower James River, near Newport News Point, is an extremely complex estuarine setting. In view of the combined influence of channel curvature, highly variable bottom topography, oscillating tidal flow, and irregular changes in fresh water inflow and the strength and direction of the wind, it is not surprising that the density field exhibits complicated patterns of variability. Underlying this variability are the usual trends of a coastal plain estuary, with moderate density increases with depth and decreases with distance from the mouth. Observations have revealed that, superimposed on these trends, are further persistent features in the density field, namely highly localized, sharp horizontal gradients (fronts) in the near-surface

density, occurring systematically at particular locations and during a particular phase of the tidal cycle.

A view of the density structure near the front, and its evolution in time, can be derived from vertical profiles of temperature and salinity sampled along longitudinal (stations A-E) and lateral (stations F-J) transects shown in Figure IIIA-4. Representative results are shown in Figure IIIA-5 as salinity contours (the density in the region is controlled by salinity). Predicted slack before flood between stations A and B was at 0545 hours.

Early in the flood (Run 1), a region of relatively strong vertical salinity gradient stands out at about 3-5 m depth at station E. This diffuse "interface" outcrops as a surface density front between stations C and B, and in the lateral transect, between stations G and H. In Run 2, an hour later, the structure has evolved somewhat, but a region of strong horizontal gradient is again found between stations C and B. Another hour later (Run 3), the front had moved upriver and over the slope at the west end of Newport News Channel, between stations D and C.

In the longitudinal sections, in addition to the horizontal translation of the surface front, there is also an apparent deepening and steepening of the frontal zone as the flood tide progresses. However, this is not a straightforward change of position and shape of a well-defined interface. Rather, higher salinity water has been incorporated into the downriver side of the high-gradient region, but the depth at which each isohaline approaches the horizontal on the upriver side remains nearly constant throughout the period of these observations.

In the lateral sections, on the right hand side of Figure IIIA-5, note that in Run 1 there was a substantial bottom layer toward the shoreward side

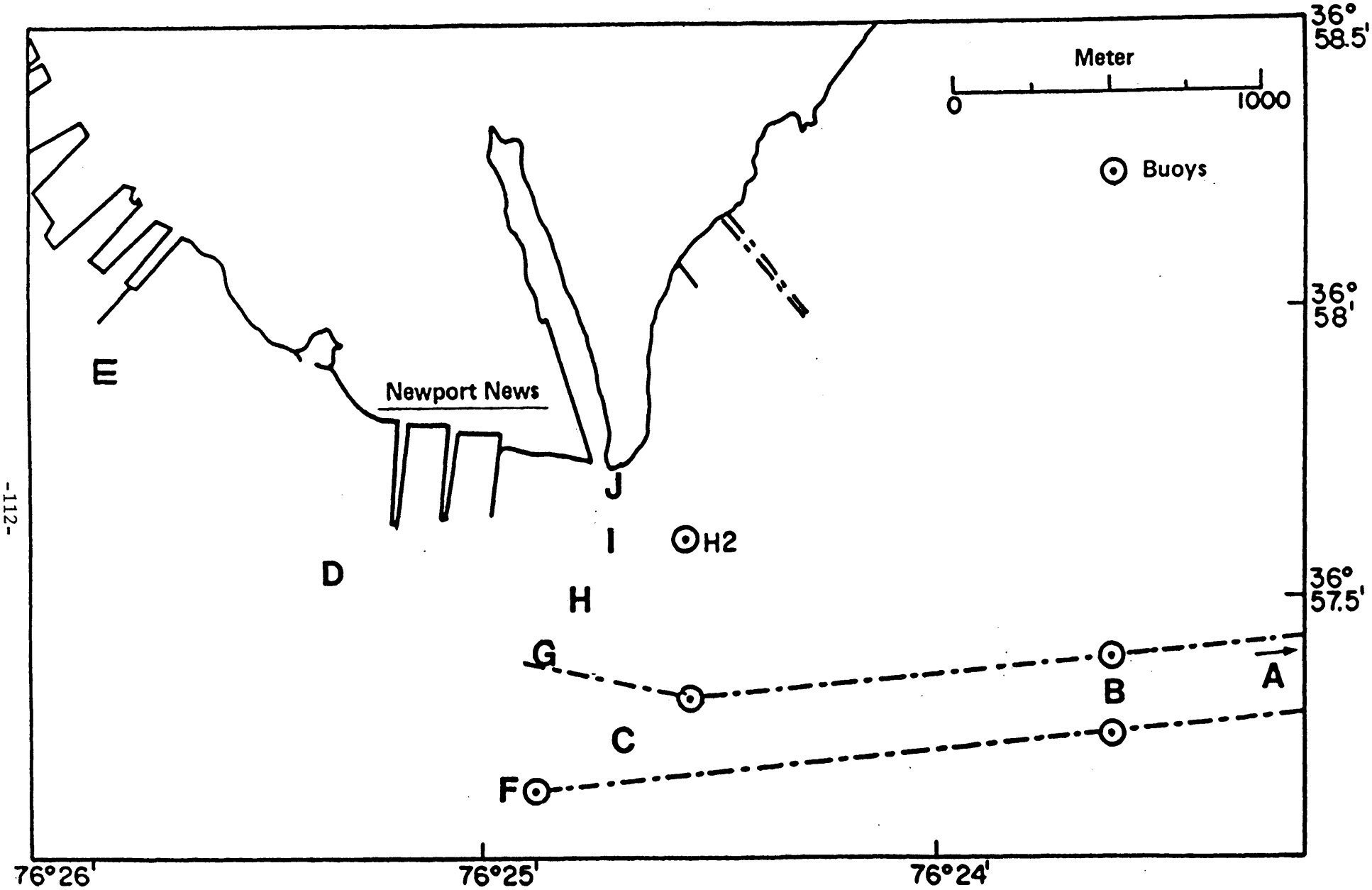

Figure IIIA-4. Station locations for vertical profiles of temperature and salinity, June 1985.

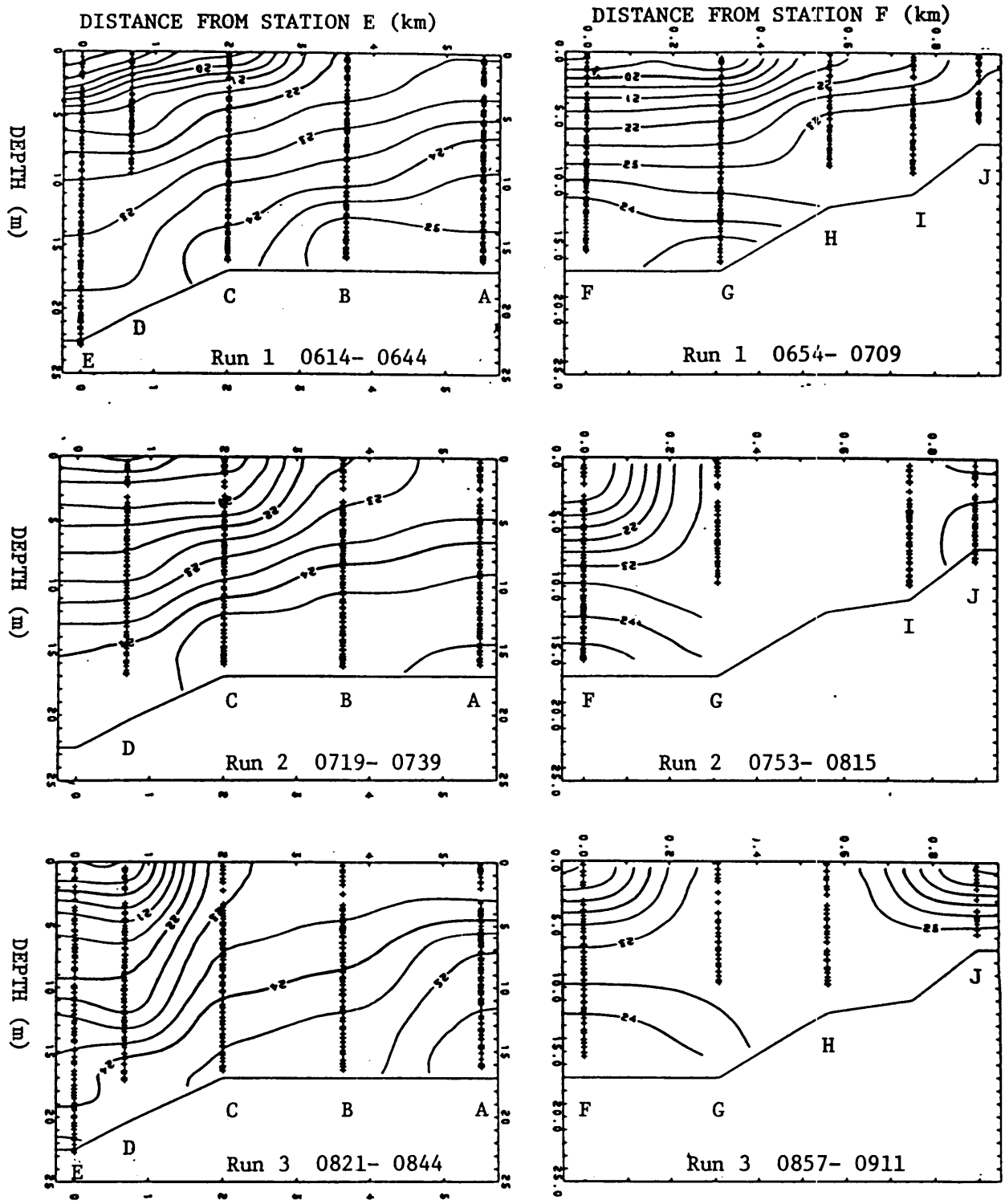

Figure IIIA-5. Salinity distribution (ppt), June 19, 1985 along transects shown in Figure IIIA-4. The "+" symbols indicate the location of each data point.

of the transect. Water of relatively uniform salinity, between 23 and 23.5 ppt, occupied half the local depth at stations H, I, and J. By the time of Run 2 and continuing through Run 3, water of this salinity filled the entire water column in the central portion of the transect.

In similar data sets obtained over the course of a year (see Appendix, section IIA-3), and in fact, even on a time scale of a week, substantial differences in some features of the salinity field were observed. For example, the vertical stratification on the downriver side of the front varied considerably, the top to bottom salinity difference ranging from about 1 to more than 8 ppt. Also, although the development of a surface salinity maximum within the lateral transect was fairly common during early flood, that salinity was not necessarily uniform to the bottom as it was on 19 June 1985. However, within these shifting patterns, the existence of strong density fronts during flood tide was a persistent characteristic of the hydrography near Newport News Point.

From other components of the field investigations, it is clear that the features referred to here as "fronts," i.e., the concentrated horizontal density gradients in the upper portion of these transects, are indeed associated with the visual surface features (color boundaries, foam lines, etc.) described in section 1 above, and thus with the location of surface convergent flow, but not necessarily in a one-to-one correspondence. Whenever surface manifestations of branch I or branch II were apparent, and two vertical profiles could be clearly identified as sampling opposite sides of the feature, a significant near-surface density difference was always observed. However, very early in the flood, relatively strong gradients

were often observed, for example between stations B and C, when corresponding surface signatures were vague and discernible only from aerial photos, if at all.

Although very useful, limitations of a density field description based on transects of vertical profiles should be kept in mind. Obviously, the horizontal resolution is limited by the inter-station spacing. When a front lies between two stations, the density "jump" may actually occur over a much shorter horizontal scale than indicated in the contour plots. Also, each transect is a slice through a complex frontal system with structure and motion in dimensions not sampled by the measurements in the plane of the transect.

B. Larval Studies

Oyster larval studies addressed the three following questions:

- Are there significant differences in numbers and sizes of larvae in the various water masses which converge at the frontal system?
- Are larvae passively transported through the frontal system?
- If larvae are passively injected into high salinity, deep, upstream flowing water at the frontal system, can they subsequently swim upwards into overlaying, low salinity water?

The first two questions were addressed by field studies in the vicinity of Newport News point. The last question was addressed by a laboratory study of oyster larval swimming behavior. Details of the design of field and laboratory studies are given below.

1. Design of Studies

a. Field. Oyster larvae are small, less than 0.3 mm length, and are capable of swimming in the water column. At the beginning of the study it was suspected that, during the oyster reproductive season in the James River (June - early October), oyster larvae occurred throughout the Hampton Roads area. From the physical oceanographic component of this report it is obvious that several distinct water masses (characterized principally by salinity signatures) converge at the frontal system off Newport News on flood tide. The objective was to know how many and what sizes of larvae occurred in each of the water masses that converge on the front. With such data in hand it would then be possible to examine larval numbers and sizes in water leaving the frontal system and, through comparison, determine whether larvae are possibly transported through the frontal system.

Oyster larvae in the water column were sampled using a plankton pump. This apparatus is described in detail in Appendix IIB-1. Plankton pump samples were collected upstream of the frontal system near the James River Bridge, south of Middle Ground in Hampton Roads, and on the northeast end of Hampton Flats. These characterize water masses a) flowing downstream in the James on the northeastern shore, b) flowing downstream on the southwestern shore and becoming part of an anticlockwise gyre in the Hampton Roads region and c) of higher salinity Hampton Roads, rather than James River, water flowing upstream toward Newport News Point on flood tide. A comparison of these "characterized" water masses was used in addressing question 1. as outlined previously.

To examine possible passive transport of larvae through the frontal system a series of stations was occupied on a transect that ran parallel to the direction of the current to bisect the frontal system. At each station the water column was at first characterized for temperature and salinity

using a conductivity-temperature-depth (CTD) profiling instrument. Distinct water masses were identified and subsequently sampled for larvae with the plankton pump. By characterizing both the water mass and the larval population at closely spaced stations across the front it was possible to determine whether or not larvae moved passively with the water masses.

b. Laboratory Studies. Downstream flowing surface water on the northeastern shore of the James at Newport News was characterized during the summer of 1985 by a salinity of 19 °/oo and a temperature of ~22°C. Upstreaming flowing surface water flowing over Hampton Flats to converge with the aforementioned downstream flowing water was characterized at 22 °/oo salinity and 22°C. At the frontal system off Newport News Point the more saline, upstream flowing water plunged beneath the downstream flowing water. The question was posed: if oyster larvae are entrained in the upstream flowing, 22 °/oo salinity surface water and are passively injected into deep, upstream flowing bottom water of the same salinity at the front can they eventually swim upwards into overlaying lower salinity water and therefore be subjected to subsequent downstream flow?

The culture of the oyster through its larval stages is now commonplace and accomplished regularly at the pilot oyster hatchery at the Virginia Institute of Marine Science (VIMS). The design of the laboratory component of the study was as follows. Oyster larvae at various stages of development were obtained from the VIMS hatchery and acclimated for a minimum of 24 hrs in the presence of food to 22 °/oo salinity water at 22°C. In an apparatus described in Appendix IIB-2 the larvae were introduced into the bottom of a laboratory generated water column in which 19 °/oo salinity water overlay 22 °/oo salinity water. The junction between the two water masses was distinct. The entire water column was maintained at 22°C. Following the

introduction of the larvae they were regularly "observed" to ascertain whether or not they would pass through the 19-22 °/oo interface and remain in the less saline water. In addition the rate of vertical movement of the larvae was recorded in order to allow estimation of the time required for a continually swimming individual to ascend through the complete water column in the James River at Newport News Point.

2. Results and Discussion

a. Field Studies. A summary of the numbers, size ranges and species composition of bivalve larvae obtained from field sampling on September 6, 19, and 20, and the sites of stations sampled are summarized in Table IIIB-1, Table IIIB-2 and Figure IIIB-1.

The plankton samples for each date are characterized, for each sampling site and depth, in terms of total larvae per 100 L of water sample, percentage of larvae of <150 μm length, and numbers of oyster larvae per 100 L in the size classes 150-250 μm and >250 μm length (Tables IIIB-3, IIIB-4 and IIIB-5).

Table IIIB-1 demonstrates the consistent presence of bivalve larvae, including oyster larvae, at all stations on all sampling days. The high numbers of larvae obtained is of special note. While it is gratifying to see such large numbers, it is appropriate to note that the data of Table IIIB-1 represent 15 man-months of sorting alone. The intensive nature of larval studies in the field is obvious.

Each of the three sampling days examined a slightly different array of stations. This "inconsistency" was forced due to the capability to sample only a limited number of stations and depths within the appropriate phase of the tide and when the frontal system was dominant as a surface feature (a period of 3-4 hours maximum). None the less, broad spatial coverage was

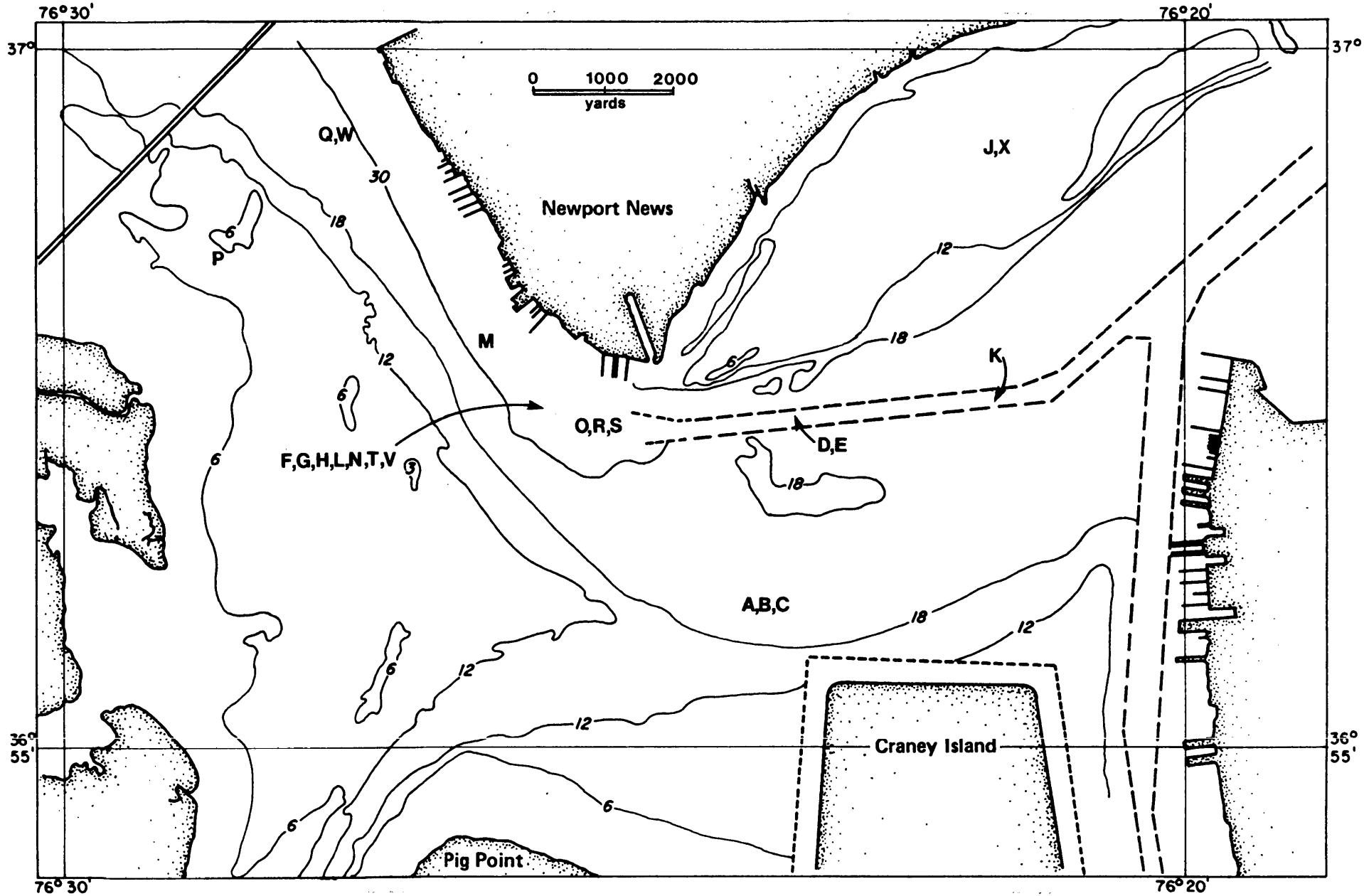

Figure IIIB-1. Location of stations sampled in Hampton Roads during field sampling, Sept. 6-20, 1986.

TABLE IIIB-1. Summary of bivalve larvae collected in field studies, Sept 6-20, 1985. All times are given as daylight savings time. For Eastern Standard Time subtract one hour e.g. 11:30 D.S.T. is 10:30 E.S.T. Station A-X is a key for sample location - see Table 4B-2. Depth and volume of sample are in m and L, respectively. Larval numbers are given as per sample and per 100L for the size classes <150 µm length (all species), 150-250 µm and >250 µm length (oysters), 150-250 µm and >250 µm (all species except oysters) and a grand total.

LARVAL COUNTS: SUMMARY

			Total						Per 100 L					
			<150	Oyster		Other			<150	Oyster		Other		
Ref/ Date Time	Depth m	Vol. L	All sp.	150-250	>250	150-250	>250	Grand Total	All sp.	150-250	>250	150-250	>250	Grand Total
9/6														
A 11:30	2	251	387	7	1	5	1	401	154	2.8	0.4	2	0.4	160
B 11:45	4	767	475	16	2	8	1	502	62	2.1	0.3	1	0.1	65
C 12:00	6	1296	841	43	6	114	13	1017	65	3.3	0.5	8.8	1	78
D 12:50	2	688	321	35	6	8	0	370	47	5.1	0.9	1.2	0	54
E 13:05	7	635	232	29	6	97	39	403	37	4.6	0.9	15	6.1	64
F 14:20	2	794	689	10	0	50	0	749	87	1.3	0	6.3	0	94
G 14:25	4	781	887	49	2	91	2	1031	114	6.3	0.3	12	0.3	132
H 14:30	7	728	794	25	3	74	15	911	109	3.4	0.4	10	2.1	125
9/19														
J 09:40	1	980	92	6	6	46	3	153	9.4	0.6	0.6	4.7	0.3	16
K 09:56	2	980	1159	22	78	361	17	1637	118	2.2	8.0	37	1.7	167
L 11:30	1.5	905	46	1	1	4	1	53	5.1	0.1	0.1	0.4	0.1	5.9
M 11:45	5	905	339*	63	20	101	8	531	38	7	2.2	11	0.9	59
N 12:10	9	905	1154	53	49	122	43	1421	128	5.9	5.4	14	4.8	157
O 12:40	5	1056	1020	52	114	224	9	1419	97	4.9	11	21	0.9	135
P 13:40	3	829	17	5	9	12	3	46	2.1	0.6	1.1	1.4	0.4	5.5
Q 14:05	5	1018	236	37	18	35	15	341	23	3.6	1.8	3.4	1.5	34
9/20														
R 12:00	7	980	930	19	13	63	7	1032	95	1.9	1.3	6.4	0.7	105
S 12:15	2	942	179	14	19	65	11	288	19	1.5	2	6.9	1.2	31
T 13:25	2	641	159	2	0	14	2	177	25	0.3	0	2.2	0.3	28
U 13:35	5	528	36	4	24	26	14	104	6.8	0.8	4.6	4.9	2.7	20
V 13:45	9	528	573	32	7	68	10	690	109	6.1	1.3	1.3	1.9	131
W 14:05	1	528	117	14	5	25	1	162	22	2.6	1	4.7	0.2	31
X 14:40	1	565	46	4	12	12	3	77	8.2	0.7	2.1	2.1	0.5	14

*mostly oysters

TABLE IIIB-2. Sampling location and station number for plankton sampling stations during field studies, Sept. 6-20, 1986.

Station	Location
A-C	Hampton Roads, middle ground
D-E	Newport News ship channel, south of Hampton Flats
F-H	Off Coal Pier, west of Newport News Point
J	Hampton Flats
K	Newport News ship channel, south of Hampton Flats
L-N	Newport News ship channel, 200m west of the frontal system
O	Newport News ship channel, 200m east of the frontal system
P	Southeast of Naseway Shoal on the southern bank of the James, south and west of the shipping channel under the James River Bridge.
Q	West-north-west of Newport News Shipbuilding, southeast of the James River Bridge and north of the shipping channel under the James River Bridge.
R-S	As for O
T-V	As for L-N
W	As for Q
X	As for J

TABLE IIIB-3. Characterization of plankton samples for September 6th. For each site and depth, samples are characterized by the following values: total number of larvae/100L, % of larvae <150 µm length, number of oyster larvae 150-250 µm length/100L, number of oyster larvae >250 µm length/100L.

Coal Pier (sta F-H)	Newport News Channel (sta D-E)
2m - 94, 92%, 1.3, 0	2m - 54, 87%, 5.1, 0.9
4m - 132, 86%, 6.3, 0.3	7m - 64, 58%, 4.6, 0.9
7m - 125, 87%, 3.4, 0.4	

Middle Ground (sta A-C)
2m - 160, 96%, 2.8, 0.4
4m - 65, 95%, 2.1, 0.3
6m - 78, 83%, 3.3, 0.5

TABLE IIIB-4. Characterization of plankton samples for September 19th. Data display as for 4B-3.

James River Bridge (sta Q)	Hampton Flat (sta J)
5m - 34, 69%, 3.6, 1.8	1m - 16, 62%, 0.6, 0.6

FRONTAL	SYSTEM
200m west (sta L-N)	200m east (sta O)
1.5m - 5.9, 87%, 0.1, 0.1	5m - 135, 72%, 4.9, 1.1
5m - 59, 64%, 7.0, 2.2	
9m - 157, 81%, 5.9, 5.4	

James River Bridge (sta P)	Newport News Channel (sta K)
3m - 5.5, 37%, 0.6, 1.1	2m - 167, 71%, 2.2, 8

TABLE IIIB-5. Characterization of plankton samples for September 20th. Data display as for 4B-3.

James River Bridge (sta W)	Hampton Flat (sta X)
1m - 31, 71%, 2.6, 1	1m - 14, 59%, 0.7, 2.1

FRONTAL	SYSTEM
200m west (sta T-V)	200m east (sta R-S)
2m - 28, 89%, 0.3, 0	2m - 31, 61%, 1.5, 2
5m - 20, 34%, 0.8, 4.6	7m - 105, 90%, 1.9, 1.3
9m -131, 83%, 6.1, 1.3	

obtained on September 6th while more intensive sampling in the frontal region was accomplished on September 19th and 20th.

Of the three stations sampled on September 6, the waters of Newport News channel east of the frontal system exhibited the lowest numbers/100L of all larvae combined; however, the numbers of oyster larvae of >150 μm length were higher than all other samples except for that from 4 m depth off the Coal Pier. The deeper sample from Newport News Channel was notably lower in <150 μm length larvae as a percentage of total larvae but contained comparable numbers of oyster larvae in the >150 μm length size classes.

The water column to the west of the frontal system and off the Coal Pier was sampled at 2, 4 and 7 m depth. The 2 m sample was characterized by a very high, 92%, proportion of <150 μm length larvae, low numbers of 150-250 μm length oyster larvae and the absence of >250 μm oyster larvae. The low values for >150 μm length oyster larvae seen in the 2 m depth sample are not comparable with those seen in the 4 m and 7 m samples. The values for the latter are more closely allied to those seen in the Newport News channel station. The percentage of <150 μm length larvae in the 4 m and 7 m samples from the DTA Coal Pier station are comparable to that recorded at 2 m in the Newport News channel. Indeed, a comparison of temperature and salinity profiles from the two stations (Figure IIIB-2) illustrates the strong similarities in physical characteristics of water at sample locations D ($27^{o}C$, 20.5 $^{o}/oo$), G ($27.5^{o}C$, 20.5 $^{o}/oo$) and H ($26.8^{o}C$, 21 $^{o}/oo$). The physical and biological data combined support the suggestions that 1) surface water originating in Newport News channel "plunges" beneath surface waters originating upstream of Newport News Point as the former moves east to west through the frontal system, and 2) larvae move passively with the "plunging" water. Note also that the deep water sample, E, from 7 m in the

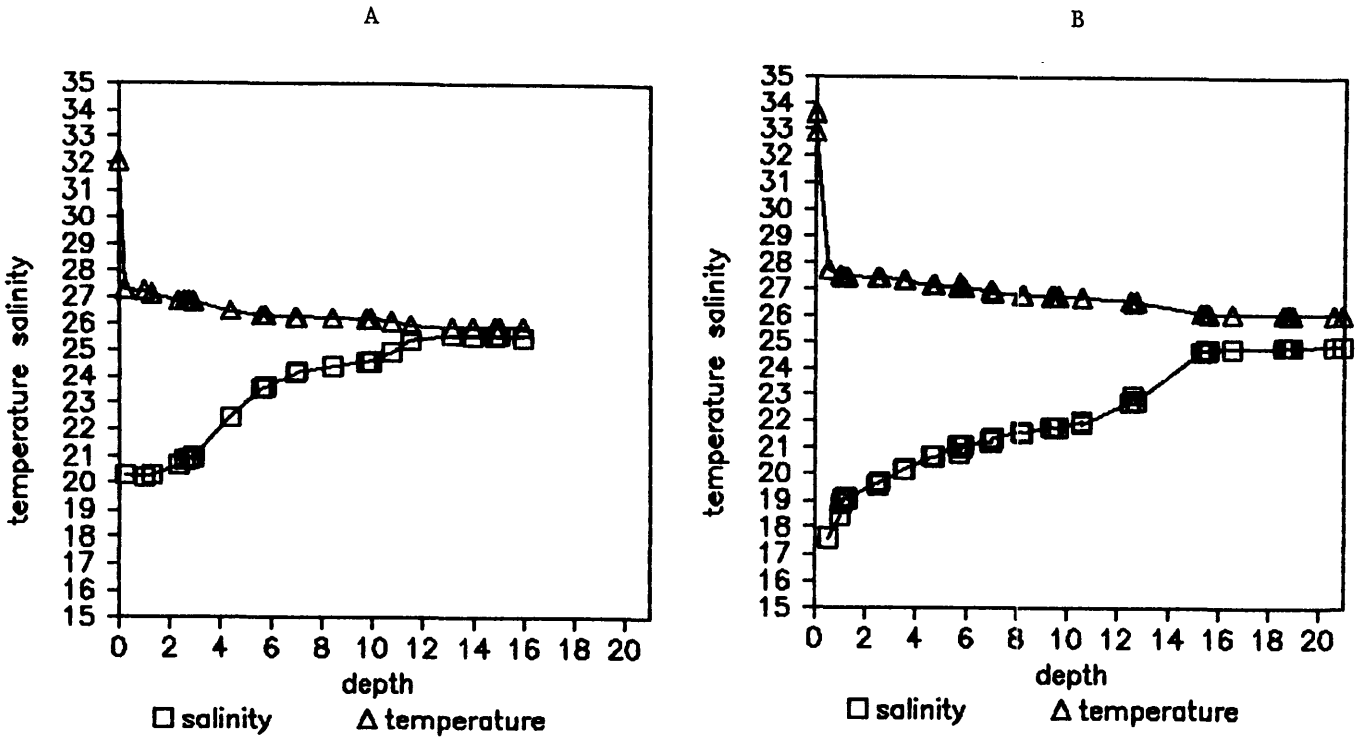

Figure IIIB-2. Temperature and salinity profiles for water column stations D-H inclusive as sampled on Sept. 6, 1985. Depths of samples were as follows: D = 2 m, E = 7 m, F = 2 m, G = 4 m, H = 7 m. Temperature in °C, salinity in °/oo. (A) corresponds to samples D and E to the east of the surface frontal feature. (B) corresponds to samples F, G, and H to the west of the frontal feature. For sample locations see Figure IIIB-1.

Newport News channel is at a temperature and salinity (26.2°C, 24 °/oo) corresponding to a depth of 15 meters upstream of the front (Figure IIIB-2)--a depth that was not sampled at the latter location.

Despite the similarities in the deeper samples from the DTA Coal Pier station and the shallow station in the Newport News channel, a considerable difference is apparent in the total number of larvae present per 100 L. The obvious question arises as to whether or not larvae are concentrated in "patches"? There is no good evidence to support or refute this suggestion with respect to mollusc larvae in estuaries. The samples collected in this study took between 4 and 10 minutes to collect and were collected in fairly rapid succession. If "patchiness" existed, it would either have been observed by the procedure or have overwhelmed it, depending upon its temporal and spatial stability and its co-occurrence with sampling. The present data cannot quantify the possible impact of patchiness; however, it may have occurred during the course of the study.

Plankton sampling on September 19th included four stations that were distant from the frontal system (Hampton Flats, J, and Newport News Channel, K, to the east, and two James River Bridge, P and Q, stations to the west) plus stations approximately 200 m east and west of the surface feature.

The Hampton Flats sample, J, contained low numbers of larvae and a comparatively low percentage of <150 µm length larvae. Some oyster larvae of >150 µm length were present. By contrast the Newport News Channel sample, K, contained over an order of magnitude greater number of larvae and a notably high number of >250 µm length oyster larvae. The sample taken at 5 m depth and 200 m east of the front, O, showed strong similarities to the Newport News Channel station in terms of numbers of larvae, percentage of larvae <150 µm length, and the presence of >150 µm oyster larvae. All three

samples came from water of similar temperature and salinity (J at 21.8°C, 23.5 °/oo, K at 22°C, 23.5°/oo, O at 22.3°C, 23.5 °/oo - see Figure IIIB-3).

An increasing number of larvae were seen with increasing depth (1.5, 5 and 9 m) to the west of the front. The 1.5 m sample, L, was characterized by a high percentage of <150 μm length larvae (the highest of any sample collected on that day and very low concentrations of >150 μm length oyster larvae. Higher (both absolute and proportionate) concentrations of >150 μm length oyster larvae were seen at 5 m, M, and 9 m, N, at the same station. These values were similar to those observed at 5 m depth and 200 m east of the front, sample O, and at the Newport News Channel station, K; however, in only the 9 m sample did the absolute numbers of larvae closely resemble sample O. Figure IIIB-3 illustrates the temperature and salinity profiles for stations J-Q inclusive as occupied on September 19th. Stations L and M are presented separately to station N in that during sampling for L and M upstream drift of the vessel was recorded (see Fig. IIIB-1). Prior to collection of sample N the vessel was repositioned closer to the front and a further temperature-salinity profile recorded --that illustrated for sample N. Note that during the intervening period, 66 minutes, the salinity of the water column had increased uniformly by 0.3 - 0.4 °/oo throughout its entire depth yet the shape of the profile changed very little. The frontal system, rather than being a boundary of fixed salinity, is a progressive feature at which salinity may increase as flood tide progresses. The 0.3 - 0.4 °/oo uniform increase in salinity seen at the fixed position corresponding to stations L and N simply reflects the progression of the front with the flood tide. Temperature and salinity characteristics of station O (22.3°C, 23.5 °/oo) were similar to station N (22.3°C, 23.2 °/oo) but of higher salinity, even allowing for the 0.3 - 0.4 °/oo temporal salinity change described

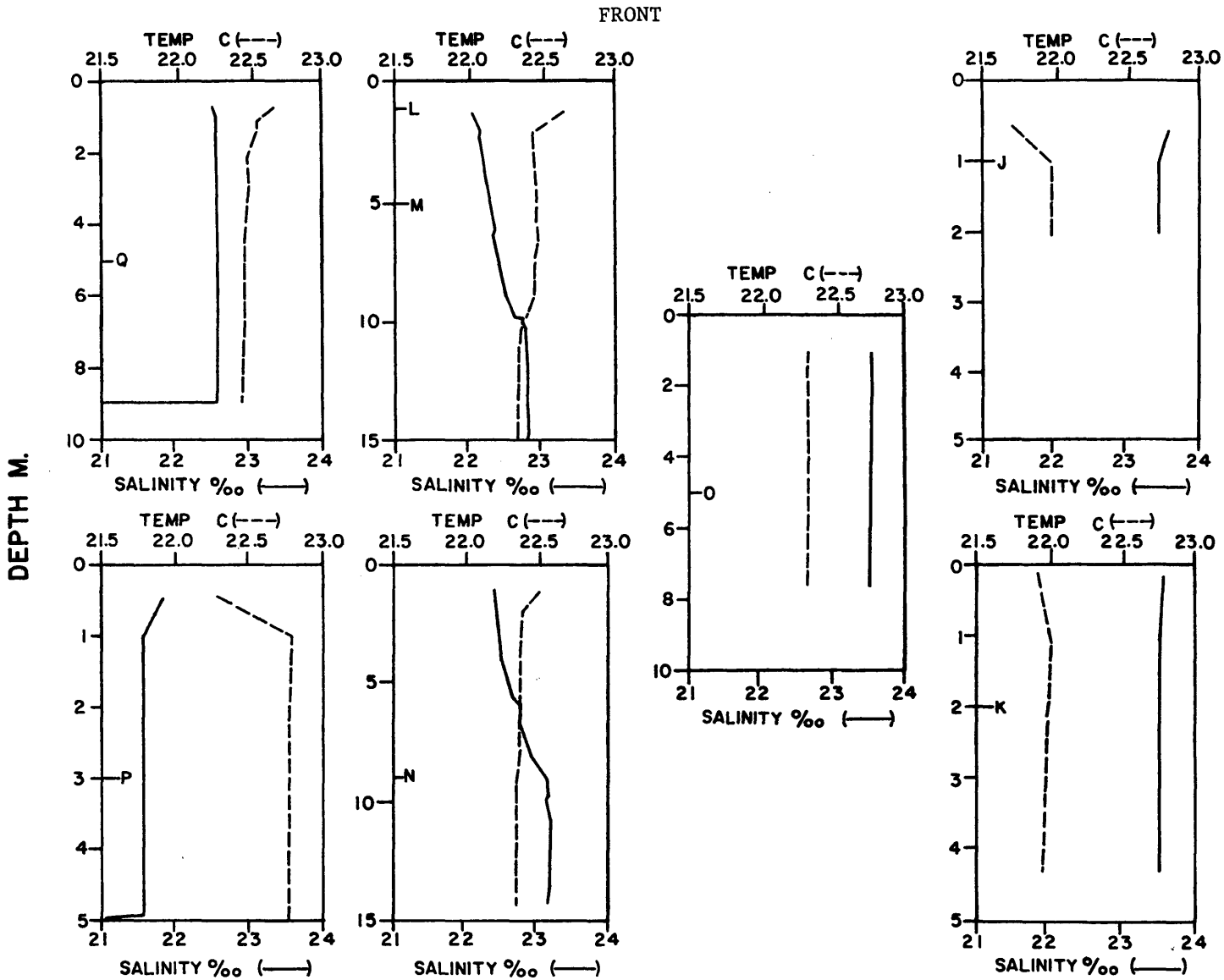

Figure IIIB-3. Temperature and salinity profiles for water column stations J-Q inclusive, as sampled on Sept. 19, 1985. Depth of sampling indicated by corresponding letter on the figure. The surface frontal feature is between samples L-N (west of front) and O (east of front). For sample location see Figure IIIB-1.

earlier, than stations M (22.4°C, 22.3 °/oo) and L (22.7°C, 22 °/oo). The physical and biological data collected at stations L, M, N and O are in close agreement in supporting a suggestion of water plunging to depth as it flows from east to west across the frontal system.

Samples collected near the James River Bridge on September 19th had both low concentrations of larvae of <150 μm length, especially so at station P on the south side of the River. At station P oyster larvae of >150 μm length represented 31% of the total larvae, a markedly high percentage compared to all other samples and higher than the 16% by number of oyster larvae of >150 μm length recorded at station Q.

Station Q was originally intended as a reference station for station L, that is surface, downstream flowing water on the north bank of the River. Table IIIB-4 clearly illustrates the difference in stations Q and L. The reason for this difference lies partly in the sampling regime used. The temperature and salinity profiles at Q suggested that the water was well mixed, at least below 2 m. A sample was taken at 5 m. In fact, the temperature and salinity values for Q (22.45°C, 22.6°/oo) are intermediate between those of M and N (see Figure IIIB-3) suggesting that Q sampled a mixture of upstream flowing high salinity water containing a high proportion of >150 μm length oyster larvae (see data from station M and N in Table IIIB-4) and downstream flowing water. Note also that the sampling regime assumes vertically homogenous distribution of larvae in the water column. Larval behaviour experiments, described elsewhere in this report, suggest strongly oriented upward swimming by smaller (<160 μm length) larvae. If indeed such larvae exhibit net surfaceward motion and aggregation at the site of station Q (perhaps in the warmer surface layer of 2 m depth) then an elevated percentage of larger larvae, when compared to a truly homogenous

water column, would be found at Q -- as in fact was the case. Sample P, like Q, was taken from an apparently well mixed water column (see Figure IIIB-3); however, salinity at this station was considerably lower than all other stations for that date.

Plankton sampling on September 20th was effected at four locations; on Hampton Flats in 1 m (X), 200 m to the east (R-S inclusive) and west (T-V inclusive) respectively of the front, and on the northern side of the James in the vicinity of the James River Bridge (W). The Hampton flats (X) and the shallow, 2 m station (R) to the east of the front both exhibit relatively low total numbers of larvae per 100L, comparable percentages of <150 μm length fractions and comparable number of oyster larvae of >150 μm length. Of special note is the greater number of >250 μm length oyster larvae than 150-250 μm length larvae in both collections. The 7 m collection(s) taken 200 m east of the front had, by comparison, higher absolute numbers of larvae and percentage of <150 μm length larvae. The oyster larvae >150 μm length were comparable in number to those at shallower depth but the 150-250 μm size range predominated.

To the west of the frontal system at 2 m depth (T) a relatively low number of larvae per 100L was again evident; however, these were predominantly <150 μm in length and oyster larvae of >150 μm length were almost absent. Clearly the composition of larvae at stations T and R, at equal depth but an opposite sides of the front, were markedly different.

On September 20th larval sampling was effected in conjunction with a dye release study. Dye was released at the surface downstream (to the east) of the front. Dye moved to the front at the surface, then plunged to be recorded at depths of 5-9 m upstream (west) of the front (for accompanying temperature and salinity data see Figure IIIB-4). Consequently larval

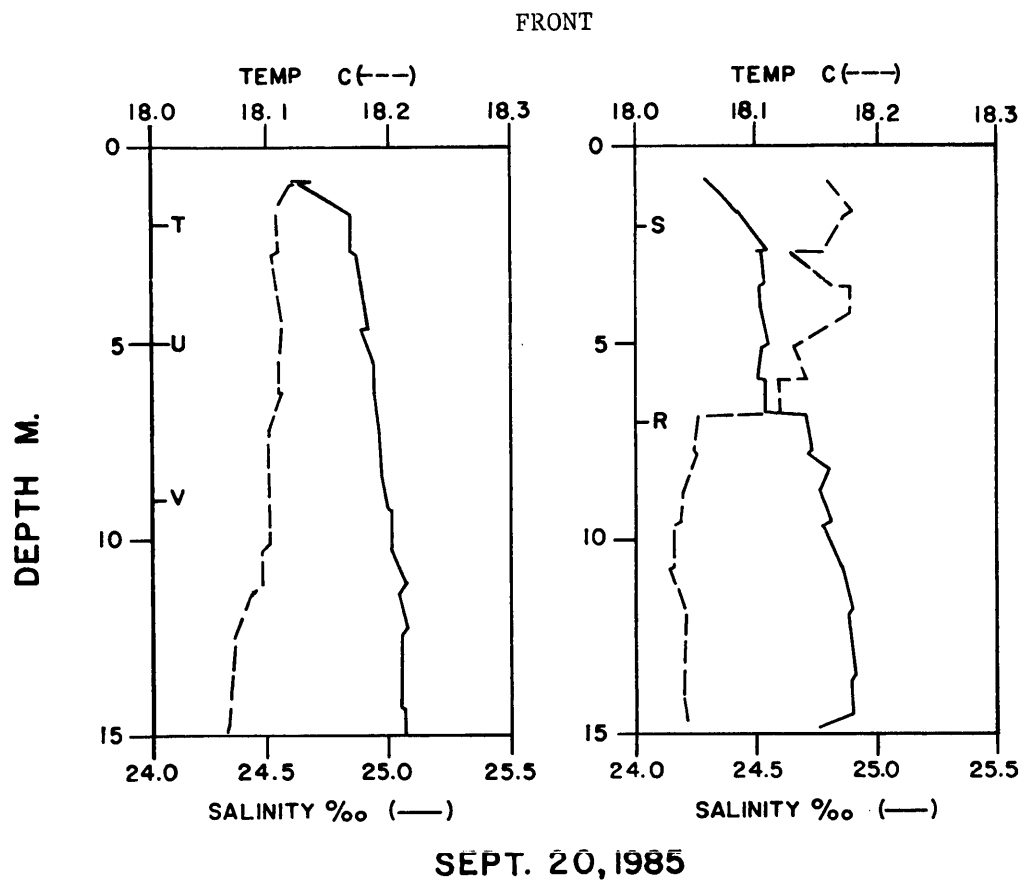

Figure IIIB-4. Temperature and salinity profiles for water column at stations R-V inclusive, as sampled on Sept. 20, 1985. Depth of sampling indicated by corresponding letter on the figure. For sample location see Figure IIIB-1. The position of the surface frontal feature lies between samples T-V inclusive (to west of front), and S-R inclusive (east of front).

sampling at stations U and V was effected at 5 and 9 m respectively. At 5 m (U) only 20 larvae/100L were observed, a value between that recorded at stations R and X to the east of the front. A further notable similarity between samples U, R and X is the low percentage of <150 μm length larvae and the proponderance of >250 μm length larvae in the >150 μm fraction. The similarity between samples U, R and X again support the contention that larvae are, like dye, transported passively at the frontal system. At 9 m depth (V) larval concentrations, size distribution and species composition closely resembled that of the slightly shallower station, S, located 200 m to the east of the frontal system suggesting continuity from S to V.

Upstream to the frontal system near the James River Bridge 31 larvae/100L were recorded. Although the <150 μm length larvae comprised a smaller percentage of this total (71%) than at T (89%) this percentage was still notably higher than at stations, U, R and X (34, 61 and 59% respectively) suggesting stronger continuity between stations W and T than X, R, U and W; however the occurrence of mixing of upstream flowing bottom water with downstream flowing water at station Q on the previous day (September 19th) has already been discussed and should be reiterated here in that W and Q occupy the same geographical location. (Stations W and Q were not; however, occupied on <u>exactly</u> the same state of tide). The aforementioned "mixing" may well provide explanation for the presence of greater numbers of >150 μm length oyster larvae at W than at T.

In summary the results of three days of intensive sampling for bivalve larvae in general (and oyster larvae in particular) in the Hampton Roads region are presented. Each day examines a slightly different aspect of larval distribution with respect to a predominant physical feature, a frontal system, which occurs in the vicinity of Newport News Point on the flood

tide. The results generally support the contention that in the immediate vicinity of the front larvae of oysters and other bivalves are passively transported - that is they are carried from east to west through the front and at the front plunge to depth as more saline water encounters less saline water. The results further suggest that this passive transport continues, at least in part, as the more saline water continues to travel upstream west of the front towards the James River Bridge. At distance upstream of the front, in the vicinity of stations Q and W, dispersal of bivalve larvae, including oyster larvae probably results from both passive movement, including that associated with mixing of upstream and downstream flowing waters, and active depth regulation through swimming.

b. Laboratory Studies. The rationale, experimental apparatus and experimental procedures used in examining the swimming behavior of oyster larvae in isothermal salinity gradients is described in detail in Appendix IIB-2.

Intensive examination of larval swimming was examined in three size ranges of larvae from three different larval cultures. Straight hinge larvae, the first shelled stage corresponding to ~24 hrs post fertilization and the <150 m stage of the field plankton samples, readily swim through a 3 °/oo salinity interface, (19 °/oo over 22 °/oo). This sharp interface is of greater magnitude than any recorded during the previously described field studies suggesting that salinity stratification in isolation does not present a barrier to vertical movement of oyster larvae of this size. One hundred and seventy measurements of larval swimming speed (defined here as rate of vertical movement in the water column; this differs from absolute velocity which incorporates the helical swimming pattern) were made for straight hinge larvae (length = 75.0 µm, S.D. = 4.7 µm, 95% C.I. = ± 1.68

μm, N=30) and a mean velocity of 0.366 mm/sec (S.D. = 0.8032 mm/sec, 95% C.I. = ± 0.121 mm/sec) recorded. At such a velocity 1 m depth of water column would be ascended in 45 minutes, a 5 m water column in 3 hrs 45 mins. Clearly, even these smallest of shelled oyster larvae can ascend through a significant portion of the water column in the James River in the time interval corresponding to one flood or ebb tide.

As oyster larvae develop and grow the hinge line is occluded by a protruding, assymetrical umbo. Such larvae are termed "umbo" larvae and generally correspond to the >150 μm length fraction in the field collected samples. Note the term "generally". Umbo development is gradual with increasing length. The 150 m length division is arbitrary. Two, independent examinations of swimming of "umboed" larvae were made. Both studies show that, like straight hinge larvae, these larger size classes also swim, without hesitation, through salinity interfaces of 3 °/oo (19 °/oo over 22 °/oo). In the first examination with 157.5 m length larvae (SD = 15.87 μm, 95% C.I. = 5.68 μm, N=30) 120 recordings of swimming speed were made and a mean value of 1.016 mm/sec (S.D. = 2.003 mm/sec, 95% C.I. = ± 0.089 mm/sec) recorded. In the second examination of 159.9 m length larvae (S.D. = 18.40 μm, 95% C.I. = ± 6.58 μm, N=30) 63 recordings of swimming speed were made and a mean value of 0.719 mm/sec (S.D. = 1.257 mm/sec, 95% C.I. = ± 0.31 mm/sec) recorded. These mean swimming speeds correspond to ascent through 1 m of water column in 17 minutes and 23 minutes respectively; 5 m water columns in 1 hr 25 mins and 1 hr 55 mins respectively. Clearly, depth regulation in the depth of the James River water column during the period of a tidal ebb or flood through swimming is tractable for umbo larvae.

Examination of swimming in larger oyster larvae was restricted by time and availability of larvae to pediveliger stage larvae. These are the

stages competent to settle, having both a velum (swimming organ) and a foot (for crawling). In extended observations in the presence and absence of oriented light and food in all combinations the investigators did not observe swimming of larvae through the salinity interface - indeed larval swimming was restricted to small (<5 cm) but frequent excursions from the chamber bottom (perhaps aptly described as "bouncing". These larvae were of large size (length = 317.2 μm, S.D. = 13.25 μm, 95% C.I. = ± 4.74 μm, N=30). Due to the "bouncing" nature of the swimming behavior no ecologically meaningful measurements of swimming speed could be made. Clearly, these results suggest that such larvae do not seek to depth regulate in the midst of the water column but, rather, near the sediment-water or substrate-water interface.

C. Significance of the Front to the Larval Transport System

The studies utilizing surface dye injection demonstrate that the upper layer of the water column downriver of the front is vertically displaced and passes beneath the overlying less saline water. This occurs at a transition to deeper water depths with enlarged section width which allows lateral spreading as well. Peak dye concentrations penetrated to depths exceeding 4 to 5 meters.

Field sampling for bivalve larvae, although limited, recovered oyster larvae at stations throughout Hampton Roads and at all depths sampled (1 to 9 meters). The results from sampling on either side of the frontal system generally support the hypothesis that larvae are passively injected to depth by the circulation induced. However, the laboratory studies demonstrate that oyster larvae less than 250 μm in size can swim upward through salinity

differences typically noted at the front ($\Delta S \simeq 3$ °/oo). Measured rates of swimming varied between 0.37 mm/sec (straight hinge, <150 μm) and 0.72 to 1.02 mm/sec (umbo stage, 150-250 μm). These swimming rates also support the contention that the larvae would be forcibly transported to depth. Results of current meter observation (Appendix IIA-2) suggest that the width of the frontal structure is of the order of 100 meters. Taking the depth of the front as 5 m the vertical velocity of the ingested surface water may then be estimated as the product of the horizontal component of the approach velocity and the aspect ratio (depth to width = 5/100 = .05). For an approach velocity of 0.5 m/sec the vertical velocity component is then approximately 25 mm/sec. Thus, the vertical injection velocity is an order of magnitude larger than the larval swimming rate.

Given the above noted range of larval swimming rates larvae could transit a five meter column of water over a time range of 1.5 to 3.75 hours if upward swimming was continuous. However, depth regulation is likely effected by the combination of upward swimming with passive or actively regulated sinking. Thus, the above noted excursion times must be viewed as minimum times.

The sum of the evidence indicates that the frontal system is a significant link in the larval transport process. During flood current phase oyster larvae in the surface waters are injected to depths where the net motion is upstream. During the following ebb current phase some of these larvae are recycled into Hampton Roads. Those that depth regulated toward the surface may be re-entrained through the front. Of the total larvae transported into Hampton Roads from the seed oyster beds some remain in Hampton Roads, some are lost due to leakage into the lower Bay and those

remaining are ultimately exposed to the upriver pumping action induced by the frontal system.

D. Theoretical Model for Front

1. Theoretical Considerations

To investigate the parameters controlling the frontal processes, in particular the diving depth of the heavier water, the dynamics of flow in the vicinity of the front are considered. The movement of the front is assumed to be sufficiently slow that a quasi-steady condition holds. In the following, a one-dimensional analysis is employed in a way analogous to that used to analyze a hydraulic jump in an open channel.

Figure IIID-1 depicts a uniform fluid of density ρ flowing toward a topographic gradient with a uniform velocity u_1, and depth y_1. If u_1 is large enough, the heavier fluid will push the lighter fluid to the right until it reaches the change in bottom elevation, which enhances the gravitational effect and stabilizes the frontal location. The heavier fluid dives beneath the lighter fluid, resulting in a sloping interface. The shear stress at the interface of two fluids will induce a slow counterclockwise circulation within the layer of lighter fluid. This is analogous to the triggering and stabilization of a hydraulic jump by a rise in bottom elevation in a supercritical open channel flow.

It is assumed that at a short distance downstream of diving, the flow of heavier fluid reaches another state of uniform flow with velocity u_2 and depth of y_2. Therefore, neglecting the entrainment of lighter fluid, the continuity equation becomes

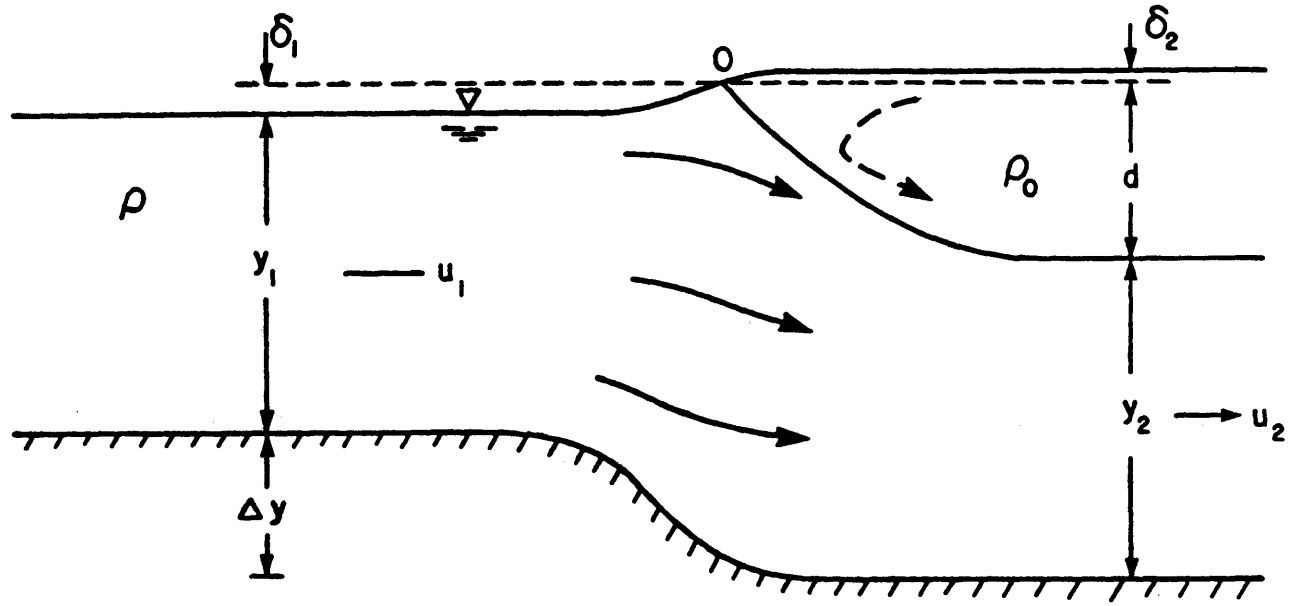

Figure IIID-1. Definition sketch for the analysis of diving of heavier fluid at front.

$$u_1 y_1 = u_2 y_2 \qquad \text{(IIID-1)}$$

Assuming that the bottom and interfacial friction is negligible over the length of flow transition and that the velocity of the lighter fluid is so small that δ_2 is also negligible, the momentum balance between sections 1 and 2 may be written as

$$\rho u_1^2 y_1 + \rho g \frac{y_1^2}{2} + \rho g (y_1 + \frac{\Delta y}{2}) \Delta y = \rho u_2^2 y_2$$

$$+ \rho_o g \frac{d^2}{2} + (\rho_o g d + \rho g \frac{y_2}{2}) y_2. \qquad \text{(IIID-2)}$$

where g is gravitational acceleration, ρ_o is the density of the lighter fluid, Δy is the drop in bottom elevation and d is the depth of diving of the heavier fluid. The last term on the left hand side of the equation represents the component of pressure force, in the direction of flow, at the sloping bottom. The second term on the right hand side of the equation represents the pressure force at the interface between the two fluids.

Substituting $d = y_1 + \delta_1 + \Delta y - y_2$, equation (IIID-2) yields

$$\frac{1}{2} \varepsilon \rho_o g (y_1^2 + \Delta y^2) = \rho (u_2^2 y_2 - u_1^2 y_1) + \frac{1}{2} \rho_o g [2\delta_1 (y_1 + \Delta y) + \delta_1^2]$$

$$+ \frac{1}{2} \varepsilon \rho_o g y_2^2 \qquad \text{(IIID-3)}$$

where

$$\varepsilon = \frac{1}{\rho_o} (\rho - \rho_o)$$

The point O in Figure IIID-1 is a stagnation point, and the pressure is zero everywhere along the free surface. Hence, by application of Bernoulli's theorem along the free surface, it follows that

$$\delta 1 = \frac{u_1^2}{2g} \qquad \text{(IIID-4)}$$

Restricting to cases with $\delta_1 \ll y_1$, and neglecting the second order term δ_1^2 equations (IIID-3) and (IIID-4) are combined to yield

$$\frac{1}{2}\,\varepsilon\rho_o g[(y_1 + \Delta y)^2 - y_2^2] = \rho(u_2^2 y_2 - u_1^2 y_1) + \frac{1}{2}\,\rho_o u_1^2\,(y_1 + \Delta y) \qquad \text{(IIID-5)}$$

Making the Boussinesq assumption in equation (IIID-5) and combining the result with equation (IIID-1) provides

$$\frac{1}{2}\,\varepsilon g[(y_1 + \Delta y)^2 - y_2^2] = u_1^2\left(\frac{y_1^2}{y_2} - \frac{y_1}{2} + \frac{\Delta y}{2}\right)$$

or

$$\frac{u_1^2}{g y_1} = \frac{y_2[(y_1 + \Delta y)^2 - y_2^2]}{2y_1^3 - y_1^2 y_2 + \Delta y\, y_1 y_2} \qquad \text{(IIID-6)}$$

or

$$F_1^2 = \frac{Y[(1 + \Delta Y)^2 - Y^2]}{2 - (1 - \Delta Y)Y} \qquad \text{(IIID-7)}$$

where the dimensionless parameters are defined as

$$Y = \frac{y_2}{y_1},$$

$$\Delta Y = \frac{\Delta y}{y_1} ,$$

and

$$F_1 = \frac{u_1}{\sqrt{\varepsilon g y_1}}$$ the densimetric Froude number

If applied to a channel of flat bottom, equation (IIID-6) is reduced to

$$\frac{u_1^2}{\varepsilon g y_1} = \frac{y_2(y_1^2 - y_2^2)}{y_1^2 (2y_1 - y_2)} \qquad \text{(IIID-8)}$$

which was derived by Benjamin (1968) in his analysis of gravity currents. Figure IIID-2 presents a graph of the dimensionless quantity Y plotted against F_1 with various values of the parameter ΔY.

The foregoing development is based on the assumption that momentum is conserved between sections 1 and 2. It is expected that the abrupt discontinuity at the point of diving of the heavier fluid involves a continuous transformation of kinetic energy of translation into kinetic energy of rotation, or turbulence, thus resulting in energy dissipation. The Bernoulli relationship between sections 1 and 2 may be written as

$$\frac{1}{2} \rho u_1^2 + \rho g(y_1 + \Delta y) = \frac{1}{2} \rho u_2^2 + \rho g y_2 + \rho_o g d + \rho g \Delta h \qquad \text{(IIID-9)}$$

where Δh is the total head loss between sections 1 and 2.

Again, applying the Boussinesq assumption and neglecting the second order term of ε, it follows that

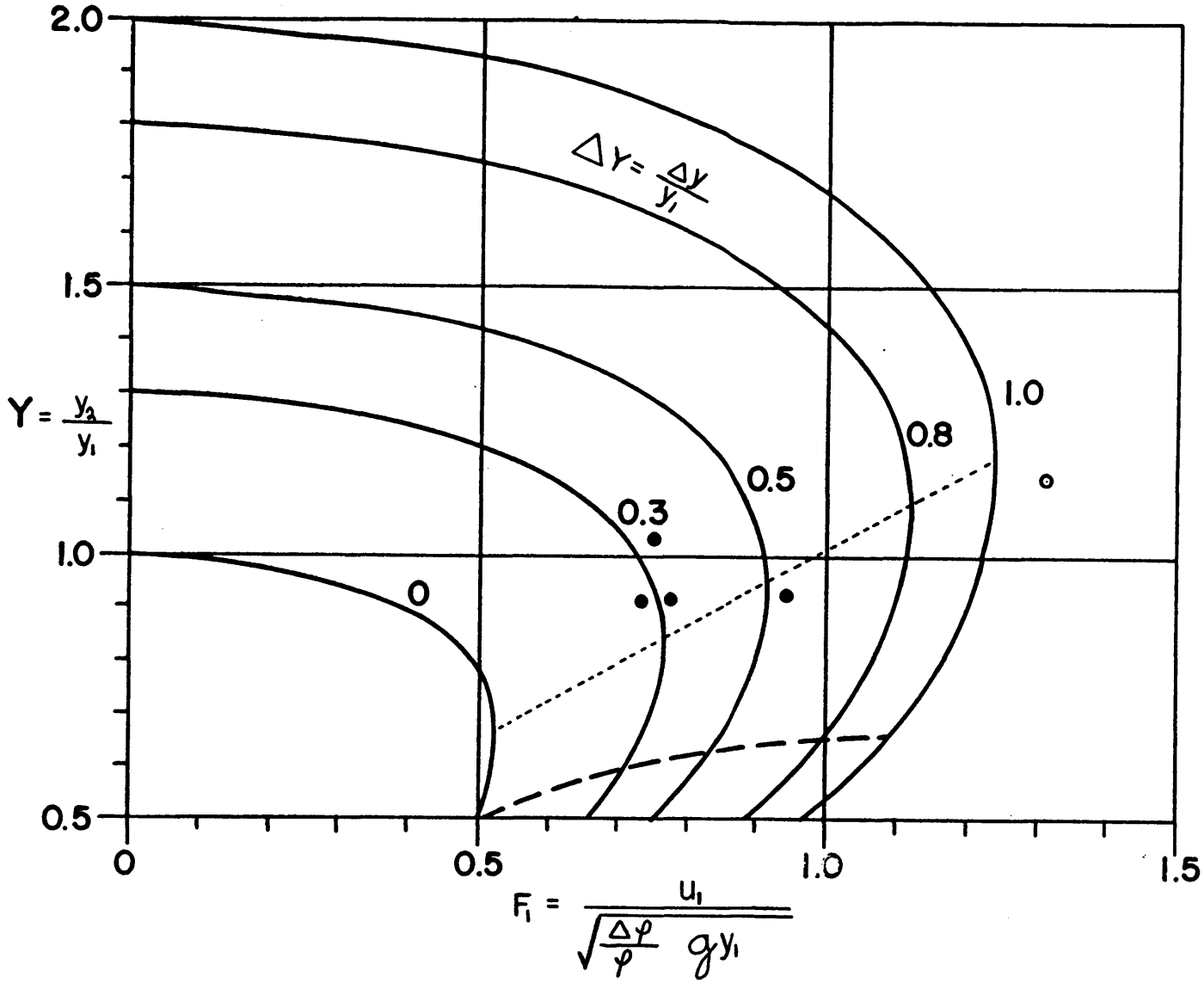

Figure IIID-2. Front characteristics as dimensionless function of the densimetric Froude number, with demensionless bottom change ΔY as parameter. (The experimental data point o is for $\Delta Y = 1.0$ data point • is for $Y = 0.3$)

$$\frac{\Delta H}{\varepsilon} = 1 + \Delta Y - Y - \frac{F_1^2}{2Y^2} \qquad \text{(IIID-10)}$$

where the dimensionless head loss

$$\Delta H = \frac{\Delta h}{y_1}$$

Since ΔH is always positive, the practically realizable flow must satisfy the condition

$$F_1^2 \leq 2Y^2(1 + \Delta Y - Y) \qquad \text{(IIID-11)}$$

Combining equations (IIID-7) and (IIID-11) provides the possible values of Y as

$$(2Y - 1)(Y-1) \leq \Delta Y(2Y^2 - 1) \qquad \text{(IIID-12)}$$

which gives

$$1/2 \leq Y \leq 1$$

for $\Delta Y = 0$. The dashed line in Figure IIID-2 marks the lower limit of Y for which flows are impossible.

Figure IIID-2 shows that, for each ΔY, there is a critical Froude number, F_c, above which no steady state solution exists. If the densimetric Froude number of the incoming flow is greater than F_c, the inertial force dominates over gravitational force, and the heavier fluid will push the

lighter fluid away. Under this condition, the analysis is applicable for the case of a flat bottom, if all velocities are taken relative to the front. Within a certain range of Froude numbers smaller than F_c, there are two possible values of downstream depth after the heavier fluid dives. It may be shown that one of the possible depth produces supercritical flow and the other subcritical flow. The two depths are related to each other by the familiar hydraulic jump equation (e.g. see Rouse 1946, p. 145),

$$\frac{y_2}{y_2'} = \frac{1}{2}\left(\sqrt{1 + 8F_2^2} - 1\right) \qquad \text{(IIID-13)}$$

where y_2' is the alternative depth and

$$F_2 = \frac{u_2}{\sqrt{gy_2}}$$

It is also seen that when $F_1 = F_c$, there is only one possible depth, y_2, which corresponds to $F_2 = 1.0$. Under this condition, the energy required to push the flow through is minimum and the flow transition dissipates the maximum allowable energy loss. This is the critical condition beyond which the diving of heavier fluid at a fixed location is impossible.

The fact that no solution exists if F_1 is greater than F_c may imply an important characteristic of the front. It may be inferred by the analogy to the critical condition, i.e., Froude number equals unity, in a homogeneous open channel flow. A result of one-dimensional analysis of open channel flow states that the critical condition is a state of flow in which, under given discharge, the specific head (or, equivalently, the energy) is minimum

and, under given specific head, the discharge is maximum. The above analysis of flow transition through the front reveals that when the densimetric Froude number of the incoming flow equals the critical value, that of the flow after transition is unity. The flow thus attains a state of minimum energy which is required to push the fluid through , or equivalently, the discharge q through the front is at the maximum allowable value

$$q_{max} = u_c\, y_1 \tag{IIID-14}$$

where

$$u_c = F_c\, \sqrt{\varepsilon g y_1} \tag{IIID-15}$$

the critical velocity corresponding to F_c under given ε and y_1. If the incoming flow has a velocity greater than u_c, the front will not be able to accommodate the discharge $u_1 y_1$. Therefore, it wil be pushed away to maintain the discharge through the front equal $u_c y_1$. The front must move with such a speed that the relative veocity of the incoming flow with respect to it be u_c. In summary, the discharge through the front is flow-limited, i.e.,

$$q = u_1 y_1, \text{ if } u_1 \leq u_c \tag{IIID-16a}$$

or front limited, i.e.,

$$q = u_c y_1, \text{ if } u_1 \geq u_c \tag{IIID-16b}$$

2. Application of the Theoretical Results

The fronts around the Newport News Point of the James River are mostly observed in the area of steep bottom slope. They move slowly upriver at a velocity of order of 10 centimeters per second or less. We will attempt to interpret our observations in light of the theoretical results presented in the previous section. The river bottom along the flow path of the flooding current is considered to be composed of a long flat bottom (the navigation channel or Hampton Flats) followed by a steep slope and then by another flat bottom of much greater depth.

The development of fronts along the Newport News Channel (Branch II of Figure IIIA-1) is depicted in Figure IIID-3. It is assumed that there is a density (salinity) discontinuity, or strong longitudinal density (salinity) gradient, somewhere in the channel at slack-water before flood ($t = 0$). When the flooding current $u_1(t)$ begins attempting to push the lighter water to the right, the Froude number F_1 is small enough that the diving of heavier water at fixed location is possible, however the diving depth would be small. As $u_1(t)$ increases, $(t = t_2)$ the diving depth increases as a result of increasing F_1. Currents measured in the channel indicate that the flood current increases with a rate faster than a sinusodial curve. As the flooding current rapidly increases and the Froude number F_1 exceeds the critical value ($F_c = 0.527$, for $\Delta y = 0$), the diving of the heavier water at a fixed location becomes impossible. The front is pushed upriver such that the Froude number remains at the critical value if u_1 is taken to be the velocity relative to the front. Therefore, the whole interfacial structure is pushed upriver rapidly without much change in shape ($t_2 \leq t \leq t_3$).

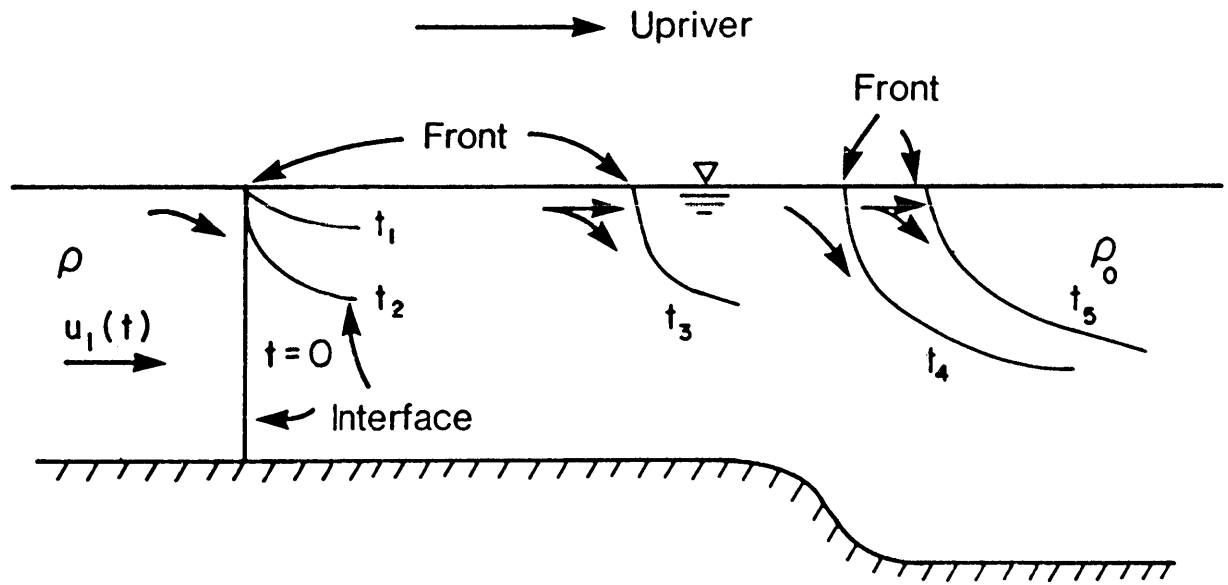

Figure IIID-3. Conceptualized model of front evolution along the Newport News Channel.

As the density interface is pushed beyond the end of the dredged channel to the region of sloping bottom, F_1 decreases because of increasing depth y_1, while F_c increases because of bottom relief. At some point where $F_1 = F_c$, the front becomes stationary, $(t = t_4)$. As the flood current continues to increase the diving location will be pushed to deeper water to maintain $F_1 = F_c$. However, the movement of the interface will be much slower on the sloping bottom than that on flat bottom. At this stage, the application of the quasi-steady condition assumed in the previous section will be most applicable.

The development of the front between Newport News Bar and the deep basin to the west of the dredged channel (Branch I of Figure IIIA-1) is better defined. Since the water on the Newport News Bar begins to flood about one and a half hours earlier than that in the deep basin, a density discontinuity between the two water masses is more likely to exist. Following the argument made in the previous paragraph, the diving of heavier water as it moves off the shallower bar to the deep basin should occur in most instances.

In the following, the results of the dye release experiments are analyzed and compared with the theoretical results. The surface dye released at buoy H2 (Figure IIIA-2) on the Newport News Bar on 21 November 1985 followed the flood current in the southwest direction and disappeared at the junction with the front (Branch I of the front, Figure IIIA-1) over the area of steep bottom slope. The water depth increases from 9 m to 18 m in a horizontal distance of 350 m. The core of dye plume was detected upriver at a depth of 8 m, and the salinities were 17 $^{o}/oo$ and 20 $^{o}/oo$ above and below the dye core respectively (Figure in Section IIA1 of Volume 2). Therefore

$y_1 = 9m$

$y_2 + d = 18m$

$y_2 = 10m$

$\Delta S = 3\ ^{o}/oo$

The density difference was calculated from salinity difference, since the contribution from the temperature was negligible. No velocity measurements were made at the time of dye release experiment. The maximum local flood current was estimated from the prediction for Chesapeake Bay entrance (NOS 1985) multiplied by the ratio of the local maximum flood current measured on 6 December 1985 to the corresponding prediction for the bay entrance. The calculated results are listed in Table IIID-1 and noted in Figure IIID-2.

Dye released near the edge of Newport News Channel was carried westward to a slope over which the depth increases from 15.0 m to 19.5 m (Branch II of the front, Figure IIIA-1). During the experiment of 19 November 1985 the velocity was measured at buoy 12 and used to calculate the Froude number. The velocities used for other experiments were estimated from the prediction for bay entrance and adjusted by the ratio of measured current on 19 November 1985 to the corresponding predicted current at the bay entrance. Since the Froude numbers were calculated based on the estimated maximum flood current, the Froude numbers may be over estimated for those cases when the dye plumes were measured before flood current reached its maximum. The results calculated from field experiment are also listed in Table IIID-1 and presented in Figure IIID-2.

Figure IIID-2 indicates that the experimental results agree well with the theoretical analysis. The values of Y and F_1 locate the data points close to the curves with the appropriate values of ΔY. It is also noted

TABLE IIID-1.

Parameter Values Associated with Dye Release Experiments

Date	Time[a]	d(m)	y_2(m)	$\Delta S(^o/oo)$	u_1(m/s)	ΔY	Y	F_1
(Section I of the front: y_1 = 9m, y = 9m)								
11/21	3.0	8	10	3.0	0.58[b]	1.0	1.11	1.31
(Section II of the front: y_1 = 15m, y = 4.5 m)								
8/23	1.0	6	13.5	4.0	0.63[b]	0.3	0.90	0.95
9/3	3.5	6	13.5	4.0	0.51[b]	0.3	0.90	0.77
9/6	1.0	4	15.5	2.5	0.40[b]	0.3	1.03	0.76
11/19	2.0	6	13.5	3.0	0.43[c]	0.3	0.90	0.75

a. Time in hours between the slackwater near dye release location and the time when dye distribution was measured. The measurements of 8/23 and 9/6 were made before flood current reached its maximum. Therefore, the Froude number was over-estimated.

b. Estimated maximum flood current during the tidal cycle when the dye release experiment was conducted.

c. Measured tidal current at time when dye distribution was measured.

List of Abbreviations and Symbols

hr - hours

m - meter

cm - centimeter

d - depth of diving of denser water

F_1 - densimetric Froude number before the front

F_2 - densimetric Froude number after the front

F_c - critical Froude number

g - gravitational acceleration

Δh - head loss across the front

ΔH - dimensionless head loss

q - discharge through the front

u_1, u_2 - velocities before and after the front

u_c - critical velocity associated with F_c

y_1, y_2 - depths of denser water before and after the front

Δy - change in bottom elevation

Y - $\frac{y_2}{y_1}$

ΔY - $\frac{\Delta y}{y_1}$

ρ - density of denser water

ρ_o - density of less dense water

ϵ - $\frac{1}{\rho_o} (\rho - \rho_o)$

that the values of Froude numbers are close to the critical values F_c in most cases. This indicates that the flood currents were strong enough to push the front upriver such that the Froude numbers were maintained at critical values. Because the movement of the front was slow, the absolute and relative velocities u, were approximately the same.

E. Two-Dimensional Model for Hampton Roads Circulation

1. Introduction

Field studies of existing conditions and parameterization of the frontogenetic process can offer insights as to what might happen in case the flow over Hampton Flats is partially blocked. A two-dimensional vertically averaged model was used to provide quantitative estimates of flow modification due to the various construction programs.

The first two-dimensional modeling effort for the James River was done for the Hampton Roads '208' study (Chen, 1979). This model covered the area from Fort Monroe to Claremont, a point upriver of the mouth of the Chickahominy, Figure IIIE-1. This model was extensively modified for the present project. A fine-grid 'nested' model was generated for the present study, covering the region from Fort Monroe to a point past Newport News Point but short of the James River Bridge. The grid configuration of this nested model allowed the option of blocking off areas corresponding to proposed island locations for artificial islands, i.e. forcing the flow to go around these areas. The following discussion will describe the workings of the model and its manner of application to the New Port Island Study. Then the modeling results will be presented and discussed.

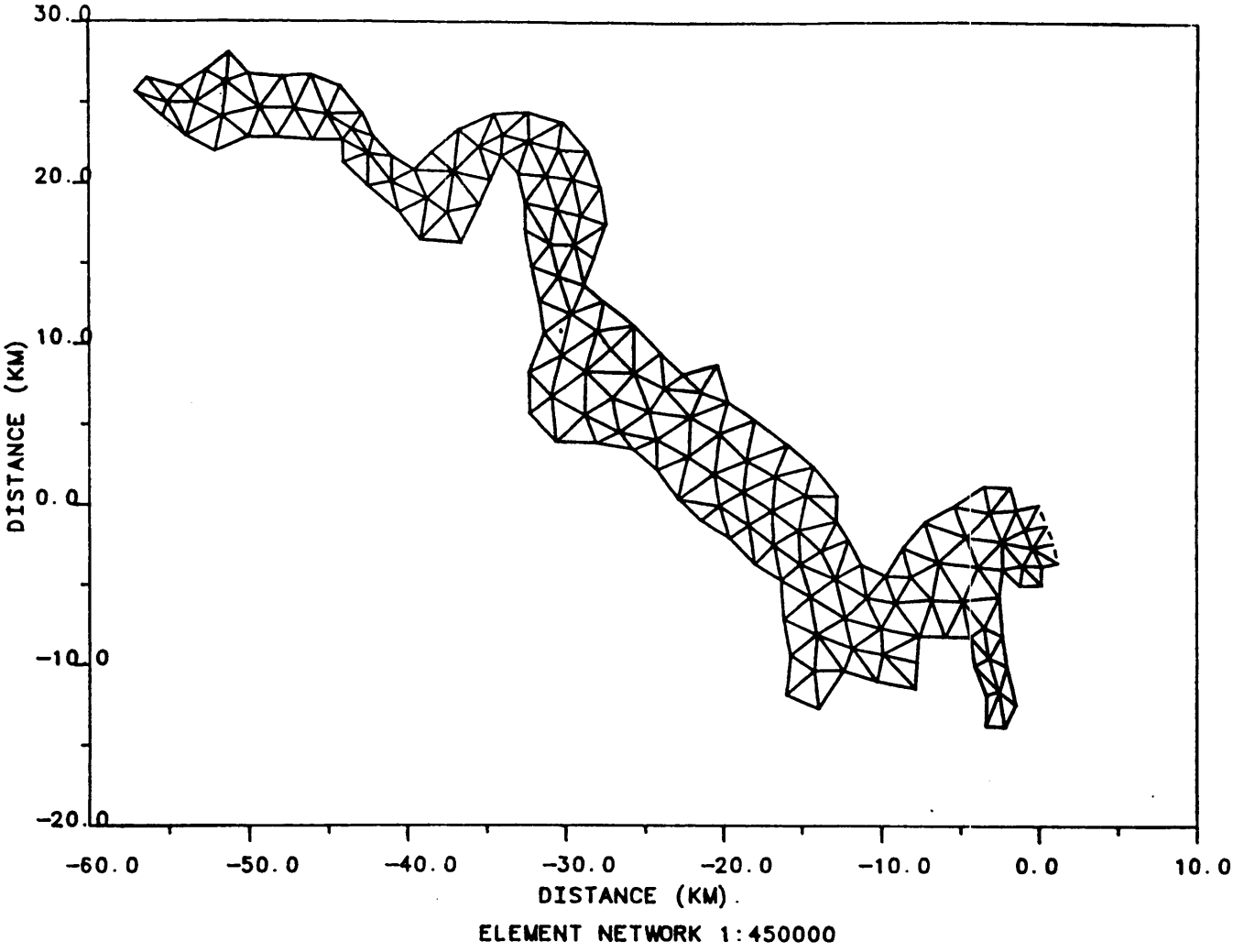

Figure IIIE-1 Large-scale two dimensional model grid for James River

The finite element model conceptually resolves the area of study into a grid of triangles of varying sizes and varying regularity. Hence the shoreline can be matched closely and finer resolution can be used in areas of particular interest. The vertices in the grid system are called nodes and the relevant equations are solved for the variables at each node. For hydrodynamic modeling the relevant equations are those for continuity (conservation of mass) and momentum. The variables to be solved for are the water surface elevation and the horizontal components of velocity, integrated from the bottom to the free surface. A time-split explicit scheme is used, wherein the continuity equation is used to predict the change in free surface elevation at the midpoint of each time step and the momentum equations are used to predict the changes in velocity at each full time step.

A quadratic formulation is used for bottom friction i.e.,

$$C_i = c_f \rho_0 H^{-2} \mathrm{sqrt}(q_x^2 + q_y^2) q_i$$

where q_x and q_y are the cartesian components of vertically integrated velocity, H is the water depth, ρ_0 is the water density, c_f is the friction coefficient and C_i is the ith component of bottom frictional stress. Values of c_f used in the model varied spatially, ranging from 0.0015 to 0.0040.

An internal friction term is also used. The stress tensor components are of the form

$$T_{ij} = E_{ij} \rho_o \left[\frac{\partial (q_i/H)}{\partial x_j} + \frac{\partial (q_j/H)}{\partial x_i} \right],$$

Where the subscript i and j can represent either of the horizontal cartesian directions. The coefficient E_{ij} was adjusted by trial. Spatially varying values in the range of 80 - 400 m^r/sec were used.

For nodes at the open boundaries (where the model limits cut across open water), tidal elevation is given and water velocity is calculated dynamically by extrapolation.

The model was modified for the present study to accept time-series water elevation records as boundary conditions at the two open boundaries. Geographically, these open boundaries correspond to the mouth near Fort Monroe at the downstream end and a transect between Sandy Point and Claremont at the upstream end. The original grid for the '208' study had 179 nodes and 254 elements.

Published tide constants for Sewell's Point were used for the downstream boundary. The synthetic downstream tide was a pure M_2 semidiurnal tide with amplitude 0.381 m. (1.25 ft.) and zero mean elevation. Observations made by VIMS in the summer of 1983 at Sandy Point were used to generate harmonic constants for the upstream boundary condition. There tide consisted of a semidiurnal tide plus two overtides plus a mean superelevation. The magnitudes of these tidal components are as follows:

semidiurnal:	0.274 m.
quarter-diurnal:	0.018 m.
sixth-diurnal:	0.015 m.
superelevation:	0.0825 m

The overtides arise because high tide propogates upstream more quickly than low tide. The superelevation is needed to drive the mean fresh water discharge in the model at a rate of 250 m^2/sec, which is apporoximately the

mean annual discharge when runoff downstream of Richmond is taken into account.

The original layout (Figure IIIE-1) proved too coarse to be useful for the Newport Island study: the proposed islands had areas of the order of a single element, making it impossible to match the shape of the islands closely. Accordingly, a fine-scale grid was generated covering only the Hampton Roads area (Figure IIIE-2). This model was 'nested', i.e. the large-scale model was run in order to provide the time-dependent boundary conditions needed to drive the fine-scale model. The fine-scale model grid included additionally a pair of 'basins' of arbitrary shape to simulate the tidal prisms of the Elizabeth and Nansemond Rivers. The basins are not shown in Figure IIIE-2, but some distortion of the Elizabeth River is evident. The fine-scale grid was also designed to match the shapes of the proposed islands and the shoreline changes occasioned by construction of I-664 (Figures IIIE-3 & IIIE-4) and to provide greater resolution in the area of Hampton Flats. The final configurations have 270 nodes and 440 elements.

2. Model Calibration

The fine-scale model was calibrated for tidal height and velocity. Tidal ranges were compared to published tide ranges (NOAA, 1985). The results are shown in Table IIIE-1. The agreement is good, except for Pig Point. However, the published value for Pig Point is based on a very short record collected before 1940, i.e. long before Craney Island was built. In order to resolve this question, a tide gauge was installed at Pig Point to be compared with one at Newport News Point. As Figure IIIE-5 indicates, the tide range at Pig Point is consistently lower than the range at Newport News Point, by about 0.05 feet on the average.

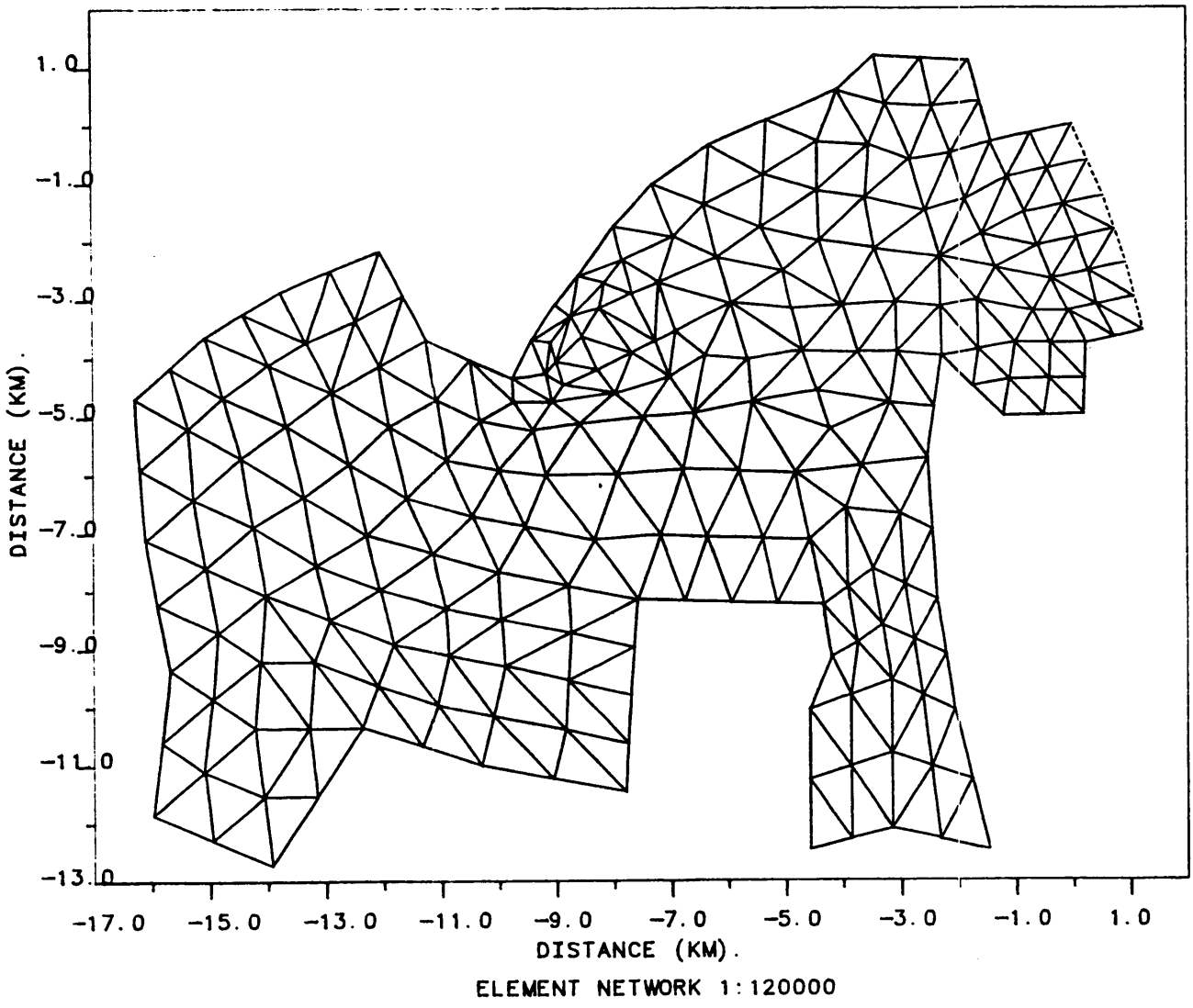

Figure IIIE-2 Fine Scale Model Grid.

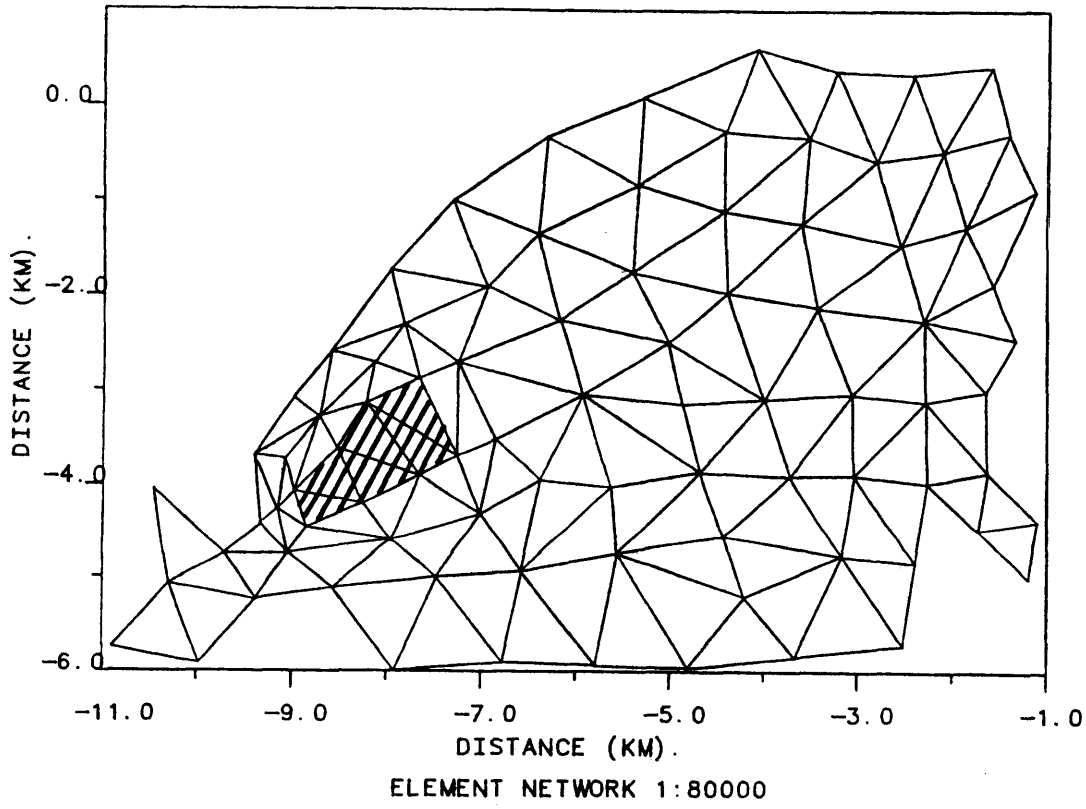

Figure IIIE-3 Model Grid Configuration for Island A

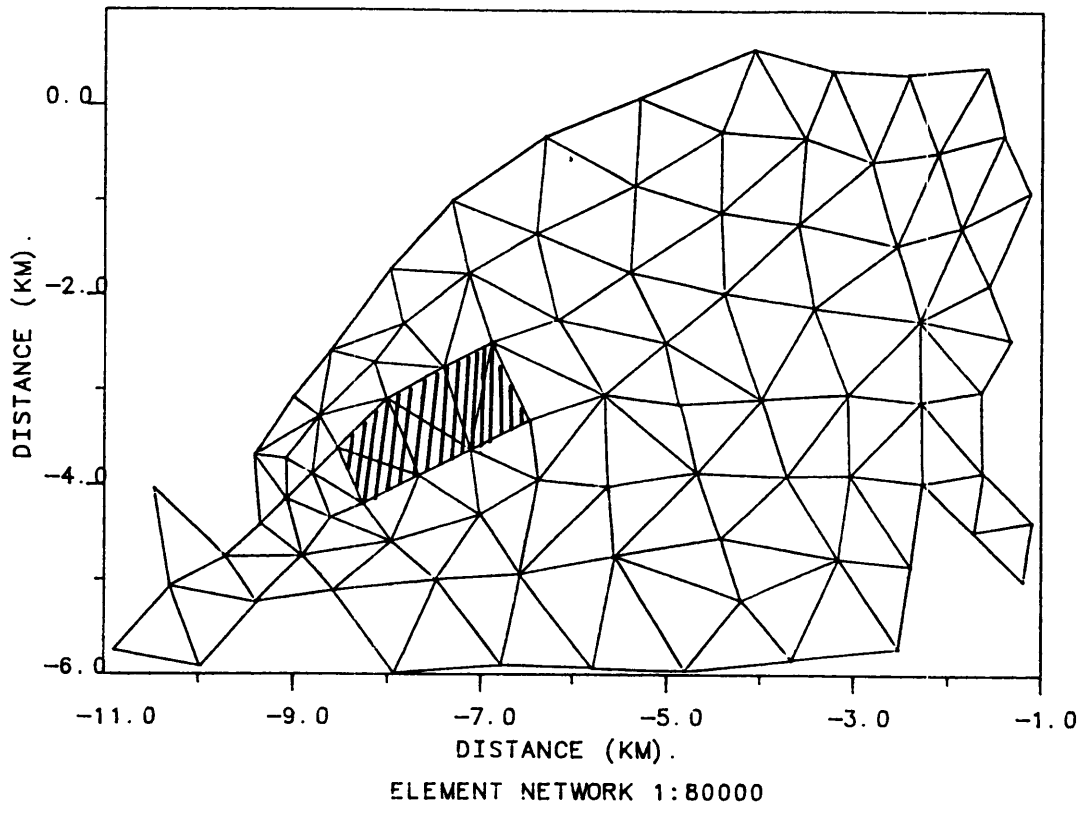

Figure IIIE-4 Model Grid Configuration for Island B

Table IIIE-1

Tidal Calibration for Two-Dimensional Model

Location	Node	Observed Tide Range (cm)	Prediced Tide Range (cm)
Sewell's Point	59	76	77
Craney Island	91	79	80
Newport News	135	79	81
Pig Point	159	85	81

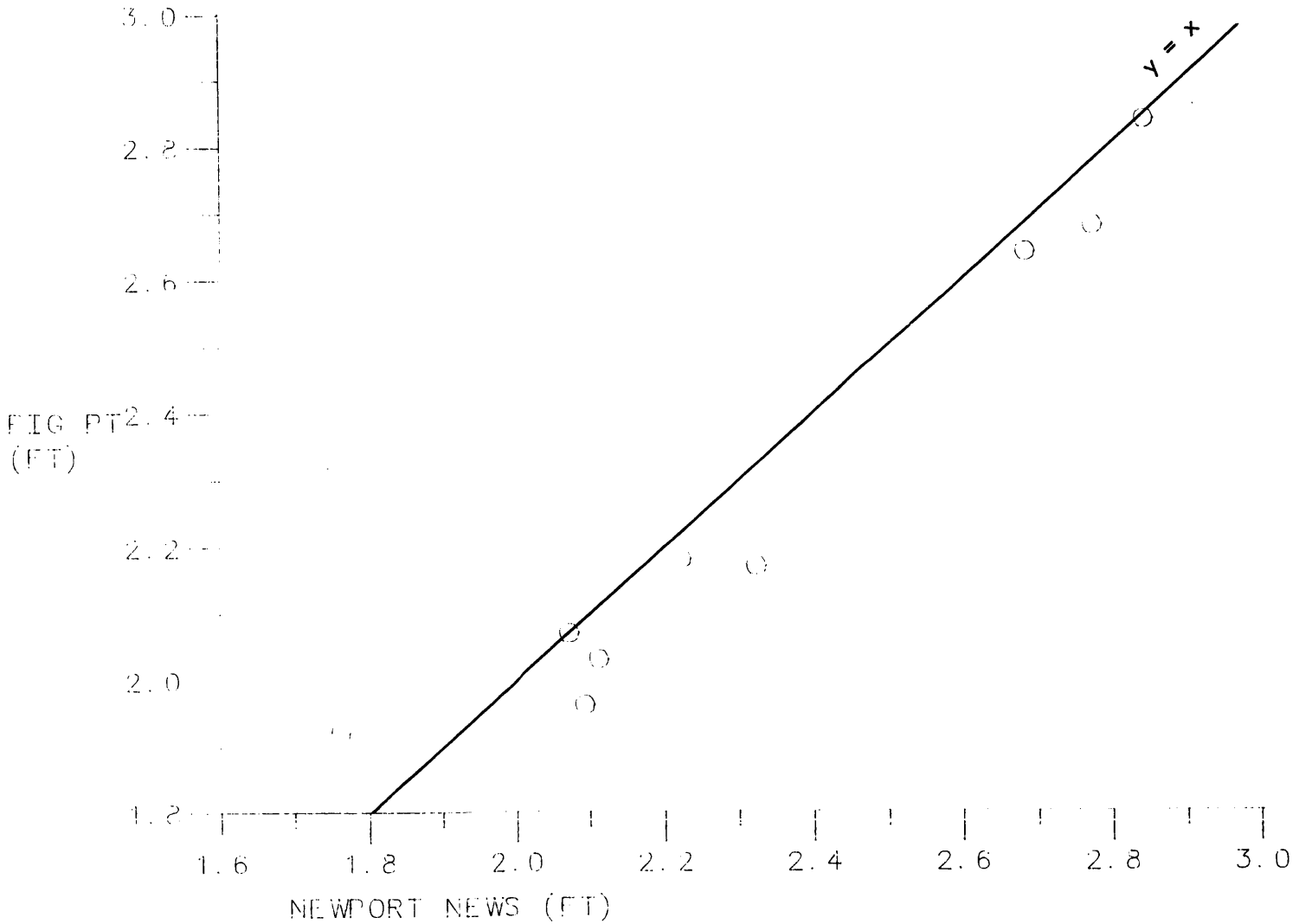

Figure IIIE-5 Observed Tide Ranges - Pig Point versus Newport News

There were two sources of data for velocity calibration. The first was the current records collected in a 1964 study termed (Operation James River, Shidler and MacIntyre, 1967). In one cruise, a transect was occupied along a line due south from Newport News Point (Figure IIIE-6). Several stations over Hampton Flats were occupied on other cruises. Current speed and direction measurements were made at each station at several depths for fifteen hours, inclusive. The vertical average on the north-south section maximum flood and ebb were calculated from these data and compared with the predicted values at the nearest model node. The results are shown in Table IIIE-2. The observed data seem to indicate a stronger flood current than ebb. This is attributed to a wind event (E. P. Ruzecki, pers. comm.), so that the average of flood and ebb magnitudes is a more reliable basis for comparison with model predictions.

Six stations over Hampton Flats proved suitable for comparison with the model predictions. The duration of these records varied from one to eight tidal cycles. Concurrent tide measurements were used to correct the speeds at stations 45-49 to mean tide range. Since such concurrent tide records were not available for stations 3 and 4, predicted tides were used to make this correction. Comparison of calculated and observed vertical average maximum flood, maximum ebb and average of the two are shown in Table IIIE-2.

Recent data also were compared to model predictions. Stations C3 and H13 from the summer of 1985 were compared with model predictions (see Appendix, IIA-2). Figure IIIE-7 shows the comparison of station C3 with model prediction at node 123. The model overpredicts, but this is to be expected since the current meter was placed at seventeen feet in a total water depth of about nineteen feet. The long record from station H13 contained several transient events, and so was analyzed using harmonic methods.

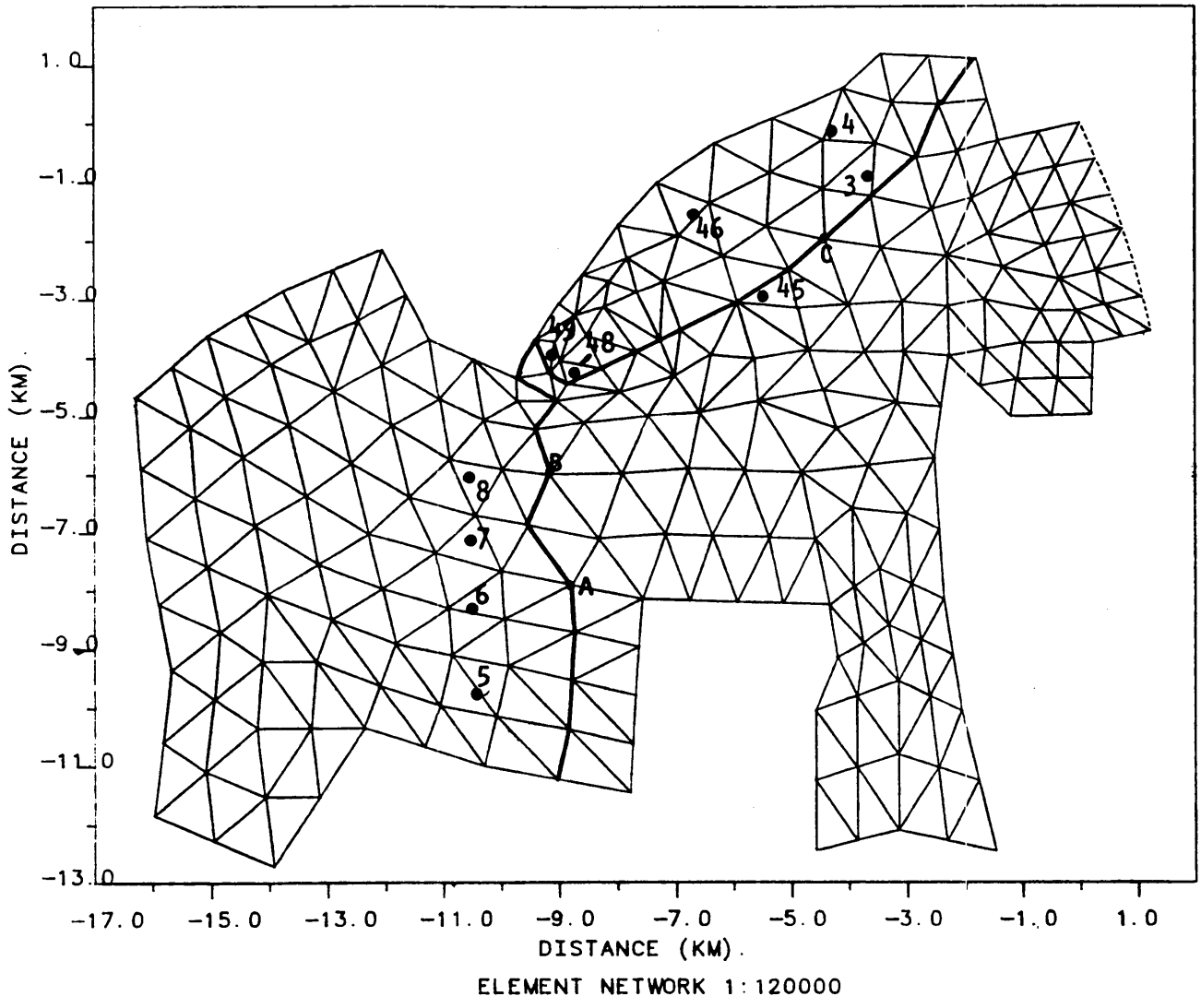

Figure IIIE-6. Transects used in Calculating Volume Fluxes and OJR (1964) Station Locations.

Transect A South Island to Vicinity of Pig Point
Transect B Newport News to South Island
Transect C Enclosing Hampton Flats

Table IIIE-2

Tidal Current Calibration for Two-Dimensional Model

Calculated				Observed (m/s)			
Node	Max Flood	Max Ebb	Average	Station	Max Flood	Max Ebb	Average
139	0.52	0.48	0.50	8	0.42	0.41	0.42
141	0.32	0.33	0.32	7	0.36	0.34	0.35
154	0.28	0.29	0.28	6	0.34	0.30	0.32
153	0.19	0.16	0.18	5	0.22	0.19	0.20
46	0.41	0.29	0.35	3	0.44	0.44	0.44
248	0.28	0.25	0.26	4	0.29	0.35	0.32
66	0.35	0.31	0.33	45	0.43	0.43	0.43
253	0.46	0.37	0.42				
94	0.27	0.24	0.26	46	0.27	0.28	0.28
64	0.27	0.25	0.26				
123	0.51	0.42	0.46	48	0.39	0.36	0.38
270	0.42	0.29	0.36	49	0.48	0.41	0.44
123	0.51	0.42	0.46	C3*	0.31	0.38	0.34
187	0.59	0.58	0.58	H13*	0.53	0.66	0.60

* Source - VIMS, 1985 all other station from OJR VIMS, 1964.

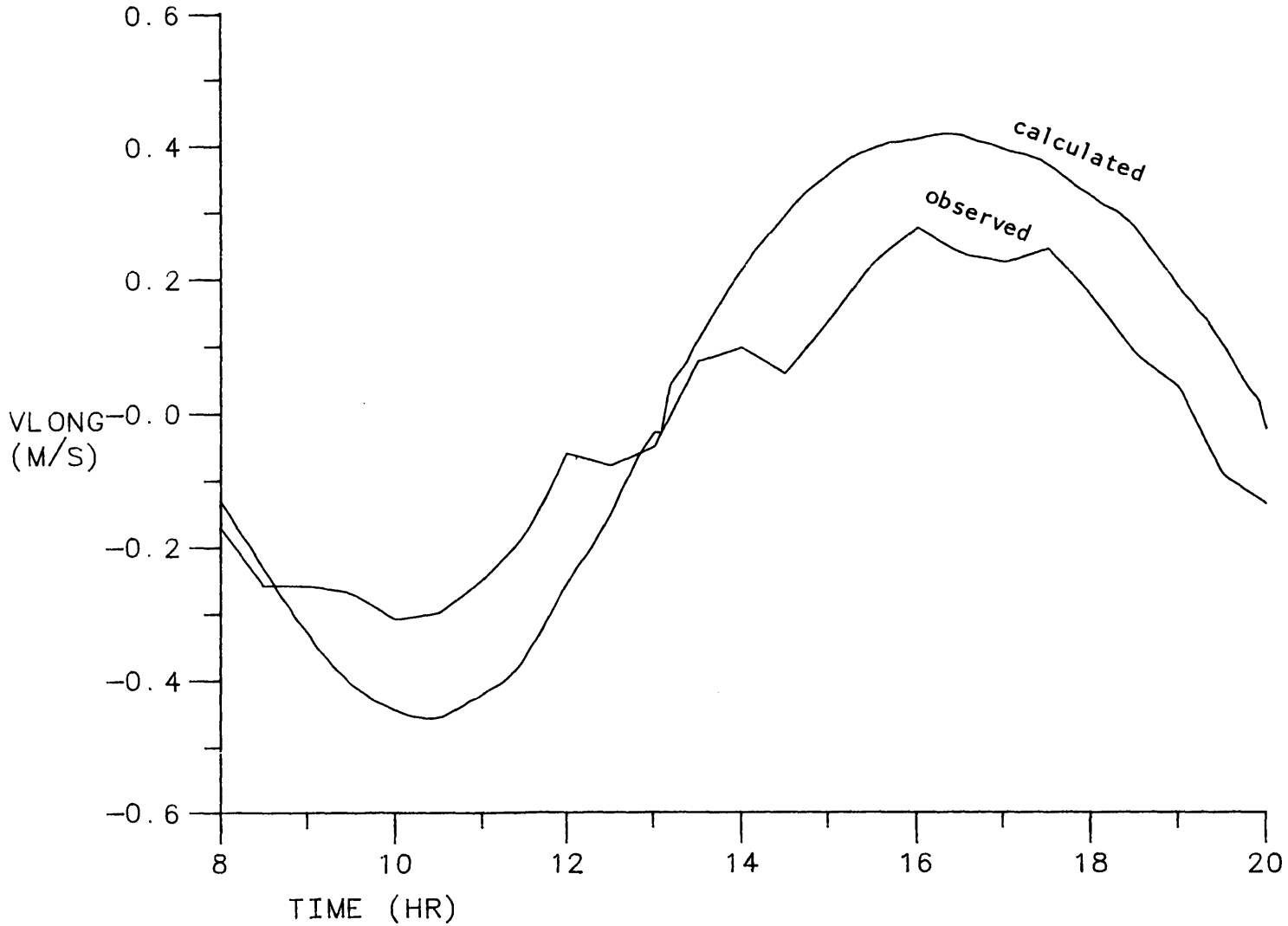

Figure III E-7 Comparison of Model Prediction with Observed Current at Station C3

The principal semi-diurnal components were extracted using a least-squares harmonic analysis method (Boon and Kiley, 1978). A synthetic record was then generated from the semi-diurnal amplitudes and phases. This record was then analyzed by complex demodulation (Bloomfield, 1976) to determine the time at which mean amplitude occurs in order to make a valid comparison with the model prediction. The observed current for mean tide is compared to the model prediction at node 187 (Figure IIIE-8) and the agreement is good. The amplitude determined by the complex demodulation procedure is empirically quite close to the root of the sum of the squares of the M2, S2 and N2 components.

3. Boundary Conditions

a. Lateral Boundaries. Since velocity calculations are performed for the nodes, velocity constraints must be applied at the nodes. Two types of constraint are possible in the model:

1) one component of velocity can be forced to zero, resulting in a constraint on the direction of flow, $\pm 180^{o}$, or

2) both components of velocity can be constrained to zero, resulting in a stagnation point at the node.

In order to establish lateral boundary conditions, the flow was constrained to be parallel to the boundary, so that there was no net flux across the rigid boundary.

The boundary nodes were spatially fixed, i.e. the shoreline did not move horizontally in response to the changing tide. In order to maintain stability and achieve satisfactory results in those places where the actual bottom slope is very gradual, the mean depth in such places was set at 1.0 meters.

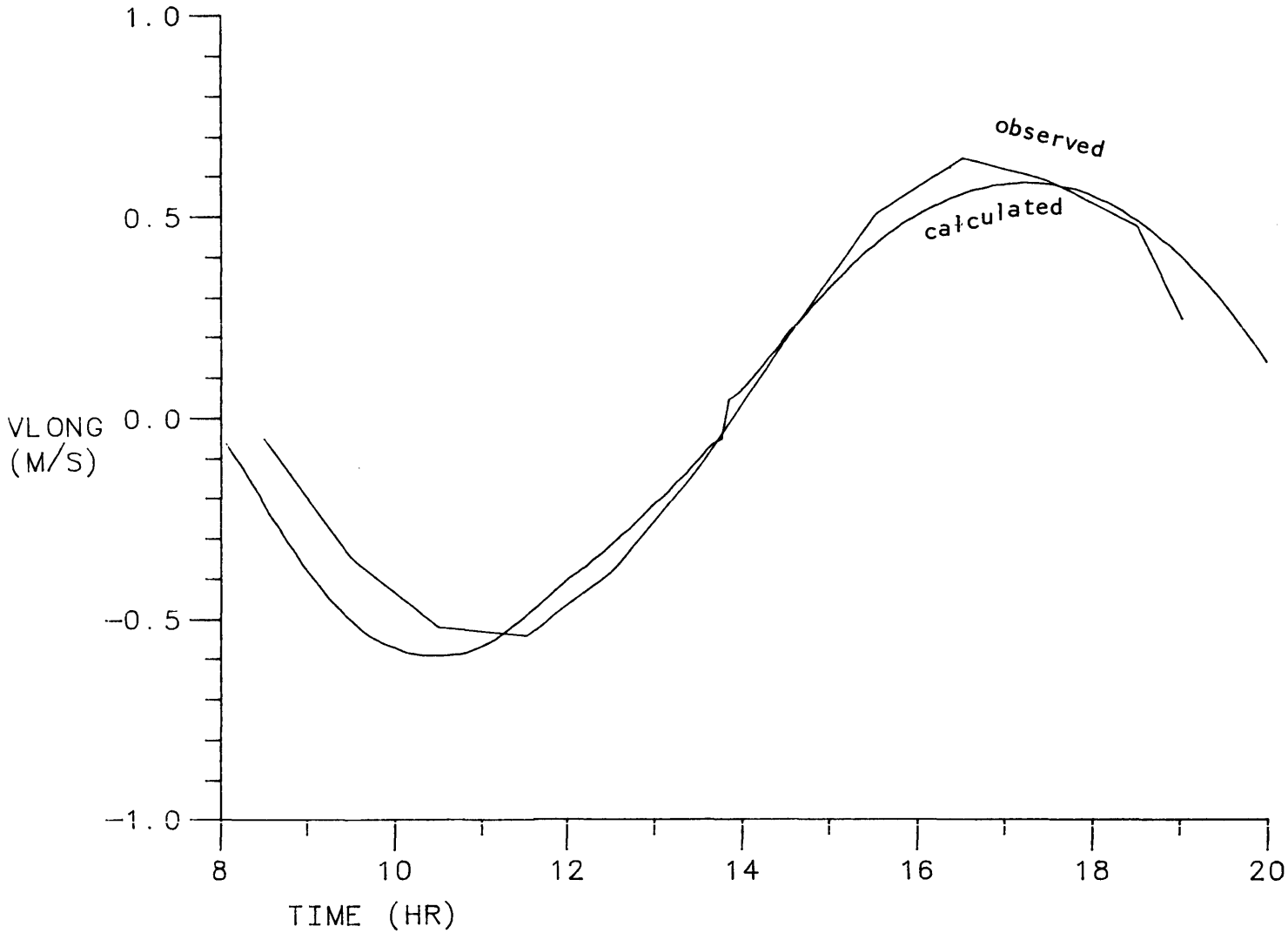

Figure IIIE-8 Comparison of Observed Current at Station H13 with Model Prediction

Tidal height was imposed at the open boundaries at the two ends. The dynamic calculations for the velocity at these nodes were carried out using the conditions in the interior only, i.e. the dynamic forcing functions were extrapolated to the boundady.

b. Jetty and New Port Island. The model grids were arranged so that certain nodes fell at the edge of the planned lcoation of an artificial island. In this way, the artificial island was represented by a set of four to eight model elements. Ideally, the boundary of this artificial island should be impermeable to flow, but in practice this is only partially true. The method of constraining velocity at the boundary nodes of an artificial island is shown below for a hypothetical island consisting of four elements with six nodes on its boundary

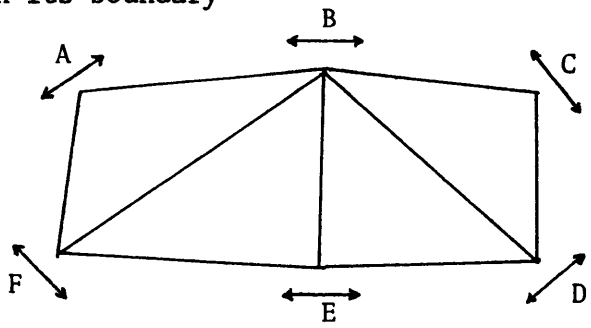

The flow at node F, for example, is constrained to be parallel to the line between nodes A and E. If each node is constrained in this manner, then there is no net flow into or out of the area representing the island. However, it is clear that nonzero flux is possible at convex boundaries. For example, there can be an inflow (outflow) between nodes A and F balanced by an outflow (inflow) between nodes F and E. Thus, the boundaries of the island are not fully impervious. In an effort to reduce the flow cutting across the corners of the island, the water depth at the boundary nodes was reduced to 1.0 m, so that frictional effects would reduce the magnitude of the velocity.

The shoreline configuration associated with the I664 crossing necessitated some modification of the model grid. The modifications were as follows:

1) Node 121 was moved to the location of the elbow on the jetty;

2) Node 268 was moved to the location of the tip of the north island; and

3) The model element with nodes 121, 268 and 134 as corners was eliminated.

Figure IIIE-2 shows the grid configuration for the base case while Figure IIIE-3 shows the shoreline modifications described above.

c. South Island I664. The bridge crossing for I664 touches down at its southern terminus at a small artificial island, (South Island). This island presented a problem for modelers since its longest dimension was shorter than the typical inter-node distances and its narrow dimension was far smaller. To approximate the effects of this island, one node (node 125) was moved to the location representing the center of this island. Then the mean water depth at this node was reduced to approximate the effects of South Island. Since the horizontal dimension of this island was shorter than the distance between nodes, an equivalent effect on discharge was calculated.

Suppose there is a vertical rectangular cross-section of width, b, depth, h and with instantaneous flow u. Suppose further that this cross-section is restricted by an obstruction of width w. Then the discharge D through the cross-section is

$$D = u(b-w)h$$

The velocity u is related to the forcing F by friction, i.e.,

$F = C \frac{u^2}{h}$, where C is some constant, so that

$$D = \left(\frac{Fh}{C}\right)^{1/2} (b-w)h$$

The same discharge can be achieved by a cross-section of width b and depth h', i.e.,

$$D = \left(\frac{Fh'}{C}\right)^{1/2} b\, h'$$

Equating these expressions and rearranging, one gets:

$$\frac{h'}{h} = \left(\frac{b-w}{b}\right)^{2/3}$$

Using the actual numbers from the model grid and the bridge plans, this ratio is

$$\frac{h'}{h} = 0.492$$

Thus, the island is simulated by a submerged obstruction of increased width and water depth equal to 0.49 of original depth.

d. Fresh Water Inflow. As explained previously, a nested model procedure was used for this project. A coarser model was run to provide boundary conditions for the fine-scale model. Neither model provided for direct input of fresh water discharge. Instead the mean surface slope controlled mean discharge. For the coarse model, a mean elevation difference of 8.25 cm between the upstream and downstream boundaries produced a mean discharge of about 250 m^3/sec, close to the observed mean annual discharge as augmented by runoff downstream of Richmond. The tidal driving function generated by this model for the fine-grid model showed a difference in mean tidal elevation of about 2.7 cm between the upstream and downstream

limits of the fine-grid model. This mean slope produced a mean discharge of 680 m^3/sec. In order to reduce this value to a more reasonable level, the tidal driving function was modified by reducing the tidal elevations at the upstream boundary by 1.36 cm. This change brought the fresh water discharge in the fine-grid model into line with the values obtained from the larger scale model.

e. Depth Compensation. The procedure for generating boundary conditions for the artificial islands includes reducing the mean water depth to 1.0 m. This procedure introduces another problem for the modeler. The cross-sectional area in the passage between the island and the mainland is drastically reduced. This reduction could make the flow through this passage unrealistically low and thus exaggerate the impact of the island. To remedy this situation, the mean water depth at the nodes lying between the island and the coast was increased sufficiently to preserve the cross-sectional area through this passage.

4. Results

a. Tidal Flux Between Hampton Roads and the Lower James. The larger scale of interest in the variation of flood current flux is that which may occur along a north-south transect between Newport News Point and the south shore of Hampton Roads. In order to include the effects of I664 the flux through individual elements was summed along a route to include the south island of I664 (node 125; Figure IIIE-9). The summary of results is shown in Table IIIE-3. For the BASE condition the total flood flux across the entire section is 212 x $10^6 m^3$ (mean tide range). This value compares well with the intertidal volume of 224 x $10^6 m^3$ calculated by Cronin (1971). Moreover, there is reasonable agreement with the value of 285 x $10^6 m^3$ obtained from a current meter transect of limited duration in 1964 (see

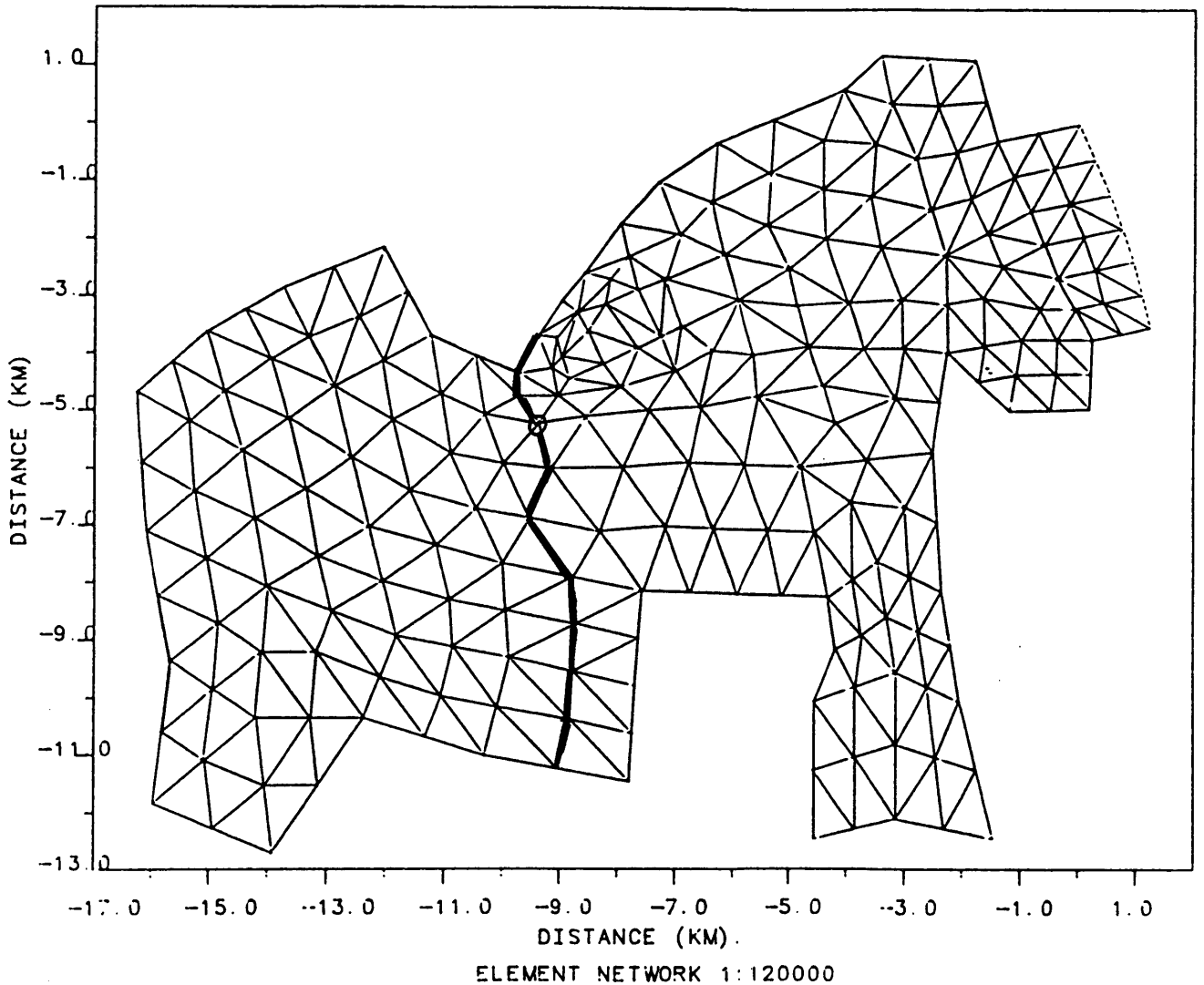

Figure IIIE-9. North-South transect for flux calculations shown in Table IIIE-3. Circle represents Node 125, South Island of 1664.

TABLE IIIE-3. Summary of Flux Estimates

	EBB FLUX ($10^6 m^3$)			FLOOD FLUX ($10^6 m^3$)		
	North Shore to Node 125	Node 125 to South Shore	(A) Sum Ebb	North Shore to Node 125	Node 125 to South Shore	(B) Sum Flood
BASE	113	110	223	114	98	212
I664-45	109	106	215	107	98	205
I664-55	118	104	222	118	93	211
Island A	113	104	217	111	96	207
Island B	116	103	219	115	94	209
Island C 45	108	105	213	106	97	203
Island C 55	118	101	219	116	92	208
Island D 55	118	102	220	116	92	208

Section IIA for further detail). The model indicates 54% of the BASE condition flood flux occurs between the north shore at Newport News Point and the planned position of the I664 south island. Calculation from field measurements at a transect somewhat upriver indicates 48 to 60% of the flux occurs in a corresponding section. The difference between the ebb and flood flux represents the fresh water discharge.

The construction of I664 with the Newport News Navigation Channel at 45 feet is estimated to result in a small reduction of total flux (up to 4 percent) with a slight redistribution of the flux. Fang et al. (1979) concluded from hydraulic model studies that if any tidal flux reduction was to be associated with I664 (45 ft channel) that change was within the accuracy of the model results, argued to be about 3 percent. Within the context of the low grid density two-dimensional mathemtical model used herein, the degree of flux impedance is dependent upon how the south island flow blockage is simulated. Thus, these results cannot be applied with quantitative confidence for estimates of flux impedance. However, the comparisons of tidal amplitude and phase throughout the river, as measured in the hydraulic model, do suggest that the flux impedance, if present, is small.

Deepening the Newport News channel to 55 feet is estimated to result in virtual restoration of the BASE condition total flux with a larger percentage passing between the north shore and the I664 south island. This agrees with expectation and the results of hydraulic model tests wherein bottom inflow is enhanced (Richards and Morton, 1983).

Addition of New Port Island (Option A or B) is estimated to result in a very small reduction (2 or 1%) of the total flux relative to the case of I664-55 foot channel. However, both New Port Island options would result in

essentially the same, or marginally larger, total flood flux than the case of I664-45 foot channel.

The tidal fluxes associated with an island in test locations C and D (see Figure IC-1a,b for location) correspond very closely with those of the respective I664 configurations. That is, island location C with a 45 ft navigation channel corresponds within 1% with I664-45 and location C with a 55 ft channel corresponds within 1.5% with I664-55.

Thus, the installation of an island of the dimensions tested would not be expected to significantly alter the total tidal fluxes to the lower James River.

b. Flux Across Hampton Flats. Observation has clearly indicated that the water flooding across Hampton Flats is involved in the frontal circulation. Due to the lead in tidal phase, the Hampton Flats water initiates one segment of the frontal system and thence contributes throughout the period of flood currents. Analysis of 1964 field measurements indicate that Hampton Flats accounts for 8 percent of the total flood flux across Hampton Roads. Since the elements of construction, I664 and the proposed New Port Island, were thought to likely modify the magnitude and/or distribution of flow across the Flats, the flood flux onto and off of the Flats was calculated.

Due to the embayed configuration of Hampton Flats, water floods onto the eastern portion of the Flats while, during the same period, water leaves the western portion. The rate of inflow exceeds the rate of outflow and the water elevation over the Flats correspondingly rises (rising tide). The flux of flood waters and its distribution onto and off of Hampton Flats was calculated via the segments shown in Figure IIIE-10a,b. For the BASE configuration approximately 35.5 x $10^6 m^3$ flows onto Hampton Flats. That flux

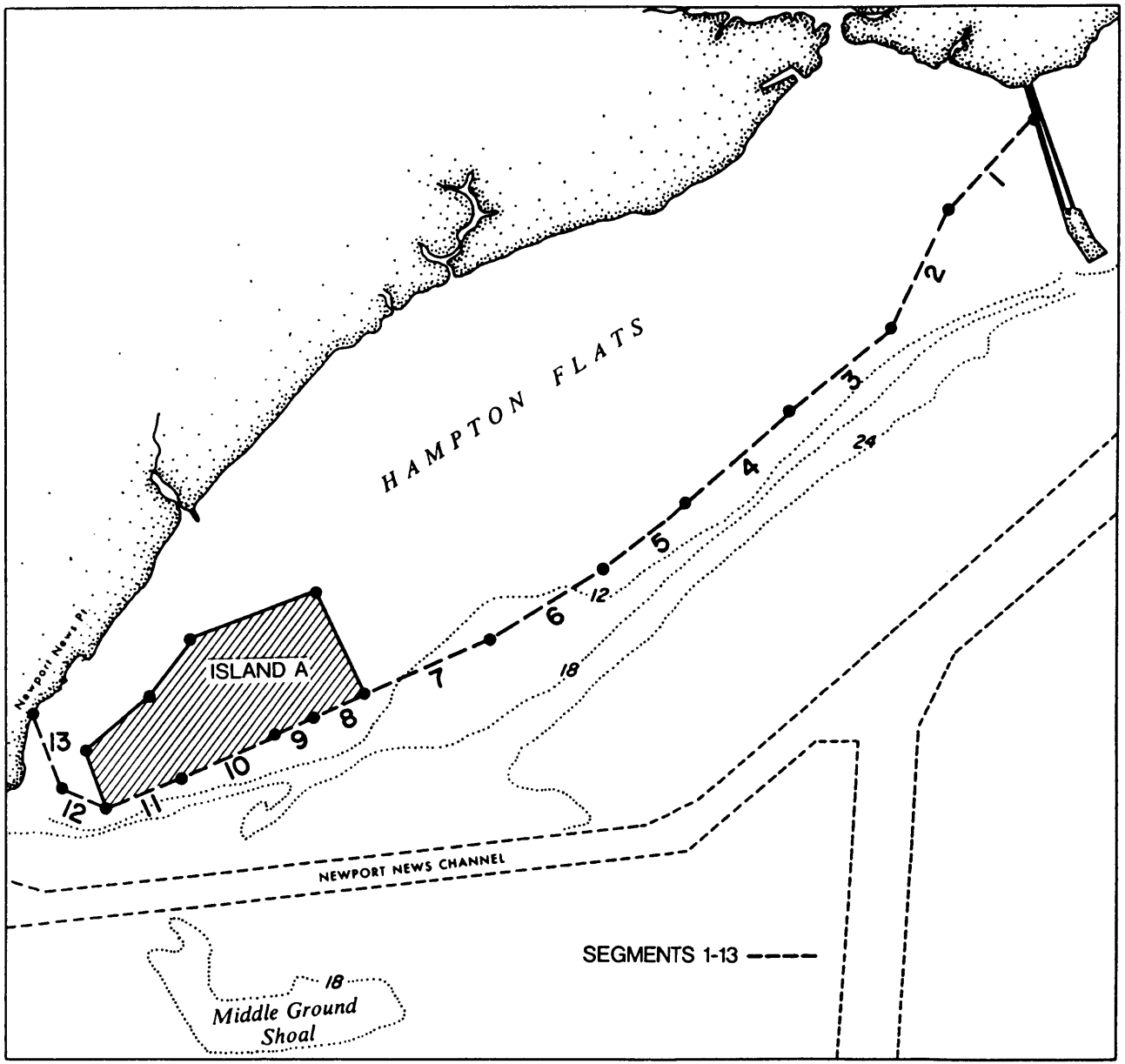

Figure IIIE-10a. Hampton Flats segments for flux calculations, Island A.

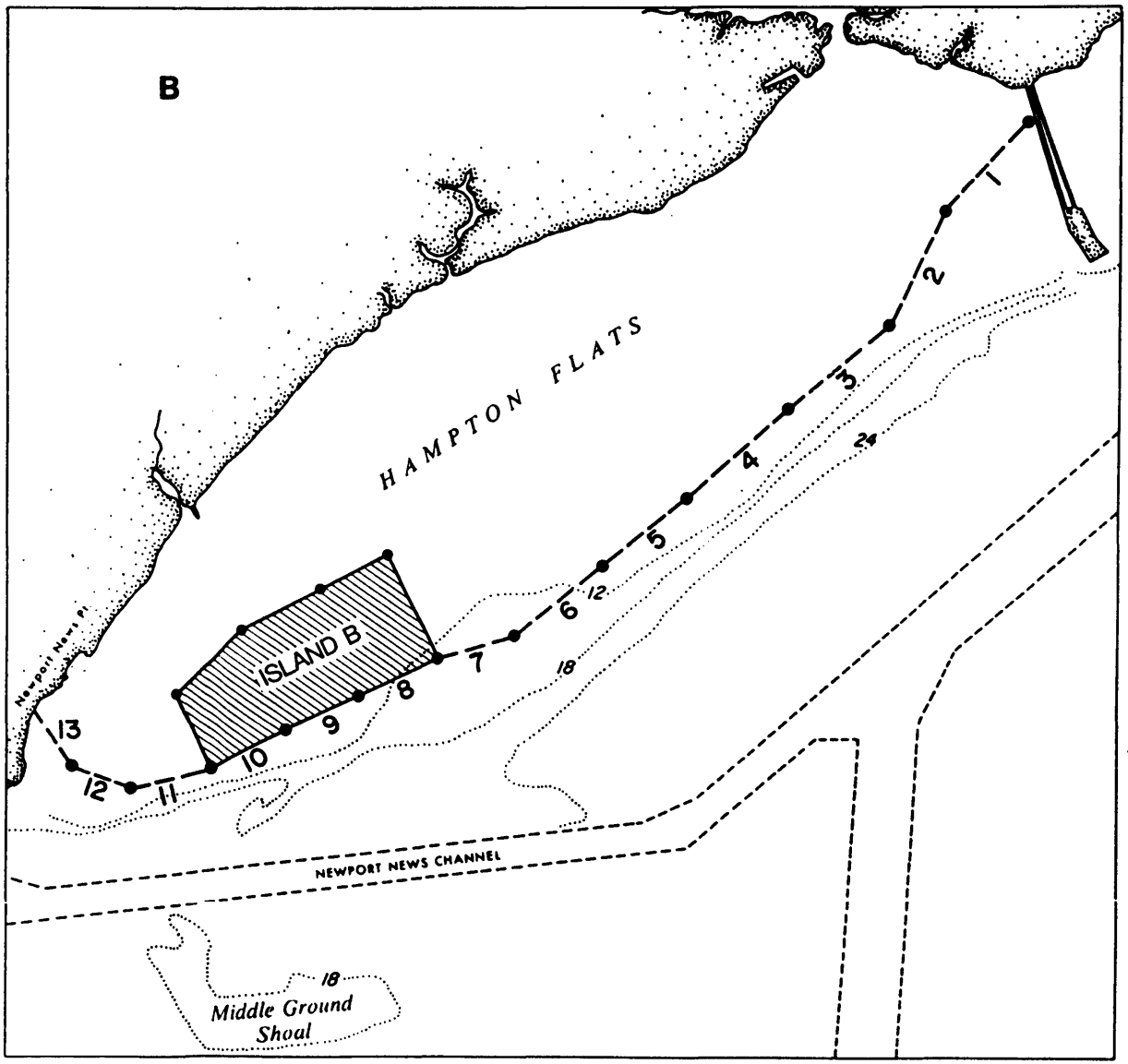

Figure IIIE-10b. Hampton Flats segments for flux calculations, Island B and test locations C and D.

is reduced by about 3 percent with the I664 configurations. However, with either of the proposed New Port Island options (A or B) the total flux onto Hampton Flats is reduced by about 14% relative to I664 due to the overall flow impedance induced by the island.

The relative distribution of flow onto and off of Hampton Flats is summarized in Table IIIE-4. For the cases of BASE, I664-45, and I664-55 flow enters along segments 1 through 6, and simultaneously exits via segments 7 through 13. This distribution corresponds with the azimuth change of the twelve and eighteen foot depth contours. Particularly noteworthy is the concentration of the exiting flow near Newport News Point. In the BASE case, 65% of the exiting flow occurs through segments 12 and 13. The jetty and north island associated with I664 result in a downriver deflection of the exiting flow such that the flow occurring in sections 12 and 13 is reduced to about 45%. However, in those cases the flux is restored with the addition of Section 11 to 69 and 66 percent for I664-45 and I664-55.

The addition of New Port Island (Options A or B) induces two important effects in addition to the previously mentioned reduction of total flux onto Hampton Flats. The Island (either Option A or B) results in flow splitting such that a large percentge of the flow exits via segments 6 and 7, positions relatively remote from the principal zone of frontal convergence activity. The time history of discharge for Segment 7 is shown in Figure IIIE-11 (discharge time histories for all segments are given in Appendix IIC). The remainder of the flow passes around New Port Island and exits near Newport News Point. In the case of the Island A Option, about 60 percent of the flow exits on the downriver (eastern) side of the island and 40 percent exits near Newport News Point. However, the volume of the exiting flow to the west of the island is only 35 percent of that of the BASE

TABLE IIIE-4. Distribution of Flood Flux Across Hampton Flats

Segment	Node	BASE % On	BASE % Off	I664 45 FT % On	I664 45 FT % Off	I664 55 FT % On	I664 55 FT % Off	ISLAND A % On	ISLAND A % Off	ISLAND B % On	ISLAND B % Off	ISLAND C % On	ISLAND C % Off	ISLAND D % On	ISLAND D % Off
	19														
1		16.6		16.7		17.0		19.3		18.9		19.8		18.1	
	23														
2		27.2		27.3		27.8		31.6		30.8		32.4		29.3	
	24														
3		16.8		16.8		16.8		18.4		18.1		14.0		17.0	
	46														
4		20.1		20.1		20.1		20.6		19.9		14.5		17.6	
	47														
5		12.0		12.1		12.1		9.4		9.6		9.6	5.3	8.2	
	65														
6		7.3		7.0	0.3	6.2		0.6	21.0	2.7	2.4	-	-	1.3	16.9
	66														
7			4.3		4.4		7.4		39.6		44.7	-	-	-	-
	269														
8			3.8		6.7		7.3					3.4	0.2	-	-
	99														
9			4.4		5.6		5.8					3.0		6.8	
	100														
10			9.5		13.9		13.7						4.2	1.6	2.9
	264														
11			12.6		21.4		20.8				2.9	14.6			13.1
	123														
12			30.9		29.7		28.4		20.9		34.0		55.6		49.2
	270														
13			34.5		17.8		16.6		18.4		16.0		19.9		18.0
	120														
TOTAL %		100	100	100	99.8	100	100	99.9	99.9	100	100	99.7	99.8	99.9	100

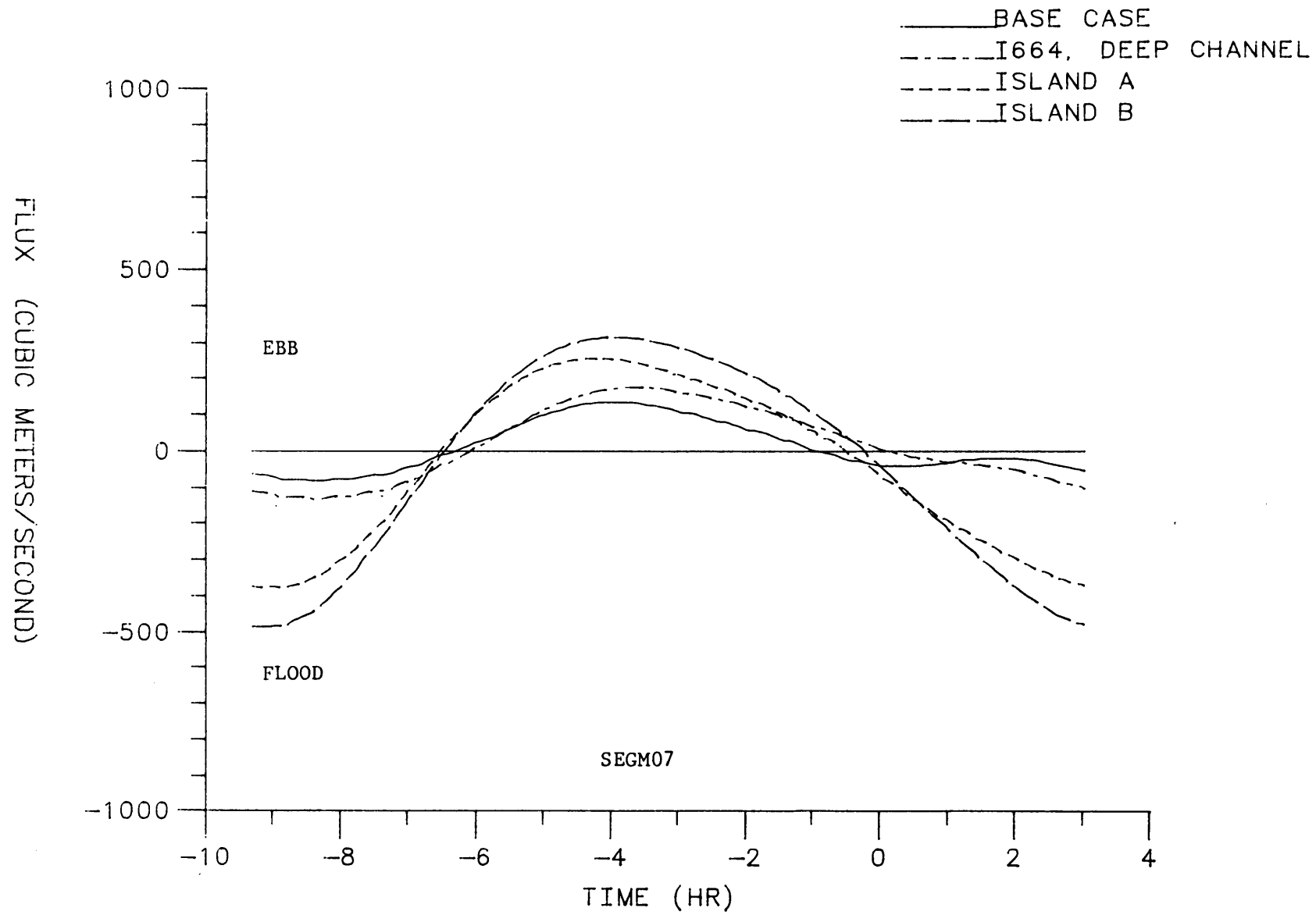

Figure IIIE-11. Discharge time history through segment 7.

condition. The Island B Option results in about 47 percent flow diversion downriver of the Island and with 53 percent exiting near Newport News Point. The flow volume thereby exiting through segments 11, 12, and 13 is about 46 percent of the volume discharged for the BASE condition. Thus, Island B Option results in less resistance to flow through the passage between the shore and island.

Tests were performed for island locations C and D (respectively 370 and 323 acres). In both of these cases the exiting flood flux through sections 11, 12, and 13 is restored to within 2 percent of that for I664-55. Approximately 76% and 67% (C and D respectively) of the flow exits via segments 11, 12, and 13.

Relative to the I664 cases the flux onto Hampton Flats is reduced by 18.6 and 12.3 percents (C and D respectively). In contrast to the cases of Options A and B there is a flux onto the Flats in the sections immediately west of the island locations.

c. Island Shape. The proposed island shapes for cases A and B were modelled by placing model nodes and elements so as to mimic the outline of the island. This was not done for the C and D cases since these tests were intended to be simple explorations of the effect of moving the island to a more easterly position. The existing grid was used and this resulted in area reduction to 370 acres (C) and 323 acres (D).

The island node geometry portrays a flat, blunt face to the flood flow. However, since the depth at the nodes is adjusted to 1 meter some flow does occur across the corners. In effect this rounds off the corners.

It is of interest to pose the question whether an island with a streamlined shape, i.e. ellipsoidal, or wedge, would materially alter the results portrayed earlier. The relatively coarse grid model used is not suitable to

test the question. Such changes could be expected to locally affect flow speeds. However, comparison of the results between the case of A and B with D indicates that the flux near Newport News Point is principally due to island location. Cases A, B, and D represent a stepped easterly shift of location with a corresponding increase of flood flux through the passage between the island and mainland.

d. Flow Patterns in Hampton Roads. Vector plots of the flow field in Hampton Roads are shown in Figures IIIE-12a,b.c for conditions of maximum flood, maximum ebb, and slack before flood for BASE, I664-55, Island A, and Island B. Similar cases for island test locations C and D are shown in Figures IIIE-13a,b,c and IIIE-14a,b,c. The complete series of vector plots is given in Appendix IIC. Figure IIIE-12c clearly depicts the flood phase over Hampton Flats while the main channel of the Hampton Roads area is at slack. Note also that the early flood flow converges at Newport News Point while the current is still ebbing in the lower James River.

F. Hampton Flats Sedimentation

Hampton Flats is a relatively shallow embayment between Old Point Comfort and Newport News Point. Sediment sources to the embayment are limited to shore erosion on the inner boundary and to suspended solids advected over the flats by tidal currents. Limited measurements over the eastern one-half of the flats and along the deeper flanks indicate normal suspended solids concentration of 5 to 15 mg/l (Boon and Byrne, 1975). In the channel area adjacent to Old Point Comfort Boon (1974) found concentrations in the upper five meters of the water column ranging up to 25 mg/l

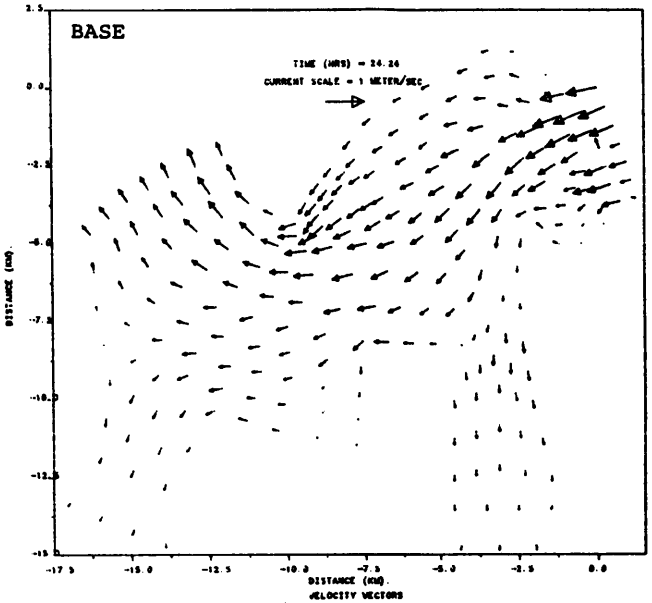

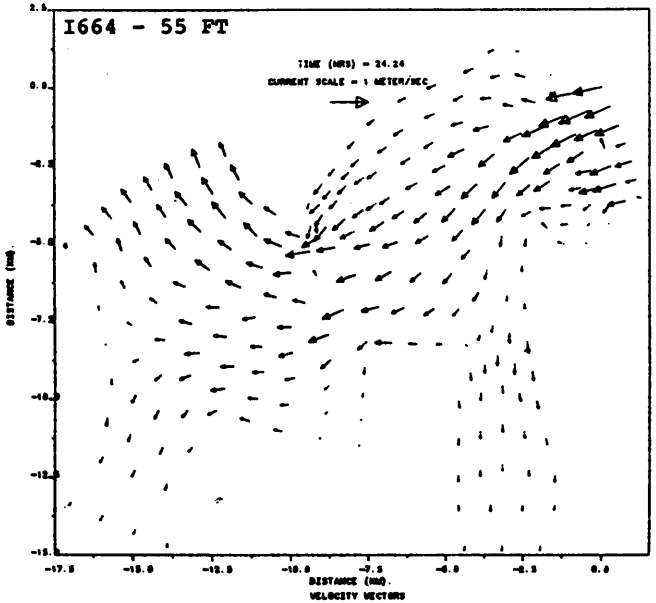

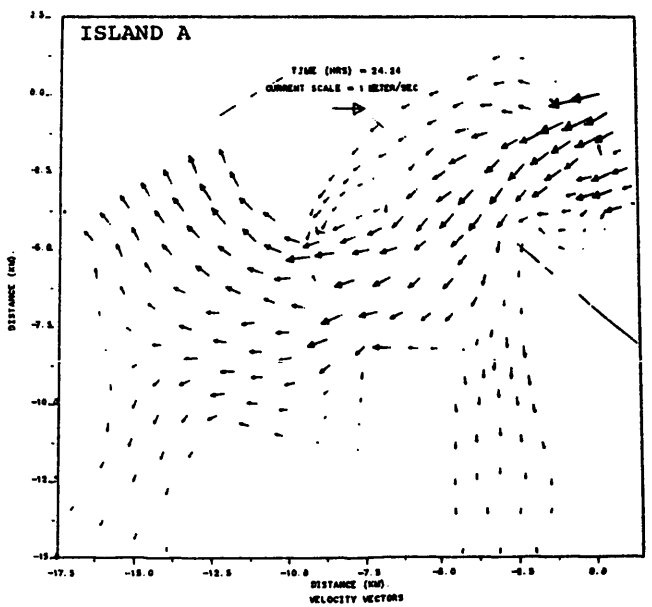

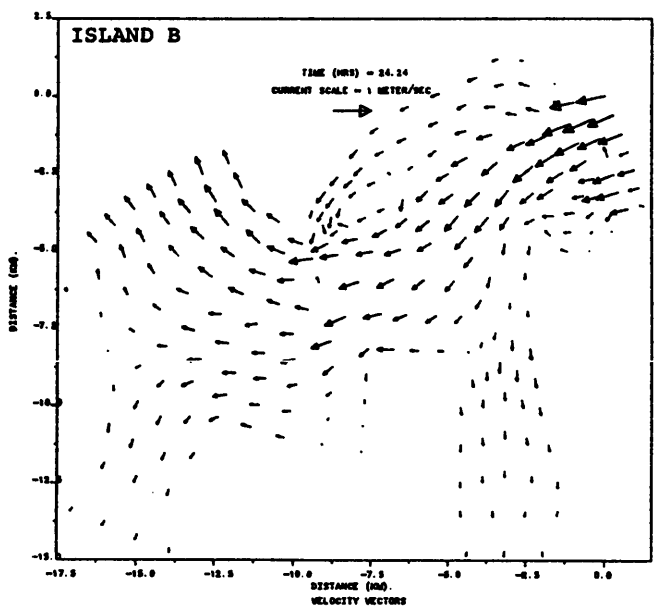

Figure IIIE-12a. Flow field in Hampton Roads, maximum flood.

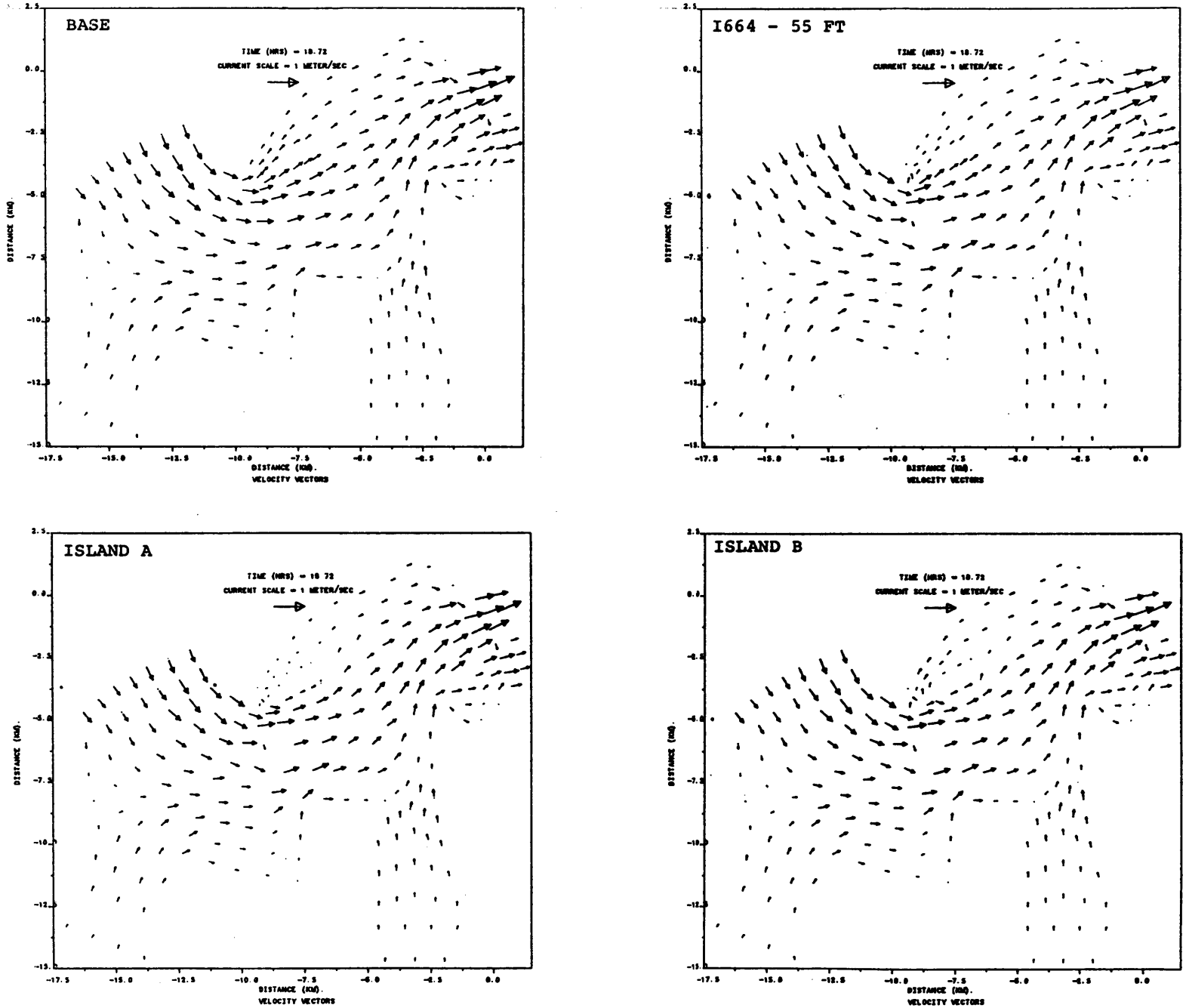

Figure IIIE-12b. Flow field in Hampton Roads, maximum ebb.

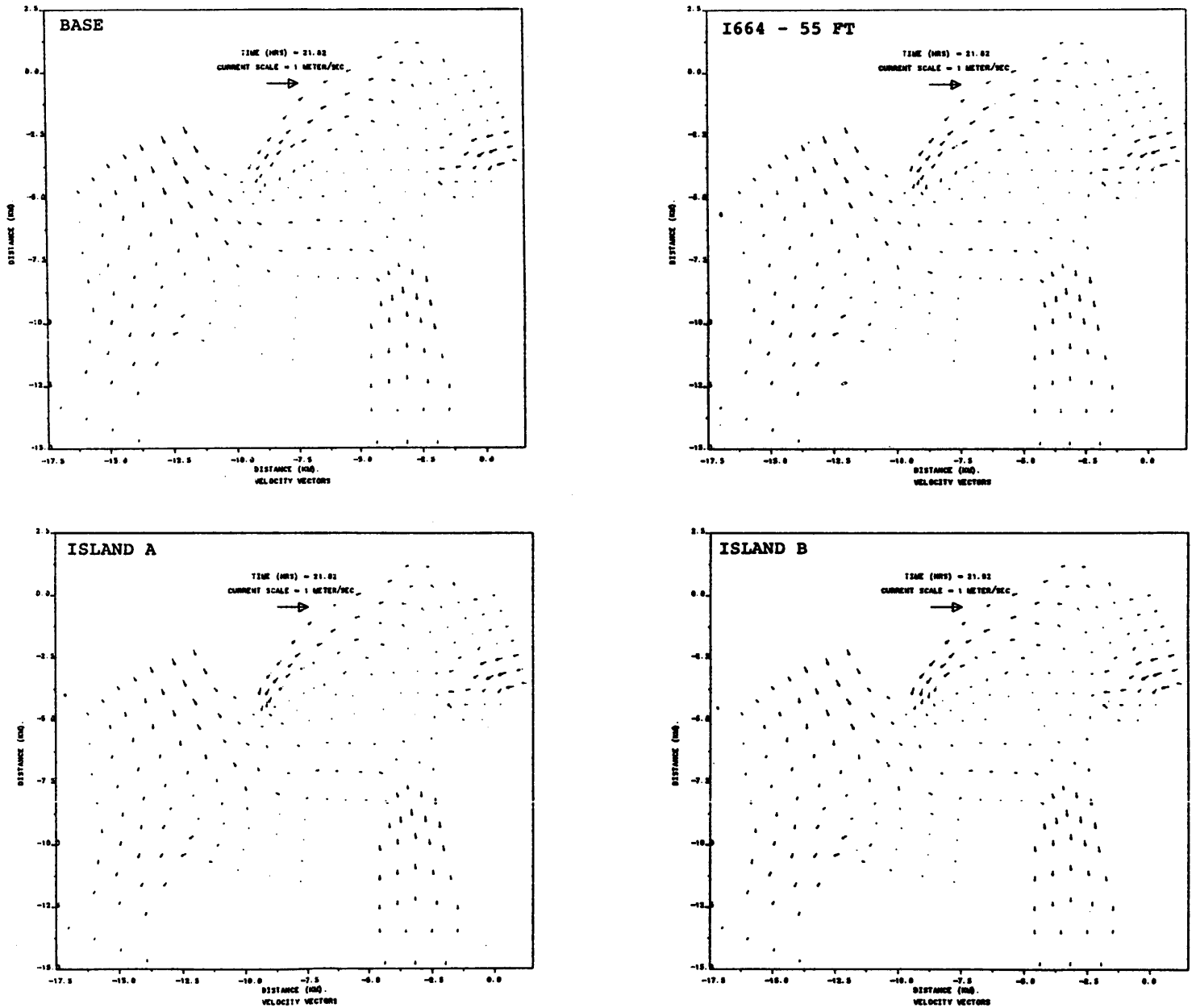

Figure IIIE-12c. Flow field in Hampton Roads, slack before flood.

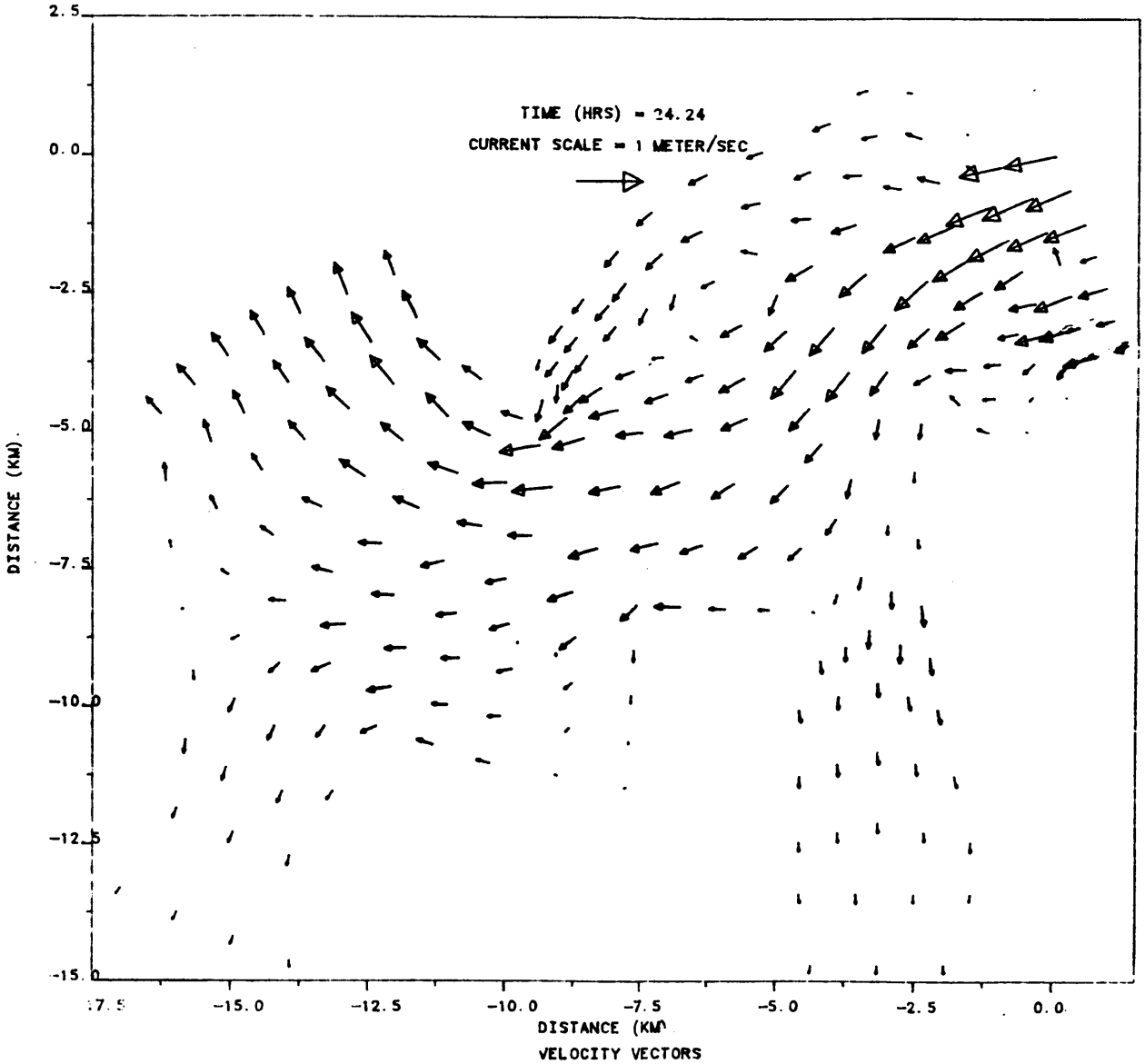

Figure IIIE-13a. Flow field in Hampton Roads, Island C, maximum flood.

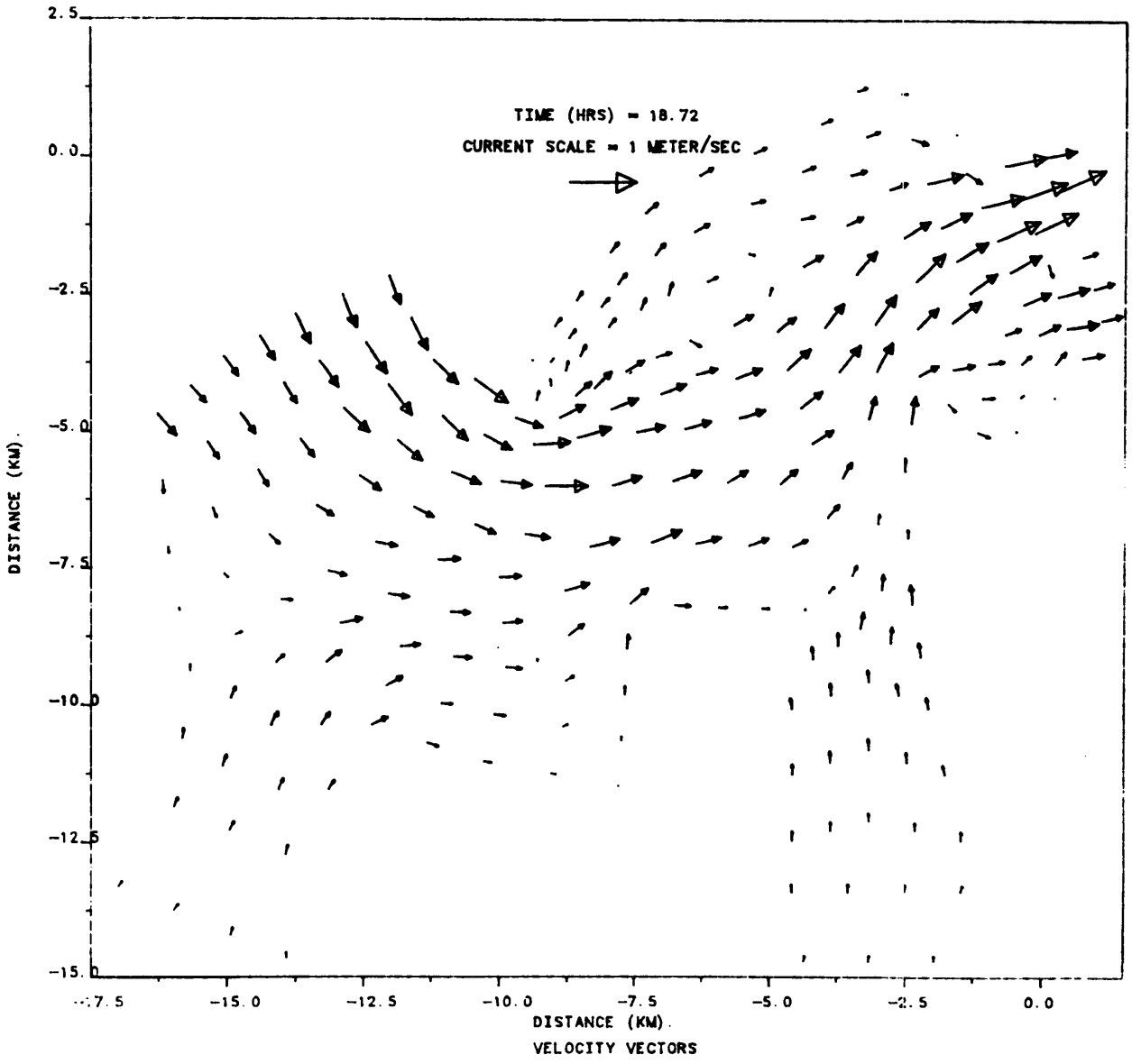

Figure IIIE-13b. Flow field in Hampton Roads, Island C, Maximum ebb.

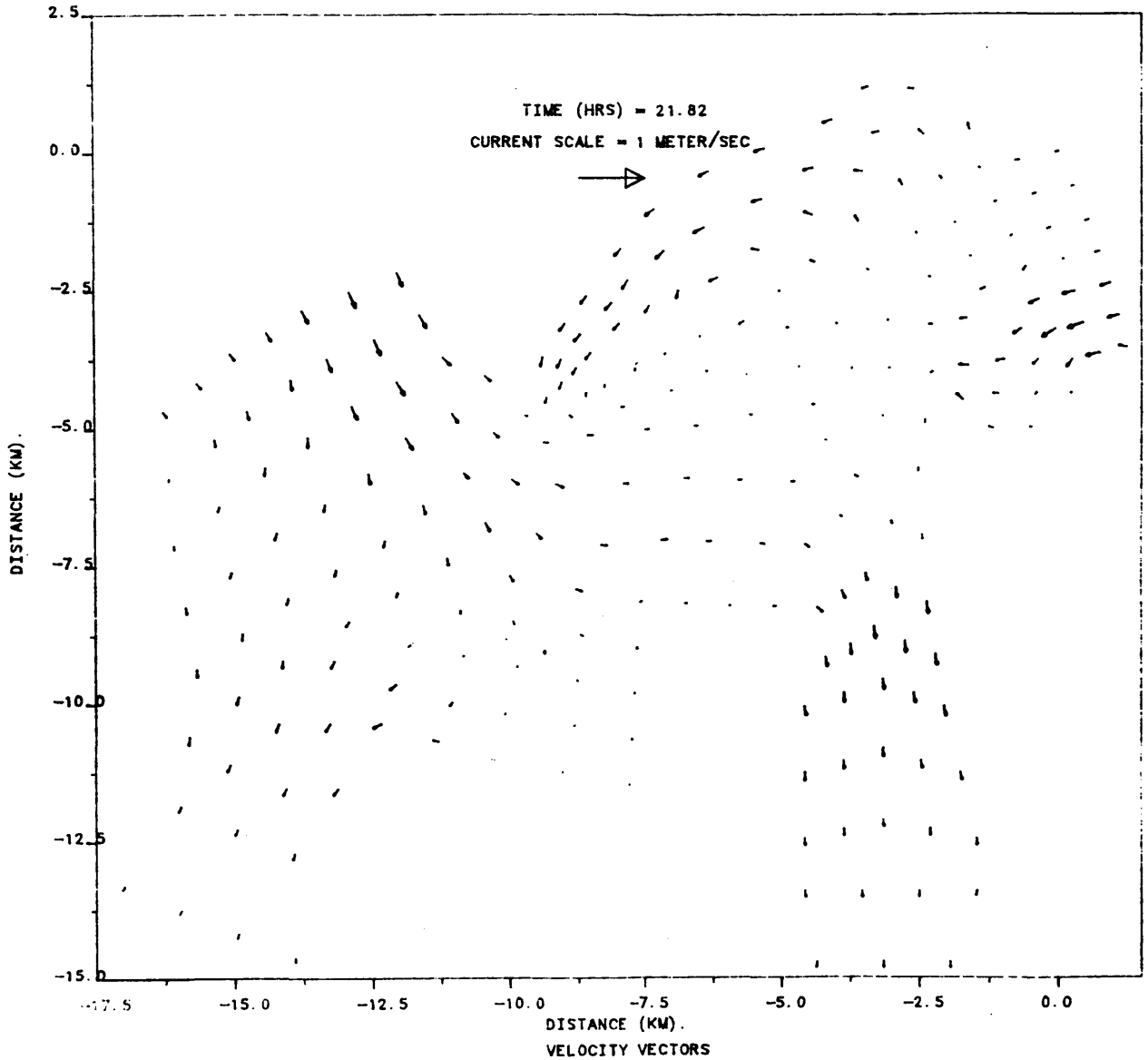

Figure IIIE-13c. Flow field in Hampton Roads, Island C, slack before flood.

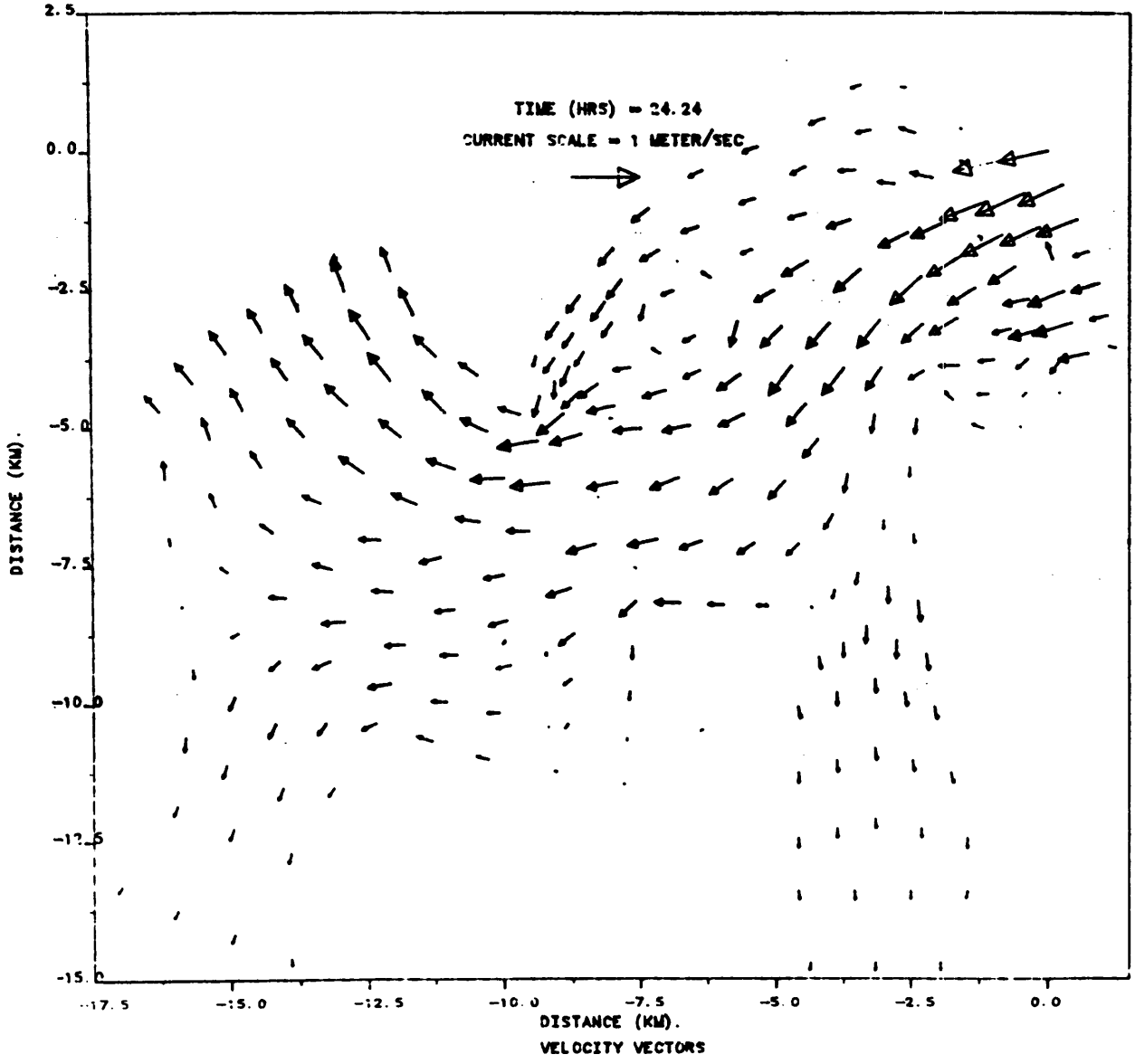

Figure IIIE-14a. Flow field in Hampton Roads, Island D, maximum flood.

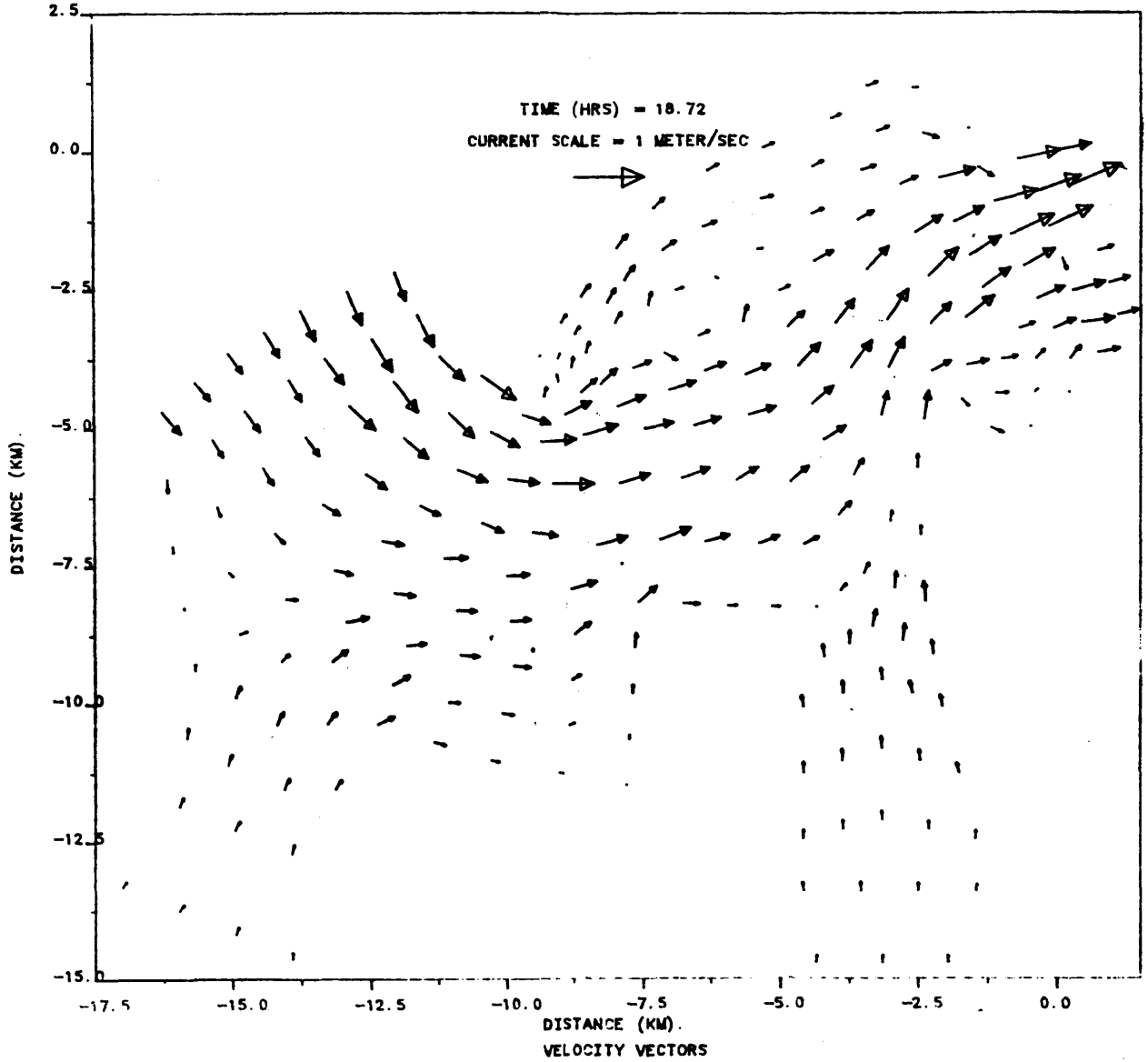

Figure IIIE-14b. Flow field in Hampton Roads, Island D, maximum ebb.

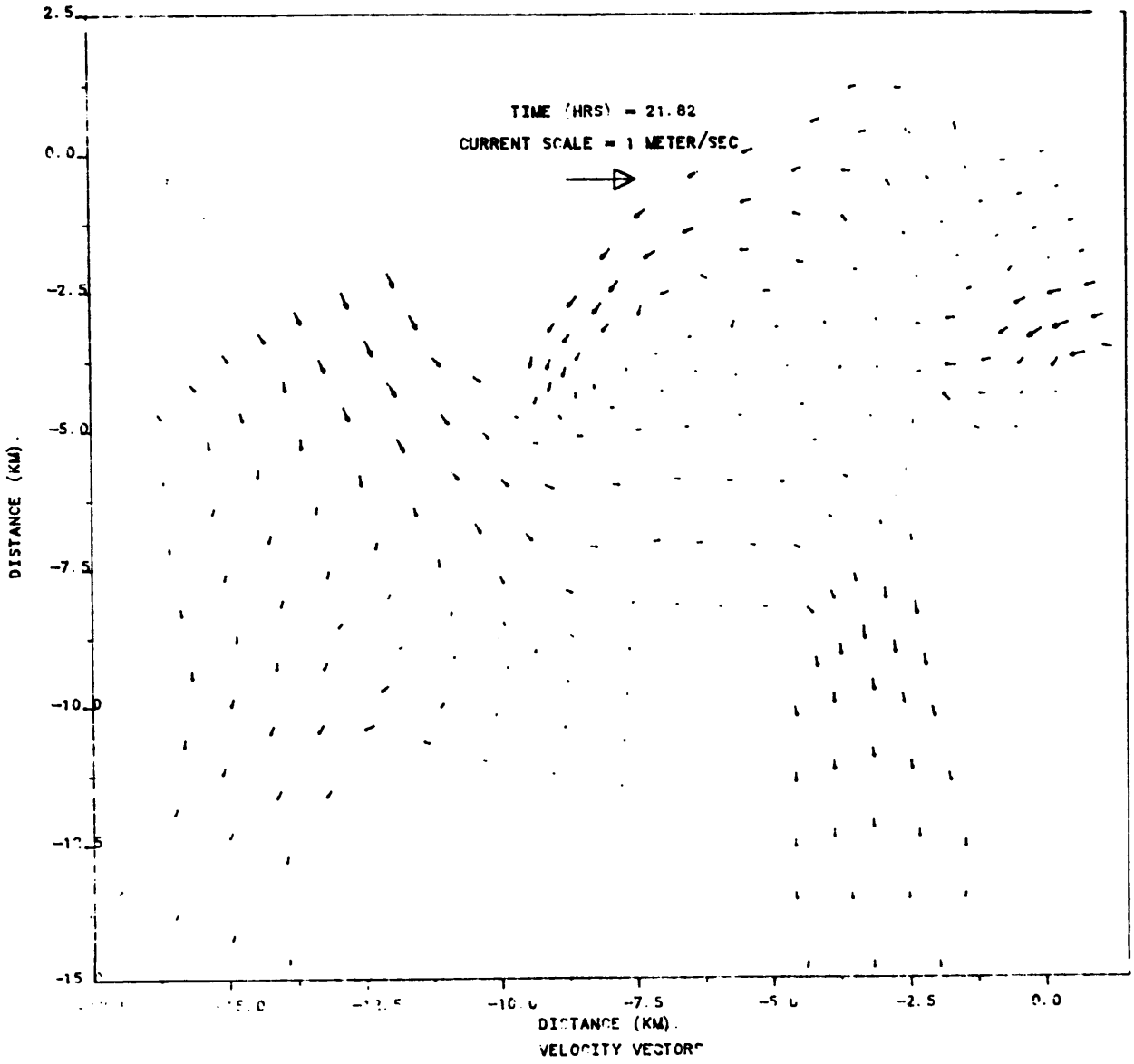

Figure IIIE-14c. Flow field in Hampton Roads, Island D, slack before flood.

during peak currents. The particulate organic fraction constituted from one-third to one-half the total dry weight.

Prior to the invasion of the oyster disese MSX in the late 1950's, Hampton Flats was a productive ground for planted oysters. With the demise of the oyster populations Hampton Flats (and its deeper flanks) have become significant hard clam harvest grounds.

Consideration of the potential changes in the sedimentation characteristics of Hampton Flats first requires an exploration of preconstruction conditions which are favorable to hard clam recruitment and growth. This required examination of the surface sediment characteristics and flow field on Hampton Flats.

1. Surface Sediments.

Sampling of surface sediments (upper 6 cm) was performed on 4 February, 1986. The surface sediments are fine to medium sands (Figure IIIF-1) with silt/clay fractions varying between 3 and 25 percent (Figure IIIF-2). The innermost, and eastern, stations contain the higher silt/clay content. The western one-third of Hampton Flats tends to be coarser than the remainder of the area. Appendix IID contains specific information on station location, details of the sediment characteristics, and methodology.

The sediment characteristics of Hampton Flats reflect a limited source of the silt/clay size fractions and/or sufficient reworking of the sediments such that only a limited amount of the finer grained material remain incorporated in the sediment column. The principal agent for incorporation into the sediment column is gravitational settling from the water column and fecal deposits of filter feeding benthos, with mixing due to bioturbation. Sedimentation reworking due to resuspension by tidal current and wave induced scour is probably the principal agent to remove the fine grained

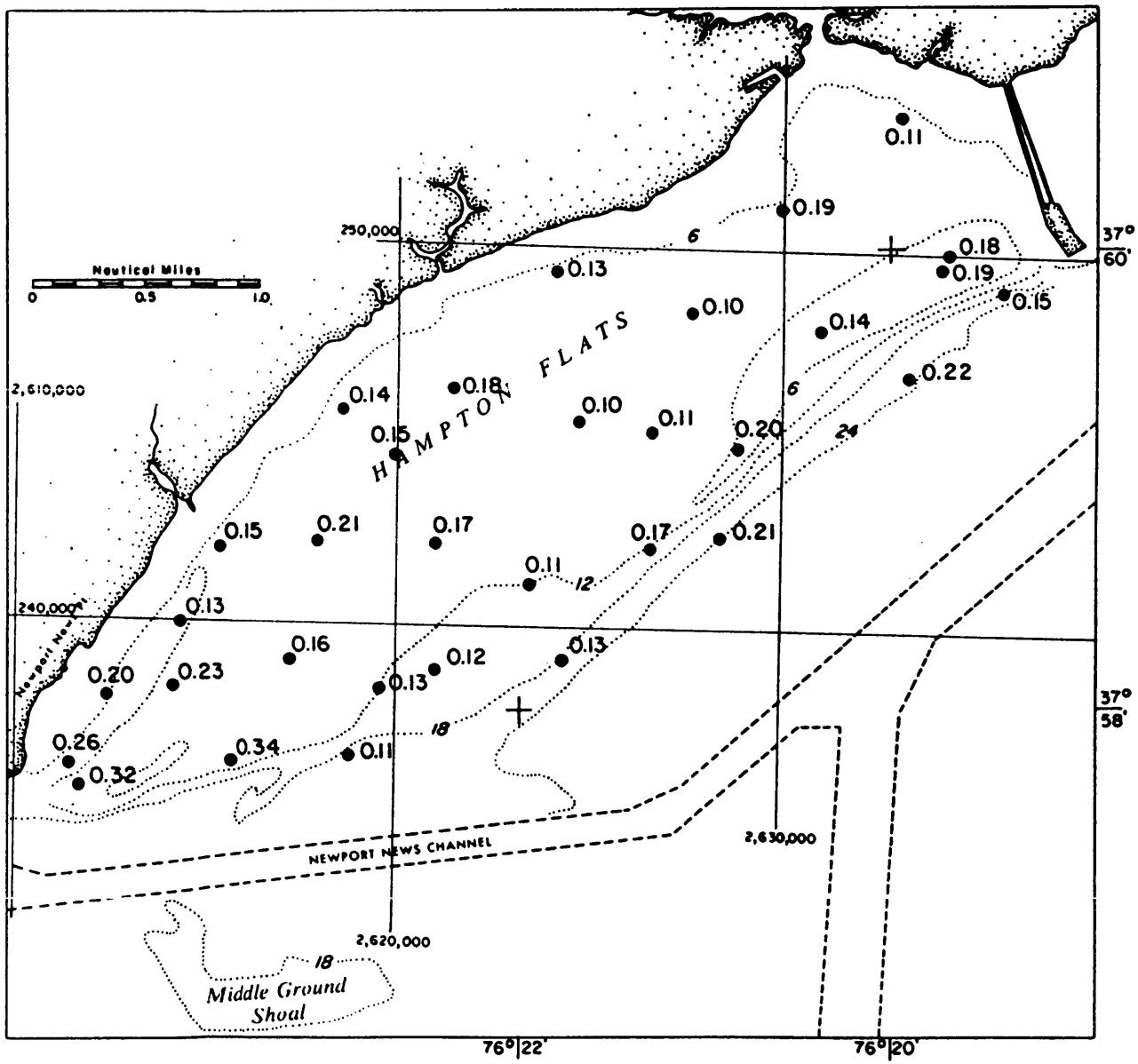

Figure IIIF-1. Median grain size of sand fraction, mm.

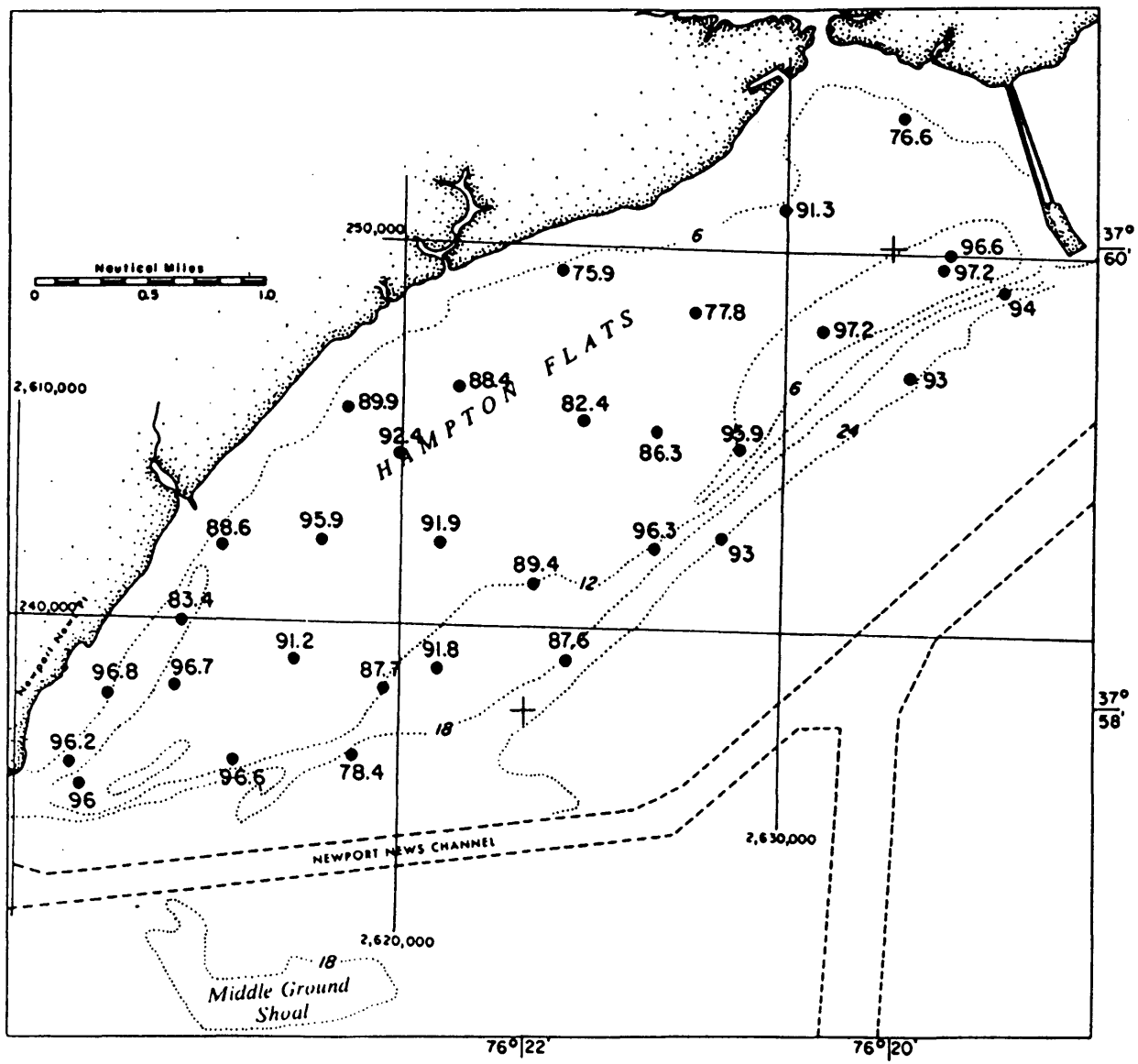

Figure IIIF-2. Percent weight of sand fraction.

fractions. However, in the Hampton Flats area sediment reworking associated with clam harvest by tongs is also likely to be a significant sediment reworking process as the fine grained fraction is returned to the water column for advection by tidal currents.

2. Tidal Currents and Sediment Resuspension Potential

The results of the two-dimensional numerical hydrodynamic model are used to describe the tidal current field on Hampton Flats. Table IIIF-1 lists the maximum ebb and flood current speeds for the mean tide range (0.76 m) identified with model nodal points shown in Figure IIIF-3. Reference may be made to Section IIIE-4 for additional information on phase relationships and vector plots.

For the BASE condition (Table IIIF-1) the maximum flood currents at virtually all stations exceed 0.25 m/s and 0.20 m/s during maximum ebb currents. At more than one-half of the nodes the maximum flood currents exceed 0.35 m/s. These values exceed the threshold velocities required to entrain fine sand. Miller et al. (1977) reanalyzed several sets of laboratory data and found the threshold velocity for quartz sand to be described by the relationship

$$u_{100} = 122.6\ D^{0.29}$$

where u_{100} = current speed 100 cm above the bed, cm/sec

D = sediment grain diameter in centimeters.

Application to the range of median sand sizes found on Hampton Flats provides the following estimates:

Grain size (mm)	Flow speeds for entrainment (cm/sec)
0.10	0.32
0.15	0.36
0.20	0.39
0.25	0.42

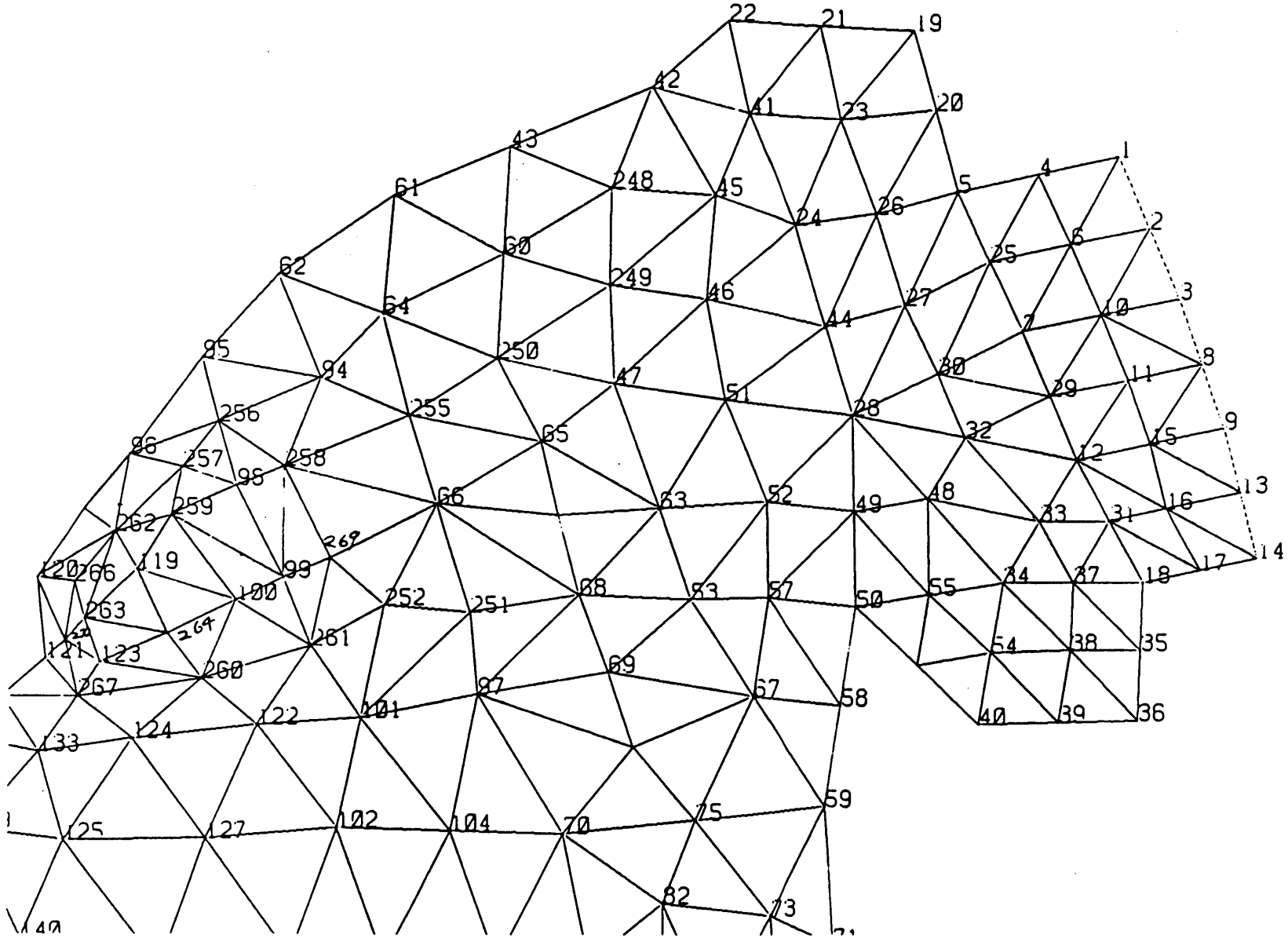

Figure IIIF-3. Position identification of node numbers listed in Table IIIF-1.

TABLE IIIF-1a. CURRENTS ON HAMPTON FLATS

NODE NO.	DEPTH AT NODE (m)	MAXIMUM FLOOD CURRENTS m/s BASE	I664 45 ft	I664 55 ft	ISLAND A	ISLAND B	ISLAND C-55	ISLAND C-45	ISLAND D-55
23	2.7	0.25	0.25	0.26	0.25	0.25	0.25	0.25	0.25
41	2.7	0.22	0.22	0.23	0.22	0.22	0.21	0.21	0.21
26	4.0	0.34	0.33	0.34	0.33	0.33	0.33	0.32	0.33
24	1.9	0.26	0.25	0.26	0.25	0.25	0.24	0.24	0.24
46	2.2	0.41	0.40	0.41	0.39	0.39	0.38	0.37	0.37
45	3.8	0.27	0.26	0.26	0.25	0.25	0.25	0.25	0.24
47	2.7	0.49	0.48	0.48	0.46	0.46	0.45	0.46	0.44
249	3.4	0.32	0.31	0.31	0.29	0.27	0.27	0.27	0.26
248	2.8	0.28	0.27	0.28	0.26	0.26	0.26	0.26	0.25
65	3.9	0.38	0.37	0.37	0.35	0.35	N/A	N/A	0.33
250	3.7	0.27	0.27	0.27	0.23	0.23	N/A	N/A	0.17
60	3.6	0.27	0.26	0.26	0.23	0.24	0.25	0.26	0.23
66	4.3	0.35	0.35	0.34	0.34	0.38	N/A	N/A	N/A
255	3.5	0.29	0.27	0.27	0.19	0.13	N/A	N/A	N/A
64	2.5	0.27	0.26	0.26	0.21	0.23	0.32	0.32	0.25
252	5.9	0.41	0.38	0.36	0.40	0.36	0.26	0.29	0.26
269	3.7	0.32	0.31	0.29	N/A	N/A	N/A	N/A	N/A
258	3.4	0.30	0.29	0.28	N/A	N/A	N/A	N/A	N/A
94	2.9	0.27	0.26	0.26	0.18	0.23	0.31	0.31	0.31
261	6.8	0.46	0.45	0.43	0.41	0.40	0.36	0.38	0.36
99	3.3	0.35	0.33	0.31	N/A	N/A	0.15	0.17	N/A
98	3.4	0.31	0.29	0.28	N/A	N/A	0.25	0.26	N/A
256	2.9	0.28	0.26	0.25	0.20	0.27	0.32	0.32	0.34
100	2.5	0.39	0.37	0.35	N/A	N/A	0.28	0.30	0.25
259	3.3	0.35	0.32	0.30	N/A	N/A	0.26	0.27	0.25
257	3.4	0.29	0.26	0.25	0.19	0.27	0.28	0.28	0.34
260	5.9	0.49	0.48	0.47	0.47	0.46	0.44	0.45	0.44
264	3.1	0.48	0.46	0.43	N/A	N/A	0.39	0.41	0.36
119	3.7	0.34	0.28	0.27	N/A	N/A	0.30	0.30	0.25
262	3.1	0.35	0.30	0.29	0.22	0.32	0.27	0.28	0.25
267	6.3	0.54	0.55	0.53	0.41	0.46	0.53	0.55	0.52
123	2.2	0.51	0.52	0.49	N/A	0.23	0.38	0.40	0.36
263	4.0	0.43	0.38	0.35	N/A	0.22	0.32	0.34	0.31
266	2.2	0.39	0.36	0.33	0.28	0.29	0.27	0.29	0.26
270	4.9	0.42	0.34	0.32	0.17	0.18	0.25	0.26	0.25

TABLE IIIF-1b. CURRENTS ON HAMPTON FLATS

MAXIMUM EBB CURRENTS
m/s

NODE NO.	BASE	I664 45 ft	I664 55 ft	ISLAND A	ISLAND B	ISLAND C-55	ISLAND C-45	ISLAND D-55
23	0.28	0.28	0.29	0.28	0.28	0.28	0.28	0.27
41	0.23	0.23	0.24	0.23	0.22	0.23	0.23	0.22
26	0.52	0.52	0.53	0.53	0.53	0.54	0.52	0.53
24	0.28	0.27	0.28	0.28	0.27	0.28	0.28	0.27
46	0.29	0.28	0.29	0.29	0.29	0.28	0.27	0.28
45	0.29	0.28	0.29	0.27	0.26	0.28	0.27	0.25
47	0.41	0.40	0.42	0.40	0.40	0.34	0.32	0.34
249	0.28	0.28	0.28	0.25	0.24	0.23	0.23	0.22
248	0.25	0.24	0.25	0.22	0.22	0.25	0.25	0.23
65	0.30	0.30	0.31	0.27	0.27	N/A	N/A	0.19
250	0.24	0.24	0.24	0.18	0.17	N/A	N/A	0.12
60	0.24	0.24	0.24	0.20	0.21	0.24	0.25	0.22
66	0.31	0.31	0.31	0.27	0.31	N/A	N/A	N/A
255	0.27	0.26	0.26	0.16	0.12	N/A	N/A	N/A
64	0.25	0.25	0.25	0.17	0.21	0.30	0.30	0.26
252	0.40	0.38	0.36	0.38	0.34	0.32	0.35	0.33
269	0.30	0.30	0.29	N/A	N/A	N/A	N/A	N/A
258	0.24	0.23	0.22	N/A	N/A	N/A	N/A	N/A
94	0.24	0.23	0.23	0.15	0.19	0.27	0.27	0.28
261	0.46	0.45	0.44	0.42	0.41	0.39	0.41	0.41
99	0.32	0.32	0.30	N/A	N/A	0.23	0.24	N/A
98	0.25	0.22	0.22	N/A	N/A	0.22	0.22	N/A
256	0.23	0.21	0.21	0.16	0.22	0.25	0.25	0.30
100	0.36	0.36	0.34	N/A	N/A	0.32	0.33	0.26
259	0.26	0.22	0.21	N/A	N/A	0.21	0.21	0.23
257	0.22	0.20	0.20	0.15	0.22	0.22	0.23	0.28
260	0.47	0.48	0.47	0.44	0.44	0.44	0.45	0.43
264	0.39	0.39	0.36	N/A	N/A	0.35	0.37	0.33
119	0.26	0.20	0.19	N/A	N/A	0.23	0.23	0.20
262	0.23	0.21	0.20	0.18	0.25	0.21	0.25	0.18
167	0.45	0.47	0.44	0.37	0.38	0.43	0.45	0.42
123	0.42	0.43	0.40	N/A	0.19	0.31	0.32	0.30
263	0.30	0.21	0.20	0.25	N/A	0.19	0.20	0.20
266	0.24	0.20	0.19	0.20	0.20	0.16	0.16	0.17
270	0.30	0.21	0.23	0.22	0.23	0.15	0.15	0.18

For the depths pertaining, u_{100} is reasonably approximated by the depth averaged velocity. However, the above values pertain to abiotic sands as opposed to mixed sediment with biological controls. For the most part the biological factors have defied quantification. Given the state-of-the-art and the problem in hand, this analysis has assumed the resuspension potential as represented by the median sand grain size. Given these approximations the results indicate that much of the area of Hampton Flats is subject to resuspension under tidal scour with the mean tide range.

The transport potential is more appropriately described in terms of the fundamental variable of shear stress, τo, induced by the flow interacting with the sediment-water interface. The transformation prcedure is described in Appendix IID. Resuspension potential is cast in terms of the ratio between the bottom shear stress to the threshold shear stress required to initiate movement, $\tau o/\tau c$. Figure IIIF-4a,b represent the BASE condition for maximum flood and ebb conditions at mean tide range (0.76 m). The flood current is sufficiently strong to initiate movement (under the embodied assumption) over most of Hampton Flats. The ratio $\tau o/\tau c$ increases over the western one-third of the area which is consistent with the flow convergence in approaching Newport News Point. In situ observations during the benthic resource sampling confirm transport reflected by active sand ripples. During the ebb current the flow over the northwestern sector is reduced such that threshold transport conditions are not exceeded. However, tide ranges exceeding the mean range but less than the spring tide range (0.88 m) would induce motion over most of Hampton Flats. Specifically, τ spring/τmean equals 1.19 so stations with values exceeding 0.84 in Figure IIIF-4a,b would have entrainment under tide range conditions between 0.76 m and 0.88 m

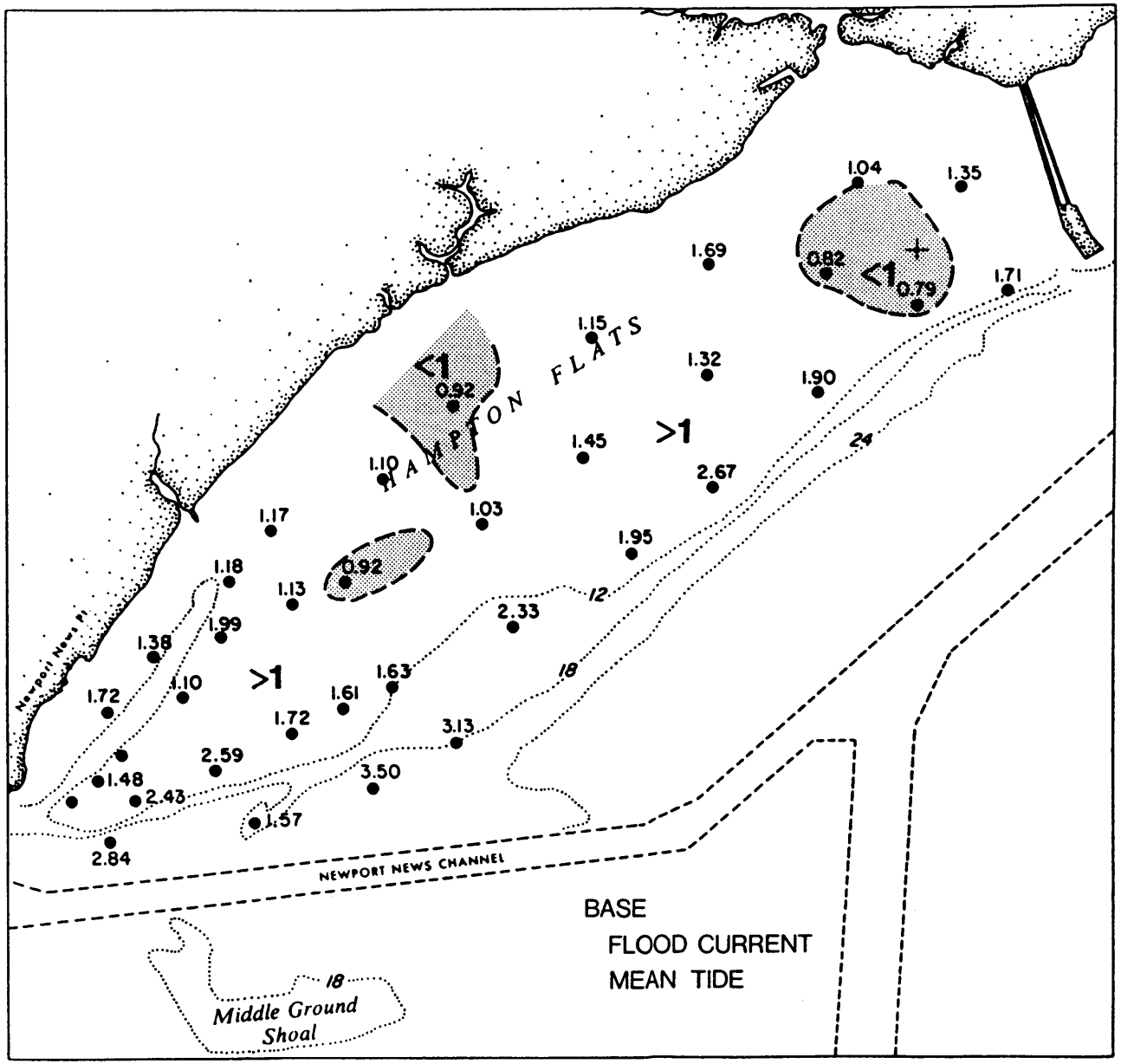

Figure IIIF-4a. Values of τ_o/τ_c for BASE condition, maximum flood current.

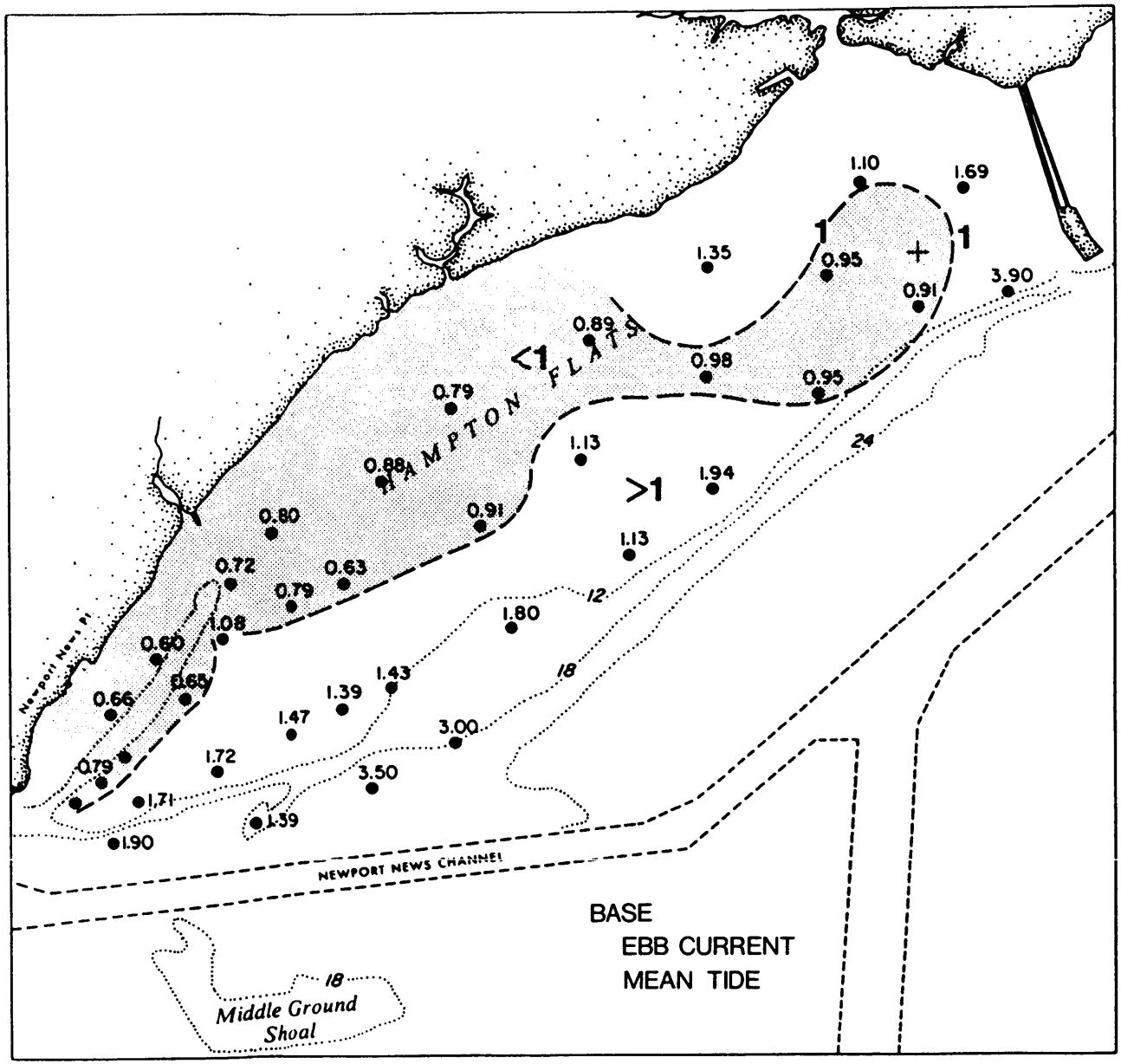

Figure IIIF-4b. Values of τ_o/τ_c for BASE condition, maximum ebb current.

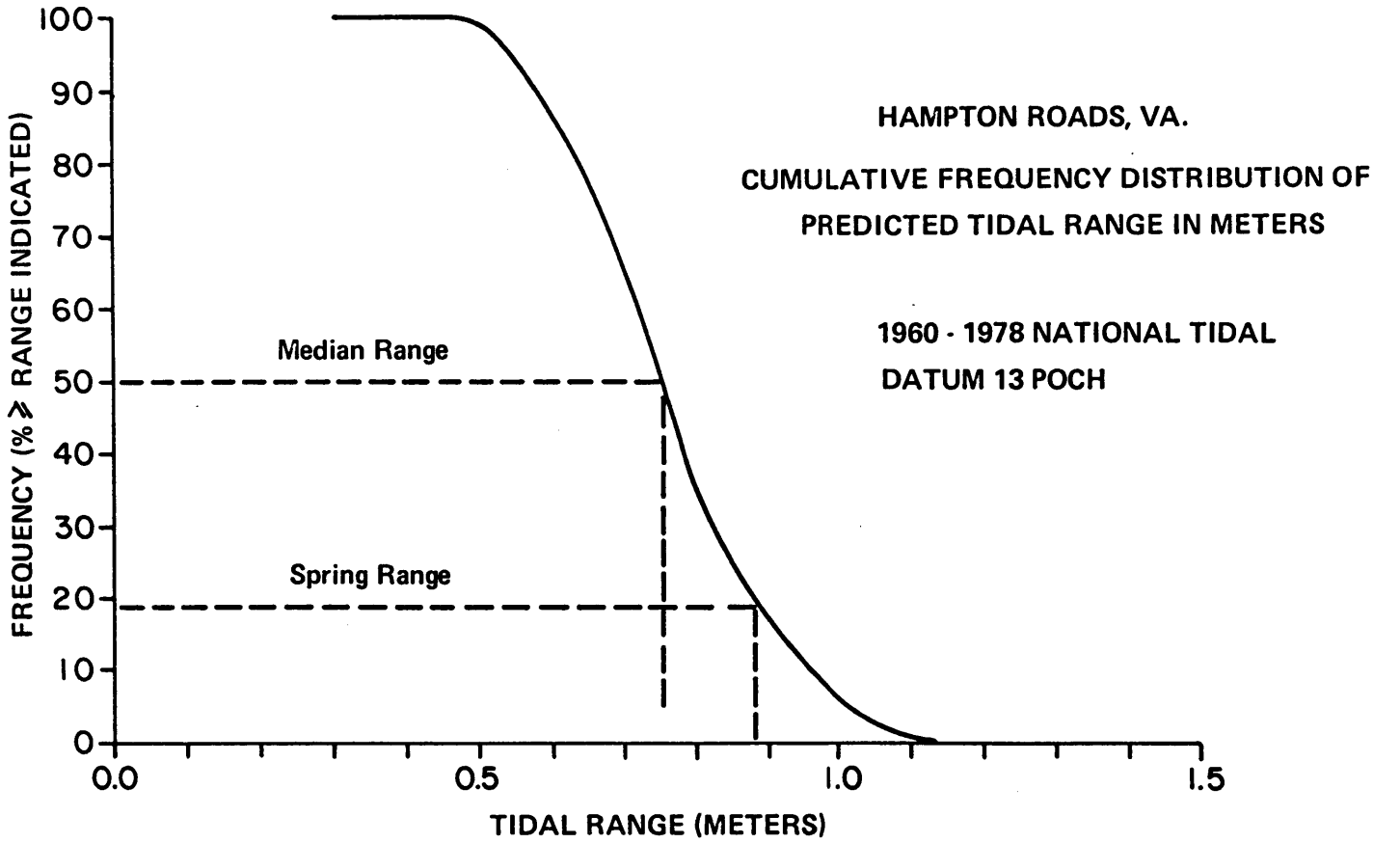

Figure IIIF-5. Cumulative distribution of tide range for 1960-1978 Tidal Datum Epoch.

(development is presented in Appendix IID). Such tide ranges are predicted to occur in 32% of the cases (Figure IIIF-5).

Surface wave-tidal current interaction also plays a role in sediment resuspension on Hampton Flats due to the fetch within Hampton Roads and exposure to waves from the lower Chesapeake Bay. The effects of the non-linear wave-current interaction (developed in Appendix IID) is shown in Figure IIIF-6 for sediment sizes, water depths, and current speeds pertaining to Hampton Flats. For a wave period of 3 seconds and wave height of 0.3 meter the combined shear stress is sufficient to entrain the sand sediment even at very low current speeds.

3. Framework for Analysis of Impacts Due to Construction

The hard clam populations of Hampton Flats occur in sandy sediments with relatively energetic current regime. The hydrodynamic regime of the BASE condition is apparently sufficient to inhibit accumulation of fine grained sediments supplied by tidal current advection. Laboratory studies of Keck et al. (1974) indicate that larvae of the hard clam prefer to set on a sandy substrate as compared to mud. Accordingly, the principal component for consideration of impact due to construction addresses whether altered conditions would induce surface accumulations of fine grained sediments. In the absence of an explicit numerical sediment transport model the criterion adopted was the entrainment potential ratio, $\tau c/\tau o$, for the sandy substrate. The rationale, simply stated, is that if the shear stress is sufficient to entrain the substrate then the sediment fluff settling to the sediment surface will be entrained into the water column and subject to tidal current advection.

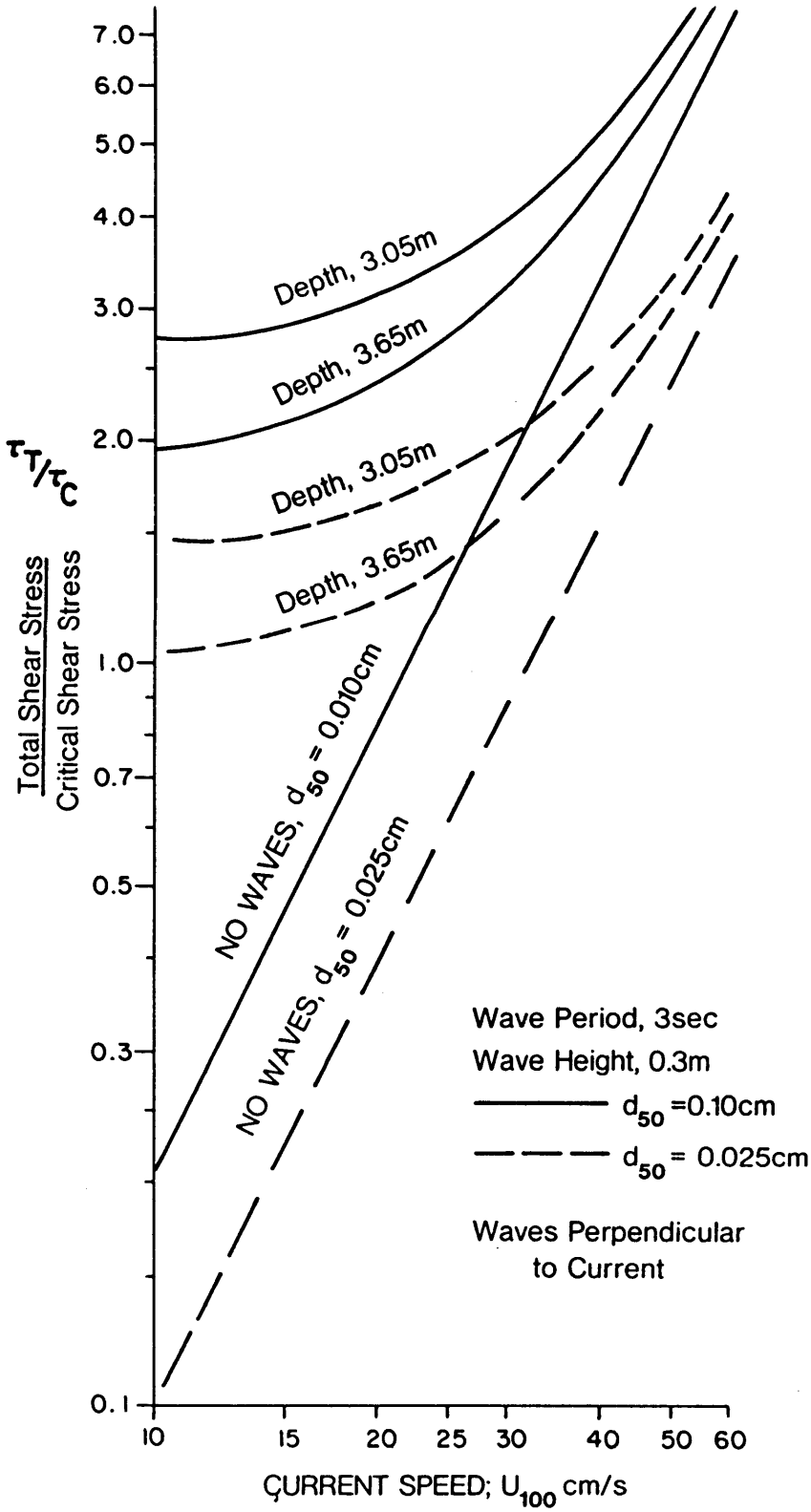

Figure IIIF-6 Total bottom shear stress to critical shear stress due to wave-current interaction.

4. Modification in Sediment Transport Potential Due to Construction

a. I664. In order to facilitate discussion of the changes due to construction the area of Hampton Flats is segmented in four zones (Figure IIF-7). Maps of the sediment transport potential for the conditions I664-45 and I664-55 are shown in Figures IIIF-8a,b and IIIF-9a,b. The results between the cases are virtually identical. Compared to the BASE condition the zone of $\tau o/\tau c<1$ is enlarged for the flood current phase. On the ebb current phase (Figure IIIF-8b) the pattern of $\tau o/\tau c<1$ is the same as the BASE condition. However, the values in Zone A (Figure IIIF-7) tend to be lower than the BASE condition. Sedimentation may be expected to be enhanced in the western sector of Zone A and along the shore boundary. This is consistent with findings of earlier studies (Fang, et al, 1972 and 1979; Heltzel, 1984) utilizing physical and numerical models. However, blanket surficial muds are not expected since the zone is exposed to surface wave action. Rather the sedimentation will probably be sands enriched somewhat in the silt/clay fraction.

b. ISLAND A. Maps of $\tau o/\tau c$ for Island A condition are shown in Figure IIIF-10a,b. Both the flood and ebb current phases exhibit markedly enlarged areas of $\tau o/\tau c<1$, with values ranging between 0.33 and 0.60 in Zone A. Thus, currents associated with spring tide range would, as well, be insufficient to entrain the substrate sands. However, the eastern portion of Zone A would still be exposed to waves from the lower Bay. Episodic resuspension could thus be expected, particularly in association with spring tide conditions. In this zone the surface sediments could be expected to have higher silt/clay content than the BASE condition. The area to the north and west of Island A would be sheltered from significant wave action. Conditions in these areas would be conducive to accumulations of fine grained sediment which, over time, may blanket the area. Prediction of

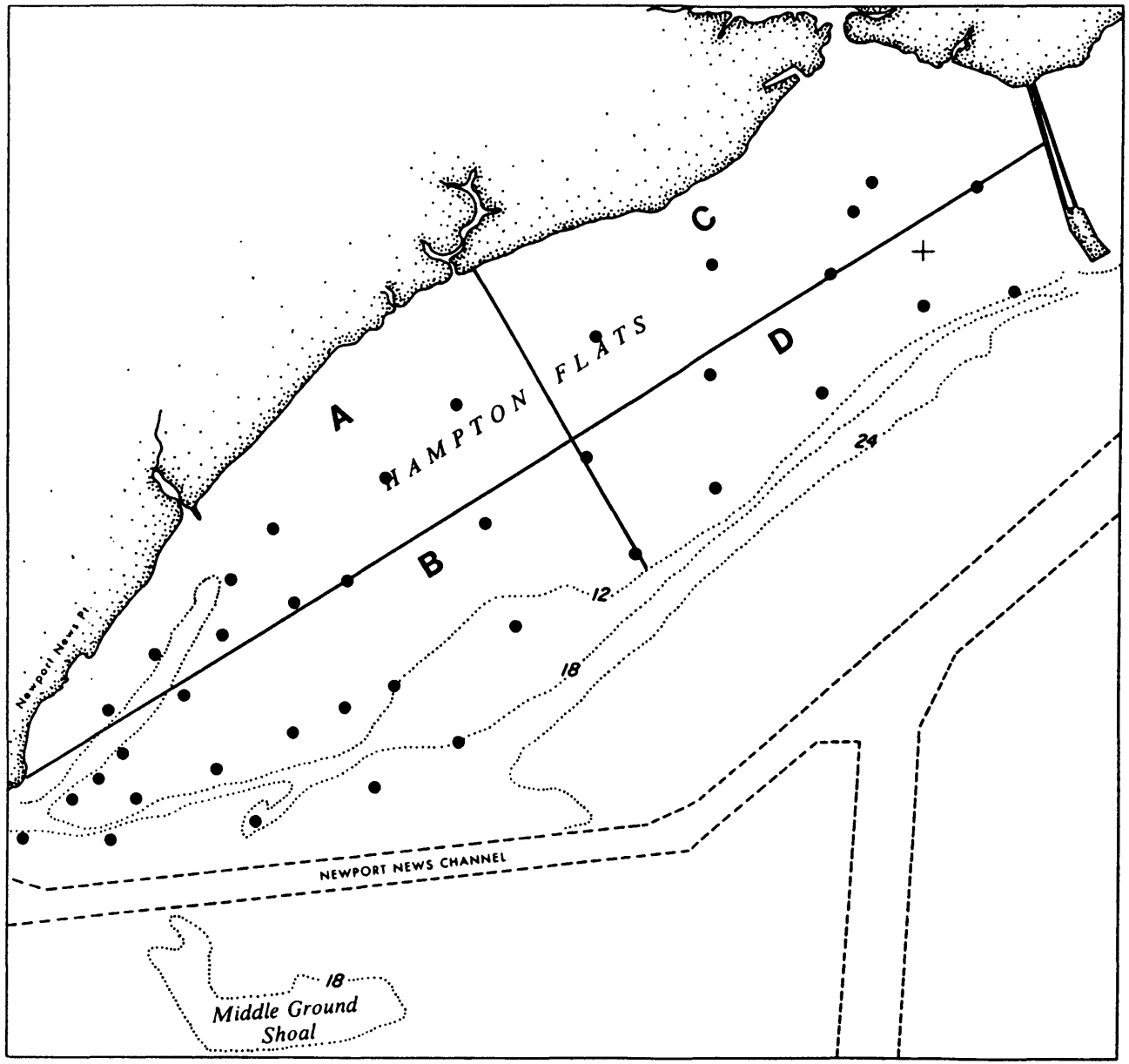

Figure IIIF-7. Segmentation of Hampton Flats.

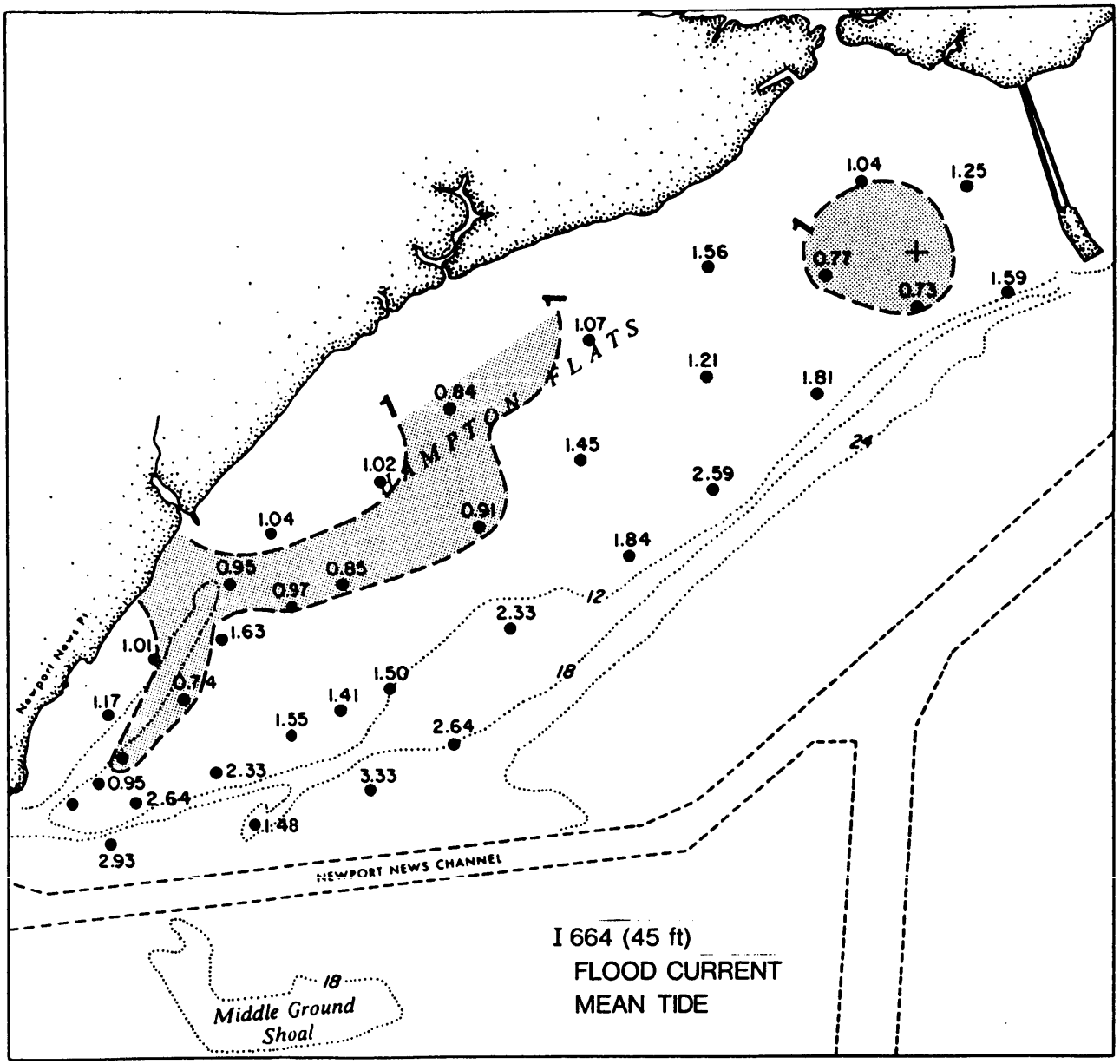

Figure IIIF-8a. Values of τ_o/τ_c for I664 (45 ft), maximum flood current.

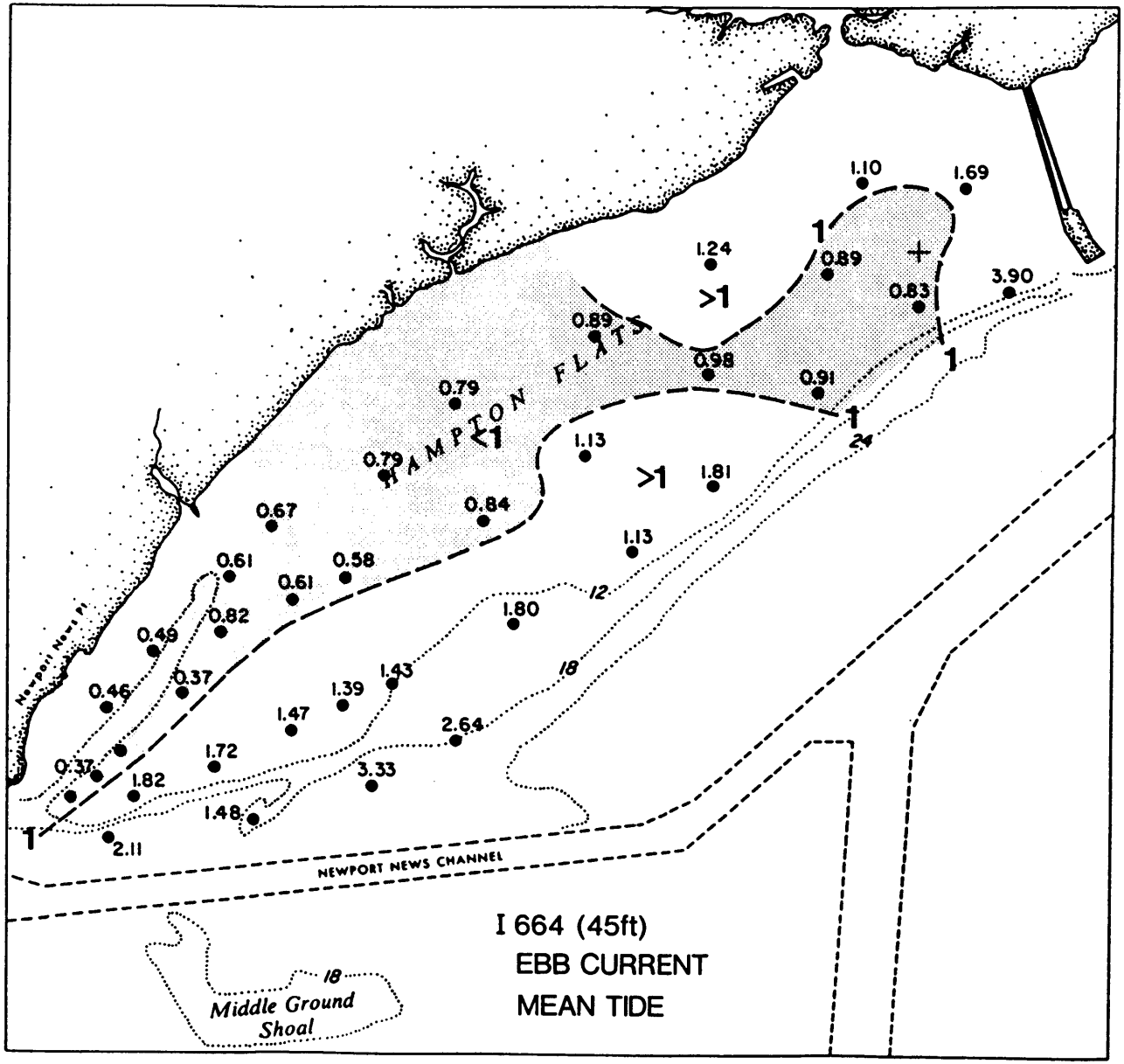

Figure IIIF-8b. Values of τ_o/τ_c for I664 (45 ft), maximum ebb current.

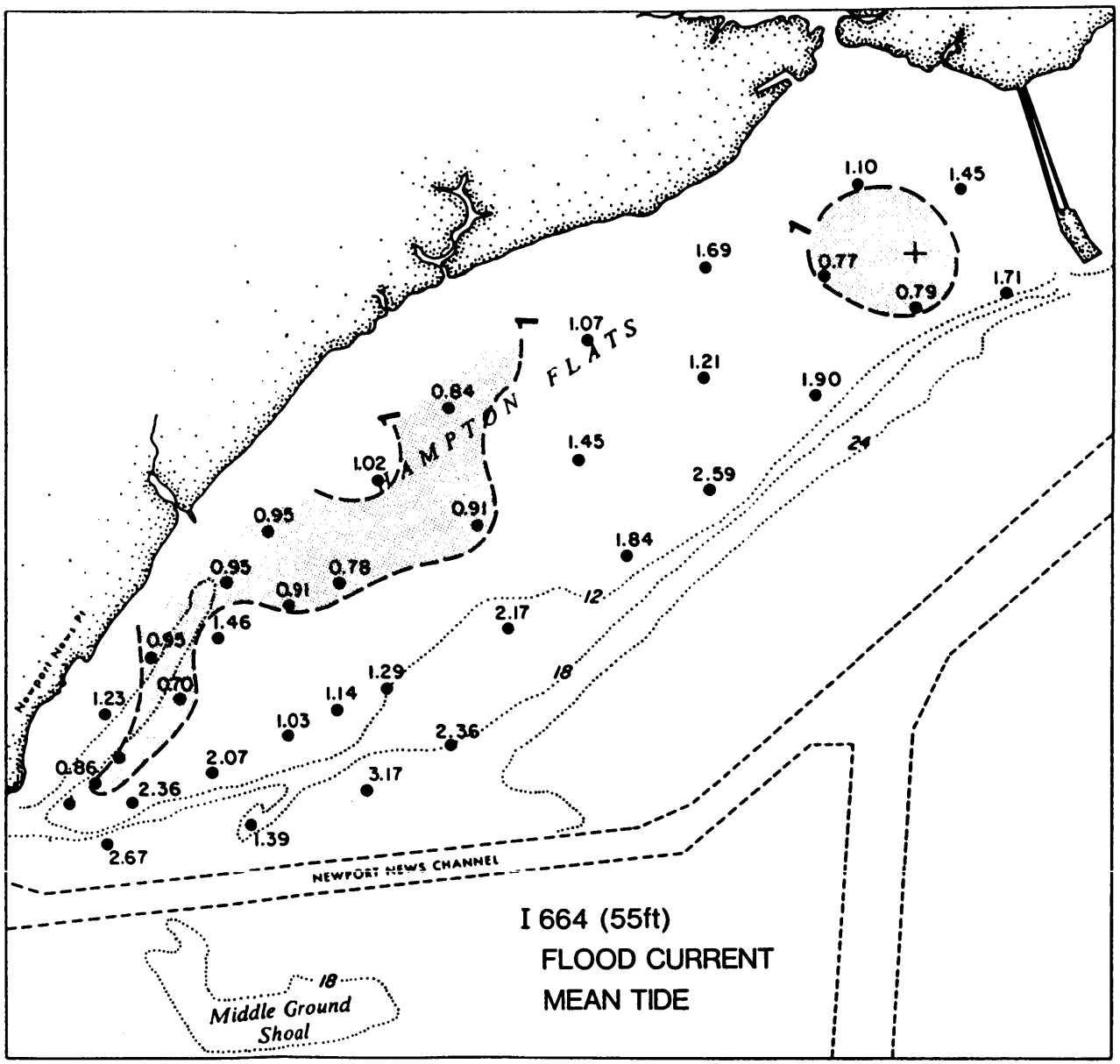

Figure IIIF-9a. Values of τ_o/τ_c for I664 (55 ft), maximum flood current.

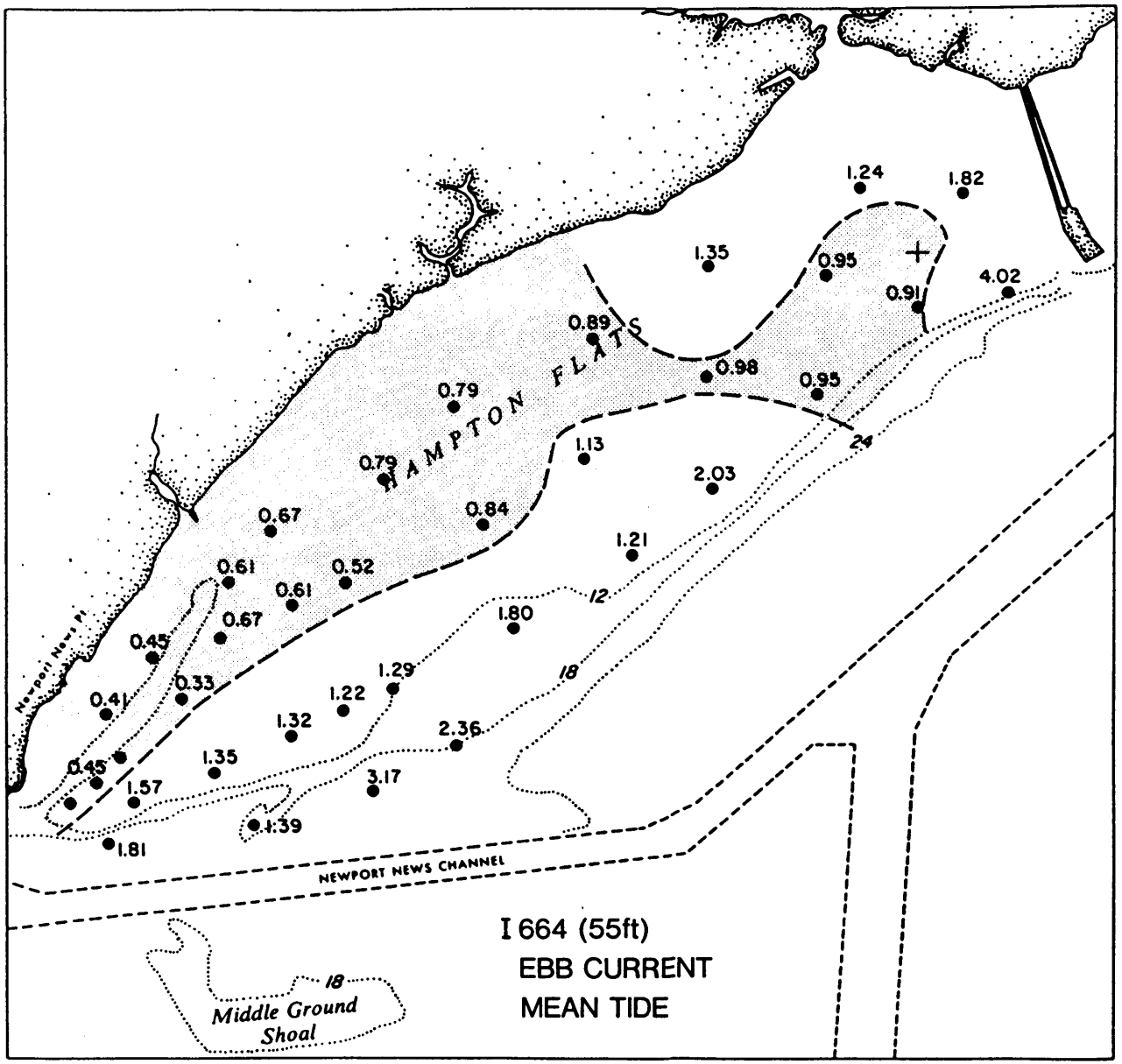

Figure IIIF-9b. Values of τ_o/τ_c for I664 (55 ft), maximum ebb current.

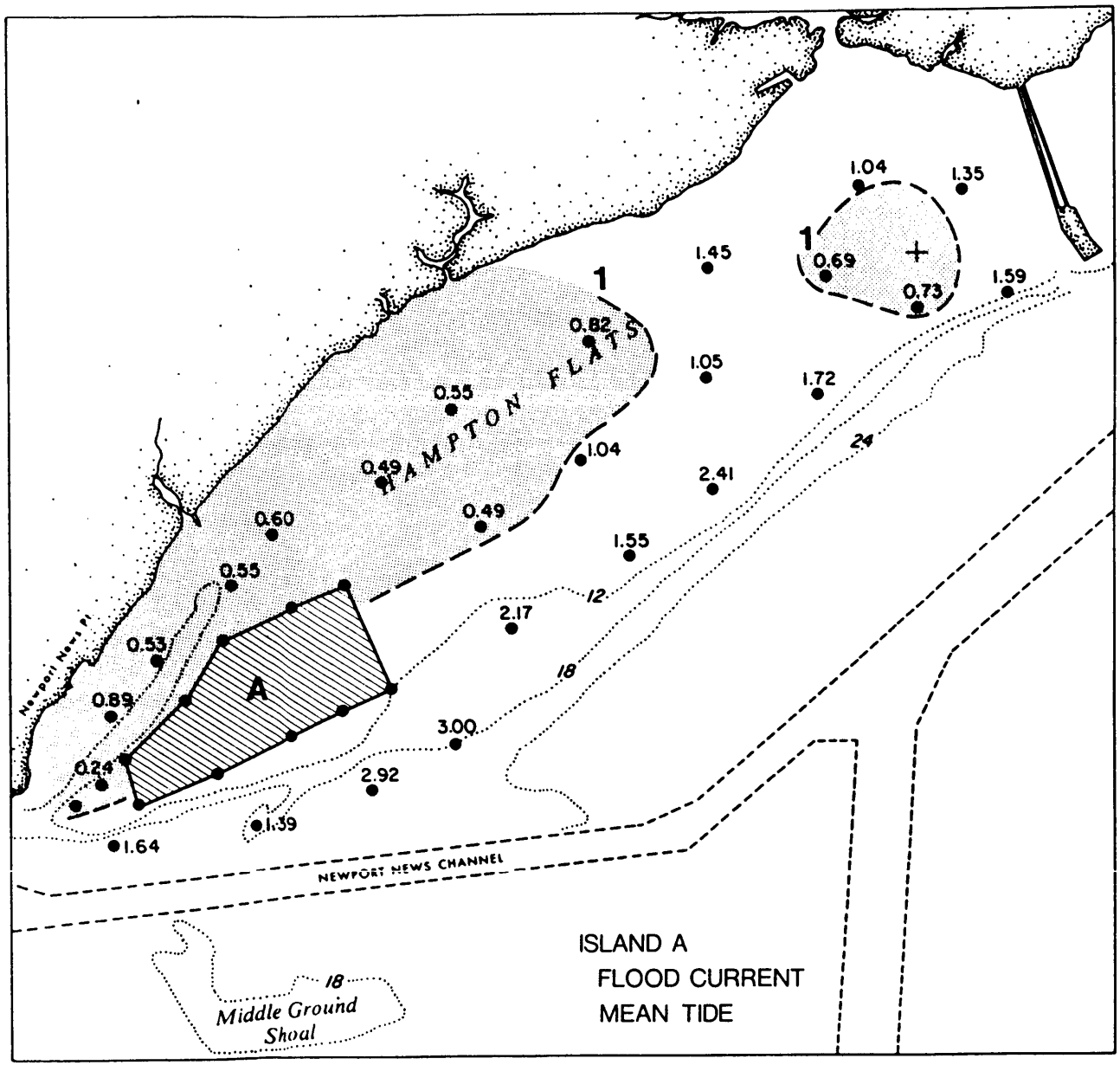

Figure IIIF-10a. Values of τ_o/τ_c for Island A, maximum flood current.

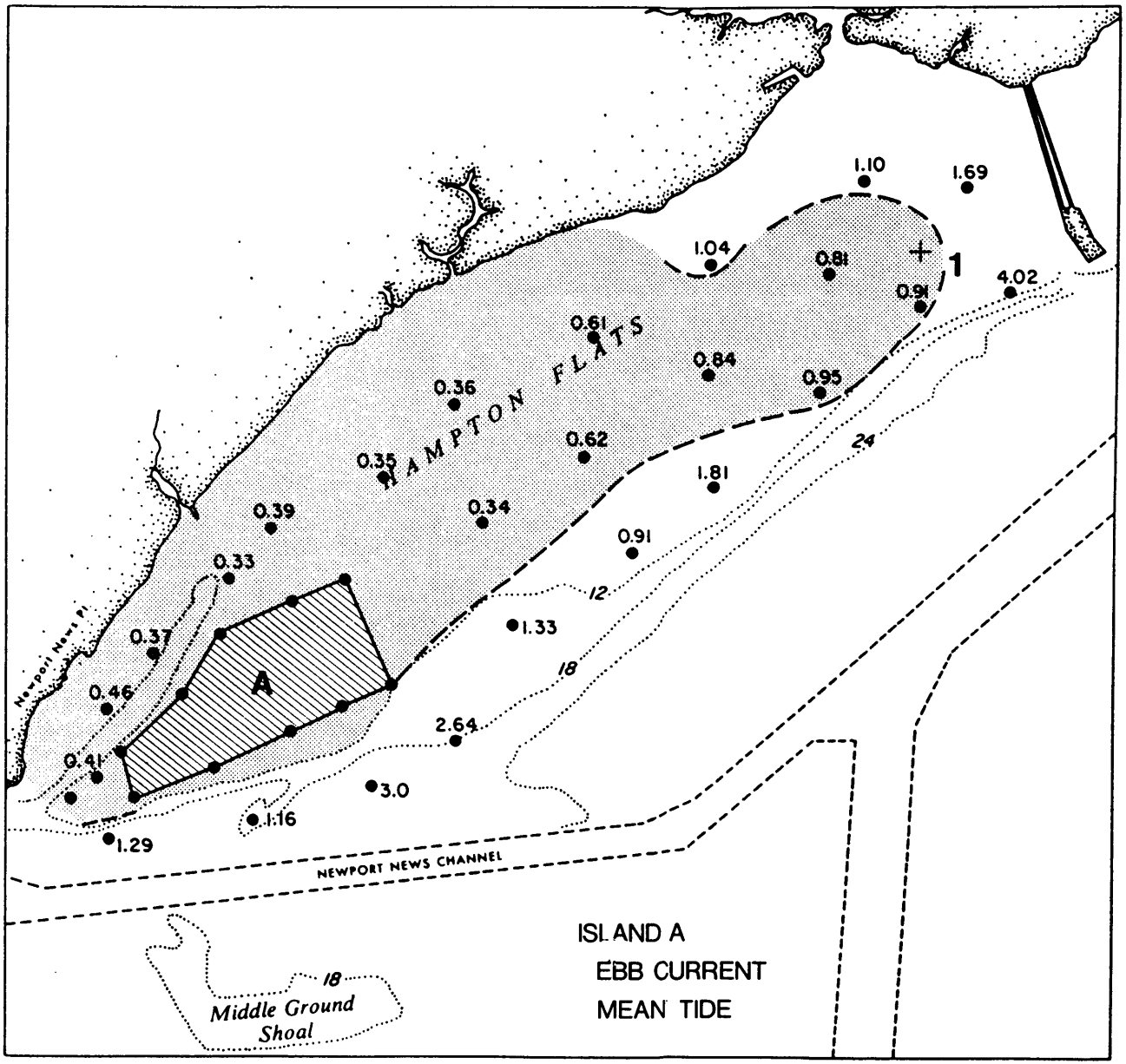

Figure IIIF-10b. Values of τ_o/τ_c for Island A, maximum ebb current.

the rate of accumulation defies quantification given the state-of-the-art. However, an order of magnitude upper limit can be estimated. Assuming a suspended solids concentration of 10 mg/l in the water column and that all of the material settled out each slack water then the deposition thickness (assuming 50% void space) would be 1 cm/yr for each meter of water depth. Given these assumptions, a 3 meter water column would provide about 3 cm of deposition per year.

c. ISLAND B. Results for the Island B configuration are shown in Figure F-11a,b. The more easterly position of Island B relative to the Island A configuration results in larger flood current flux through the northwest passage around the island. Consequently, for mean tide range the values of $\tau o/\tau c$ exceed unity through much of that zone. The lobe of reduced transport potential ($\tau o/\tau c<1$) extends further eastward than the case of Island A but much of the area would be entrained at spring tide range, and/or with significant wave action (see Figure IIIF-6). A station with a $\tau o/\tau c$ value as low as 0.20 (without waves) would be subject to entrainment under a wave of 0.3 m height and period of 3 seconds.

On ebb current the area of the reduced transport potential for Island B is essentially the same as for Island A. However, the significant difference is that values of $\tau o/\tau c$ are considerably higher in Zone A. With few exceptions the values of $\tau o/\tau c$ are comparable in the other zones.

In contrast to the Island A configuration, the Island B condition would not likely result in the blanket accumulation of fine sediments. However, the percentage of fines in the sediment column would be expected to increase in the western sector of Zone A and the northeast sector of Zone B.

d. ISLAND C. The results for Island C (370 acres) are shown in Figure IIIF-12a,b. In this case there are lobes of decreased transport

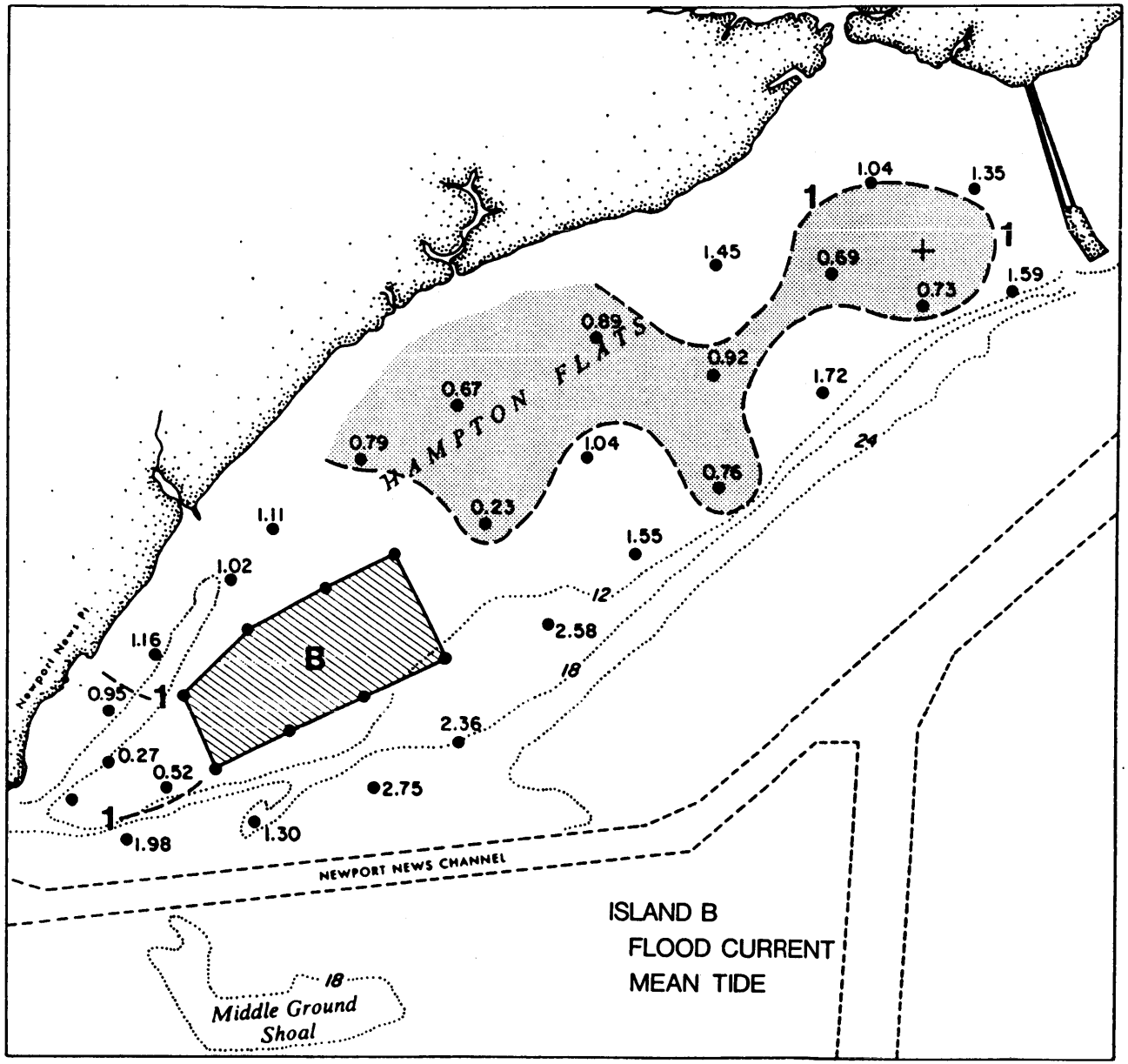

Figure IIIF-11a. Values of τ_o/τ_c for Island B, maximum flood current.

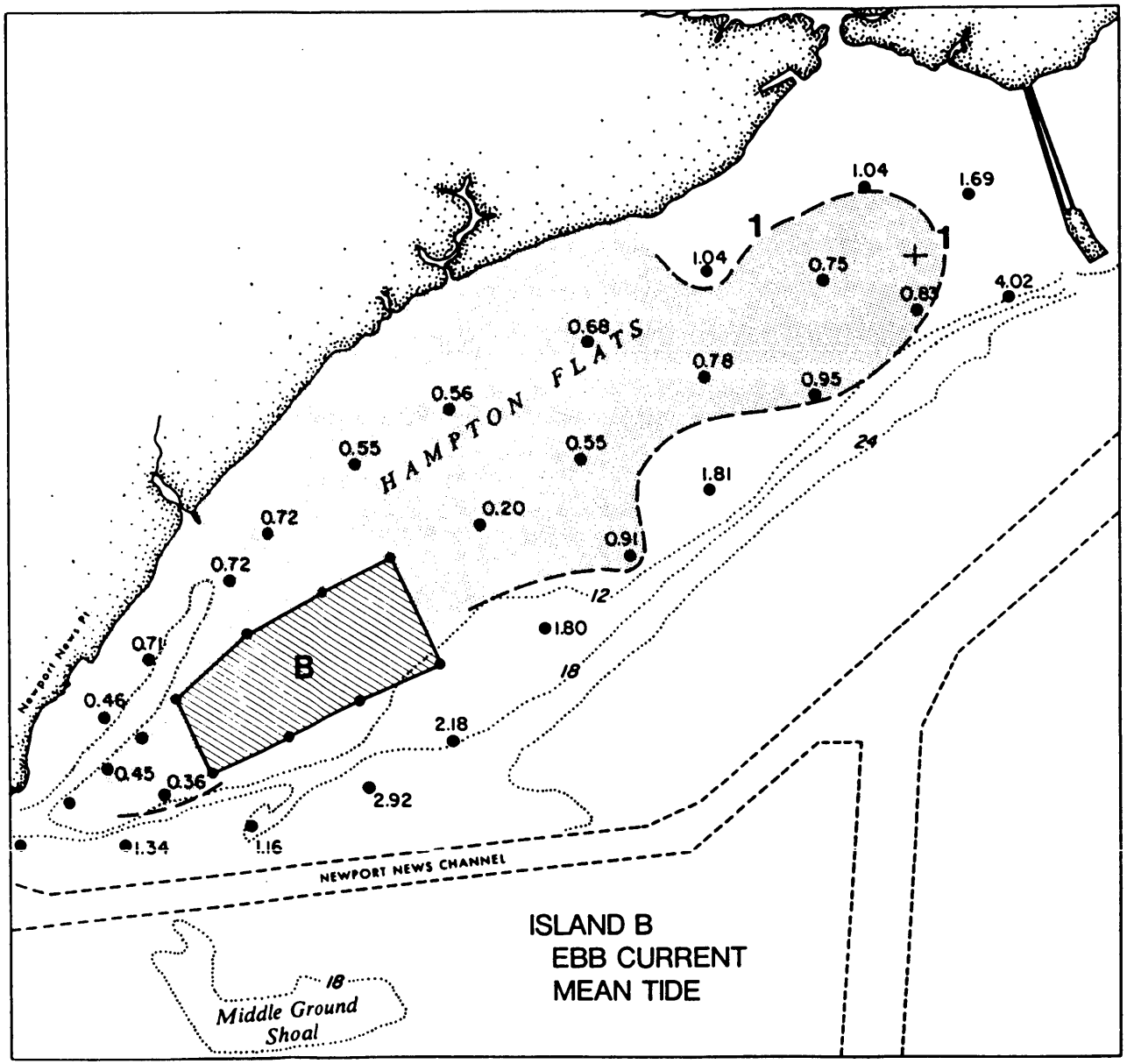

Figure IIIF-11b. Values of τ_o/τ_c for Island B, maximum ebb current.

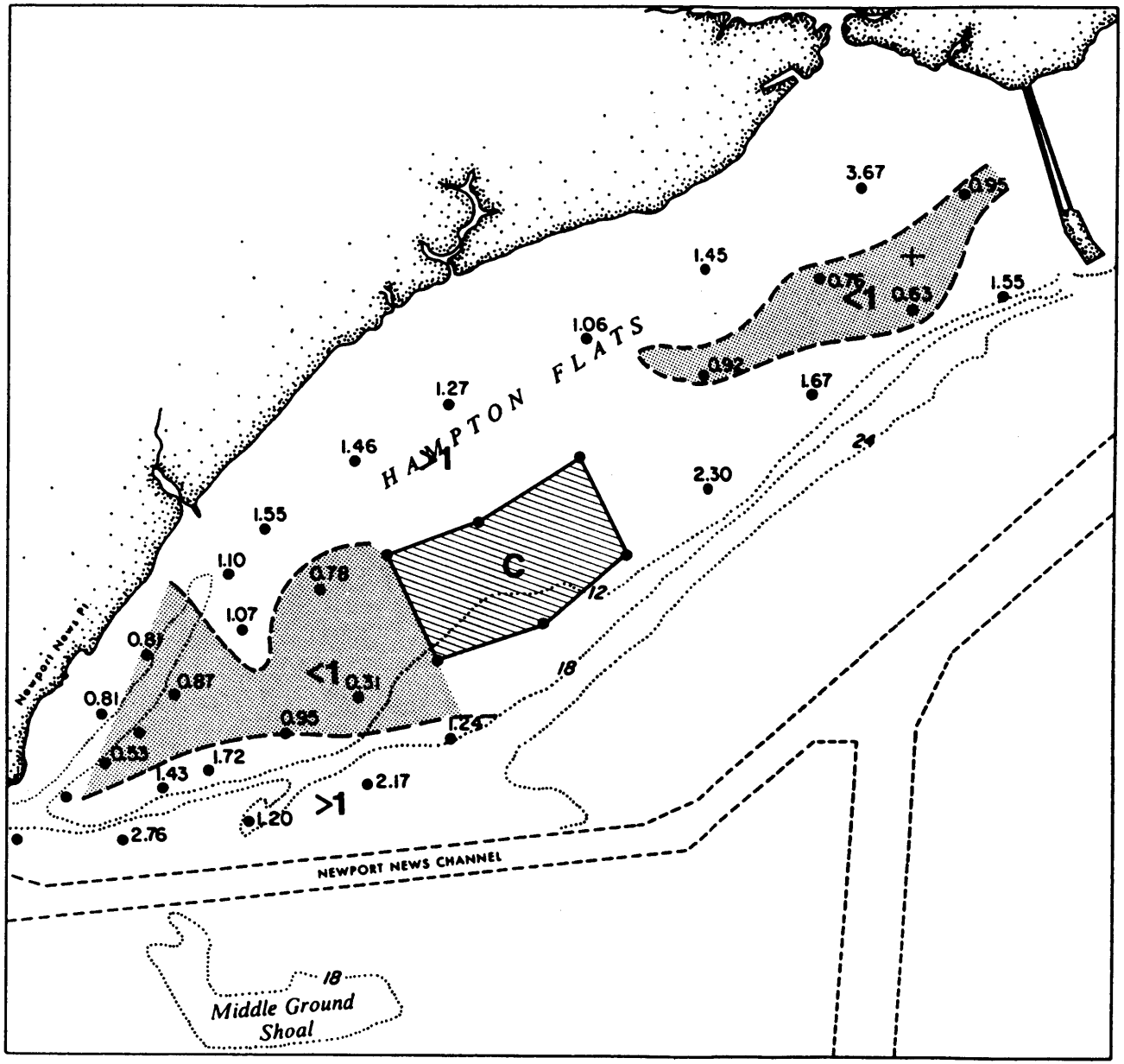

Figure IIIF-12a. Values of τ_o/τ_c for Island C, maximum flood current.

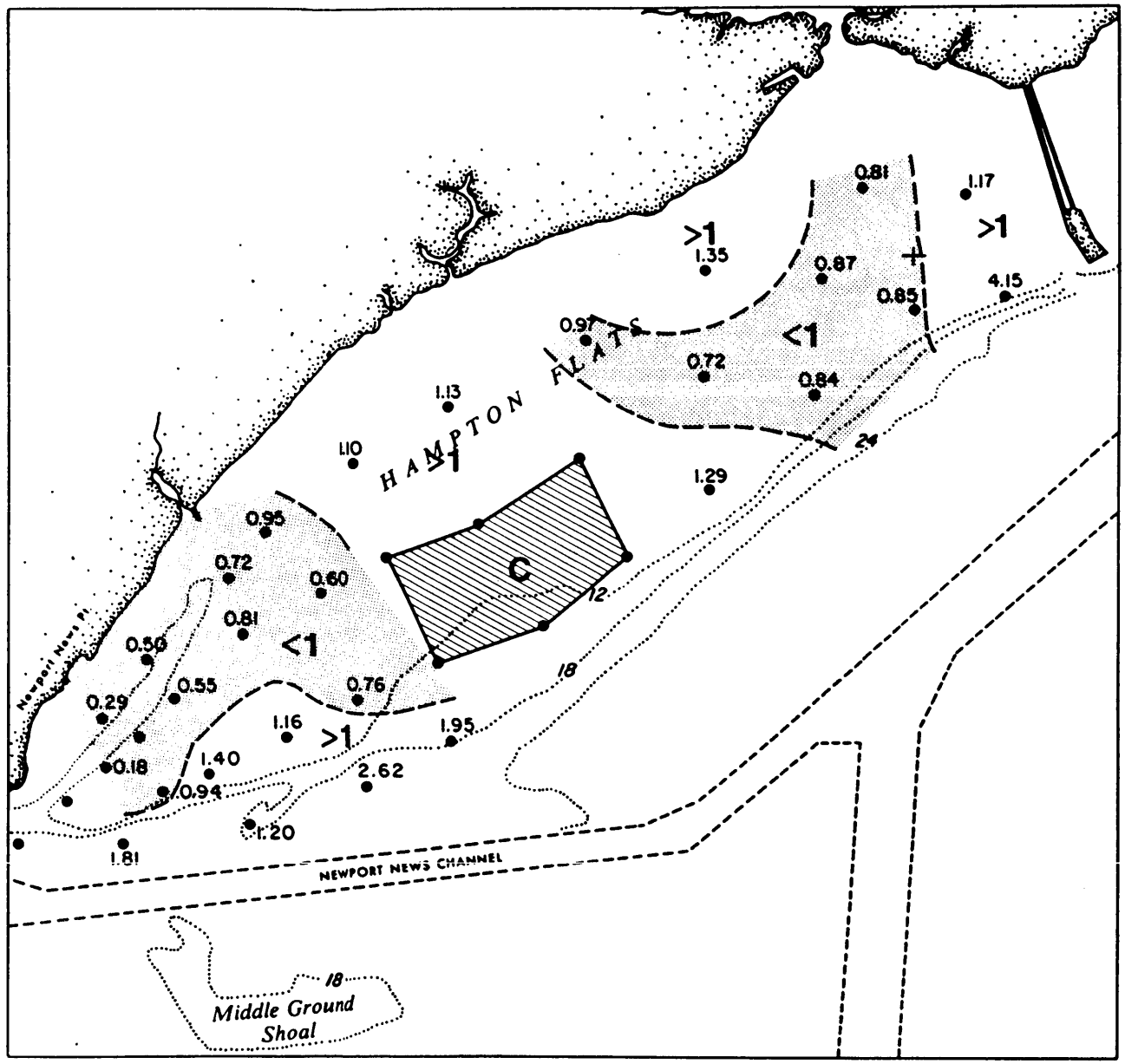

Figure IIIF-12b. Values of τ_o/τ_c for Island C, maximum ebb current.

potential to the west and east of the island position for both flood and ebb current phases. The area of reduced transport potential is markedly smaller than either the Island A or B configuration, and the values are generally within the range where currents associated with the spring tidal range and/or wave action would effect entrainment. The corridor north of the Island C location exhibits current speed enhancement relative to the BASE condition with correspondingly higher potential transport rates. Thus, even though the Island C location would partially shield the corridor from wave action the tidal currents are sufficiently strong to effect entrainment. Given the $\tau o/\tau c$ values and the exposure to wave action, blanket accumulation of fine grained sediments would not be expected. In addition, sediment column enrichment with fine grained material would be less than that associated with either of the proposed island locations.

e. ISLAND D. The results for Island D (323 acres) are shown in Figure IIIF-13a,b. The area of reduced transport potential is larger on both the flood and ebb current phases than the case of Island C configuration. However, as in the Island C condition the transport potential is enhanced in the passage between the island and the mainland on both ebb and flood currents. Given the $\tau o/\tau c$ values and the exposure to wave action, blanket accumulation of fine grained sediment would not be expected. As in the case of Island C the sediment column enrichment with fine grained sediments would be less than that associated with either of the proposed island locations.

f. SUMMARY. The previous discussion considered the patterns of the transport potential as reflected by $\tau o/\tau c$ for the currents associated with mean tide range (0.76 m). These results may be further synthesized by considering the values of $\tau o/\tau c$ that would be associated with tide range

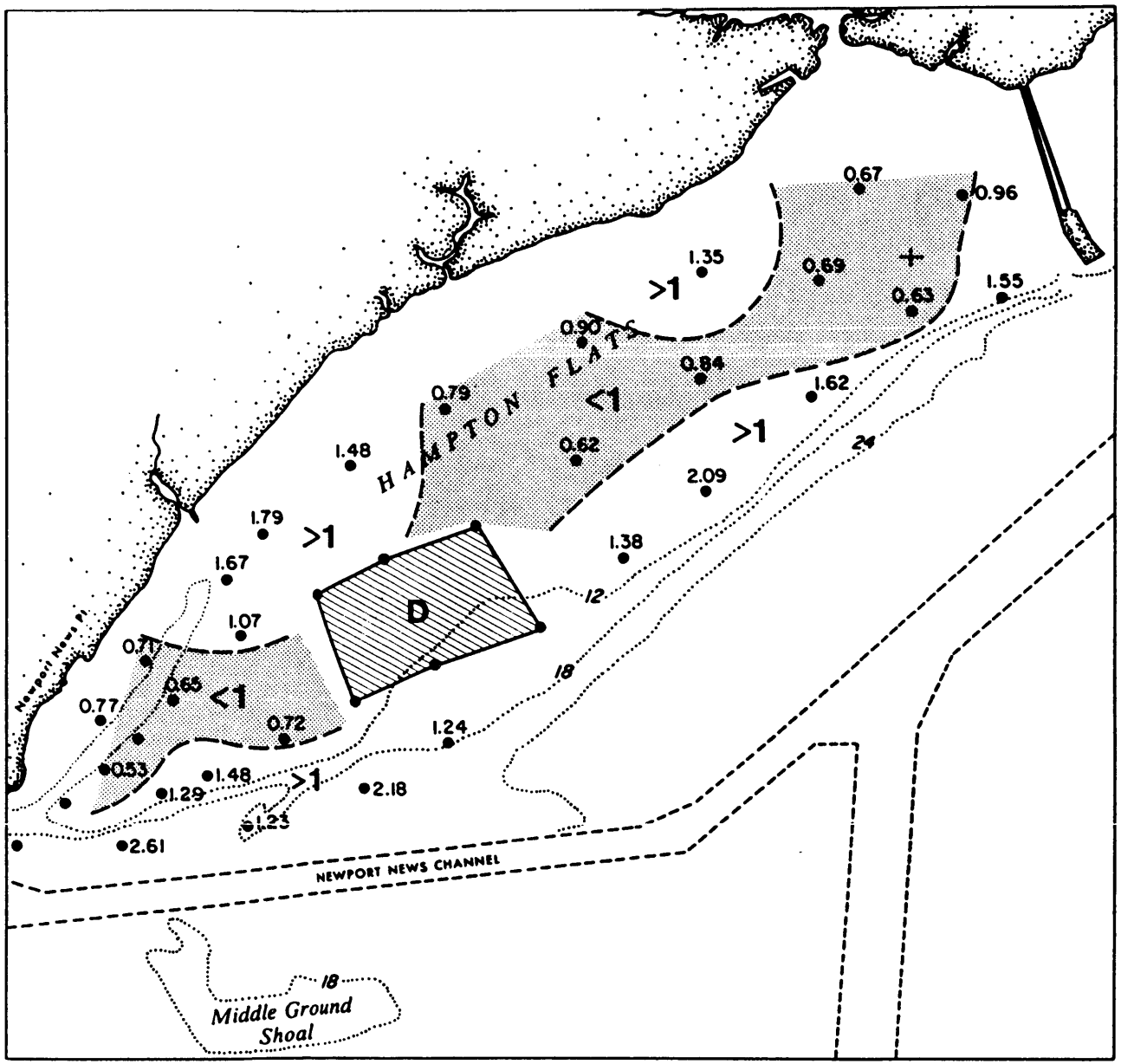

Figure IIIF-13a. Values of τ_o/τ_c for Island D, maximum flood current.

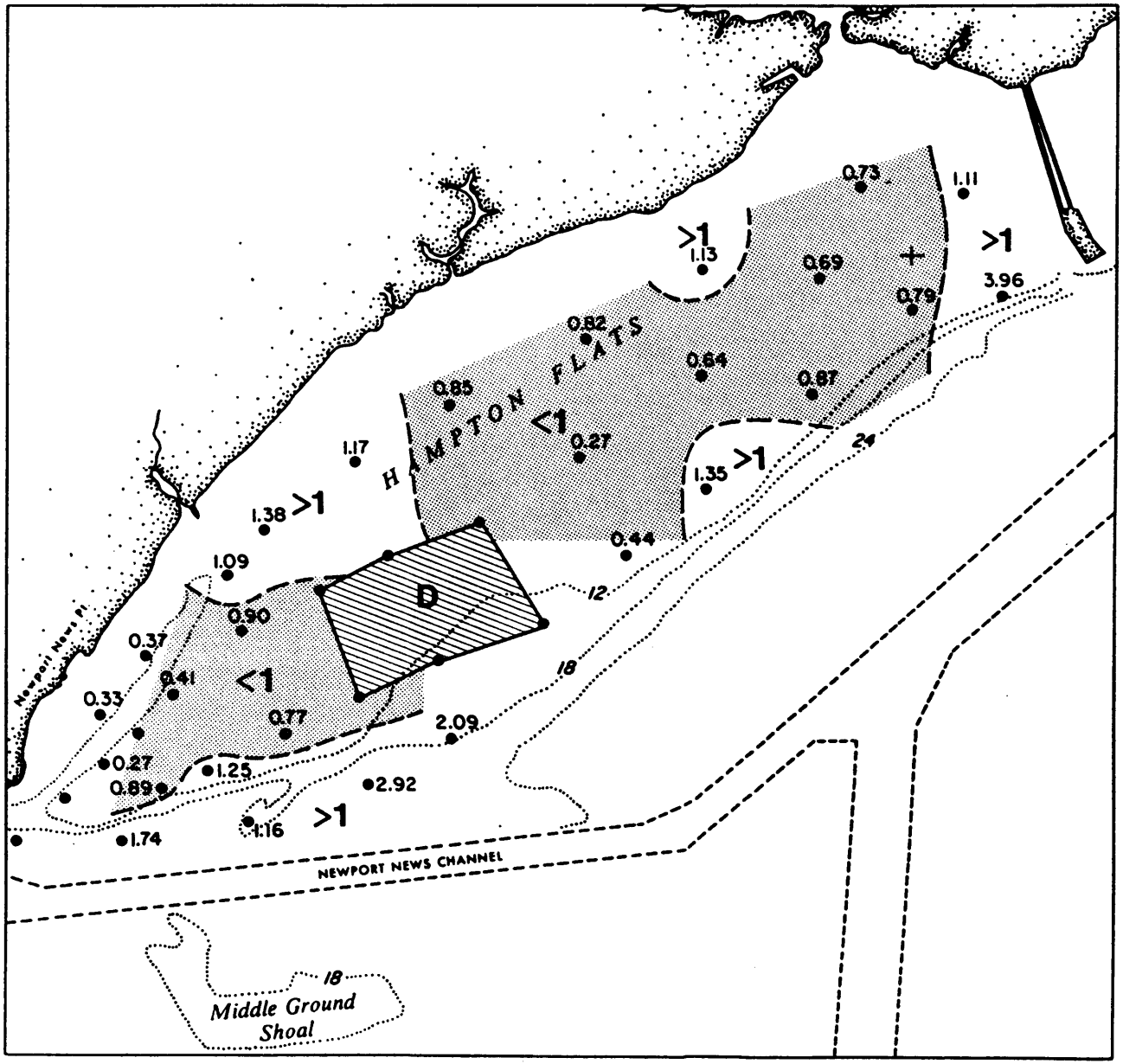

Figure IIIF-13b. Values of τ_o/τ_c for Island D, maximum ebb current.

intervals. It has already been noted that values $1>\tau o/\tau c>0.84$ correspond to tide ranges between the mean (0.76) and spring (0.88 m) conditions. $\tau o/\tau c$ values within that range would be sufficient for sediment entrainment. Reference to Figure IIIF-5 indicates that predicted tide ranges exceeding 1.05 m occur in only 2 percent of the cases. Specifically, $\tau_{(2\%)}$ τ_{mean} equals 1.39 so the presented $\tau o/\tau c$ values less than 0.72 in Figure IIIF-4a,b represent entrainment in fewer than 2 percent of the predicted tide ranges.

Five classes of potential transport are presented as a qualitative means to compare the conditions examined. These classes are derived from $\tau o/\tau c$ calculated from currents associated with the mean tide range.

Class		Class Description
1	$\tau o/\tau c \geq 1$	Transport is expected for tide ranges less than or equal to the mean range; either flood or ebb current.
2	$1>\tau o/\tau c \geq 0.84$	Transport is expected for tides between mean and spring ranges (0.76 m and 0.88 m); either flood or ebb current.
3	$0.84>\tau o/\tau c \geq 0.72$	Transport is expected for tide ranges between 0.88 m and 1.05 m; both flood and ebb currents.
4	$\tau o/\tau c \leq 0.72$	Transport expected only when tide range exceeds 1.05 m; both flood and ebb currents.
5	$\tau o/\tau c \leq 0.72$	As in Class 4 but also sheltered from wave exposure.

Increase in numerical rank represents the increasing tendency for incorporation of fine grained sediments in the sediment column. Class 5 represents a strong likelihood of blanket fine grained accumulation.

The application of these criteria to the values of $\tau o/\tau c$ shown in Figures IIIF-4,8,9,10,11,13 are shown in Figure IIIF-14a through g. The BASE condition (Figure IIIF-14a) is characterized by Class 1 over most of

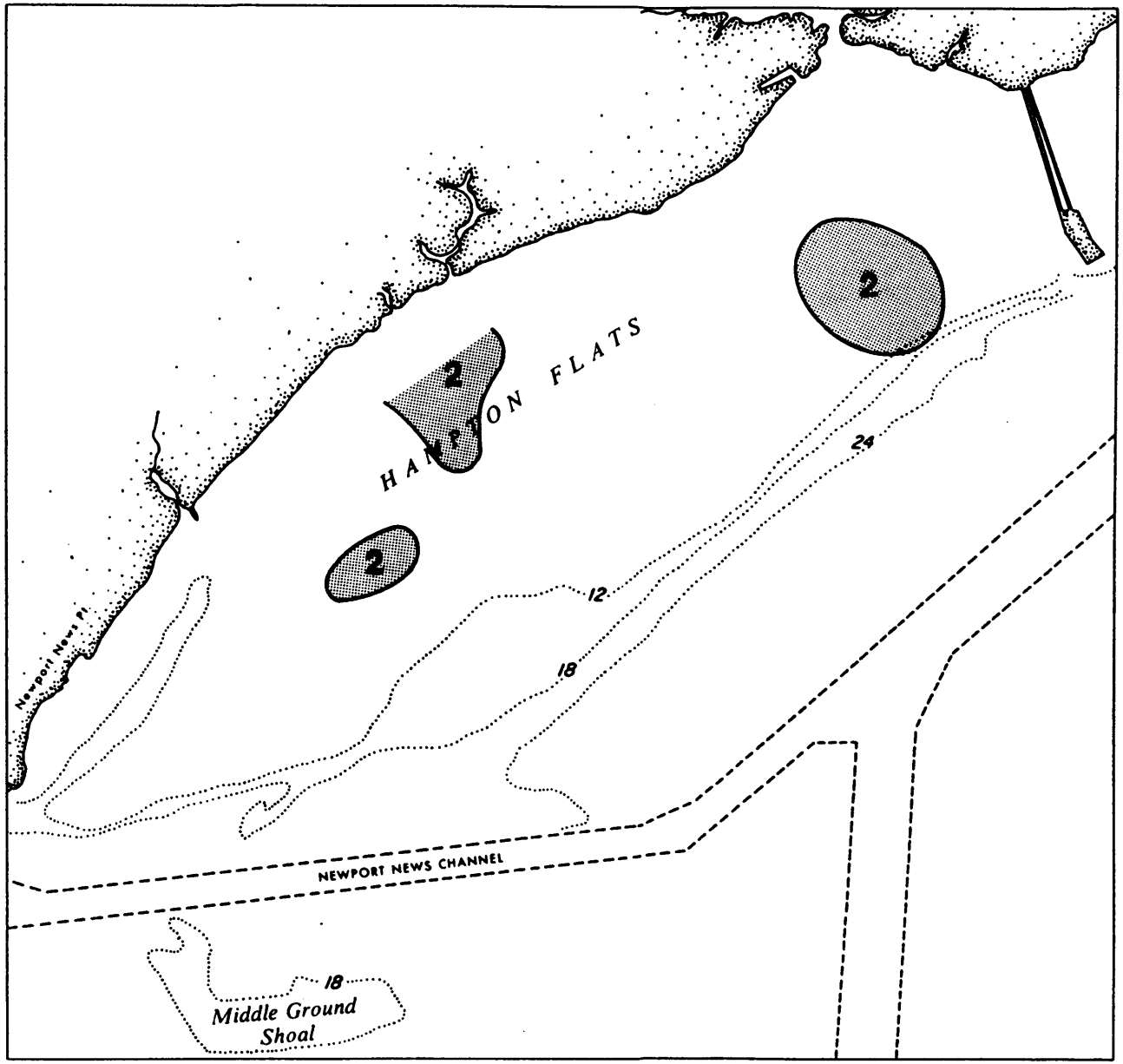

Figure IIIF-14a. Deposition potential for BASE condition. Reference text for code.

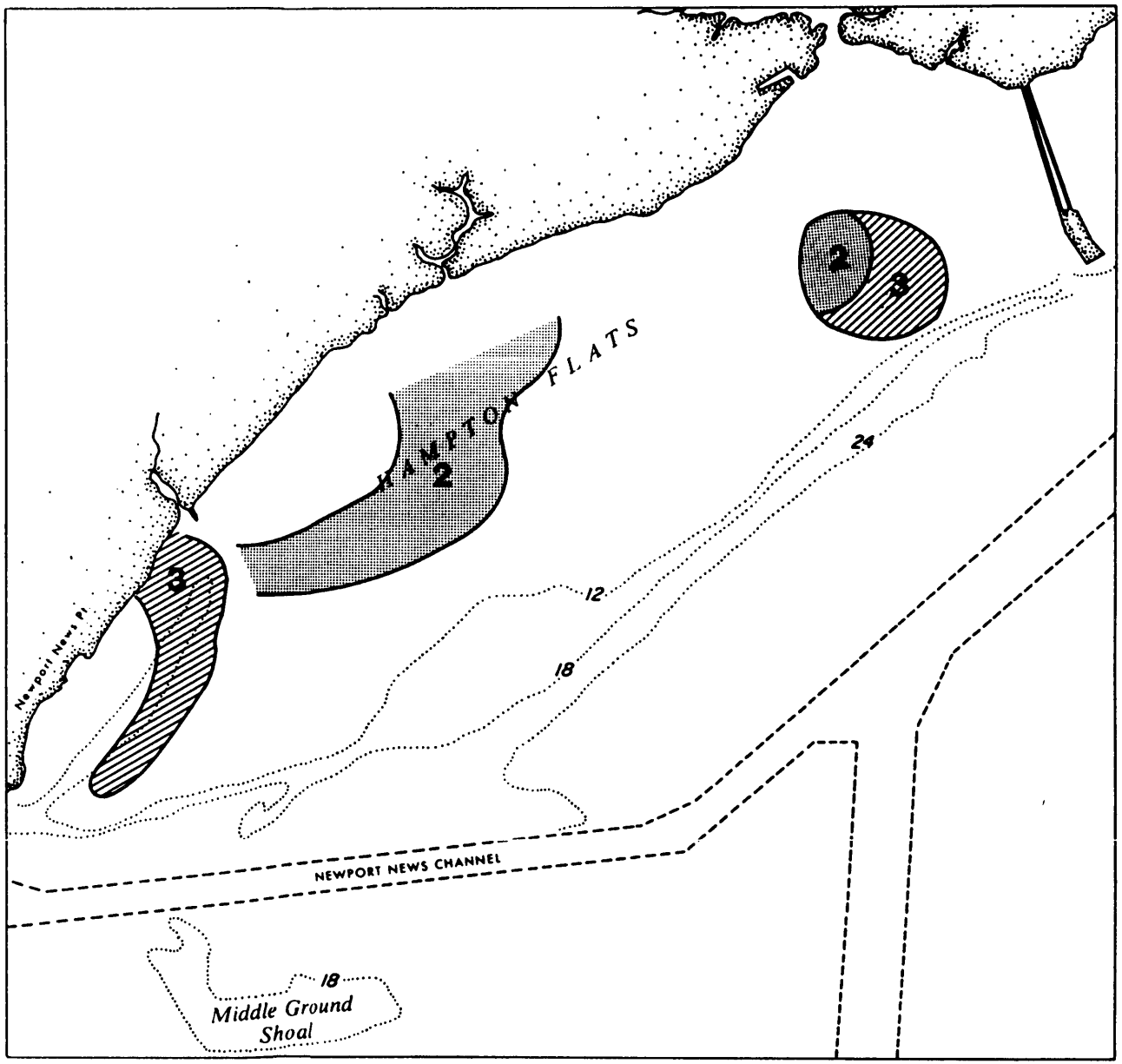

Figure IIIF-14b. Deposition potential for I664-45 condition. Reference text for code.

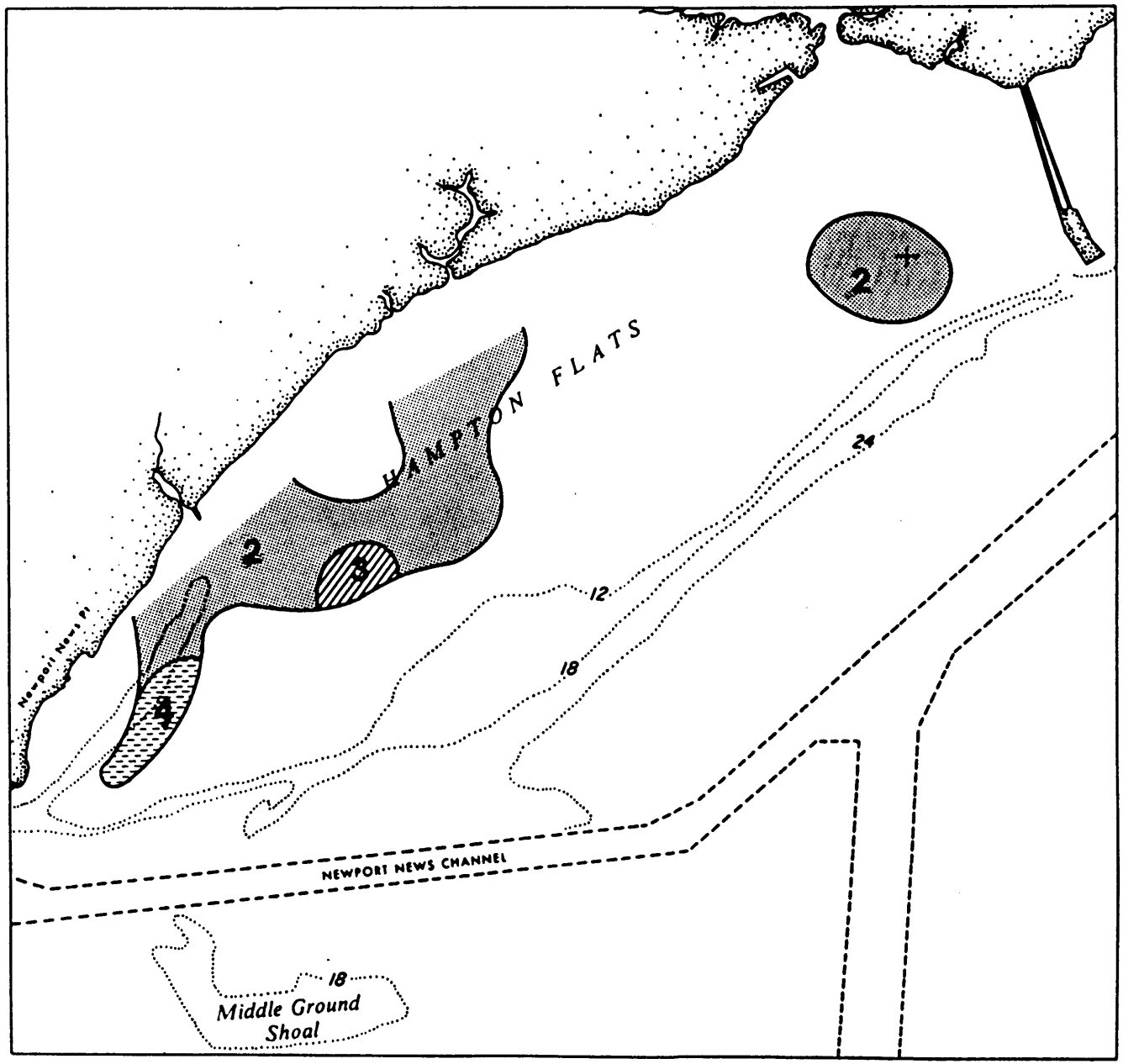

Figure IIIF-14c. Deposition potential for I664-55 condition. Reference text for code.

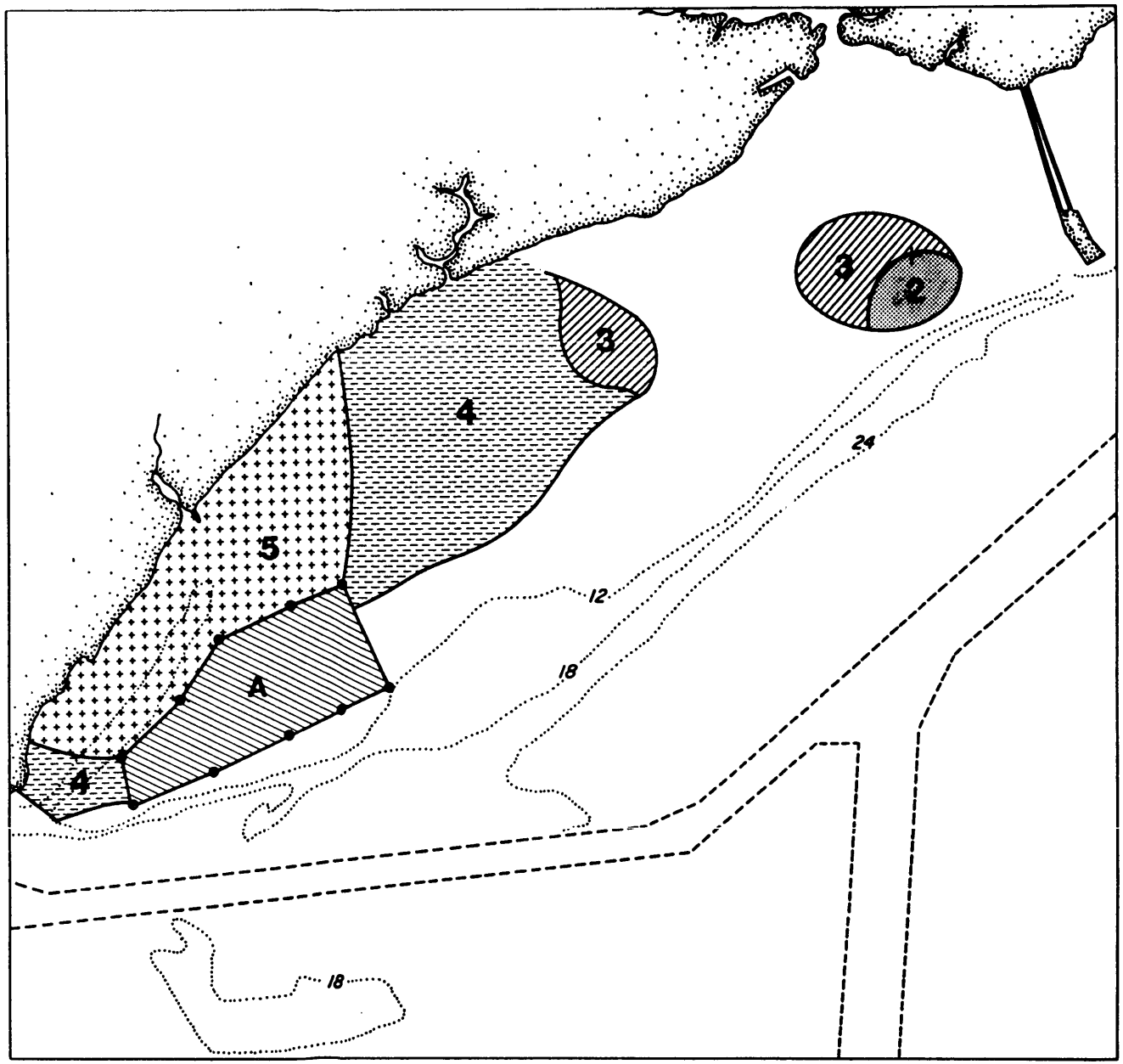

Figure IIIF-14d. Deposition potential for Island A. Reference text for code.

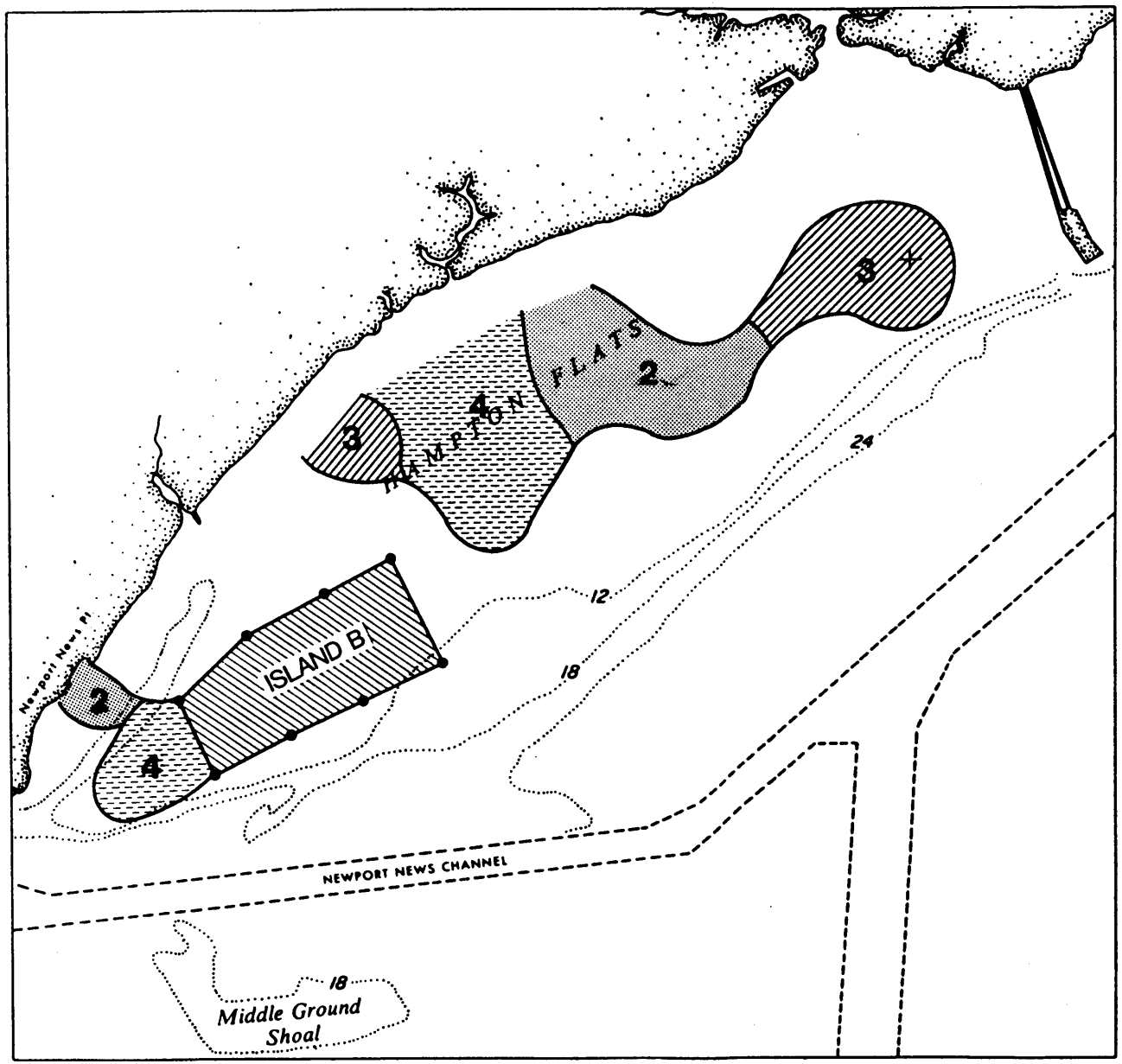

Figure IIIF-14e. Deposition potential for Island B. Reference text for code.

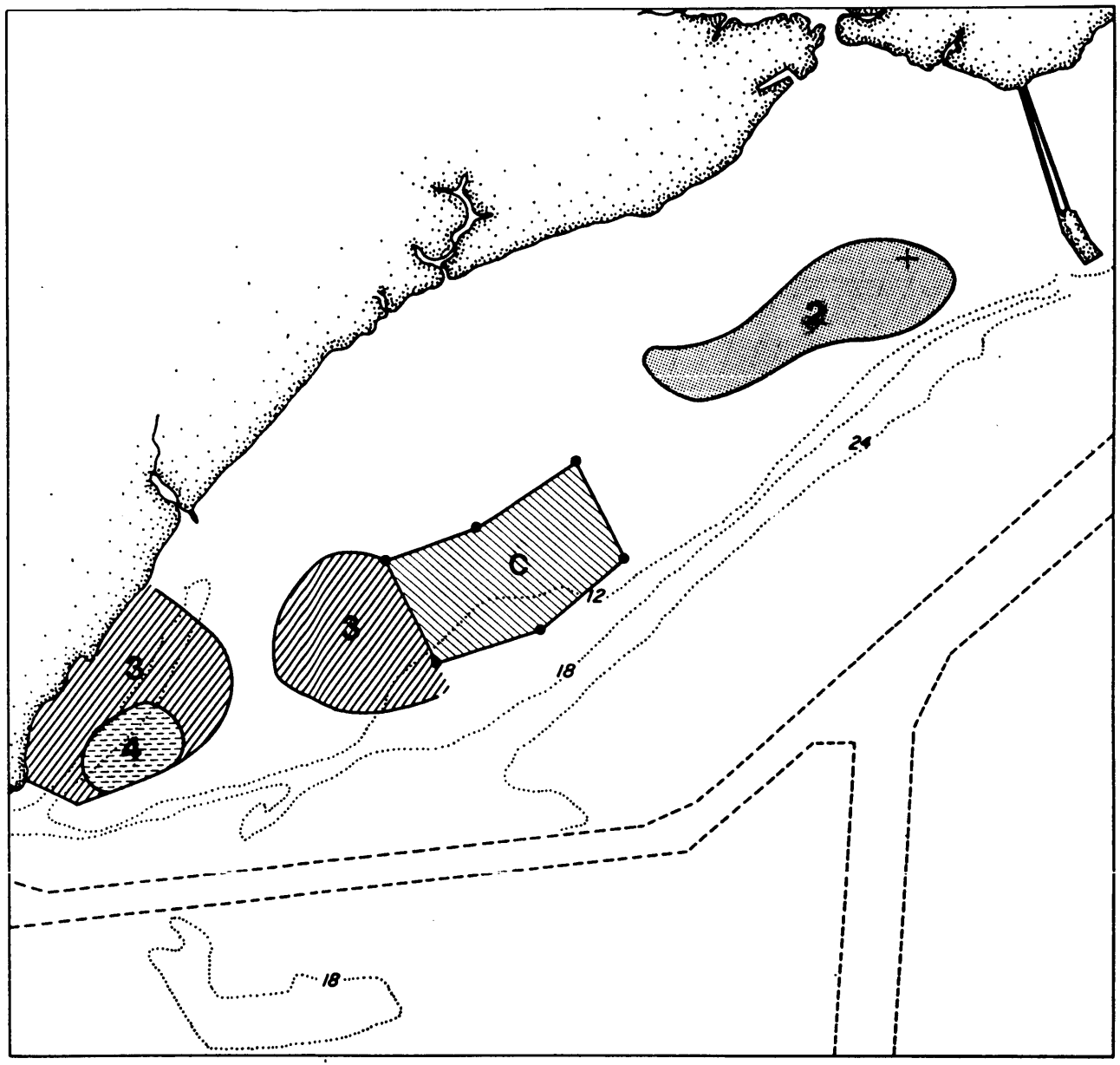

Figure IIIF-14f. Deposition potential for Island C. Reference text for code.

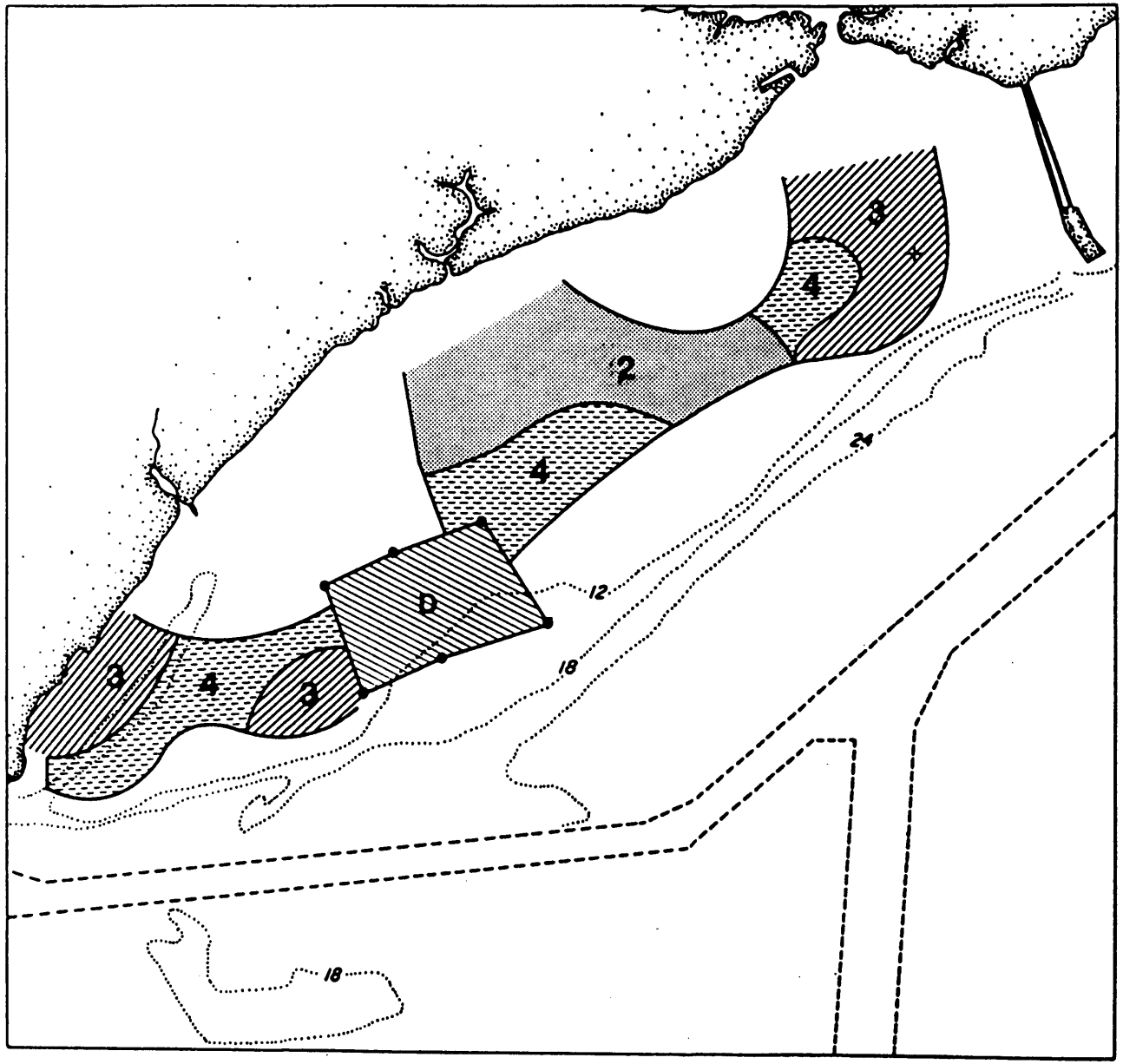

Figure IIIF-14g. Deposition potential for Island D. Reference text for code.

the area of Hampton Flats and Class 2 in the remainder. Thus, during either flood or ebb current associated with mean tide range (and smaller) most of Hampton Flats is subject to entrainment of the surface sediments and, it is argued, thereby a condition not conducive to deposition of fine grained sediments. It is this condition to which the others must be compared.

I664-45 and I664-55 exhibit similar characteristics. Most of the area is Class 1 but the northwest portion (Zone A) is predominantly Class 2. Thus, some increase in the fine grained sediment fraction could be expected. However, relative to the BASE condition the degree of exposure to wave driven resuspension is unchanged.

Relative to the BASE and I664 conditions the ISLAND A configuration has a markedly enlarged area susceptible to increased fine grained sedimentation. A substantial area (Class 5), subject to slow tidal currents and reduced exposure to wave action, has conditions conducive to blanket accumulation of mud.

In contrast to ISLAND A the configuration for ISLAND B has no Class 5 condition since the tidal currents are sufficient for entrainment without wave action. The flow through the passage between the island and mainland shifts that area from Class 5 to Class 1, and tends to cancel the tendency for accumulation induced by I664.

The ISLAND C configuration is characterized by Class 1 conditions over much of Hampton Flats (Figure IIIF-14f). The subareas of Classes 2 and 3 tend to be closer to the outer boundaries of Hampton Flats and therefore more susceptible to wave driven resuspension.

The pattern associated with the ISLAND D configuration is similar to that associated with ISLAND B (Figure IIIF-14g). Both contain a central lobe of Class 2, 3 and 4 subareas. However, in the case of ISLAND D the

Class 4 subarea is relatively more exposed to wave induced resuspension. As in the cases of ISLAND B and ISLAND C, the relatively high current speeds in the passage between the respective island positions and the mainland tend to cancel the sedimentation tendencies induced by I664.

Keeping in mind the coarseness of the model grid and the assumptions embodied in assessing sediment transport and deposition the results portrayed in Figure IIIF-14 do permit a ranking, relative to the BASE, of the expected perturbations to the deposition of fine grained sediments. In order of increasing deposition tendency the ranking is:

I664-45
I664-55
ISLAND-C
ISLAND-D
ISLAND-B
ISLAND-A

G. Benthic Resources in the Proposed Island Locations

1. Introduction

The subtidal bottom upon which the New Port Island is proposed is part of the marine ecosystem of Hampton Roads which contributes a portion of the total biomass produced in Hampton Roads. This biomass is in the form of crabs, clams, and other invertebrate species that serve as food for finfish species.

The objective is to provide an estimate of the bottom resources that would be lost with island construction. The assessment of the bottom resources focuses on the invertebrates that serve as food for finfish and crabs. It is based on invertebrate data collected from Newport News Bar, Hampton Flats, and Hampton Bar between 1969 and 1981, and a survey done

February, 1986 using a Sediment Profiling Camera (SPC). The SPC is a instrument that provides in situ photos of surface sediments which can be used to determine the general biological conditions. In operation a prism is driven into the sediment and a vertical cross-section is photographed. The resulting image provides a means to identify sediment surface roughness as well as the general characteristics of the epifauna and infauna.

2. Determination of Resource Value

The benthic resource value of an area is directly linked to its total productivity and availability of this productivity to fisheries species. While productivity cannot be determined without quantitative field sampling, resource value can be inferred from abundance and species composition data which is available from the surface SPC photographs and the living position of the benthic species.

Benthic data from areas of similar sediment and depth were summarized by major taxonomic group. These data were then compared to data from other areas in the lower Bay (Willoughby Bar, Crumps Bank, Thimble Shoals, and Horseshoe Bank) to provide a relative comparison of resource value (Hobbs et al. 1985).

3. Benthic Data

Benthic data from four studies were compiled by major taxonomic groups (Table IIIG-1). Studies considered were those by Boesch (1971), Hyland (1972), Diaz and Boesch (1978) and Bowen (1984). Locations of stations for these studies are contained in Figure IIIG-1. When the data were summarized by year it can be seen that there are year-to-year differences in the communities. For polychaetes and crustaceans the highest abundance years were 1969, 1972, 1975 (Table IIIG-2). Molluscs were most abundant in 1974, 1975, and 1980.

Table IIIG-1. Abundance of major groups from benthic data sets around the New Port Island location.

Station	Date	Abundance/m^2 Polychaetes	Crustaceans	Molluscs	Total Individuals	Total Species	Area
D1	8/69	2343	1276	357	4810	39	Newport News Bar
D1	8/72	1220	1353	127	23340	35	Newport News Bar
1	2/74	185	15	475	715	18	Hampton Bar
2	2/74	65	10	110	185	9	Hampton Bar
3	2/74	75	25	185	295	16	Hampton Bar
4	2/74	205	30	575	820	20	Hampton Bar
5	2/74	425	110	170	970	27	Hampton Bar
6	2/74	50	25	0	75	6	Hampton Bar
7	2/74	395	65	170	905	20	Hampton Bar
10	2/74	90	10	100	210	9	Hampton Bar
11	2/74	65	5	65	140	8	Hampton Bar
12	2/74	135	45	695	900	23	Hampton Flats
1	1/75	870	265	160	1420	32	Hampton Bar
3	1/75	110	5	225	370	14	Hampton Bar
4	1/75	530	75	375	1010	28	Hampton Bar
5	1/75	850	70	445	3435	28	Hampton Bar
7	1/75	1310	115	510	4335	36	Hampton Bar
10	1/75	160	15	40	265	11	Hampton Bar
11	1/75	110	20	50	285	14	Hampton Bar
12	1/75	1230	1325	430	3035	38	Hampton Flats
13	1/75	350	20	355	780	21	Hampton Bar
1	1/76	755	225	495	1705	35	Hampton Bar
3	1/76	200	50	220	480	23	Hampton Bar
4	1/76	370	420	175	1500	27	Hampton Bar
5	1/76	1320	315	200	3610	48	Hampton Bar
7	1/76	2050	520	245	3130	47	Hampton Bar
11	1/76	295	15	110	420	17	Hampton Bar
12	1/76	295	230	190	725	25	Hampton Flats
13	1/76	145	5	25	180	9	Hampton Bar
C1	10/80	370	249	411	1030	22	Hampton Flats
C2	10/80	691	315	418	1424	26	Hampton Flats
PT	6/81	1385	101	161	1647	25	Hampton Flats

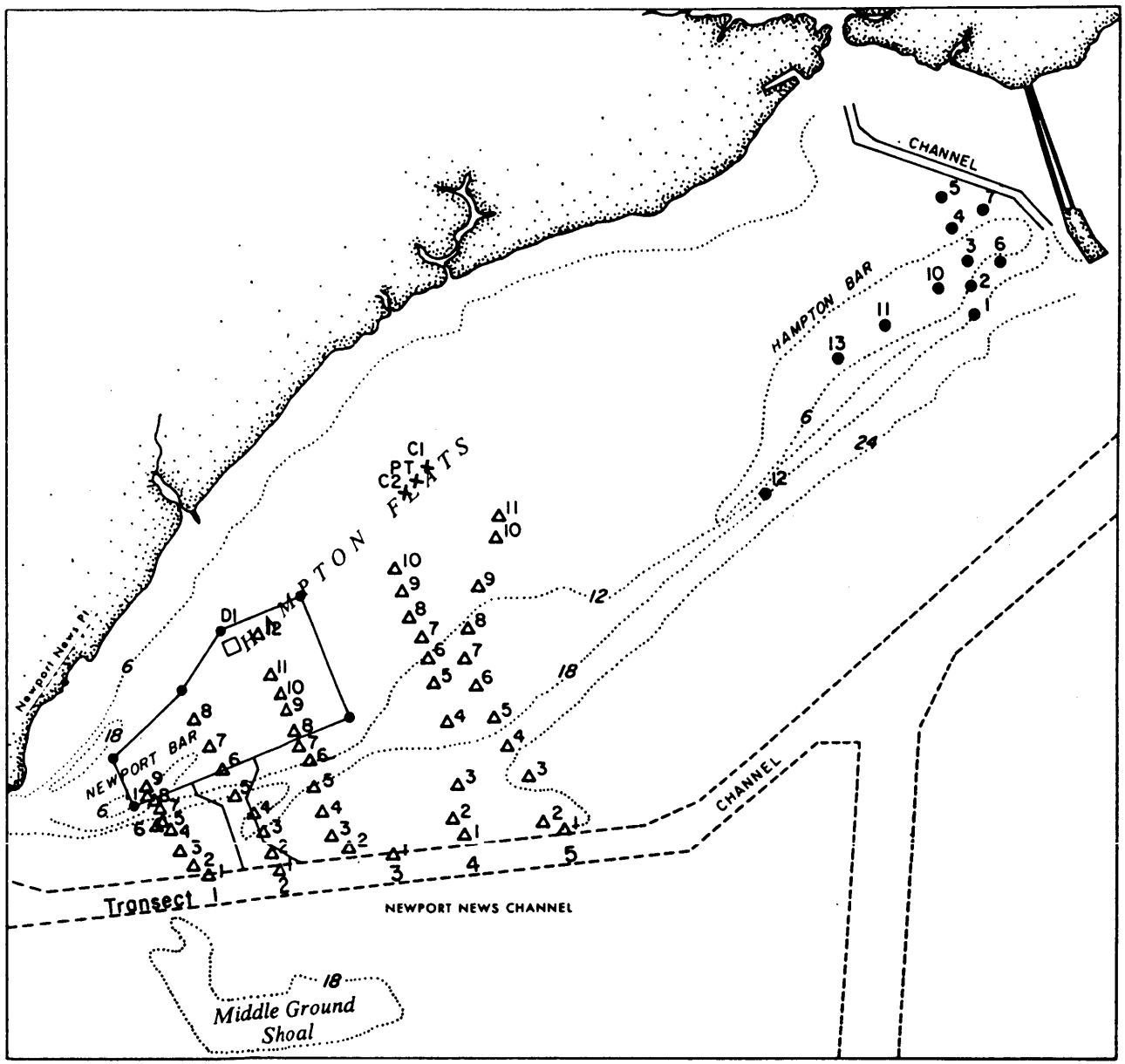

Figure IIIG-1. Location of Benthic sampling stations used in resource assessment of the proposed Newport Island location.

Table IIIG-2. Summary of benthic data used in resource evaluation of the area around the New Port Island location.

Summary by Year and Area:

	Polychaetes			Crustaceans			Molluscs		
Year	NNB*	HF	HB	NNB	HF	HB	NNB	HF	HB
1969	2343	--	--	1276	--	--	357	--	--
1972	1220	--	--	1353	--	--	127	--	--
1974	--	135	171	--	45	35	--	695	192
1975	--	1230	536	--	1325	73	--	430	270
1976	--	295	734	--	230	221	--	190	241
1980	--	530	--	--	282	--	--	414	--
1981	--	1385	--	--	101	--	--	161	--
$\bar{x}$	1781	715	480	1314	397	110	242	378	234

Summary By Depth:

Depth (cm)	Polychaetes	Crustaceans	Molluscs
<2	188	49	174
2-5	1183	421	222
>5	543	376	390

* NNB - Newport News Bar
HF - Hampton Flats
HB - Hampton Bar

When averaged by area there was a trend for there to be higher abundances of polychaetes and crustaceans in the western areas. Newport News Bar was highest followed by Hampton Flats and then Hampton Bar. Molluscs were most abundant in Hampton Flats (Table IIIG-2). Much of this trend could be explained by depth. Hampton Bar stations were overall shallower than Hampton Flats or Newport News Bar stations (Table IIIG-3). Depths shallower than 2 m, at mean low water, had the lowest abundances of polychaete, crustaceans, and molluscs. Depths from 2 to 5 meters had highest abundances of polychaetes and crustaceans. Depths greater than 5 m had highest mollusc abundance (Table IIIG-2). Species richness also followed the same trend.

Almost all of the crustaceans in Hampton Roads are epifaunal and live on the sediment surface or attached to hydroid colonies. About 70% of the molluscs were epifaunal snails occupying the same habitat as the crustaceans. About 50% of the polychaetes were also epifaunal, most attached to shell or other hard substrates. From the viewpoint of utilization, the fauna is then very accessible to finfish and crabs.

4. Surface Profiling Camera Data

Locations of SPC stations are presented in Figure IIIG-1. Measurements taken from image analysis of the SPC photos are presented in Table IIIG-4. The SPC camera acts as a dead weight penetrometer so depth of penetration is a function of sediment mass properties (grain size, water content, porosity). Surface features that were measured include bed forms, shells, epifauna, and diatom mats. Subsurface features measured were sediment grain size, burrows, and feeding voids.

Overall the bottom in the area is very hard and camera penetration was generally limited to about 2 to 5 cm. This reflects the high sand content

Table IIIG-3. Physical parameters from benthic community stations.

Station	Depth (m)	Sand (%)	Silt (%)	Clay (%)	Study
D1	3.3	99	0.5	0.5	Boesch 1971
D1	3.3	91	4	5	Hyland 1972
1	6.1	78	12	8	Diaz and Boesch 1978
2	0.9	87	9	4	" " " "
3	1.5	90	4	6	" " " "
4	1.5	94	3	3	" " " "
5	3.1	82	14	4	" " " "
6	1.2	89	6	5	" " " "
7	2.6	79	17	4	" " " "
10	1.5	80	17	3	" " " "
11	1.5	96	1	3	" " " "
12	5.4	89	4	6	" " " "
13	1.5	96	2	2	" " " "
C1	3.3	--	--	--	Bowen 1984
C2	3.3	--	--	--	" "
PT	3.3	--	--	--	" "

Table IIIG-4. Measurements made from REMOTS photographs taken in the area of the proposed New Port Island.

Station	Depth of Penetration	Surface Features: Bed forms	Shells	Epifauna	Diatom mats	Subsurface Features: Grain size	Burrows	Feeding Voids
1-1	5.6 cm	+*	+			MCS**		
1-2	15.5					FS	+	+
1-3	3.2		+			MS		
1-4	4.1	+				MCS		
1-5	2.9	+				MCS		
1-7	2.0			+	+	FS		
1-8	4.2	+				MS		
1-9	2.9	+				MCS		
1-11	4.3	+				MCS		
2-1	4.3	+	+			MCS		
2-3	3.5			+	+	MS	+	
2-4	1.2		+			CS		
2-5	7.8				+	FS	+	
2-6	2.4	+	+			FS		
2-7	2.5		+			CS		
2-8	4.8	+	+	+		FS		
3-2	3.4		+		+	FS		
3-3	1.2		+			MS		
3-4	0.0		+			--		
3-5	2.8	+		+		MS		
3-6	0.7	+				MS		
3-7	2.6	+				MS		
3-9	0.0			+	+	--		
3-10	0.0			+	+	--		
3-11	0.0					--		
3-12	1.2				+	FS		
4-1	20.4					FS	+	+
4-2	5.8	+				MCS		
4-3	5.4			+		FS		
4-4	9.8					FS		
4-5	5.6	+?			+	FS		+
4-6	3.5	+			+	FS		
4-7	2.1	+			+	FS		
4-8	1.8				+	FS		
4-9	2.6	+			+	FS		
5-2	13.5			+		FS		
5-3	5.3		+	+		MS		

Table IIIG-4 (continued)

Station	Depth of Penetration	Surface Features				Subsurface Features		
		Bed forms	Shells	Epifauna	Diatom mats	Grain size	Burrows	Feeding Voids
5-4	10.9				+	FS	+	
5-5	6.8				+	FS		
5-6	5.4					FS	+	
5-7	7.0				+	FS	+	+
5-8	0.0			+	+	--		
5-9	1.1	+?			+	FS		
5-10	5.3				+	FS		
5-11	1.0				+	FS		

* + - present
** CS - coarse sand
MCS - medium coarse sand
MS - medium sand
FS - fine sand

of the substrate. Only at five stations did the approximately 300 lb. camera penetrate to 10 or more cm (Table IIIG-4). Many of the stations showed bed forms (sand ripple) that indicated a hydrodynamically active bottom (Fig. IIIG-2). Other surface features, that enhance the resource value of the area, were diatom mats (Fig. IIIG-3), epifauna (Fig. IIIG-3), and shell (Fig. IIIG-4). Diatom mats covered the bottom at approximately 40% of all SPC stations. These mats are important sources of primary production in shallow estuarine habitats and can be as productive as salt marshes (Rizzo & Wetzel 1985).

Epifauna was found at 25% of the stations. The most abundant epifaunal species was the hydroid Sertularia argentea, commonly known as grass. While this hydroid is not utilized directly by fish or crabs it is the major substrate in Hampton Roads upon which grow the amphipods that are a major food item for fish. Amphipods are a dominant faunal element in Hampton Roads (Boesch 1973) because of the widespread abundance of this hydroid (Diaz and Ruzecki 1981). Shells and shell hash also provide habitat heterogeneity that attract epifaunal species, mainly polychaete worms. Shells were present at about 25% of the stations (Table IIIG-4).

Subsurface features visible in the SPC photos were sediment grain size and other biological structures, such as burrows and feeding voids (Table IIIG-4). The sediments were mainly fine sands with some coarser sands on the westernmost transects (1 and 2). Grain size analysis of sand samples from the area collaborate the image interpretation. Biologically produced structures, burrows and feeding voids, were present at 17% of the stations. These structures indicate the presences of organisms (Figs. IIIG-3 and IIIG-5) and give a relative measure of community density. Polychaete worms were observed in the photographs at 11% of the stations (Fig. IIIG-5).

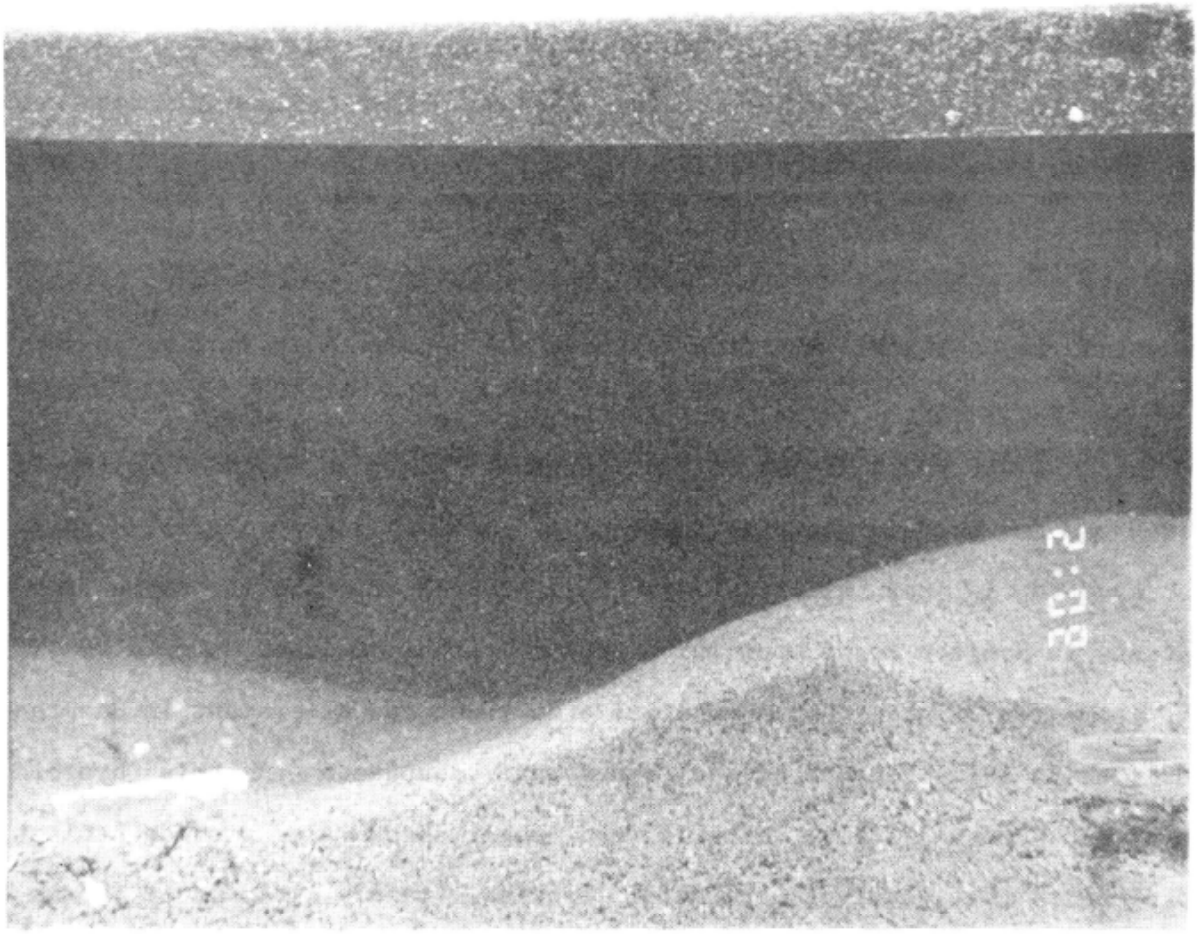

Figure IIIG-2. Sand ripple at Transect 2, Station 6. Scale is 1X.

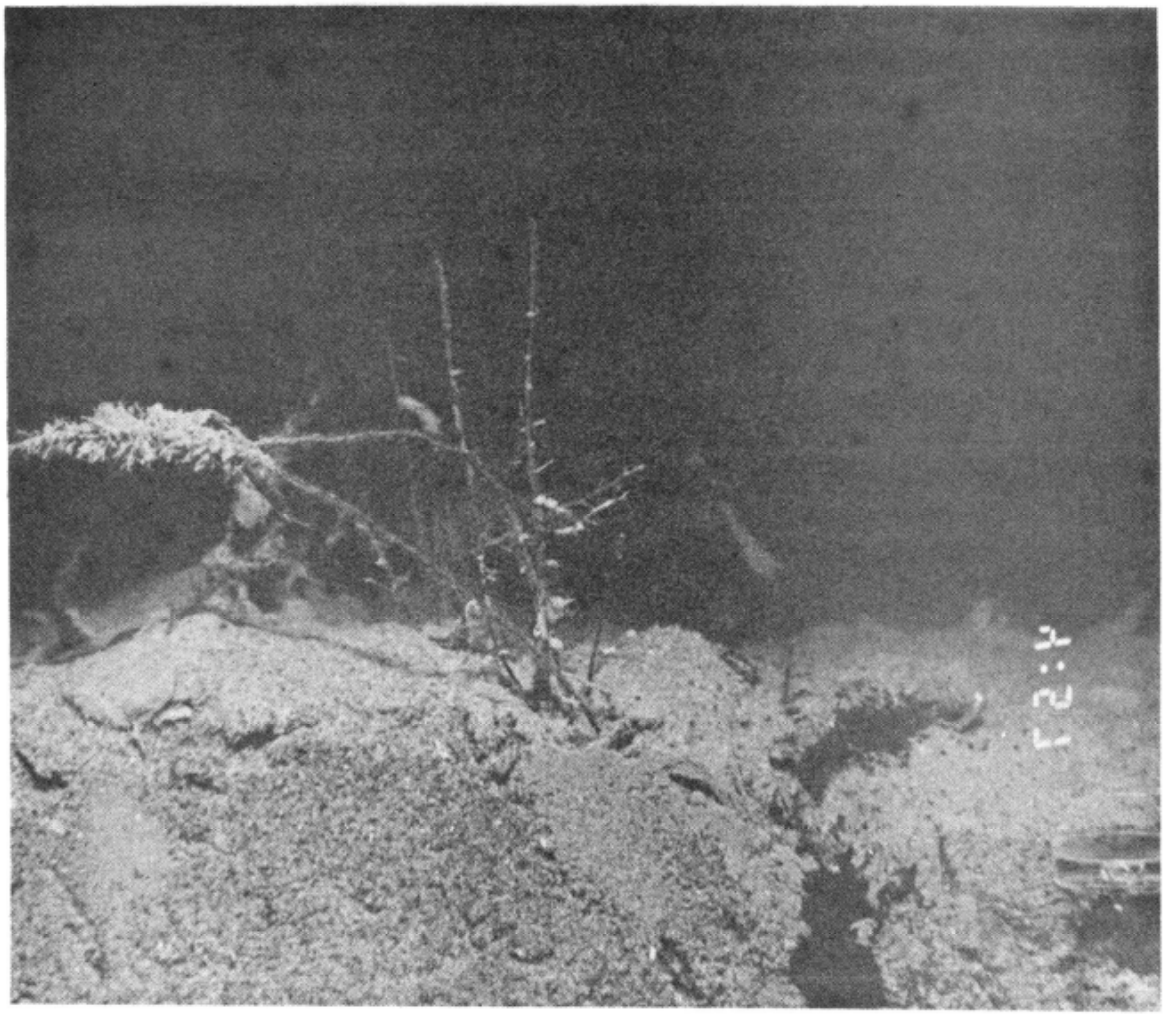

Figure IIIG-3. Diatom mat, epifauna, and burrow at Transect 2, Station 3. Scale is 1X.

Figure IIIG-4. Shell hash at Transect 2, Station 1. Scale is 1X.

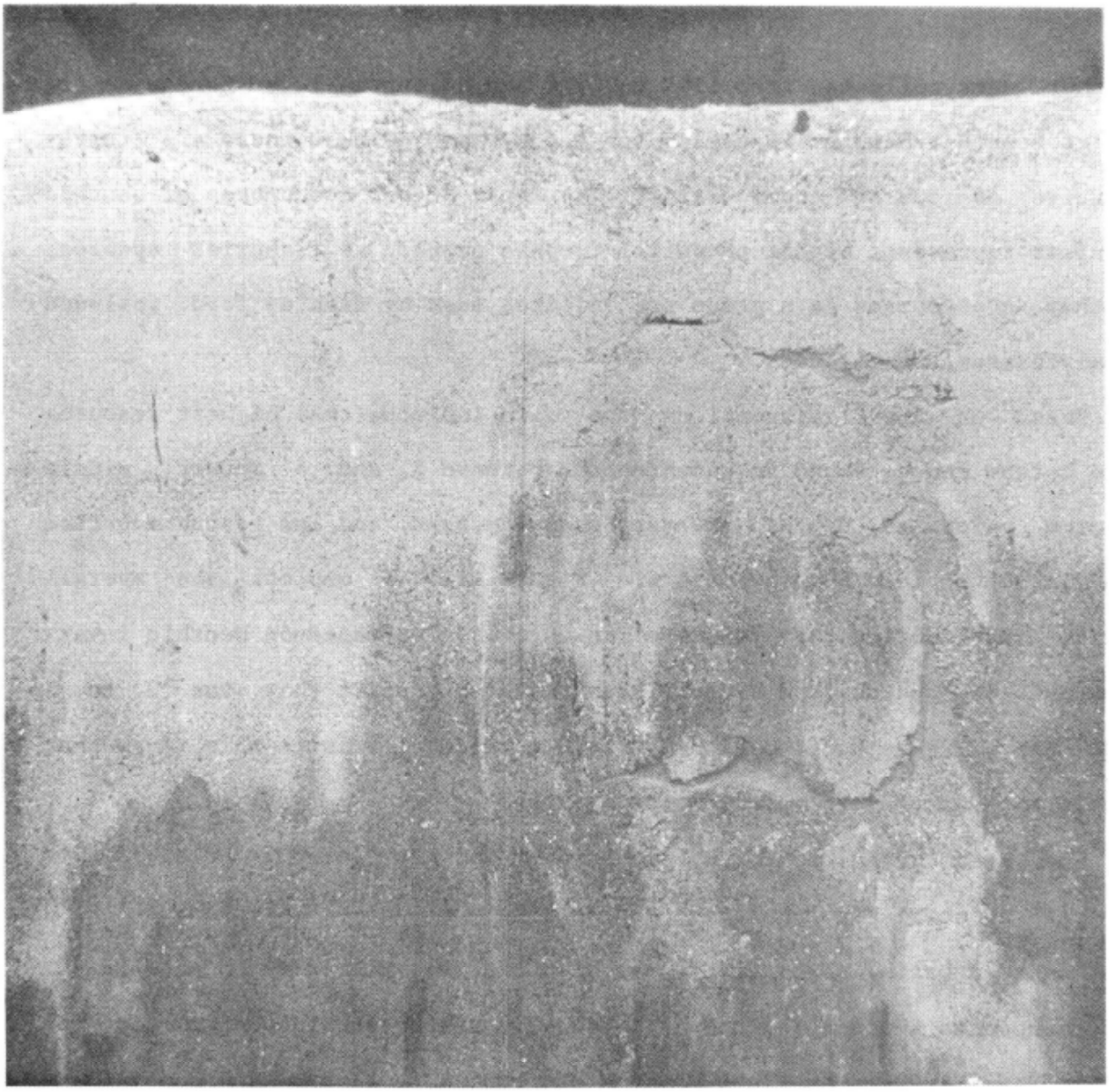

Figure IIIG-5. Feeding void and polychaete worm at Transect 4, Station 1. Scale is 1X.

5. Estimation of Resource Value

The estimation of resource value is based on several assumptions: a) that data collected from 1969 to 1976 can be extrapolated to the entire Newport News Bar-Hampton Flats-Hampton Bar system and that these are representative of current communities; b) that higher abundances of benthic organisms represents higher potential trophic support to fisheries species; c) that crustaceans as a group are utilized most by fish as food, followed by polychaetes and molluscs.

Based on these assumptions the data indicate that highest resource value bottom can be found in water depths between 2 and 5 meters, middle resource value at depths greater than 5 meters, and low resource bottom value in depths less than 2 meters. Figure IIIG-6 depicts the overall spatial distribution of relative resource value based on benthic invertebrates. SPC photos from Newport News Bar also confirm that the 2 to 5 meter depth range has the higher resource value. It is in this range that most of the diatom mats and hydroids occurred.

The area which would be covered by New Port Island (Option A) will eliminate about 1240 polychaetes, 480 crustaceans, and 280 molluscs on a meter squared basis. Extensive areas of diatom mat will also be eliminated. This represents about 9% of the high relative resource value bottom in the Newport News Bar-Hampton Flats-Hampton Bar system.

The overall resource value of the Newport News Bar-Hampton Flats-Hampton Bar system was found to be most similar to Crumps Bank, which had the highest resource value of the four areas studied by Hobbs et al. (1985). Willoughby Bar, which best matched the depth of the Newport Island location, had the lowest resource value (Hobbs et al. 1985). Sediments on Willoughby Bar were medium sands reflecting the higher energy environment. Newport

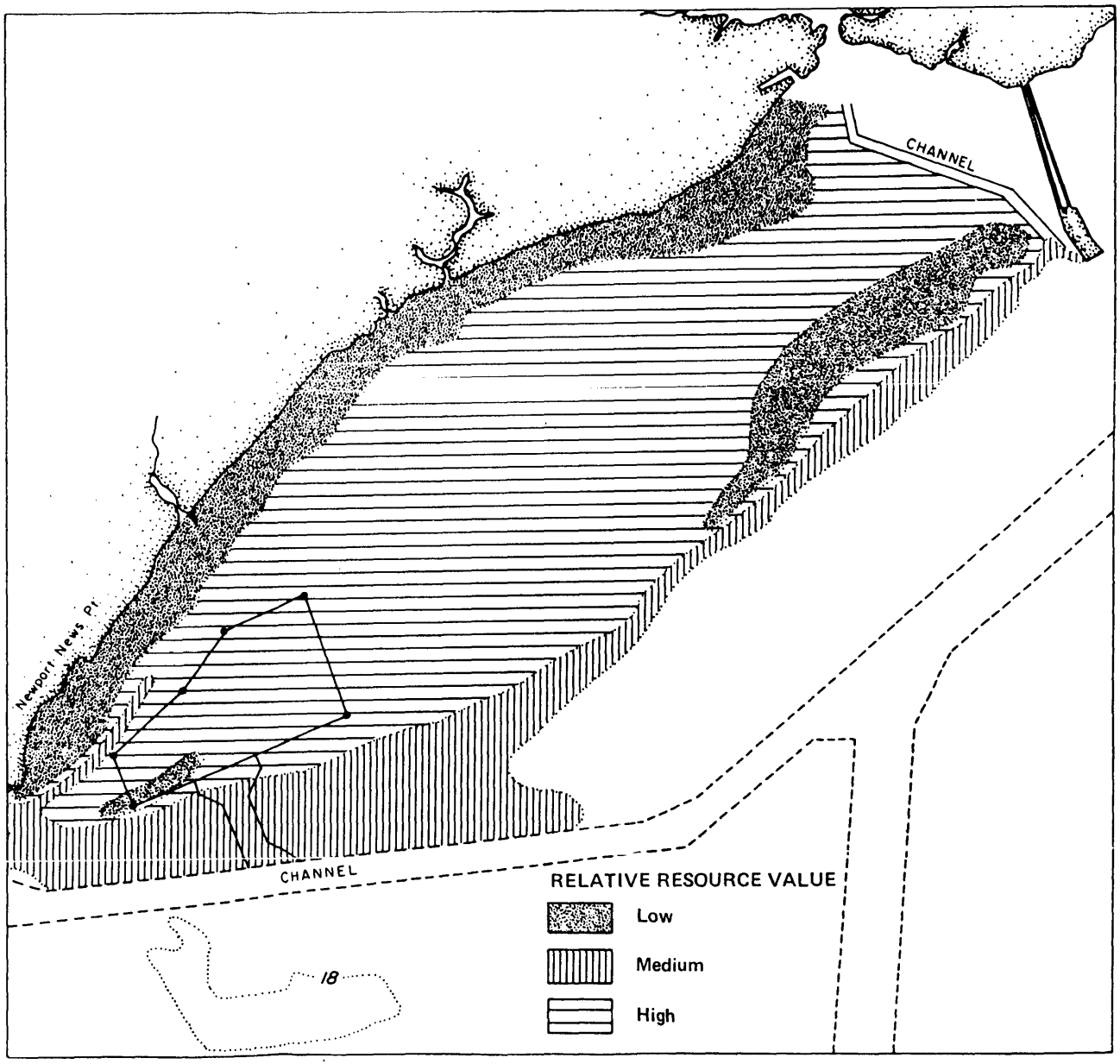

Figure IIIG-6. Relative resource value of Newport News Bar-Hampton Flats-Hampton Bar.

News Bar is fine sand, which tends to support higher densities of benthic organisms. Therefore the Newport News Bar resource value was most closely aligned to the finer sand deeper areas studied by Hobbs et al. (1985). Only areas less than 2 meters in depth were found to have as low a resource value as Willoughby Bar.

IV. EVALUATION OF IMPACT DUE TO CONSTRUCTION

A. Impact to Transport through the Frontal System

The state-of-the-art does not permit the direct translation of the mechanics of the circulation associated with, or induced by, the frontal system to quantitative assessment of oyster larvae settlement on the James River seed oyster beds. Therefore, the assessment of impact centers on the degree to which the various elements of construction change the flux (volume transport) of water through the frontal system. The primary importance of the frontal system centers on the fact that "surface" waters are injected to depths where the gravitational circulation induces net upriver movement. Based upon a 29 day (July 1985) integration of currents in a transect near the James River Bridge (Figure IIA-10) the depth level of 4 meters appears to be a good representation of the level of no net motion. The vertical displacement of surface waters may also be expected to force the deeper waters to somewhat greater depths with enhanced net upriver transport. The displacement of surface water is shown in Figure IVA-1 which contrasts, schematically, the cases of flow passing into the increasing depths of the lower James with and without the front. The central premise is that were the front not present the net downstream movement of surfce waters would result in reduced larval retention in the James/Hampton Roads system.

The assessment focuses on the flux of water passing through the frontal system. Estimates of flux differentials are determined by use of the 2-D hydrodynamic model coupled with application of the theoretical results developed in this study (Section IIID). As well, the analysis of impact

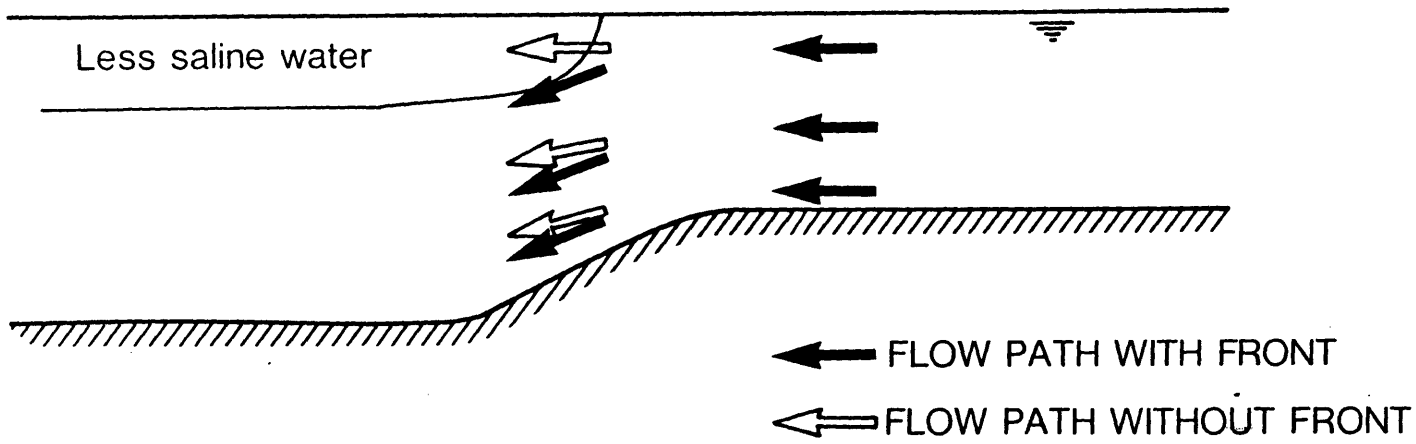

Figure IVA-1. Effect of front on flow displacement.

utilized the findings of other studies as they are germane to the salinity distribution.

1. Framework for the Analysis

As discussed in Section IIIA-1, the flows contributed to the frontal system may be considered to be composed of three parts, each passing through one segment of the river on the downriver side of the front (Figure IVA-2a,b). Segment 1 represents the flow exiting near Newport News Point and Segment 2 represents flow along the fringe of Hampton Flats to the north of the navigation channel. As well, the selected alignment includes the boundaries for Island Options A and B. This selection ensures that the entire flux is included for the island cases. Segment 3 is composed of the channel and channel fringe areas. The position of Segment 3 corresponds to the observed seaward limit of the overlying lens of less saline water at slack before flood. The boundary of Segment 1 was selected to incorporate the principal contribution of Hampton Flats water while Segment 2 is positioned to capture the residual Hampton Flats flux and the parabathic flux component near Hampton Flats. Our analysis of the potential impacts of construction incorporates several important approximations:

a. The theory developed and herein applied is for the two-dimensional case while the phenomenon approximated is intrinsically three-dimensional. Moreover, the theory considers flows involving two fluids of discretely different density while the case approximated is generally continuously stratified. The theory considers steady and sectionally uniform flow. The phenomenon addressed is neither spatially uniform nor steady.

b. The frontal system is treated as two discrete branches although it is recognized that the system is interactive.

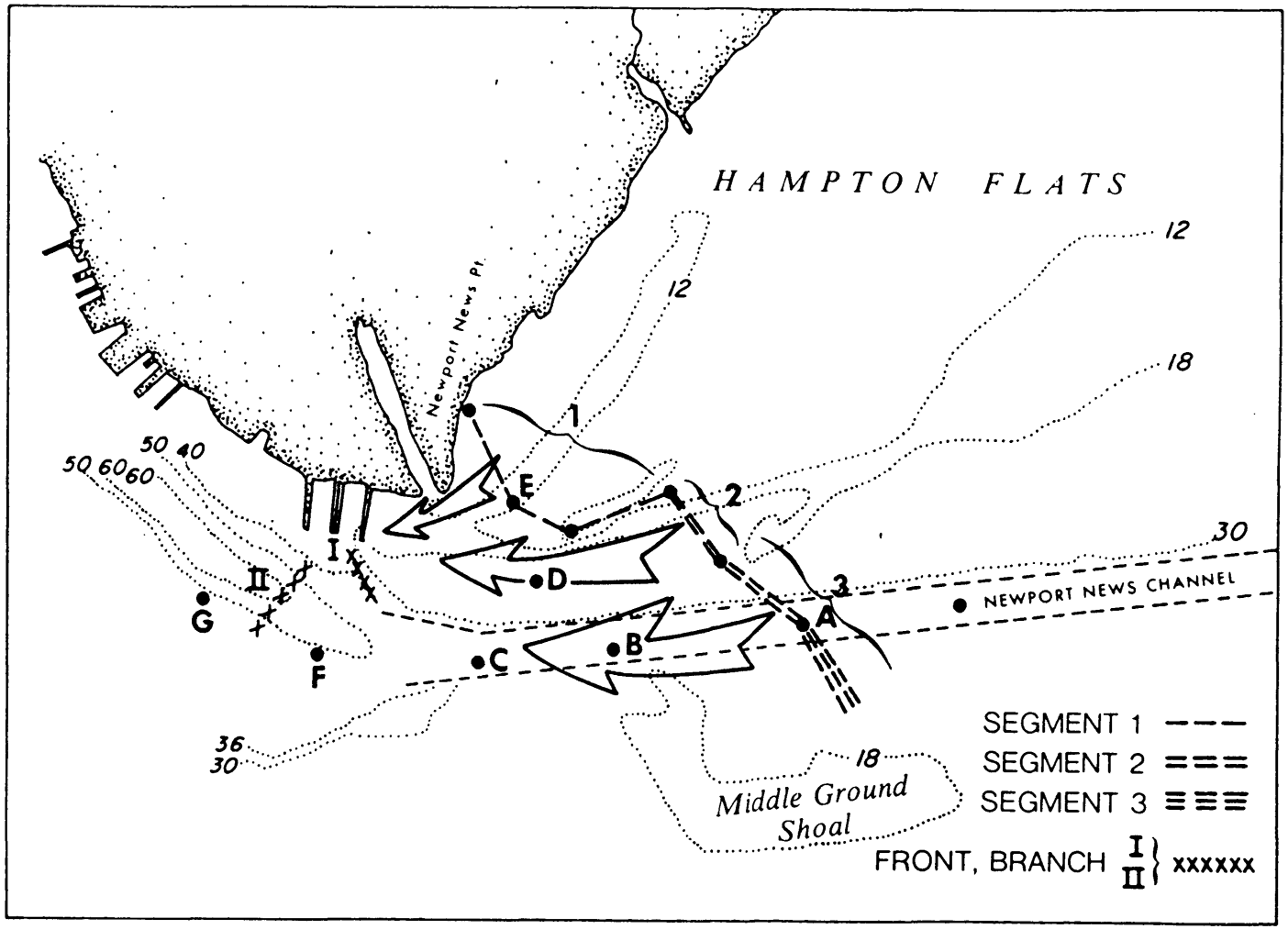

Figure IVA-2a. Segments used in calculation of flux to the frontal system, BASE condition. Reference text for details.

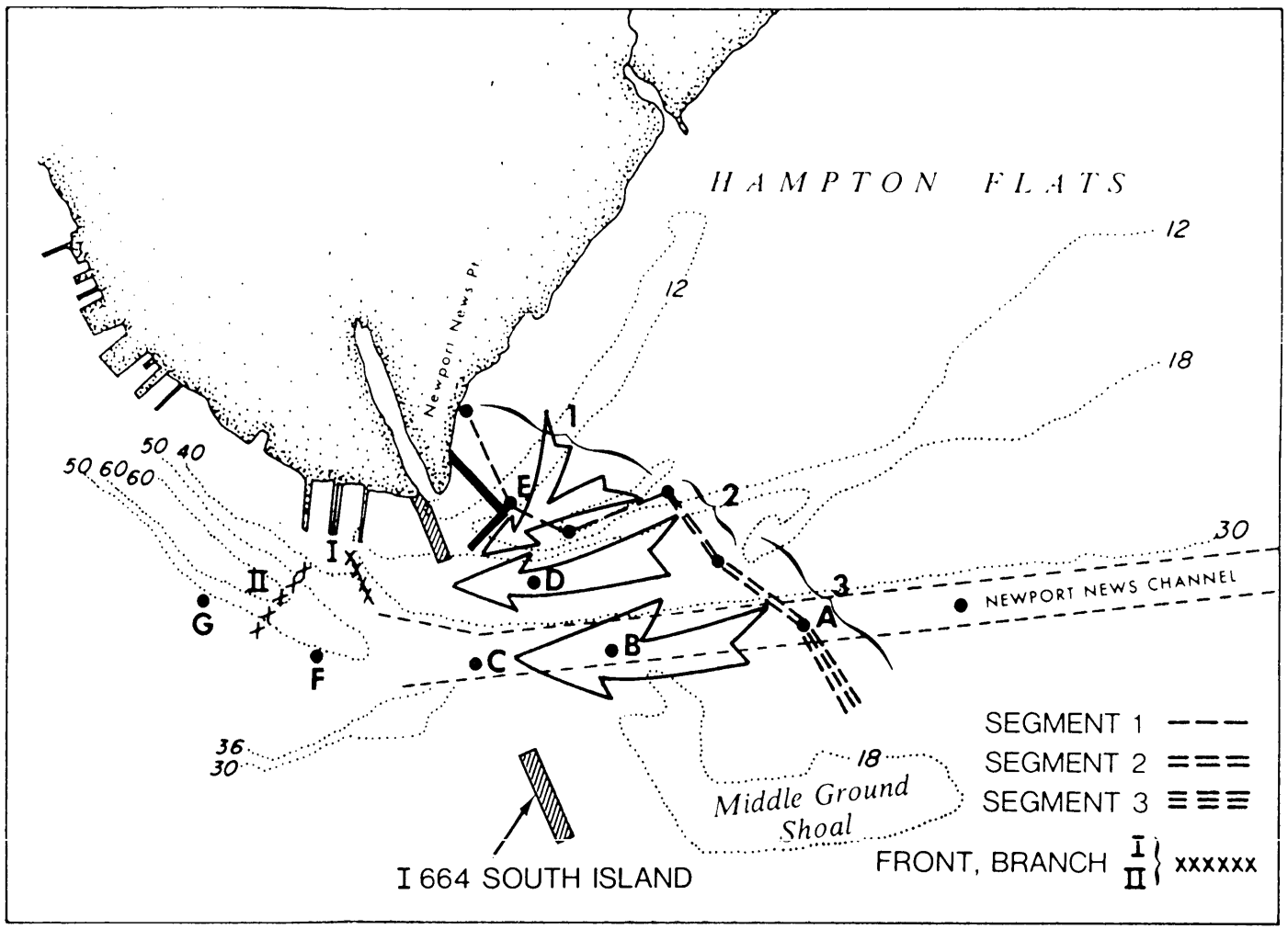

Figure IVA-2b. Segments used in calculation of flux to the frontal system, 1664 and Island conditions. Reference text for details.

c. As previously mentioned, interest is focused primarily on the frontal injection of water in the upper four meters of the water column. Estimates of flow partition were derived for Segment 3 by assuming a uniform distribution over the navigation channel and a logarithmic distribution over the fringing platforms. The details of estimation are presented in Appendix IIIA-2.

d. The position of the front components varies with time. This is particularly striking in the case of the transverse component over the Newport News Channel, the Branch II. Our analysis explicitly treats only the condition when the frontal system has migrated to the bathymetric transition in the vicinity of Newport News Point. The upriver limit of the front excursion has been observed to occur within a one kilometer zone.

2. Salinity Changes Due to Construction

This study attempts to differentiate the effects of the three sequential elements of construction (I664, channel deepening, and island) on the frontal system transport. With respect to salinity variation, past hydraulic model studies have treated the construction elements separately. That is, the I664 crossing investigations did not include channel deepening and the investigation on channel deepening did not include the I664 crossing. The numerical hydrodynamic study (Heltzel, 1984) did include both construction elements but salt transport was not incorporated. Therefore, estimates of salinity changes must be inferred from the individual study elements. The horizontal salinity gradient between Hampton Roads and the lower James is of particular importance.

In order to ascertain the effects of the I664 crossing on salinity the model studies of 1972 were selected, since the sampling station density was greater than that of the 1979 study. Those results (presented in Appendix

IIIA-1) indicate no significant changes in the horizontal or vertical salinity gradients in the area of interest due to the I664 crossing.

In order to ascertain the horizontal salinity gradient differences due to channel deepening the data of the hydraulic model tests (Richards and Morton, 1983) were analyzed. Of over 700 salinity gradient changes considered, 27% exceeded the gradient change induced by a 1 ppt salinity change, which is the accuracy claimed for salinity differences. Closer examination shows that the bulk of the 27% involved salinity changes less than 2 ppt over a distance of 4.7 km. From these results it can be concluded that changes in horizontal salinity gradients attributable to channel deepening are too small to affect frontal dynamics.

Thus, neither the I664 crossing nor channel deepening are considered to materially influence frontal dynamics by alteration of the horizontal salinity gradient. It is necessary to assume that the joint effect is also inconsequential. The addition of an island on Hampton Flats may induce highly localized salinity gradients changes. However, the gradients of concern are of larger scale. It is therefore reasonably assumed that island construction will not significantly alter the gradients responsible for the formation of the frontal system.

3. Application of 2-D Model Results and Front Theory

Equation (IIID-16) indicates that the critical velocity imposes an upper limit on the amount of surface water that the front can inject into the lower horizon of net upriver transport. Therefore, the capacity of a frontal system is controlled by the critical velocity, u_c, as well as the velocity, u_1, of the approaching flow. Table IVA-1 lists u_c and u_1 associated with Branch I and Branch II of the frontal system. The depth of approach flow y_1 is taken

Table IVA-1. Parameter Values Associated with the Frontal System off Newport News Point.

	Branch I	Branch II	
		45 ft. Channel	55 ft. Channel
y_1 (meters)	9.0	15.0	17.4
Δy (meters)	9.0	4.5	2.1
ΔY	1.0	0.3	0.12
F_c	1.24	0.265	0.623
u_c (m/s)			
ΔS = 3 o/oo	0.5	0.44	0.39
ΔS = 4 o/oo	0.64	0.51	0.45
u_1 (m/s)			
maximum flood current predicted by model	Node 267	Node 133	Node 133
Base	0.54	0.60	
I664/45	0.55	0.67	
I664/55	0.53		0.63
Island A	0.41		0.60
Island B	0.46		0.62
Island C-55	0.53		0.63
Island D-55	0.52		0.63
Island C-45	0.55	0.66	
Prototype data			
Buoy 13[1]		0.61	
Buoy 13[2]		0.65	
Buoy 12[2]		0.76	

Note: 1. November 1985 data, average over 46 tidal cycles.
2. March 1986 data, average over 18 tidal cycles.

at the brink of Hampton Flats for Branch I, and the dredged channel for Branch II respectively. The depth increases over the steps were taken along the directions of approach flows as they reach the topographic gradients. Given $\Delta Y = \frac{\Delta y}{y_1}$, the critical densimetric Froude number may be obtained from Figure IIID-2.

It is important to note that the parameter ΔY changes only for Branch II of the front in association with channel deepening. Construction of I664, with or without New Port Island, does not change the value of ΔY for Branch I. Field observations in June, 1986, after construction of the jetty associated with the north I664 tunnel approach, indicate that Segment 1 flow is simply diverted around the jetty.

Field observation utilizing dye injection reveals that the salinity difference across the front generally ranges from 2.5 to 4.0 $^{o}/oo$. As noted in previous discussion, the hydraulic model studies for I664, and for channel deepening, indicate that those construction elements taken individualy will not significantly alter the longitudinal salinity gradient in the section of the river affecting frontal transport. Moreover, placement of an island on Hampton Flats may be reasonably assumed not to significantly alter the salinity distribution in so far as the frontal activity is concerned. Therefore, salinity differences of 3 and 4 o/oo were used to evaluate the density difference used to calculate u_c by equation (IIID-15).

The velocity of the approaching flow, u_1, was predicted by the two-dimensional numerical model. Table IV-2 lists the maximum flood current speeds at the model nodes appropriate to this discussion (and referenced to the locations noted in Figure IVA-2a,b). Several points warrant note:

Table IVA-2. Maximum Flood Current Speeds at Selected Model Nodes (m/s).

NODE:	A* 122	B 124	C 133	D 267	E 270	F 136	G 160
Condition							
Base	0.49	0.55	0.60	0.54	0.42	0.50	0.52
I664-45	0.45	0.56	0.67	0.55	0.34	0.44	0.48
I664-55	0.44	0.54	0.63	0.53	0.32	0.48	0.51
Island A	0.45	0.55	0.60	0.41	0.22	0.48	0.51
Island B	0.46	0.53	0.62	0.46	0.23	0.47	0.51
Island C	0.43	0.52	0.63	0.53	0.25	0.47	0.50
Island D	0.43	0.51	0.63	0.52	0.25	0.47	0.50

*Letters refer to points shown in Figure IVA-2a,b.

a. The velocity at model node 267 (Point D in Figure IVA-2a,b) is an appropriate choice for the approach velocity, u_1, for Segment 2 of Branch I.

b. Model node 267 was also used to estimate u_1 for Segment 1 of Branch I. While node 270 (Point E in Figure IVA-2a,b) would seem more appropriate, field observations indicate that the flow from Segment 1 is entrained with the more rapid parabathic flow represented by node 267 for all cases with I664 in place. A more realistic value would be given by a velocity intermediate to those represented by nodes 270 and 267. Table IVA-1 was used to demonstrate that Branch I (a & b) are flow limited by using node 267 velocity. If node 270 velocity is used, Branch 1a is still flow limited. When the effect on discharge through front was assessed, the appropriate actual fluxes calculated by 2-D model were used for Branch Ia and Ib separately.

c. Node 133 was chosen to represent the approach velocity for Branch II of the front. This node represents the limit of accelerating flood current along the channel section (see points A,B,C in Table IV-2 and Figure IVA-2a,b), and the node is at the downriver side of the front. The average values of maximum flood currents measured at the western end of the dredged channel are also included in Table IVA-1 for comparison. The prototype data are in general agreement with that calculated by the numerical model.

Table IVA-1 shows that u_1 is less than or equal to u_c for Branch I of the front under all cases considered. Therefore, the capacity of Branch I is flow-limited; i.e., the front will inject all of the approaching flow. Since the flow through Segment 1 floods earlier than that through Segment 2, all the flow through Segment 1 will be injected to depth by the frontal activities.

Some portion of the flow passing through Segment 2 at the later phase of flood tide will not reach the front. Hence the total flux of flood flow through Segment 2 needs to be discounted with a factor. The method used to determine this factor is described in Appendix IIIA-3.

For Branch II of the front, u_1 is greater than u_c for all cases. Therefore, the capacity of this branch is front-limited; i.e., the discharge through the front is limited by u_c and y_1, regardless of how strong u_1 is. When $u_1 > u_c$, the excessive velocity only serves to push the front forward. The fraction of the flow injected by the front decreases with increasing u_1, since the displacement of the front will be larger. As in Segment 2, some portion of the flow passing Segment 3 will not reach the position of the front (Appendix IIIA-3 provides the procedure used).

Table IVA-3 summarizes the results of flux calculated for all cases studied. The 'volume' under each case was calculated from results of 2-D numerical model. It represents the total volume passing each segment during the flood phase of tide. The flux through Segment 3 was further partitioned between those above and below 4 m depth. Each of the 'volume' was divided into 'contributing' and 'noncontributing' components; i.e., those injected by the front and those not participating in the frontal activity. The noncontributing component represents the flux passing through Segments 2 and 3 in the later stages of flood current and which does not transit the position of the front. As discussed earlier, all flux through Segment 1 is considered to contribute to the frontal process. The velocity used for this determination is that calculated by 2-D model at node 260, which lies at the middle of Segment 2. The distance between the front and Segment 2 was derived from field observation to be 2.30 km. The discount factor for Segment 3 was

Table IVA-3. Front Flux Budget.

	BRANCH I		BRANCH II				% Change Relative to I664-45	
	Segment 1	Segment 2	Segment 3 <4m	Segment 3 >4m	SUBTOTAL <4m	TOTAL FLUX	<4m	Total
BASE								
Volume	20.4*	15.2	41.2	41.2				
Contributing	20.4	10.0	22.2	22.2	52.6	74.8	N/A	N/A
Noncontributing	-0-	5.2	19.0	19.0	24.2	43.2		
I664-45								
Volume	16.0	14.7	38.3	36.8				
Contributing	16.0	9.7	22.7	21.8	48.4	70.2	N/A	N/A
Noncontributing	-0-	5.0	15.6	15.0	20.6	35.6		
I664-55								
Volume	14.9	14.2	41.9	43.7				
Contributing	14.9	9.2	22.4	23.4	46.5	69.9	- 3.9	- 0.4
Noncontributing	-0-	5.0	19.5	20.3	24.5	44.8		
ISLAND A								
Volume	6.7	11.5	42.5	44.2				
Contributing	6.7	7.5	22.4	23.4	36.6	60.0	-24.4	-14.5
Noncontributing	-0-	4.0	20.1	20.8	24.1	44.9		
ISLAND B								
Volume	9.4	10.3	40.8	44.3				
Contributing	9.4	6.6	22.4	23.4	38.4	61.8	-20.7	-12.0
Noncontributing	-0-	3.7	18.4	20.9	22.1	43.0		
ISLAND C-45								
Volume	15.6	14.1	39.3	37.3				
Contributing	15.6	9.0	22.7	21.8	47.3	69.1	- 2.2	- 1.6
Noncontributing	-0-	5.1	16.6	15.5	21.7	37.2		
ISLAND C-55								
Volume	14.9	13.8	38.8	40.3				
Contributing	14.9	8.7	22.4	23.4	46.0	69.4	- 5.0	- 1.1
Noncontributing	-0-	5.1	16.4	16.9	21.5	38.4		
ISLAND D-55								
Volume	14.6	13.2	38.4	40.0				
Contributing	14.6	8.3	22.4	23.4	45.3	68.7	- 6.4	- 2.1
Noncontributing	-0-	4.9	16.0	16.6	20.9	37.5		

*All values x $10^6 m^3$.

estimated using velocity at model node 122, and a distnce of 3.2 km between the segment and front at the end of flood tide. This estimate was made for the base condition only. As discussed earlier, the total contributing flux from Segment 3 is front-limited. Therefore, the contributing flux remains unchanged as long as the navigation channel is not deepened. For the cases of the deepened channel, the contributing fluxes were estimated from the BASE condition by multiplying with a ratio of $u_c y_1$ for the deepened channel to that for the original channel.

4. Discussion

As noted earlier, particular interest is placed upon the disposition of surface waters (<4 m) intersecting the frontal system since it is this component which is injected to depths with net upriver motion. Correspondingly, this component is the more important in evaluating impacts due to construction. Inspection of Table IVA-3 for the BASE condition indicates that of the 52.6 x $10^6 m^3$ of surface water contributing to the frontal system about 39% ($20.4 \times 10^6 m^3$) is derived from Segment 1.

Comparison between the BASE and I664-45 conditions indicates the surface water contribution would be reduced by 8% and the total transport through the front reduced by 6%. However, comparison between these conditions must be considered indeterminate since the flow partitioning to either side of the South Island of I664 is determined by the treatment of local boundary conditions at the node representing the island. However, all cases besides BASE employ the same treatment of the South Island and may be intercompared. Due to the assumptions embodied in the application of the theory and the accuracy of a relatively coarse grid numerical model the differences portrayed in Table IVA-3 must be considered rather gross estimates.

The proposed locations of New Port Island (Island A or Island B in Table IVA-3) are seen to result in a marked reduction in the volume of surface waters transported through the front. Island A configuration results in a reduction of 24.4% and the reduction with Island B is 20.7%. The reduction is principally due to the blockage of flow from Hampton Flats (Segment 1). Both locations result in a reduction of flood tidal flow onto Hampton Flats of about 14% relative to the BASE condition (see Discussion in IIIE-4). Of the flow entering Hampton Flats a significant volume is deflected toward the channel at the eastern ends of the islands, a position remote from the front. Both configurations result in dramatically reduced outflow through the passage between the island and the mainland. Consequently, the transport effectiveness of Segment 1 is reduced. For the I664-45 condition Segment 1 contributes 33% of the total volume of surface water to the frontal system. For island locations A and B the contributions are respectively reduced to 18 and 24 percent.

The analyses conducted for the proposed locations suggested that an island location further to the east may have less impact on the frontal transport system. Additional analyses were performed as a diagnostic test for two conditions. These are Islands C and D (Figure IC-1) which represent areas of 370 and 323 acres respectively. The configurations were dictated by the grid layout of the numerical model. Both configurations, with channel depth at 55 feet, result in a reduction of the tidal flow onto Hampton Flats, reductions of 19% for Island C and 12% for Island D. However, the entering and exiting flow over Hampton Flats is redistributed such that the contribution to Segment 1 of the frontal system is essentially maintained.

The analysis indicate, in a diagnostic sense, a remarkable difference compared to the proposed locations (Option A or B). Relative to I664-45 the

percent change of surface transport is -5% and -6.4% for C-55 and D-55 respectively. However, relative to I664-55 the change is respectively, -1.0% and -2.6% for surface transport. The change then in total transport is within 2% for both cases. The values noted for Islands C and D configurations are considered to be within the accuracy of the present analysis.

B. Impact to Sedimentation Processes on Hampton Flats and Inferences on the Hard Clam Resources

1. Habitat Sensitivity

The bottoms of Hampton Flats and adjacent slopes contain a significant component of the local hard clam (**Mercenaria mercenaria**) fishery. The prinicpal concern was whether the proposed island construction would so alter the circulation patterns on Hampton Flats to induce deposition of fine grained sediments, and thereby degrade the substrate suitability for clam settlement. Laboratory studies (Keck, et al, 1974) indicate that a sandy substrate is preferred to mud for setting. Moreover, sandy or sand-shell hash substrates tend to reduce the predation effectiveness of the blue crab and thereby enhance the survival of natural set (Kraeuter and Castagna, 1977; see also Stanley, 1985, for review of environmental requirements).

Results previously discussed (Section IIIF) demonstrate that the substrate of Hampton Flats is medium to fine sands with silt/clay content ranging between 3 and 25 percent. Moderate suspended load concentrations of 5 to 15 mg/l are supplied by tidal advection from Hampton Roads. The substrate of Hampton Flats is thus favorable for hard clam settlement. The tidal current regime appears to be sufficiently energetic to inhibit accumulation of fine grained material.

Suspended sediment loads can also affect the feeding efficiency and growth of the hard clam (Bricelj and Malouf, 1984; Bricelj et al. 1984). These laboratory studies with 32 mm and 13 mm clams utilized mixtures of algae and silt. Algal ingestion rate decreased with increasing sediment loads. While the loss of algae in pseudofaeces increased with sediment concentration the maximum loss of algae cleared from suspension was 18 percent (at silt concentration of 40 mg/l). In growth rate studies Bricelj et al. found, for 9 mm clams, that sediment concentrations up to 25 mg/l did not significantly reduce growth rate. However, significant reduction did occur at sediment loads of 44 mg/l. Recent field studies (Grizzle, 1986) also suggest that growth rates are positively correlated with near-bottom tidal current speed as it contributes to the food provision rate. Thus, water current speed, food, and sediment appear to be major environment variables affecting the growth rates of hard clams. The relative effects are still incompletely understood and remain topics of active research.

It appears reasonable to argue that the hard clam habitat value of Hampton Flats would thus be altered by:

a. Blanket deposits of fine grained sediments (mud) as the substrate for settlement, and post-settlement survival, would be degraded.

b. Pronounced enrichment of the sediment column with fine grained sediments as episodic resuspension may yield suspended sediment loads sufficient to inhibit feeding efficiency.

c. Pronounced reduction in current speed which might affect food provision rates.

The evidence for substrate settlement selection and post-settlement survival is relatively well accepted. While numerous studies have shown that adult hard clams are more likely to live on sandy bottoms, muddy substrates are not

excluded. There is insufficient evidence to quantitatively define clam abundance as a function of the sediment size distribution.

2. Impacts Due to Construction

The present investigations permit only qualitative assessment of the tendency for deposition of fine grained sediment. The results discussed in Section IIIF indicate the following ranking in order of increasing deposition tendency (see also Figure IIIF-14):

I664-45

I664-55

ISLAND-C

ISLAND-D

ISLAND-B

ISLAND-A

a. ISLAND A. This configuration represents the most severe perturbation of sedimentation patterns. The area of expected deposition includes at least the entire northwest sector of Hampton Flats. More importantly the conditions would likely be conducive to the blanket accumulation of mud in the passage between the island and the mainland. Correspondingly, the substrate would be less suitable settlement substrate for the hard clam.

b. ISLAND B. This configuration is also projected to induce sedimentation in 25 percent of the Hampton Flats area. In contrast to configuration A, blanket mud accumulations are not expected in the passage between the island and the mainland since the tidal currents are projected to be sufficient to entrain the sediment fluff. However, the area of highest deposition tendency is located in the center of Hampton Flats, coincident with

the sector with the highest clam abundance (as reflected in the 1980 survey; see Section IIB).

c. ISLAND D. While total area of bottom projected to have somewhat higher sedimentation potential is similar to Island B, the subarea with the highest tendency is relatively more exposed to wave driven resuspension. Nonetheless, the areas with projected sedimentation enhancement are again coincident with the central area of Hampton Flats which had higher clam abundance.

d. ISLAND C. Of the four island locations considered, the Island C location is projected to have the least amount of bottom area with enhanced potential for deposition of fine grained sediments. The amount of area impacted is about the same as that projected for the I664 construction and part of the respective zones coincide.

3. Flood Tide Flux onto Hampton Flats

As indicated in the discussion of Section IIIE the hydrodynamic model predicts a reduction in the volume of water entering Hampton Flats during flood current. With respect to the I664 configuration these values are:

ISLAND-A	14.5%
ISLAND-B	14.2%
ISLAND-C	18.6%
ISLAND-D	12.3%

Recall that the model configurations for Island C and D were 370 and 323 acres respectively. Enlargement to 400 acres may have altered values. The reduction in flood flux could be expected to reduce the supply of clam larvae from external sources. However, since the relative roles of recruitment versus post-settlement differential survival is indeterminate it cannot be stated whether the volume reduction would result in any measurable impact.

REFERENCES

Andrews, J. D. 1951. Seasonal pattern of oyster setting in the James River and Chesapeake Bay. Ecol. 32, 752-758.

Andrews, J. D. 1954. Setting of oysters in Virginia. Proc. Natl. Shellfish. Ass. 45, 38-46.

Andrews, J. D. 1968. Oyster mortality studies in Virginia. VII. Review of epizootiology and origin of Minchinia nelsoni. Proc. Natl. Shellfish. Assoc. 58:23-36.

Andrews, J. D. 1979. Pelecypoda: Ostreidae. In: Reproduction of marine invertebrates, pp. 293-341. Ed. by A. C. Geise and J. S. Pearse. New York: Academic Press.

Andrews, J. D. 1982. The James River public seed oysters areas in Virginia. Special Report in Applied Marine Science and Ocean Engineering No. 261:1-60. Virginia Institute of Marine Science.

Andrews, J. D., D. S. Haven & D. B. Quayle. 1959. Fresh water kill of oysters (Crassostrea virginica) in the James River, Virginia, 1958. Proc. Natl. Shellfish. Assoc. 49:29-49.

Baylor, J. B. 1894. Method of defining and locating natural oyster beds, rocks, and shoals. Oyster Records (pamphlets, one for each Tidewater, VA, county, that listed the precise boundaries of the Baylor Survey). Board of Fisheries of Virginia.

Bayne, B. L. 1963. Responses of Mytilus edulis larvae to increases in hydrostatic pressure. Nature, Lond., Vol. 198, pp. 406-407.

Bayne, B. L. 1964. The responses of the larvae of Mytilus edulis L. to light and to gravity. Oikos, Vol. 15, pp. 162-174.

Bayne, B. L. 1976. Marine mussels: their ecology and physiology. Cambridge University Press. 506 pp.

Benjamin, T. B. 1968. Gravity currents and related phenomena. J. Fluid Mech, 31(2):209-248.

Bloomfield, P. 1976. Fourier Analysis of Time Series. New York, (Wiley.)

Boesch, D. F. 1971. Distribution and structure of benthic communities in the Hampton Roads area, Virginia. Tech. Rpt. Hampton Roads Sanitation Dist. Comm., Spec. Rpt. No. 15.

Boesch, D. F. 1973. Classification and community structure of macrobenthos in the Hampton Roads area, Virginia. Mar. Biol. 21:226-244.

Boon, J. D. III. 1974. Final report on the environmental effects of the second Hampton Roads Bridge- Tunnel construction: Sediment distributions and bottom characteristics. Virginia Institute of Marine Science, 25 pp.

Boon, J. D. III and R. J. Byrne. 1975. Borrow site monitor of turbidity and sedimentation, Hampton Bar dredging project. Final report to Newport News Shipbuilding and Dry Dock Co., 46 pp.

Boon, J. D. III and K. P. Kiley. 1979. Harmonic analysis and tidal prediction by the method of least squares. Special Report in Applied Marine Science and Ocean Engineering No. 186, Virginia Institute of Marine Science.

Bousfield, E. L. 1955. Ecological control of the occurrence of barnacles in the Miramichi estuary. Bull. Nat. Mus. Canada 137: 1-69.

Bowen, B. 1984. Effects of hydraulic clam dredge on benthos. Data Report, VIMS.

Bowman, M. J. and R. L. Iverson. 1978. Estuarine and plume fronts. Oceanic fronts in coastal processes, M. J. Bowman and W. E. Esaias, ed., pp. 87-104.

Bricelj, V. M. and R. E. Malouf. 1984. Influence of the algal and suspended sediment concentration on the feeding physiology of the hard clam Mercenaria mercenaria. Marine Biology 84:155-165.

Bricelj, V. M., R. E. Malouf, and C. de Quillfeldt, 1984. Growth of juvenile Mercenaria mercenaria and the effect of resuspended bottom sediments. Marine Biology 84: 167-173.

Brooks, T. J. and C. S. Fang. 1983. James River slackwater data report, temperature, salinity, disolved oxygen, 1971- 1980. Data report No. 12, Virginia Institute of Marine Science.

Byrne, R. J., A. Y. Kuo, J. M. Brubaker, P. V. Hyer, E. P. Ruzecki and J. H. Posenau. 1986. Effects of the proposed Newport Island on the circulation in Hampton Roads. SRAMSOE. Va. Inst. of Marine Science.

Carriker, M. R. 1951. Ecological observations on the distribution of oyster larvae in New Jersey estuaries. Ecol. Monogr. 21: 19-38.

Carriker, M. R. 1961. Interrelation of functional morphology, behavior and autecology in early stages of the bivalve Mercenaria mercenaria. J. Elisha Mitchell scient. Soc., Vol. 177, pp. 168-242.

Castagna, M. and J. N. Kraeuter. 1981. Manual for growing the hard clam Mercenaria mercenaria. VIMS SRAMSOE No. 249.

Chen, H. S. 1979. A two- dimensional hydrodynamic and biogeochemical water quality model and its application to the lower James River. Special Report in Applied Marine Science and Ocean Engineering No. 183, Virginia Institute of Marine Science.

Clarke, G. L. 1970. Light conditions in the sea in relation to the diurnal vertical migrations of animals. In: Farquhar, G. B. (ed.) Proceedings of an international symposium on biological sound

scattering in the ocean. Maury Center for Ocean Science, Department of the Navy, Washington, D.C., pp. 41-50.

Clarke, G. L. and E. J. Denton. 1962. Light and animal life. In: Hill, M. N. (ed.) The sea. Interscience Publishers, New York, pp. 456-468.

Cragg, S. M. 1980. Swimming behaviour of the larvae of Pecten maximus (L.) (Bivalvia). J. mar. biol. Ass. U.K. 60: 551-564.

Cragg, S. M. and L. D. Gruffydd. 1975. The swimming behaviour and the pressure responses of the veliconcha larvae of Ostrea edulis (L.). In: Proceedings of the Ninth European Marine Biology Symposium, Oban, Scotland, 1974 (ed. H. Barnes), pp. 43-57. Aberdeen: Aberdeen University Press.

Cronin, W. B. 1971. Volumetric, area and tidal statistics of Chesapeake Bay and its tributaries. Special Report No. 20, Chesapeake Bay Institute, The Johns Hopkins University, Baltimore, Maryland.

deWolf, P. 1973. Ecological observations on the mechanisms of dispersal of barnacle larvae during planktonic life and settling. Neth. J. Sea Res. 61: 1-129.

deWolf, P. 1974. On the retention of marine larvae in estuaries. Thalassia Jugoslavica 10: 415-424.

Diaz, R. J. and D. F. Boesch. 1978. Environmental effect of subaqueous sand fill acquisition on the benthic communities of Hampton Bar, James River, Virginia. Rpt. Newport News Shipbuilding and Drydock Co. 73 pp.

Diaz, R. J. and E. P. Ruzecki. 1981. Study to investigate source and transport route of marine organisms (Hydroids and Bryozoans) in Hampton Roads and current velocity profiles of the Pier 12 area Naval Station, Norfolk, Virginia. Rpt. NAVFAC, Norfolk Naval Base. 75 pp.

Fang, C. F., et al, 1972. Physical and geological studies of the proposed bridge-tunnel crossing of Hampton Roads near Craney Island. Special report in Applied Marine Science and Ocean Engineering No. 24, Virginia Institute of Marine Science, 42 pp.

Fang, C. F. et al. 1979. James River hydraulic model study with respect to proposed third bridge- tunnel causeway in Hampton Roads. Special report in Applied Marine Science and Ocean Engineering No. 212, Virginia Institute of Marine Science, 160 pp.

Fang, C. S. and B. Neilson, 1975. Oceanography, water quality and modeling studies for the outfall for a proposed Nansemond waste water treatment plant. Vol. V. Special Report in Applied Marine Science and Ocean Engineering, Virginia Institute of Marine Science. No. 86, 1-88.

Flugel, H. 1972. Pressure - animals. In: Marine Ecology, vol. 1, part 3, O. Kline, ed., pp. 1407-1450. Wiley-Interscience.

Foxon, G. E. H. 1934. Notes on the swimming methods and habits of certain crustacean larvae. J. mar. biol. Ass. U.K. 19: 829-849.

Fortier, L. and W. C. Leggett. 1983. Vertical migrations and transport of larval fish in a partially mixed estuary. Can. J. Fish. Aq. Sci. 40: 1543-1555.

Fraenkel, G. S. and D. L. Gunn. 1961. The orientation of animals. Dover Publ. NY.

Gibbons, M. C. and M. Castagna. 1984. Serotonin as an inducer of spawning in six bivalve species. Aquaculture 40:189-191.

Garvine, R. W. and J. D. Monk. 1974. Frontal structure of a river plume. Jour. Geophys. Res., 79: 2251-2259.

Grizzle, R. E. 1986. Preliminary studies on the effects of tidal currents, food concentration, and sediment characteristics on ontogenetic growth of Mercenaria mercenaria. Journal of Shellfish Research [abst], in press.

Harder, W. 1968. Reactions of plankton organisms to water stratification. Limnol. Oceanogr. 13: 156-160.

Haskin, H. H. 1964. The distribution of oyster larvae. In: Symposium on Experimental Marine Ecology. N. Marshall, H. P. Jeffries, T. A. Napora and J. M. Sieburth, eds., pp. 76-80. Occasional Publication no. 2, Graduate School of Oceanography, University of Rhode Island.

Haskin, H. H., A. Stauber & J. Makin. 1966. Minchinia nelsoni n. sp. (Haplosporida, Haplosporidiidae): causative agent of the Delaware Bay oyster epizootic. Science 153:1414-1416.

Haven, D. S. and J. G. Loesch. 1972a. Hampton Roads corridor survey report for the Virginia Department of Highways. Final Report. 12 pp + 6 tables. Virginia Institute of Marine Science.

Haven, D. S. and J. G. Loesch. 1972b. An investigation into commercial aspects of the hard clam fishery and development of commercial gear for the harvest of molluscs. Annual contract report for the period 1 July 1971 through 30 June 1972. Contract 3-124-R with the Virginia marine Resources Commission, for the National Marine Fisheries Service. 50 pp. Virginia Institute of Marine Science.

Haven, D. S., J. G. Loesch and J. P. Whitcomb. 1973. An investigation into commercial aspects of the hard clam fishery and development of commercial gear for the harvest of molluscs. Final Reporet, contract 3-124-R with the Virginia Marine Resources Commission, for the National Marine Fisheries Service. 119 pp. Virginia Institute of Marine Science.

Haven, D. and P. Kendall. 1974. A final report to the Virginia Department of Highways on hard clam (Mercenaria mercenaria) populations in the

vicinity of Hampton Roads Bridge Tunnel (I-64). 16 pp. + 6 tables + 18 figures. Virginia Institute of Marine Science.

Haven, D. and F. Kendall. 1975. A survey of commercial shellfish in the vicinity of Newport News Point and Pig Point in the lower James River. Final Report to McGaughy, Marshall and McMillan - Hazen and Sawyer. In: Fang, C. S., (Project Manager): Oceanographic, Water Quality and Modeling Studies for the Outfall from a Proposed Nansemond Waste Water Treatment Plant, Volume 4. pp. 1-28 and summary. Special report No. 86 in applied Marine Science and Ocean Engineering. Virginia Institute of Marine Science.

Haven, D. S., W. J. Hargis, Jr., J. G. Loesch & J. P. Whitcomb. 1976. The effect of Tropical Storm Agnes on oysters, hard clams, soft clams, and oyster drills in Virginia. Haven, D. S., W. J. Hargis, Jr., J. Loesch, and J. P. Whitcomb, eds. The Effects of Tropical Storm Agnes on the Chesapeake Bay Estuarine Systems. Baltimore, MD: John Hopkins Press. (CRC Publ. 54:488-407).

Haven, D. S. and R. Morales-Alamo. 1980. Estimate of the total weight of kepone in the major ccomponents of the molluscan fauna of the James River, Va. Virginia Institute of Marine Science: internal report.

Haven, D. S., J. P. Whitcomb & P. Kendall. 1981a. The present and potential productivity of the Baylor Grounds in Virginia. Special Report in Applied Marine Science and Ocean Engineering, No. 243:1-154, Virginia Institute of Marine Science.

Haven, D. S., W. J. Hargis, Jr. & P. Kendall. 1981b. The oyster industry of Virginia: to status, problems and promise. 1981 (revised). Special Report in Applied Marine Science and Ocean Engineering, No. 4: 1024 pp., Virginia Institute of Marine Science.

Haven, D. S. and J. P. Whitcomb. 1983. The origin and extent of oyster reefs in the James River, Virginia. Jour. Shellfish Res. 3(2): 141-151.

Hebbert, B., J. Imberger, I. Loh, and J. Patterson. 1979. Collie River underflow into the Wellington Reservoir. Jour. of Hydraulic Div., ASCE, 105(HY5), 533-546.

Heltzel, S. B. 1984. I664 Bridge Tunnel study: sedimentation and circulation investigation. Draft Technical Report. U. S. Army Corps of Engineers Waterways Experiment Station.

Hidu, H. and H. H. Haskin. 1978. Swimming speeds of oyster larvae Crassostrea virginica in different salinities and temperatures. Estuaries 1: 252-255.

Hobbs, C. H., R. J. Byrne, R. A. Gammisch, and R. J. Diaz. 1985. Sand for beach nourishment in Lower Chesapeake Bay. Proc. 4th Sym. Coastal and Ocean Manag. pp. 790-811.

Huzzey, L. M. 1982. The dynamics of a bathymetrically arrested estuarine front. Estuarine, Coastal and Shelf Sci. 15:537-552.

Hyland, J. 1972. The effects of Hurricane Agnes on the benthic diversity in the Hampton Roads, Virginia, area. VIMS Manuscript. 27 pp.

Ippen, A. T. 1966. Estuary and coastline hydrodynamics. McGraw-Hill. New York.

Keck, R., D. Maurer and R. Malouf, 1974. Factors influencing in setting behavior of larvaal hard clams, Mercenaria mercenaria. Proc. National Shellfish Assoc. 64: 59-67.

Kennedy, V. S. (ed.) 1982. Estuarine Comparisons. Academic Press. N.Y.

Klemas, V. and D. F. Polis. 1977. Study of density fronts and their effects on coastal pollutants. Remote Sensing of Environ. 6:95-126.

Knight-Jones, E. W. and E. Morgan. 1966. Responses of marine animals to changes in hydrostatic pressure. Oceanography and Marine Biology, an Annual Review, 4: 267-299.

Korringa, P. 1952. Recent advances in oyster biology. Q. Rev. Biol. 27; 266-308; 339-365.

Kraeuter, J. N. and M. Castagna. 1980. Effects of large predators on the field culture of the hard clam, Mercenaria mercenaria. U. S. Natl. Mar. Fish. Serv. Bull. 78(2): 538-541.

Kunkle, D. E. 1957. The vertical distribution of larvae in Delaware Bay. Proc. Nat. Shellfish. Assoc. 48: 90-91.

Lamb, H. 1932. Hydrodynamics. 6th edition. Dover Publications, New York.

Loesch, J. G., D. S. Haven & J. P. Whitcomb. 1975. An investigation of the seed oyster reserves in Virginia and testing and identifying gear to harvest oysters. Gloucester Point, VA: Va. Inst. Mar. Sci. Final Rep. Contract No. 3 - 193R, Natl. Mar. Fish. Serv.; 133 p.

Loosanoff, V. L. 1932. Observation on Propagation of Oyster in the James and Corrotoman Rivers and the Seaside of Virginia. Newport News, VA: Virginia Comm. Fish.; 46 p.

Loosanoff, V. L. and H. C. Davies. 1963. Rearing of bivalve molluscs. Adv. Mar. biol. 1:1-136.

Lutz, R. A., R. Mann, J. G. Goodsell and M. Castagna. 1982. Larval and early post larval development of the Ocean Quahog Arctica islandica. J. mar. biol. Ass. U.K. 62: 745-769.

Mann, R. 1982. The seasonal cycle of gonad development in Arctica islandica on the Southern New England shelf. Fishery Bulletin 80(2):315-326.

Mann, R. (in press). Sampling of bivalve larvae. Can. J. Fish. Aq. Res.

Mann, R. and C. C. Wolf. 1983. Swimming behaviour of larvae of the ocean quahog Arctica islandica in response to pressure and temperature. Mar. Ecol. Prog. Series 13: 211-218.

Marshall, N. 1954. Changes in the physiography of oyster bars in James River, Virginia. Va. J. Sci. 5(3):23-28.

Mileikovsky, S. A. 1973. Speed of active movement of pelagic larvae of marine bottom invertebrates and their ability to regulate their vertical position. Marine Biology, 23: 11-17.

Miller, M. C., I. N. McLane and P. D. Komar. 1977. Threshold of sedimentation under unidirectional currents. Sedimentology 24: 507-527.

Moore, H. F. 1911. Condition and extent of oyster beds in the James River. U.S. Bur. Fish. Doc. No. 729:83 p.

National Ocean Survey. 1985. Tide current table: East Coast of North and South America. US Dept. of Commerce.

Naylor, E. and R. J. A. Atkinson. 1972. Pressure and the rhythmic behaviour of inshore marine animals. Symposia of the Society for Experimental Biology, no. 26: 395-415.

Nelson, J. 1911. Report of the biologist. Rep. New Jers. St. agric. exp. Stn. June, 1910, 183-218.

Nelson, T. C. 1953. Some observations on the migrations and setting of oyster larvae. Proc. Natl. Shellfish Assoc. 43: 99-104.

Nelson, T. C. 1955. Observations on the behaviour and distribution of oyster larvae. Proc. Natl. Shellfish Assoc. 45: 23-28.

Nelson, T. C. and E. B. Perkins. 1931. Annual Report of the Department of Biology for the year ending June 30, 1930. N. J. Agric. Exp. Sta. Bull. 522: 1-47.

Nunes, R. A. and J. H. Simpson. 1985. Axial convergence in a well-mixed estuary. Estuarine Coastal and Shelf Sci. 20:637-649.

Pritchard, D. W. 1951. The physical hydrography of estuaries and some applications to biological problems. Trans. N. Am. Wildl. Conf. 16: 368-376.

Pritchard, D. W. 1952. Distribution of oyster larvae in relation to hydrographic conditions. Proc. Gulf Caribb. Fish. Inst. Nov. 1952, 1-10.

Pritchard, D. W. 1952. Salinity distribution and circulation in the Chesapeake Bay estuarine system. J. Mar. Res. 11, 106-123.

Pritchard, D W. 1953. Distribution of oyster larvae in relation to hydrographic conditions. Proc. Gulf Carib. Fish. Inst. 5, 123-132.

Pritchard, D. W. 1967. What is an estuary: physical viewpoint. Estuaries, Amer. Assoc. Aolv. Sci., Pub. No. 83, G. H. Lauff, ed., pp. 3-5.

Pritchard, D. W. 1985. Estuarine classification- a help or a hindrance? Paper presented at William and Mary Founders Day symposium on circulation in Estuaries, Gloucester Point, Virginia, 31 Jan.- 1 Feb.

Quayle, D. B. 1952. Structure and biology of the larva and spat of Venerupis pullastra (Montagu). Trans. R. Soc. Edinb. 62: 255-297.

Redfield, A. C. 1950. The analysis of tidal phenomenon in narrow embayments. Paper in Phy Oceans and Meteor. IX (4), WHOl, Mass.

Richards, D. R. and M. R. Morton. 1983. Norfolk Harbor and channel deepening study, Report 1, physical model results. Tech. Rep. Hl-83-13. U. S. Army Corps of Engineers Waterways Experiment Station Hydraulics Laboratory.

Rouse, H. 1946. Elementary mechanics of fluids. John Wiley and Sons, Inc., New York.

Rizzo, W. M. and R. L. Wetzel. 1985. Intertidal and shoal benthic community metabolism in a temperate estuary: Studies of spatial and temporal scales of variability. Estuaries 8:342-351.

Ruzecki, E. P. and R. W. Moncure. 1968. Dye distribution results from point release in the James River model, pp. 1-22. In: Utilization of physical and mathematical models in marine water resources research, planning and management. A report for the period Sept. 1967-Dec. 1968. Ed. by W. J. Hargis, Jr. Gloucester Point: Virginia Institute of Marine Science.

Ruzecki, E. P. and R. W. Moncure. 1969. Dye distribution resulting from point releases in the James River. Appendix IV in Hargis, W. J. Jr., 1969. Utilization of physical and mathematical models in marine water resources research, planning, and management. A report for the period 1 Sept. 1967- 31 Dec. 1968 to the Office of Water Resources Research, U. S. Dept. of Interior.

Ruzecki, E. P. and W. J. Hargis, Jr. 1985. Interaction between circulation of the estuary of the James River and transport of oyster larvae. Paper presented at William and Mary Founders Day Symposium on circulation in estuaries, Gloucester Point, Virginia, 31 Jan.- 1 Feb. 1985.

Schubel, J. R. and H. H. Carter. 1984. The estuary as a filter for fine-grained suspended sediment. In: The Estuary As a Filter, V. S. Kennedy, ed., Academic Press, New York.

Seliger, H. H., J. A. Boggs, R. B. Rivkin, W. H. Biggley and K. R. Aspden. 1982. The Transport of Oyster Larvae in an Estuary. Marine Biology 71: 57-72.

Shidler, J. K. and W. G. MacIntyre. 1967. Hydrographic data collections for "Operation James River- 1964." Virginia Institute of Marine Science data report No. 5.

Simpson, J. E. 1982. Gravity currents in the laboratory, atmosphere, and ocean. Ann. Rev. Fluid Mech., 14: 213-234.

Simpson, J. H. and J. R. Hunker. 1974. Fronts in the Irish Sea. Nature. London, 250:404-406.

Simpson, J. H. and R. A. Nunes. 1981. The tidal intrusion front: an estuarine convergence zone. Estuarine, Coastal and Shelf Sci 13: 257-266.

Simpson, J. H. and W. R. Turrell. 1986. Convergent fronts in the circulation of tidal estuaries. In: Estuarine Variability. Proceedings of 8th Int. Estuarine Res. Conf., Durham, New Hampshire.

Spooner, G. M. 1933. Observations on the reactions of marine plankton to light. J. mar. biol. Ass. U.K. 19: 385-438.

Stanley, J. G. 1985. Species profiles: life histories and environmental requirements of coastal fishes and invertebrates (mid-Atlantic)- hard clam. U. S. Fish and Wildlife Serv. Biol. Rep. 82(11.41). U. S. Army Corps of Engineers, TR EL-82-4, 24 pp.

Thorson, G. 1950. Reproductive and larval ecology of marine bottom invertebrates. Biol. Rev. 25: 1-45.

Thorson, G. 1964. Light as an ecological factor in the dispersal and settlement of larvae of marine bottom invertebrates. Ophelia 1: 167-208.

Tyler, M. A. and H. H. Seliger. 1978. Annual subsurface transport of a red tide dinoflagellate to its bloom area. Water circulation patterns and organism distributions in the Chesapeake Bay. Limnol. Oceanogr. 23: 227-246.

Tyler, M. A. and H. H. Seliger. 1981. Selection for a red tide organism. Physiological responses to the physical environment. Limnol. Oceanogr. 26: 310-324.

U. S. C. & G. S. 1963. Tidal current tables of the Atlantic Coasts of North America. U. S. Dept. of Commerce, Washington, D. C.

Vogel, S. 1981. Life in moving fluids. W. Grant Press, Boston, MA 52 pp.

Welch, C. S. and B. J. Neilson: Newport News circulation study. Spec. Sept. Appl. Mar. Sci. Ocean Eng., Va. Inst. Mar. Sci. No. 87, 1-105 (1975).

Wood, L. and W. J. Hargis. 1971. Transport of bivalve larvae in a tidal estuary. In: Proceedings of the Fourth European Marine Biology

Symposium, Bangor, 1969 (ed. D. J. Crisp), pp. 29-44. Cambridge: Cambridge University Press.